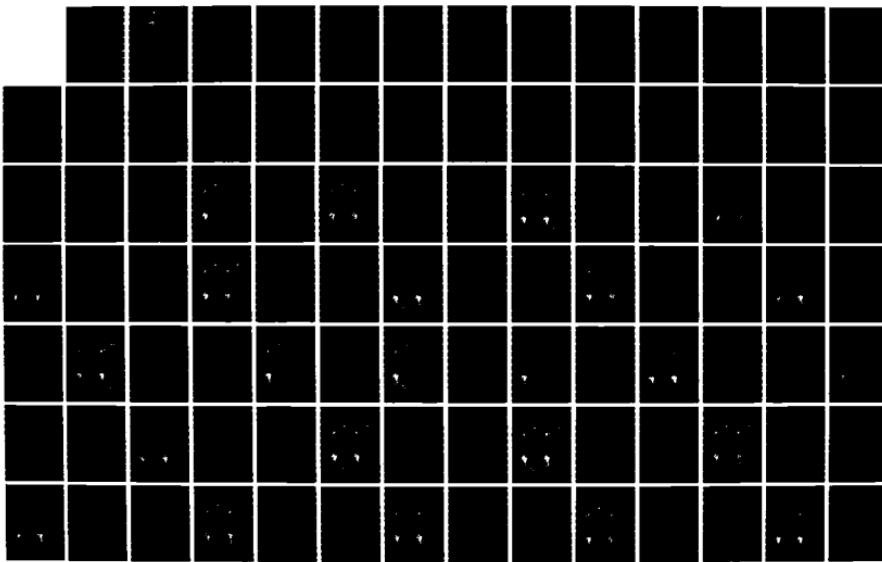


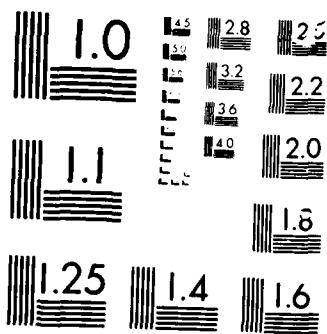
RD-A168 852 MONTHLY AND SEASONAL CLIMATOLOGY OF THE NORTHERN WINTER 1/2
OVER THE GLOBAL T. (U) NAVAL POSTGRADUATE SCHOOL
MONTEREY CA J S BOYLE ET AL. MAY 86

UNCLASSIFIED NPS-63-86-002-VOL-3

F/G 4/2

ML





MIN. RES. 1.0 2.8 2.5 3.2 3.6 4.0 1.8 1.6

NAVAL POSTGRADUATE SCHOOL

Monterey, California

AD-A168 852



DTIC
SELECTED
JUN 20 1986
S P

Monthly and Seasonal Climatology of the Northern
Winter over the Global Tropics and
Subtropics for the Period 1974 to 1983

Volume III. Surface Winds

by

James S. Boyle and C.-P. Chang

May 1986

Technical Report May 1985 - May 1986

Approved for public release; distribution unlimited.

Prepared for: National Oceanic and Atmospheric Administration
Washington, D.C. 20233

DTIC FILE COPY

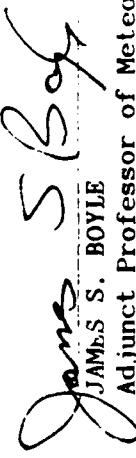
NAVAL POSTGRADUATE SCHOOL
Monterey, California 93943

Rear Admiral R. H. Shumaker
Superintendent

D. A. Schraday
Provost

The work reported herein was supported by the National Oceanic and Atmospheric Administration, under Research Contracts NAG3AAG03828 and 40AAW503656.

This report was prepared by:



James S. BOYLE
Adjunct Professor of Meteorology

C.-P. CHANG
Professor of Meteorology

Publication of the report does not constitute approval of the findings or conclusions. It is published for information and for the exchange and stimulation of ideas.

Reviewed by:



ROBERT J. REWARD
Chairman
Department of Meteorology

Released by:



JOHN N. DYER
Dean of Science and Engineering

UNCLASSIFIED

SECURITY CLASSIFICATION OF THIS PAGE (When Data Entered)

REPORT DOCUMENTATION PAGE		READ INSTRUCTIONS BEFORE COMPLETING FORM
1. REPORT NUMBER NPS-63-86-002	2. GOVT ACCESSION NO AD-A168852	3. RECIPIENT'S CATALOG NUMBER 52
4. TITLE (and Subtitle) Monthly and Seasonal Climatology of the Northern Winter over the Global Tropics and Subtropics for the Period 1974 to 1983. Volume III. Surface Winds	5. TYPE OF REPORT & PERIOD COVERED Technical Report for May 1985 - May 1986	6. PERFORMING ORG. REPORT NUMBER NA83AAG03828 & 40AAANW503656
7. AUTHOR(s) James S. Boyle and C.-P. Chang	8. CONTRACT OR GRANT NUMBER(s) NOAA Research Contracts	9. PERFORMING ORGANIZATION NAME AND ADDRESS Naval Postgraduate School Monterey, California 93943
10. PROGRAM ELEMENT, PROJECT, TASK AREA & WORK UNIT NUMBERS	11. CONTROLLING OFFICE NAME AND ADDRESS Climate Analysis Center/NMC National Oceanic and Atmospheric Administration Washington, D.C. 20233	12. REPORT DATE May 1986
13. NUMBER OF PAGES 142	14. MONITORING AGENCY NAME & ADDRESS (if different from Controlling Office)	15. SECURITY CLASS. (of this report) UNCLASSIFIED
16. DISTRIBUTION STATEMENT (of this Report) Approved for public release; distribution unlimited.	17. DECLASSIFICATION/DOWNGRADING SCHEDULE	

17. DISTRIBUTION STATEMENT (of the abstract entered in Block 20, if different from Report)

18. SUPPLEMENTARY NOTES

19. KEY WORDS (Continue on reverse side if necessary and identify by block number)

Interannual Variations
Tropical Climatology
Winter Circulations

20. ABSTRACT (Continue on reverse side if necessary and identify by block number)

This atlas of the surface circulation field contains northern winter monthly and seasonal mean wind analyses, velocity potential and streamfunction from 40°S to 60°N over a global belt for the period 1974 through 1983. In addition, the deviations of the individual annual seasonal and monthly means from their respective nine-year means are presented for the same variables. The basic wind data used are the operational Global Band Analyses of the United States Navy's Fleet Numerical Oceanography Center.

DD FORM 1 JAN 73 EDITION OF 1 NOV 68 IS OBSOLETE
S/N 0101-014-66011

UNCLASSIFIED
SECURITY CLASSIFICATION OF THIS PAGE (When Data Entered)

CONTENTS

	page
<i>Abstract</i>	<i>i</i>
1. INTRODUCTION	1
2. DATA SOURCES, ANALYSIS AND COMPUTATIONAL PROCEDURES	2
Global Band Analysis Computation of streamfunction and velocity potential	2
3. DISCUSSION	4
REFERENCES	6
<i>Figure I</i>	9
<i>Figure II</i>	10
<i>Figure III</i>	11
<i>Figure IV</i>	12
<i>Figures A1 - A3</i>	13
<i>Figures B1 to B27</i>	14
<i>Figures C1 to C9</i>	15
<i>Figures D1 to D81</i>	16
<i>Dist</i> / <i>Avail. and/or Specifi</i>	16
<i>Ability Codes</i>	16
<i>Dist</i> / <i>Avail. and/or Specifi</i>	16
<i>A-1</i>	16

ORIC
COPY
SPECIFIC

For
CRA&I
TAB
Avail
Specifi
Ability Codes
Avail and/or
Specifi

ABSTRACT

This atlas of the surface circulation field contains northern winter monthly and seasonal mean wind analyses, velocity potential and streamfunction from 40°S to 60°N over a global belt for the period 1974 through 1983. In addition, the deviations of the individual annual seasonal and monthly means from their respective nine-year means are presented for the same variables. The basic wind data used are the operational Global Band Analyses of the United States Navy's Fleet Numerical Oceanography Center.

1. INTRODUCTION

This atlas depicts the wintertime (December, January, February) seasonal and monthly mean atmospheric surface motion fields for the period 1974/1975 to 1982/1983. The charts display surface streamfunction, wind vectors, isotachs, and velocity potential from 40°S to 60°N. In addition, to the nine-year seasonal and monthly means and the individual annual seasonal and monthly averages, the deviations of the individual seasonal and monthly means from their nine-year averages are also presented. The seasonal calculations are based on the months of December, January, and February. The data used as the basis for these motion fields are the Global Band Analysis (GBA) of the United States Navy's Fleet Numerical Oceanography Center (FNOC). The procedure used in producing these analyses are described in section 2.

The motion fields for the winters from 1974/75 to 1982/83 are of interest since the data cover a period not previously examined in other collections of data. Other works such as Oort (1983) and Krishnamurti et. al. (1983) have presented detailed analysis of the decade prior to 1974. The 1974 - 1983 period contains two El Niño/Southern Oscillation (ENSO) events, one occurring in 1976/77 and the other in 1982/83. The latter event is the most intense ENSO event yet observed. Also, the analyses presented here allow the FGGL winter to be placed in a longer term perspective since the FGGL/WMONEX experiment took place in the midst of the period.

2. DATA SOURCES, ANALYSIS AND COMPUTATIONAL PROCEDURES

2.1 GLOBAL BAND ANALYSIS

The wind data set used in this work are the operational analyses of the Global Band Analyses of FNOC. These data are produced four times daily by objective procedures on a mercator grid which extends from 40°S to 60°N . The use of the mercator secant projection results in a change in the actual distance between grid points from 140 km at 60°N to a maximum value of 280 km at the equator. The objective scheme is designed to take advantage of all the reports in the operational data base, surface synoptic, aircraft, pilot balloons, rawindsonde and satellite data.

The analysis is performed every six hours for the surface, 700, 400, 250 and 200 mb levels. The first guess field used as input for the objective analysis is the six hour persistence field. The approach is to first interpolate the irregularly spaced data to grid points using a successive corrections technique based on Cressman's (1959) method. The successive corrections method takes several scans through the data reducing the scan radius on each successive scan. Analyses are performed of both wind and temperature by this method. These fields are then adjusted to be consistent with a set of numerical variational analysis (NVA) equations which have incorporated the dynamical constraints of the momentum equations with friction included in the surface layer, (Lewis and Grayson, 1972). Temperature and wind fields are adjusted subject to mutual constraints on the fields. However, the surface and 200 mb wind data serve only as a lower and upper boundary condition for the NVA and are not subject to an adjustment.

2.2 COMPUTATION OF STREAMFUNCTION AND VELOCITY POTENTIAL

The streamfunction (Ψ) and velocity potential (χ) were computed from the following equations:

$$\nabla^2 \chi = \delta$$

$$\nabla^2 \Psi = \zeta$$

where:

ζ is the relative vorticity = $\partial v / \partial y - \partial u / \partial x$ and
 δ is the divergence = $\partial u / \partial x + \partial v / \partial y$. Both ζ and δ were computed using centered differences on
the GBA mercator grid taking the appropriate map scale factor into account.

Equation (2) was solved using the boundary condition that $\chi = 0$ on the north and south
boundaries which are at 60°N and 40°S respectively. The method used to compute Ψ was essentially
the method II of Shukla and Saha (1974). This technique uses the previously computed values of χ to
formulate boundary conditions for Ψ .

The depiction of the divergence field appears reasonable away from the boundary. Comparison with the global fields produced by the National Meteorological Center (NMC) for the years since the NMC χ fields have become available indicate that the effect of the boundary conditions on χ is not significant between 40°N and 30°S . Thus, the Ψ and χ fields in the equatorial regions are sufficiently removed from the boundaries that we can assume that these values are not unduly affected by the choice of boundary conditions.

In addition, the windfield was directly decomposed into its rotational and divergent components using the method of Endlich (1967). This method does not require any assumption about the boundary conditions. The divergent wind vectors shown in the figures are not computed from χ but are those computed by the Endlich technique. The excellent agreement between the χ field and the divergent winds over the entire grid gives confidence in the accuracy of the computations.

3. DISCUSSION

The winter (DJF) mean nine-year data (Figs. A1 - A3) are in reasonable agreement with the data of Yu et. al. (1983), Wright et. al. (1985) and Newell et. al. (1974). The familiar features of all these data compilations are prominent in the present work. The Aleutian and Icelandic lows, the subtropical highs, the Siberian anticyclone and the west Australian heat low are all apparent. The χ field shows a broad band of equatorial convergence, with maxima over South America, Africa and a zonally elongated

maxima centered on New Guinea. These features are consistent with the tropical outgoing longwave radiation (OLR) data, (Boyle and Chang, 1984). However, the South Pacific convergence zone (SPCZ) which is in evidence in the OLR data does not appear to be a distinct feature in the surface χ field.

Figure 1 is a time, longitude plot of χ winter, seasonal anomalies along the Equator. The sense of anomalies is that positive anomaly maxima imply convergence relative to the mean. The largest anomalies are found in the winters of 1981/82 and 1982/83, evidently in association with the strong ENSO event. These data indicate that one of the largest anomalies of 82/83 occurs over Africa (00 to 30°E). The relative suppression of convection west of 150°E and enhancement to the east, seen in the OLR anomalies, is also suggested by the χ field. However, examination of the anomalies do not indicate as strong a relationship between the χ_{sfc} and the OLR anomalies as exhibited between the χ_{200mb} and OLR anomalies, Boyle and Chang (1983).

Further overviews of the interannual, seasonal variations are provided by Figs. II, III and IV. These are time, longitude plots of surface wind winter season anomalies along 40°N, 20°N and the Equator. In Fig. II the 82/83 ENSO event is prominent, with very large westerly anomalies around the dateline. The subtropical flow of Fig. III indicates a change in the zonal flow regime from the 78/79 winter to the 79/80 winter, probably a reflection in a shift in the position/strength of the subtropical anticyclone. The midlatitude flow in Fig. IV has the largest variations in the Pacific circulation; the strong variability is also seen in the data of Wright et. al. (1985). The large variations from 60°E to 90°E are in a region of very high terrain and thus, are of uncertain value.

REFERENCES

Boyle, J. S. and C.-P. Chang, 1984: Monthly and seasonal climatology over the global tropics and subtropics for the decade 1973 to 1983. Vol. I: 200 mb winds. Tech. Rep. NPS-63-84-006, Dept. of Meteorology, Naval Postgraduate School, Monterey, CA 93943, 172 pp.

Boyle, J. S. and C.-P. Chang, 1984: Monthly and seasonal climatology over the global tropics and subtropics for the decade 1973 to 1983. Vol. II: Outgoing longwave radiation. Tech. Rep. NPS-63-84-006, Dept. of Meteorology, Naval Postgraduate School, Monterey, CA 93943, 112 pp.

Cressman, G. P., 1959: An operational objective analysis system. *Mon. Wea. Rev.*, **87**, 367-374.

Eindlich, R. M., 1967: An iterative method for altering the kinematic properties of wind fields. *J. Appl. Meteor.*, **6**, 837-844.

Fu, C., J. Fletcher and R. Slutz, 1983: The structure of the Asian monsoon surface wind field over the ocean. *J. Clim. Appl. Met.*, **22**, 1242-1252.

Grayson, T. H., 1971: Global band sea level pressure and surface wind analysis. Fleet Numerical Weather Central Tech. Note 71-3, 22pp. Available from Librarian, Fleet Numerical Oceanography Center, Monterey, CA 93943

Krishnamurti, T. N., H.-L. Pan, R. Pasch and D. Subrahmanyam, 1983: Interannual variability of the tropical motion field. FSU Report No. 83-3, Department of Meteorology, Florida State University, Tallahassee, Florida 32306.

Lewis, J. M., 1972: An operational upper air analysis using the variational method. *Tellus XXIV*, **6**, 514-530.

Lewis, J. M. and T. H. Grayson, 1972: The adjustment of surface wind and pressure by Sasaki's variational matching technique. *J. Appl. Meteor.*, **11**, 586-597.

Newell, R.E., J. W. Kidson, D. G. Vincent and G. J. Boer, 1974; *The General Circulation of the Tropical Atmosphere* vol. 2. Massachusetts Institute of Technology, Boston, MA 02139, 371pp.

Oort, A. H., 1983: Global atmospheric circulation statistics, 1958 - 1973. NOAA Professional Paper 14. U. S. Department of Commerce (available from the Superintendent of Documents, U. S. Government Printing Office, Washington, D. C. 20402

Shukla, J. and K. R. Saha, 1974: Computation of non-divergent streamfunction and irrotational velocity potential from the observed winds. *Mon. Wea. Rev.*, **102**, 419-425.

Wright, P. B., T. P. Mitchell and J. M. Wallace, 1985: Relationships between surface observations over the global oceans and the southern oscillation. NOAA Data Report IRI. PMEL-12, Pacific Marine Environmental Laboratory, Seattle, Washington, 61pp.

FIGURE 1

Time versus longitude plot of winter season anomalies of surface velocity potential averaged from 5°N to 5°S about the Equator. The ordinate labels refer to the year of the January of the winter involved. The contour interval is $0.25 \times 10^6 \text{ ms}^{-2}$. Dashed lines are negative, solid lines are positive values. The zero contour is suppressed.

FIGURE II

(a) As in Fig. 1 except for the zonal wind component. The contour interval is 0.25 ms^{-1}
(b)
As in (a) except for the meridional wind component.

FIGURE III

As in Fig. II except the reference latitude is 20°N .

FIGURE IV

As in Fig. II except the reference latitude is 40°N .

FIGURES A1 - A3

Nine winter season (1974/75 - 1982/83) mean circulation fields at the surface. Variables displayed are wind vectors and isolachs streamfunction, and velocity potential. Contour interval for the streamfunction is $2.0 \times 10^6 \text{ m}^2 \text{s}^{-1}$, for the velocity potential it is $1.0 \times 10^6 \text{ m}^2 \text{s}^{-1}$, and for the isolachs it is 2.5 ms^{-1} . The vector scale is given in the upper right portion of the wind vector isolach plots. The grid intervals of the INOC Global Band Analysis mercator grid are shown on the left hand side and bottom of each figure. The longitude grid is marked every 30° from the Greenwich meridian on the extreme left and the latitude is marked every 10° from 40°S at the bottom of the figure. The black dots on the wind vector plots indicate terrain heights greater or equal to 1000 m, smoothed to the GBA grid. The contour plots use the convention that negative values are dashed, positive values are solid. Although the sign of the streamfunction and velocity potential has no meaning in itself, this plotting convention allows the principal maxima and minima in these fields to be more readily discerned.

FIGURES B1 TO B27

Individual winter season mean and deviation circulation fields at the surface for the winters from 1974/75 to 1982/83. The deviations are differences from the nine-year seasonal mean (Figs. A1 to A3). The figures are labeled with the year corresponding to the year of the January of the winter. Variables displayed are the wind vectors and isotachs, streamfunction, and velocity potential. For the mean fields the contour interval for the streamfunction is $2.0 \times 10^6 \text{ m}^2 \text{s}^{-1}$, for velocity potential it is $1.0 \times 10^6 \text{ m}^2 \text{s}^{-1}$, and for the isotachs it is 2.5 ms^{-1} . For the deviation fields the contour interval for the streamfunction is $1.0 \times 10^6 \text{ m}^2 \text{s}^{-1}$, for velocity potential it is $1.0 \times 10^6 \text{ m}^2 \text{s}^{-1}$, and for the isotachs it is 1.5 ms^{-1} . On the deviation plots the contours corresponding to negative values are dashed, those corresponding to positive values are solid. The zero contour is not drawn. The vector scale is given in the upper right part of the wind vector plots.

FIGURES C1 TO C9

Nine year (1974 to 1983) monthly mean circulation fields at the surface. The months displayed are December, January and February. Variables displayed are the wind vectors and isotachs, streamfunction and velocity potential. The contour interval for the streamfunction is $2.0 \times 10^6 \text{ m}^2 \text{s}^{-1}$, for velocity potential it is $1.0 \times 10^6 \text{ m}^2 \text{s}^{-1}$, and for the isotachs it is 2.5 ms^{-1} . The vector scale is given in the upper right part of the wind vector plots.

FIGURES D1 TO D81

Individual monthly mean and deviation circulation fields at the surface for the months from December 1974 to February 1983. The deviations are differences from the nine-year monthly mean (Figs. C1 to C9). The months displayed are December, January, and February. Variables displayed are the wind vectors and isotachs, streamfunction, and velocity potential. For the mean fields the contour interval for the streamfunction is $2.0 \times 10^6 \text{ m}^2 \text{s}^{-1}$, for velocity potential it is $1.0 \times 10^6 \text{ m}^2 \text{s}^{-1}$, and for the isotachs it is 2.5 ms^{-1} . For the deviation fields the contour interval for the streamfunction is $1.0 \times 10^6 \text{ m}^2 \text{s}^{-1}$, for velocity potential it is $1.0 \times 10^6 \text{ m}^2 \text{s}^{-1}$, and for the isotachs it is 1.5 ms^{-1} . On the deviation plots the contours corresponding to negative values are dashed, those corresponding to positive values are solid. The zero contour is not drawn on the deviations. The vector scale is given in the upper right part of the wind vector plots.

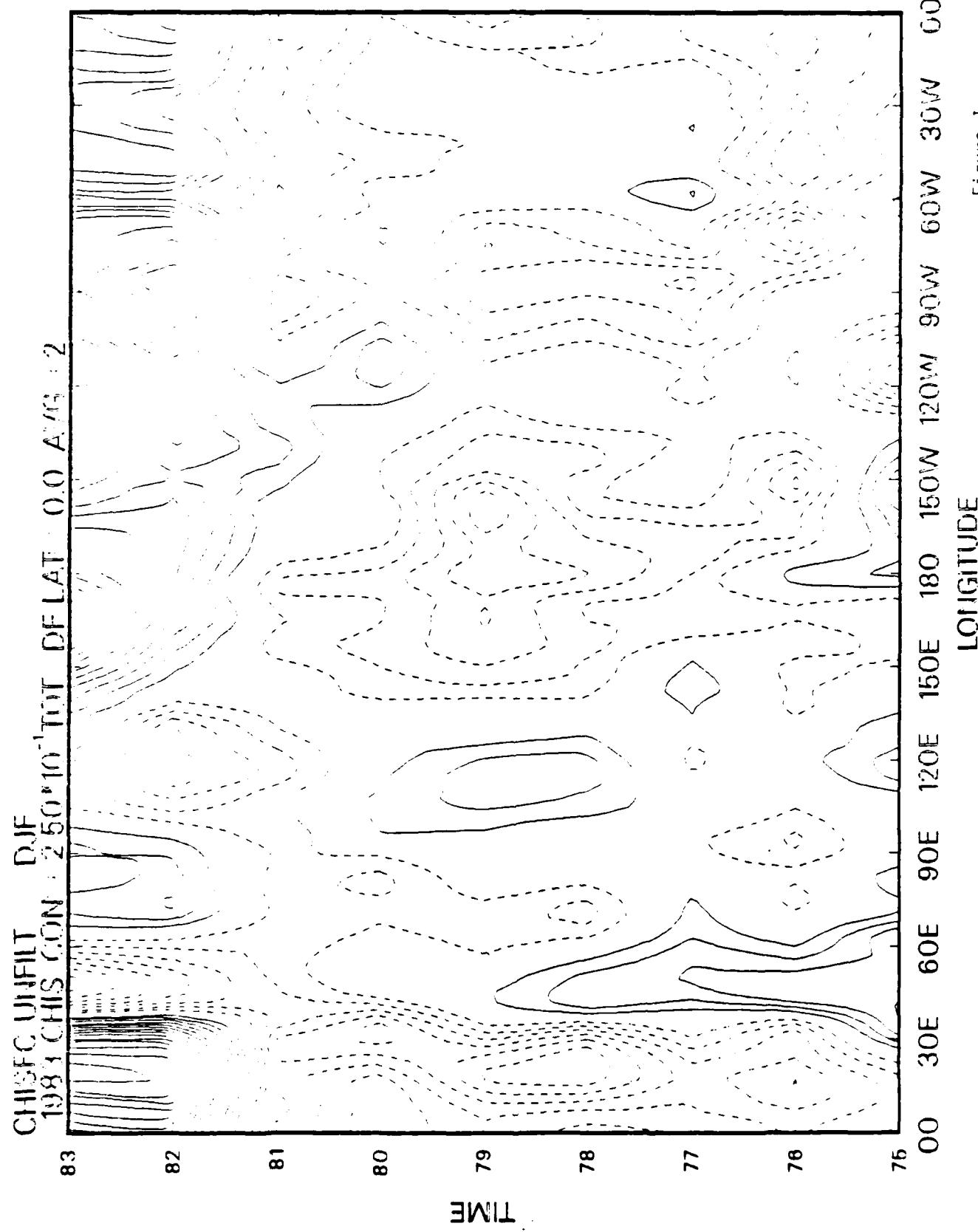


Figure 1

USFC UNFI DIF
1983 USFC CON : 2 50*10⁻¹TOR DF LAT: 0.0 AVG: 2

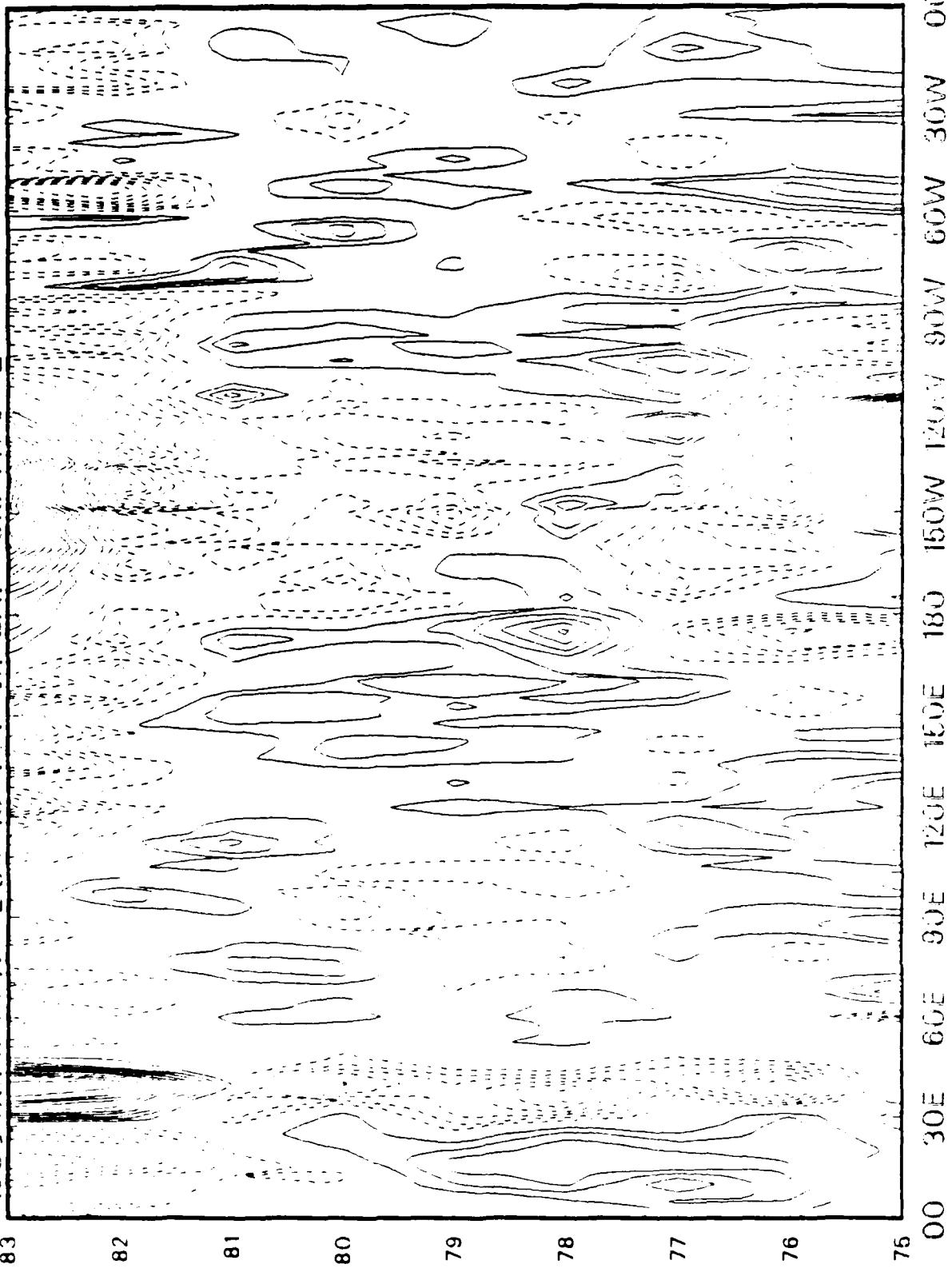


Figure 11a

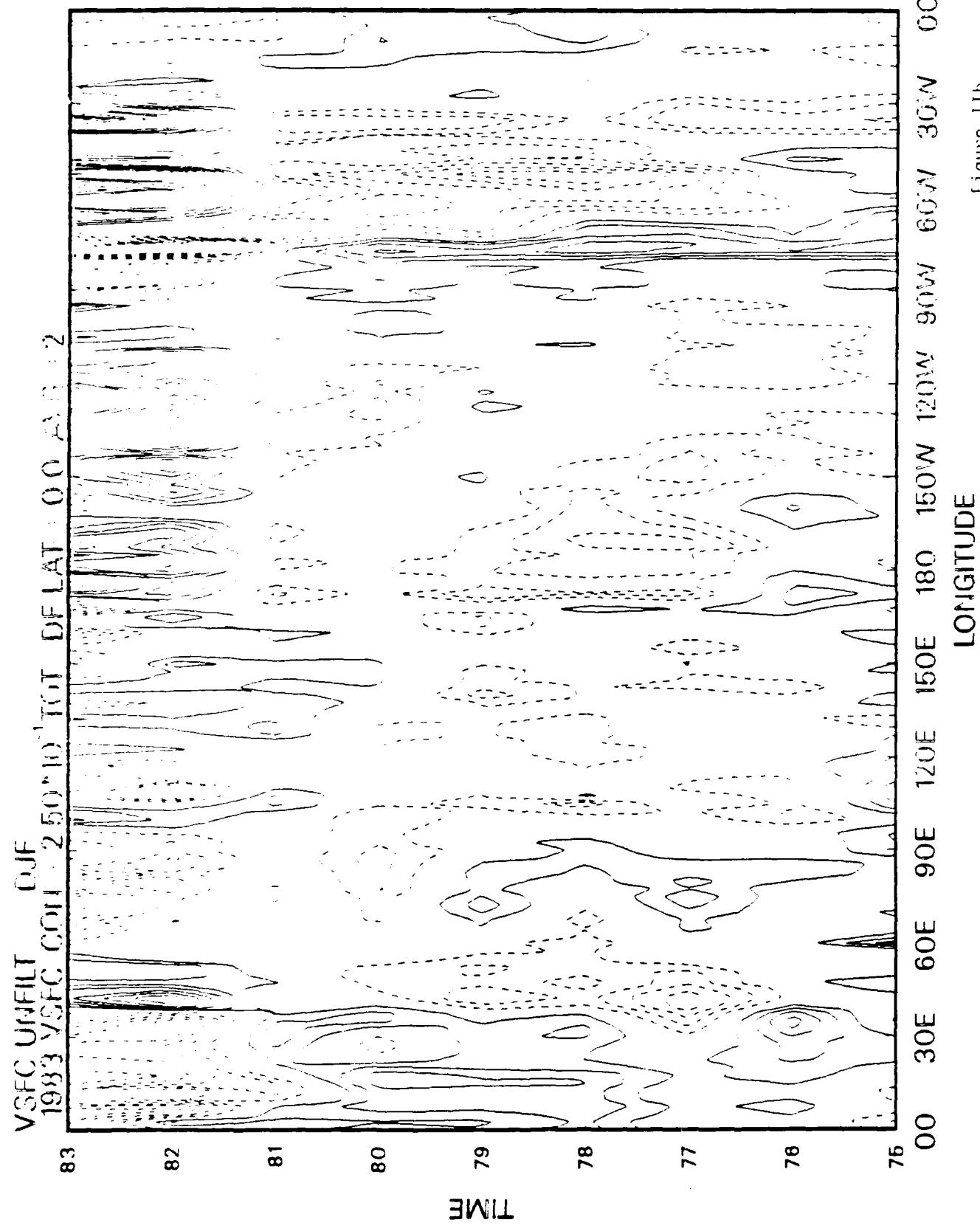


figure 11b

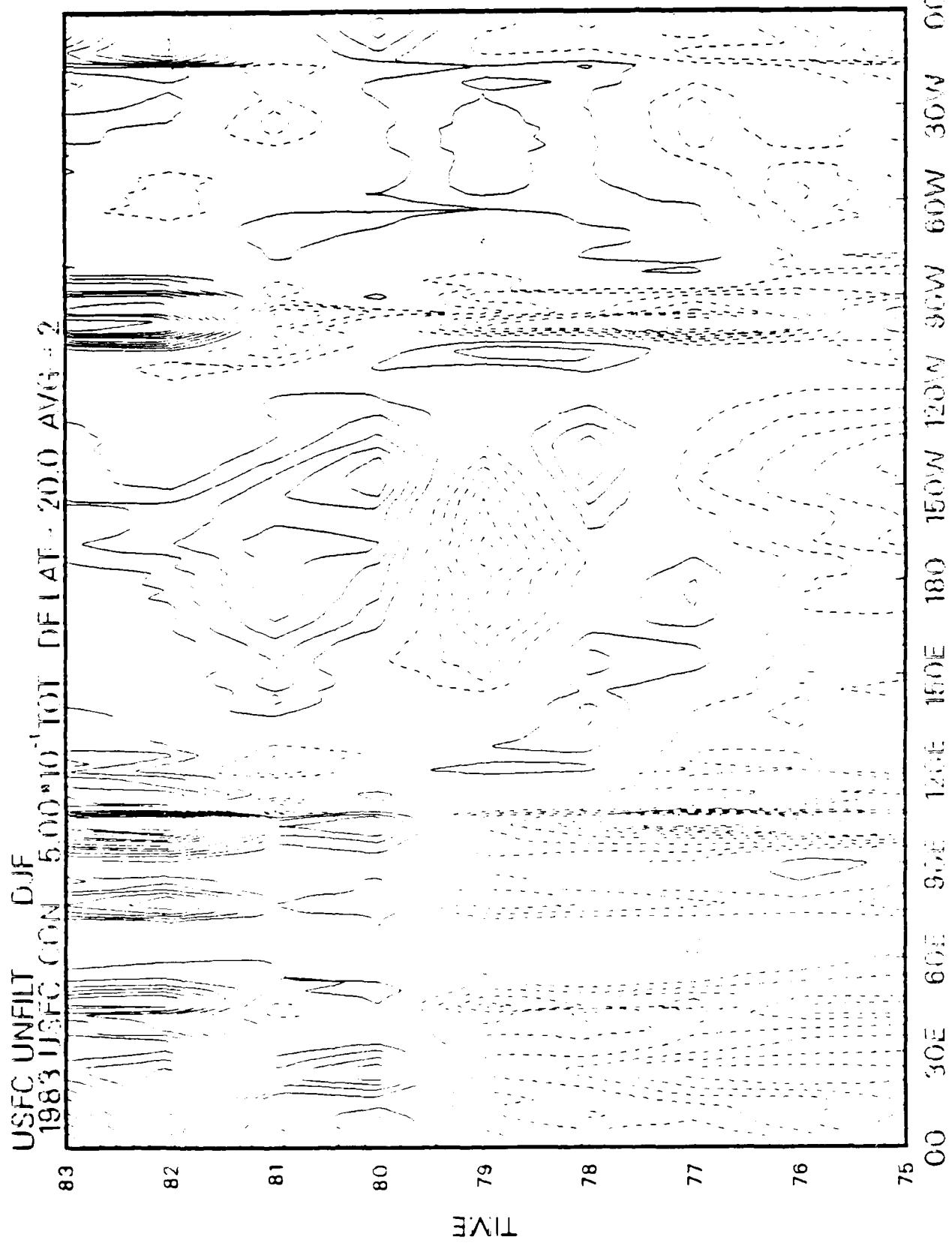


Figure IIIa

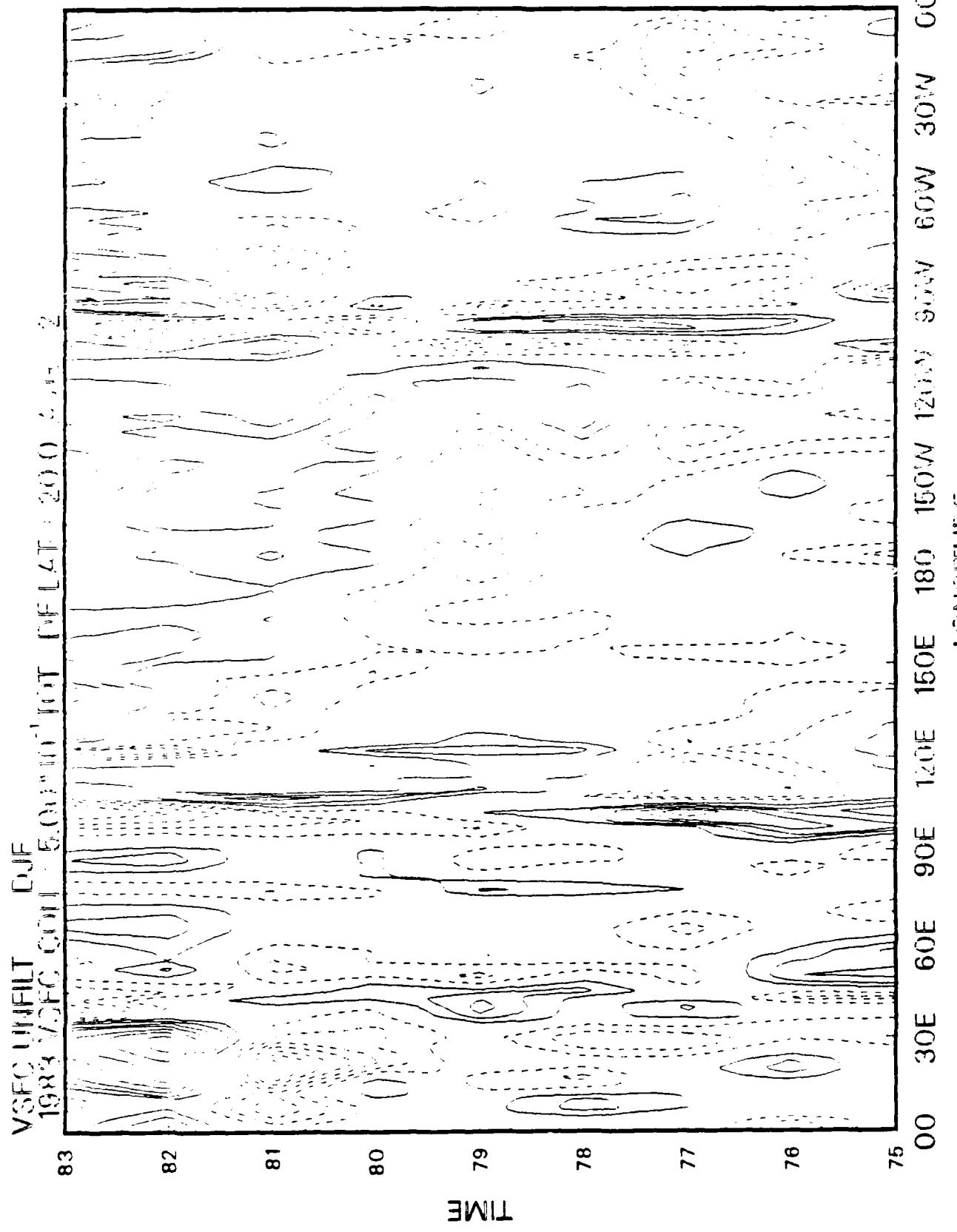


figure IIIb

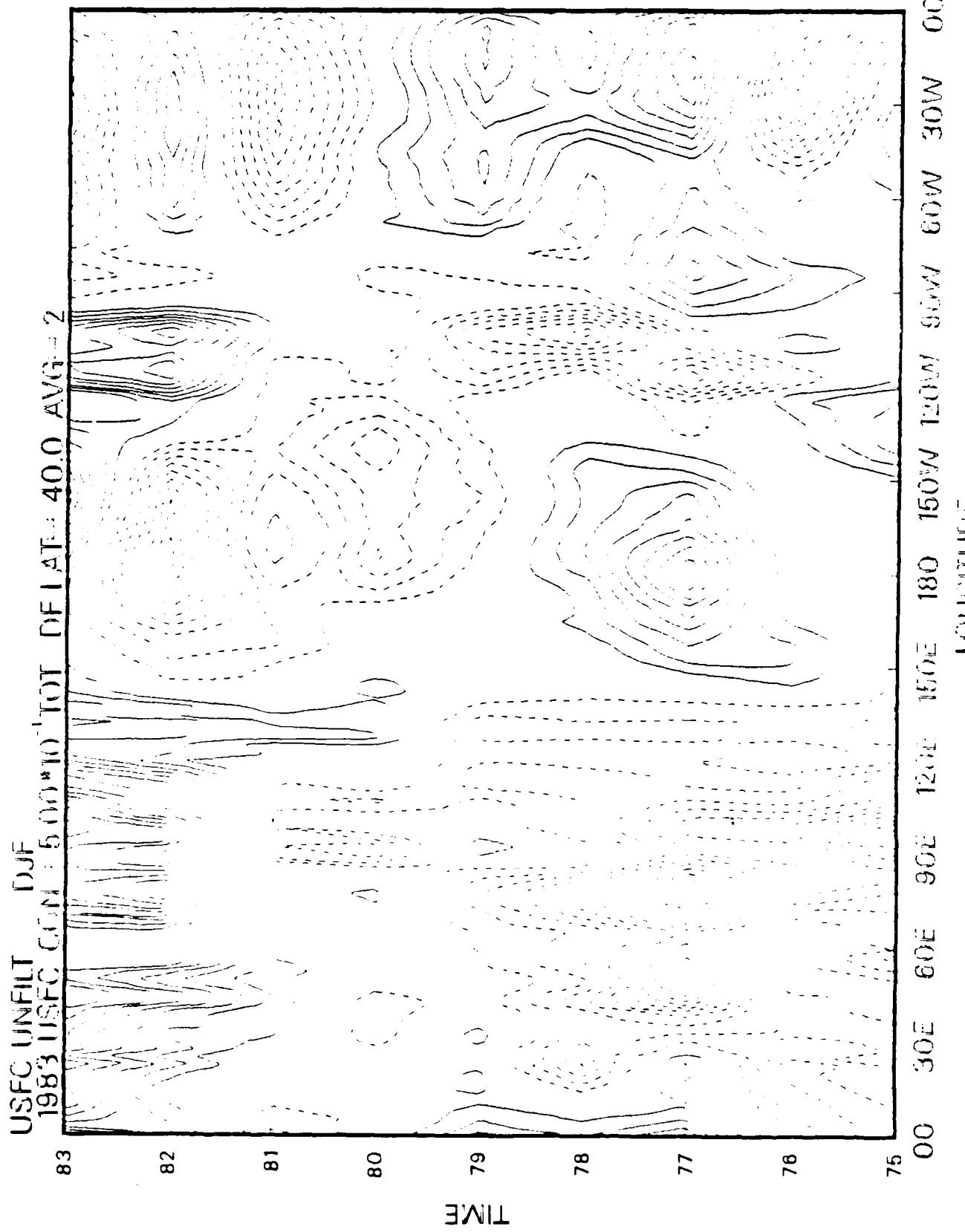


Figure IVa

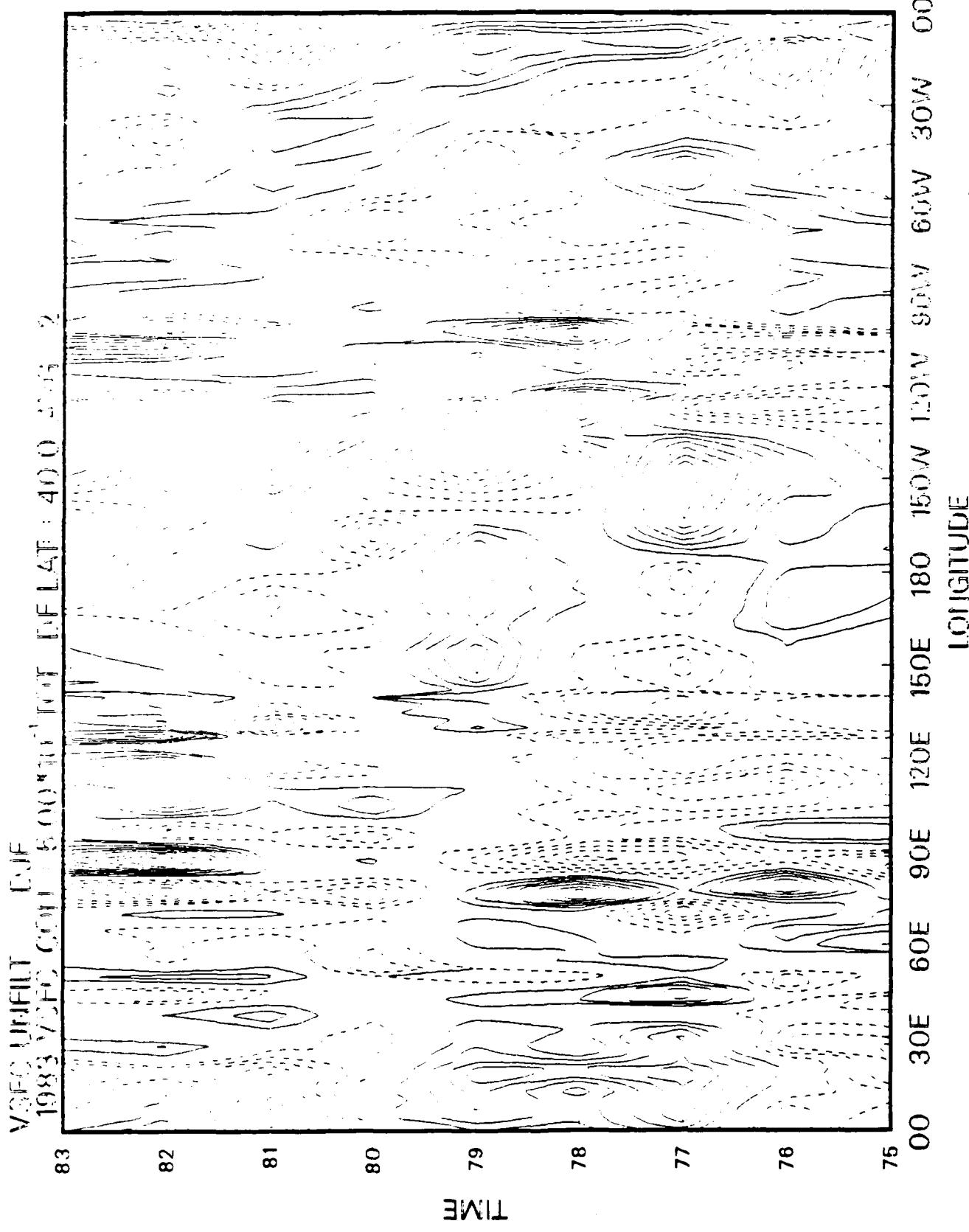
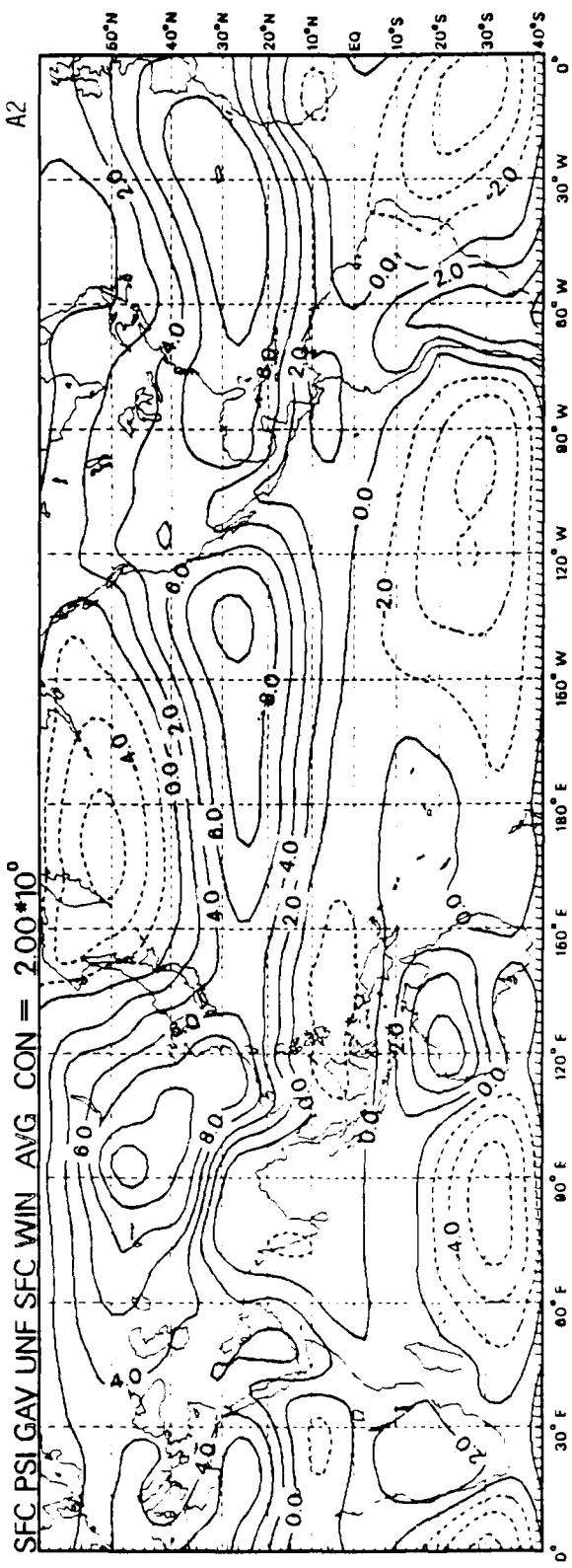
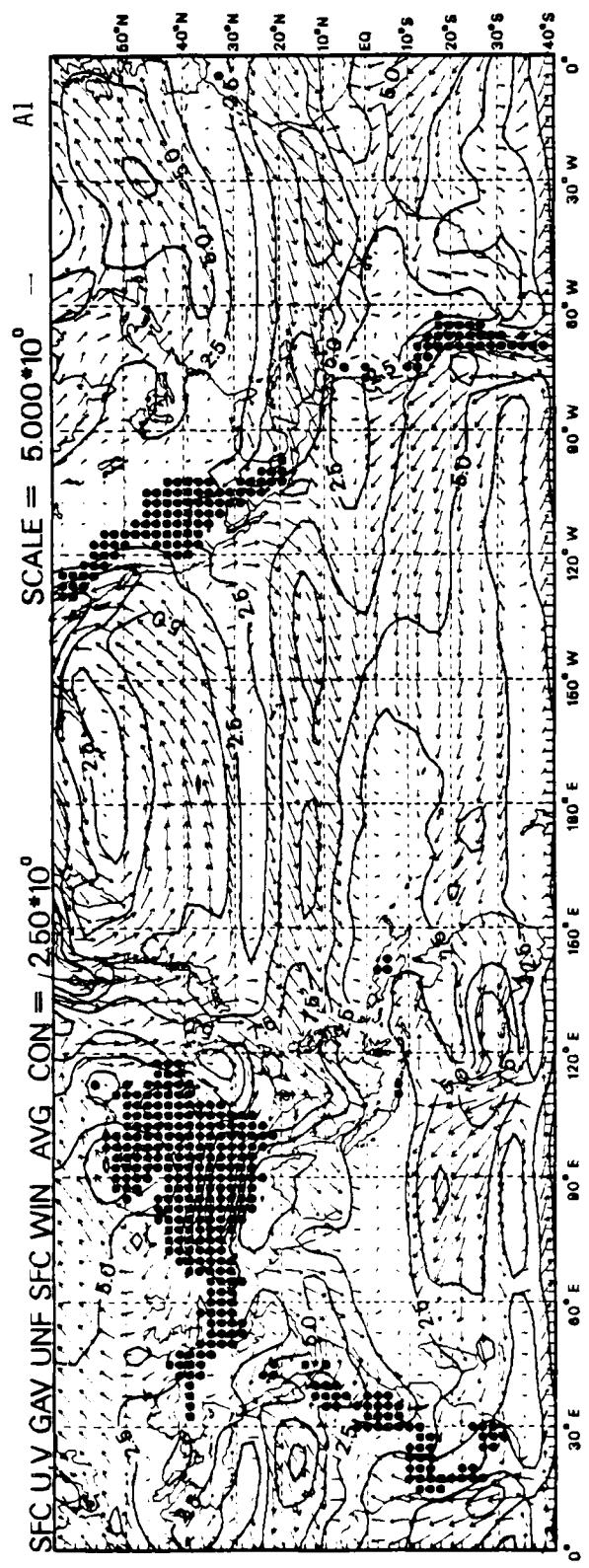
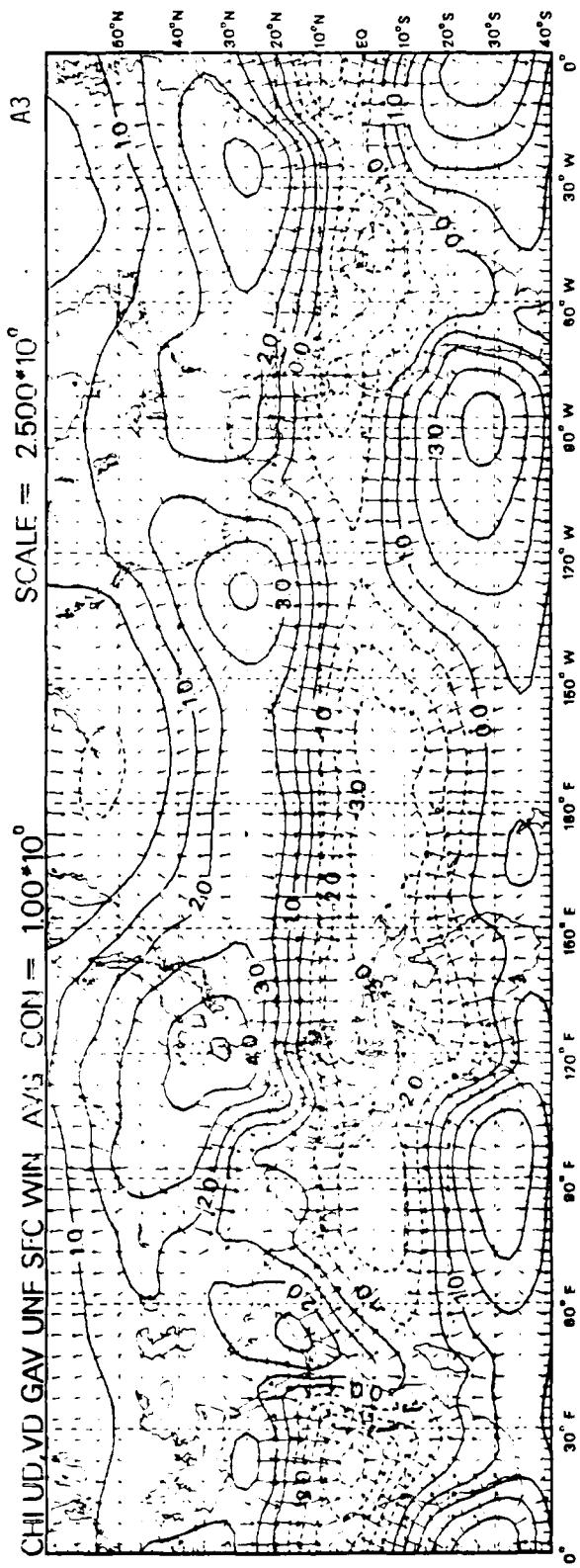
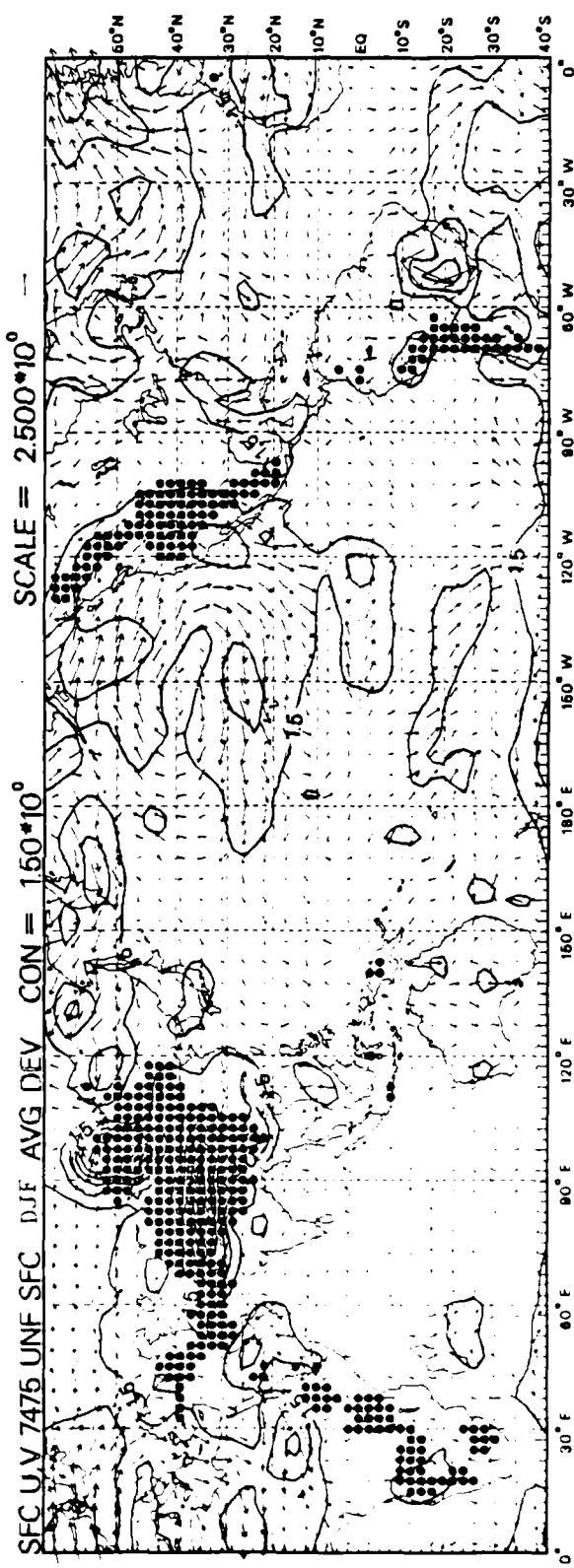
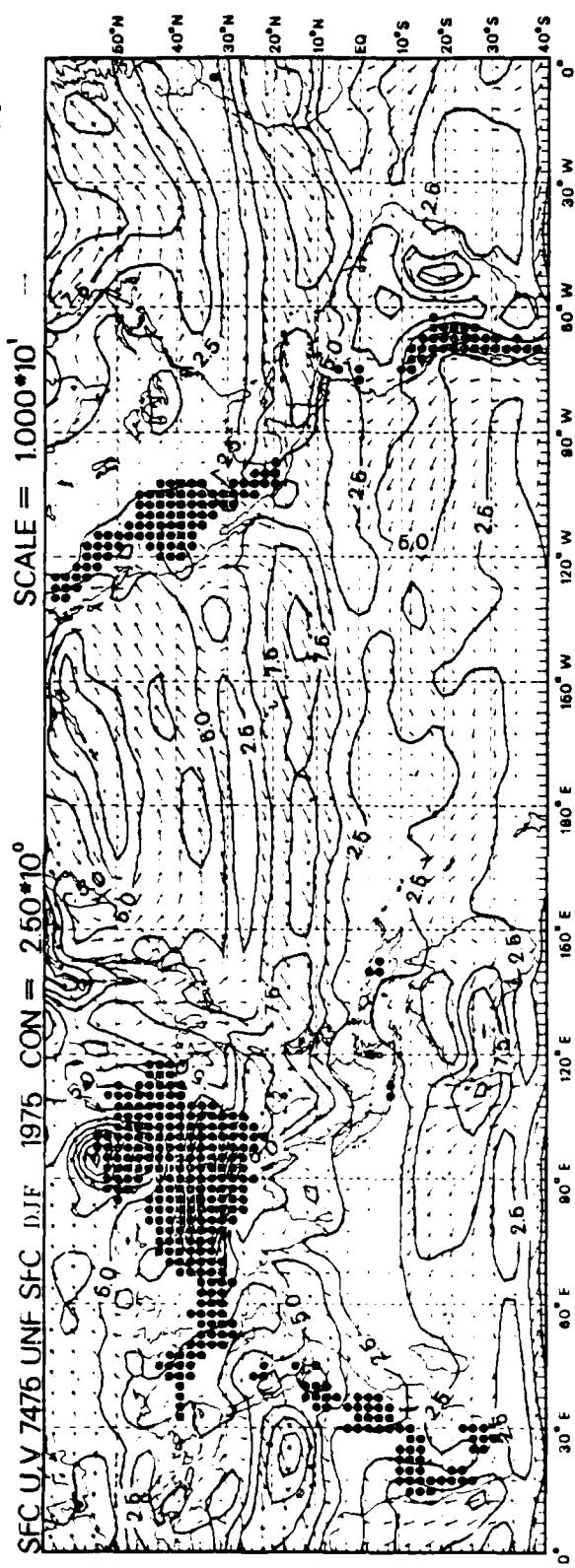


Figure IVb

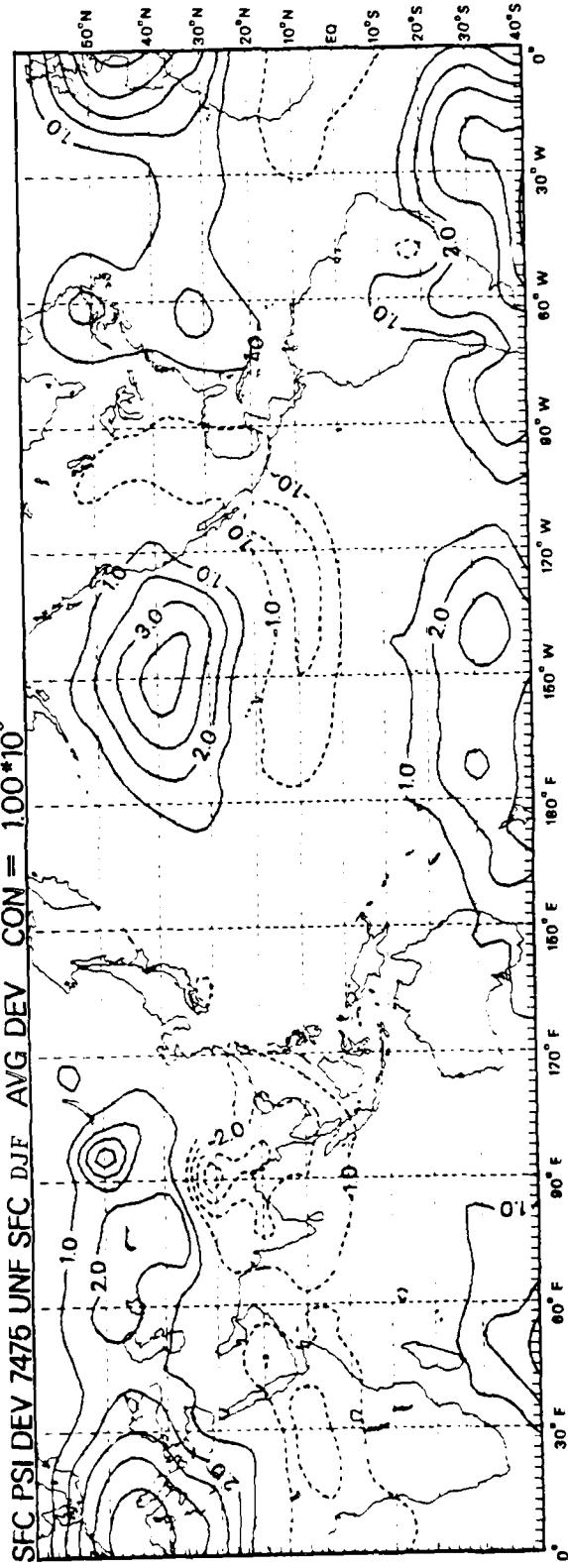
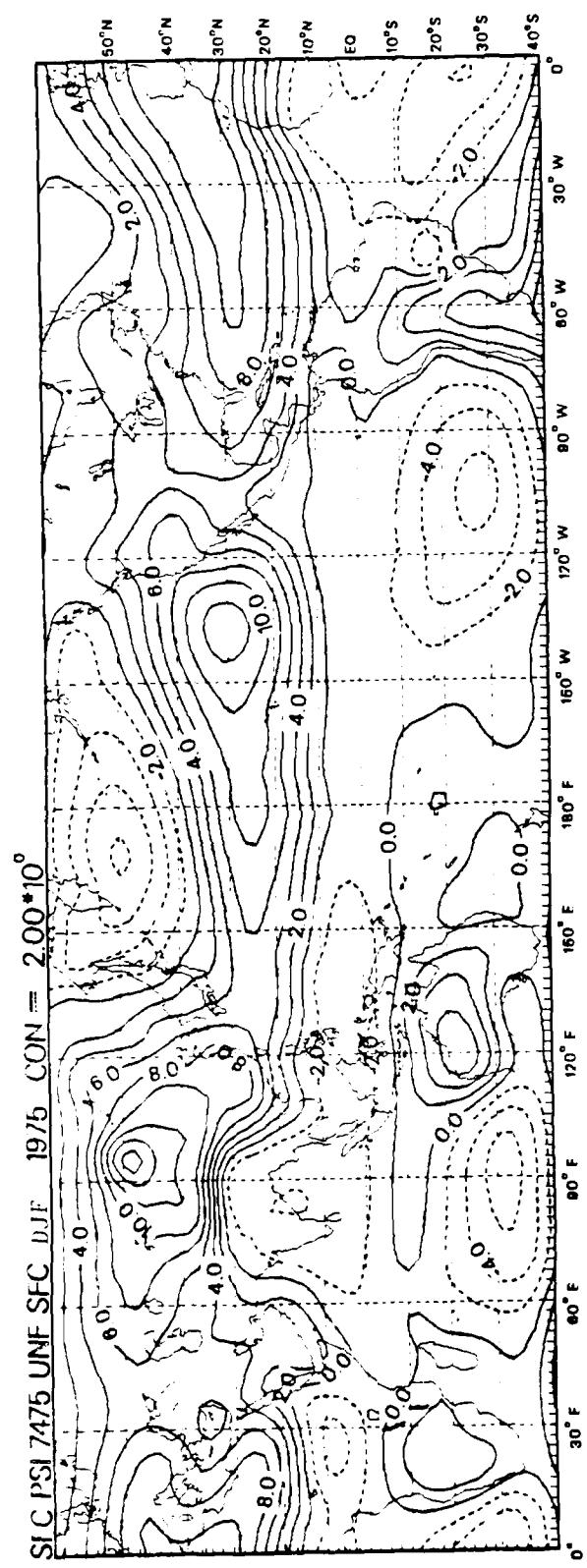




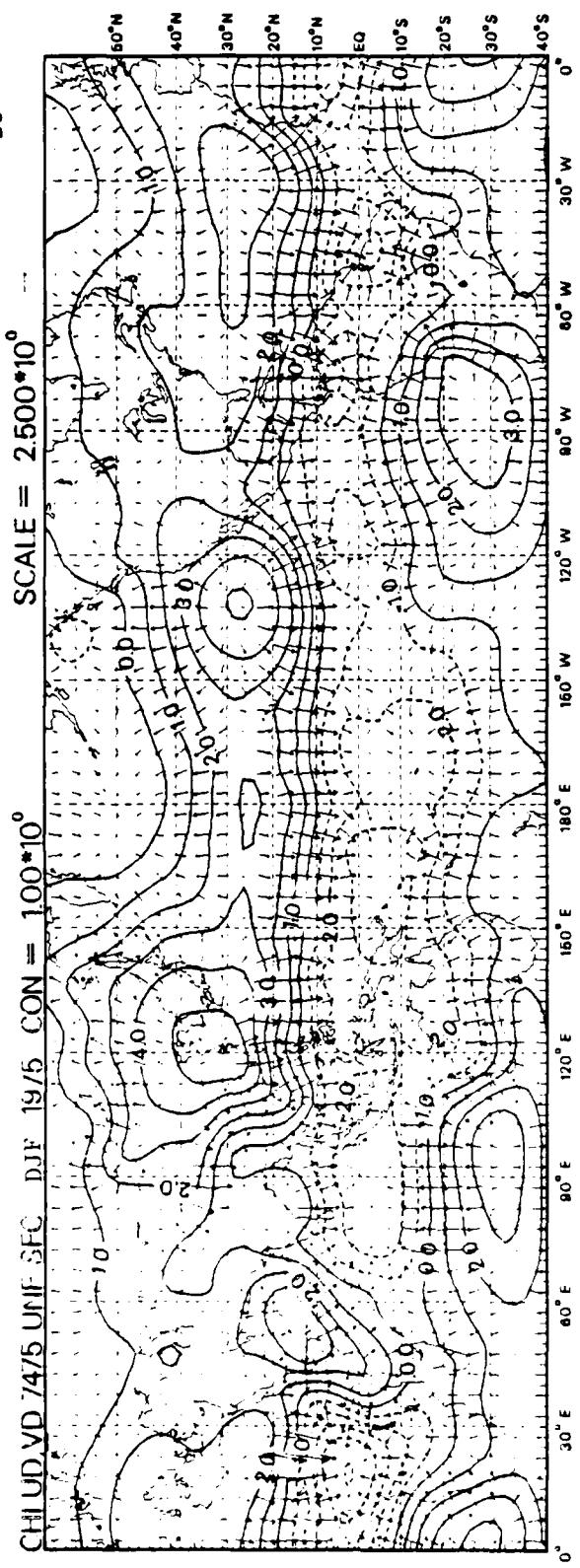
B1

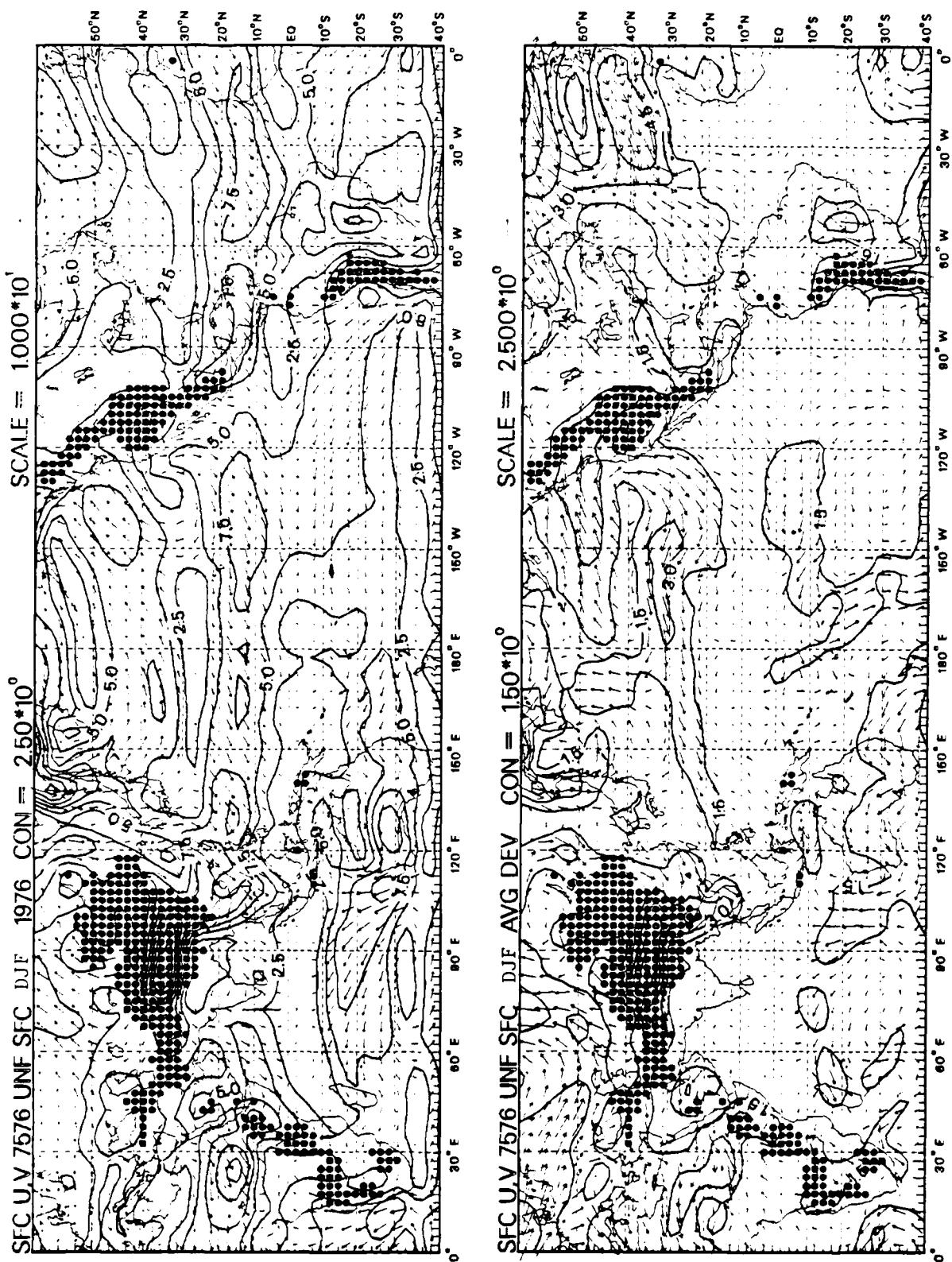


B2

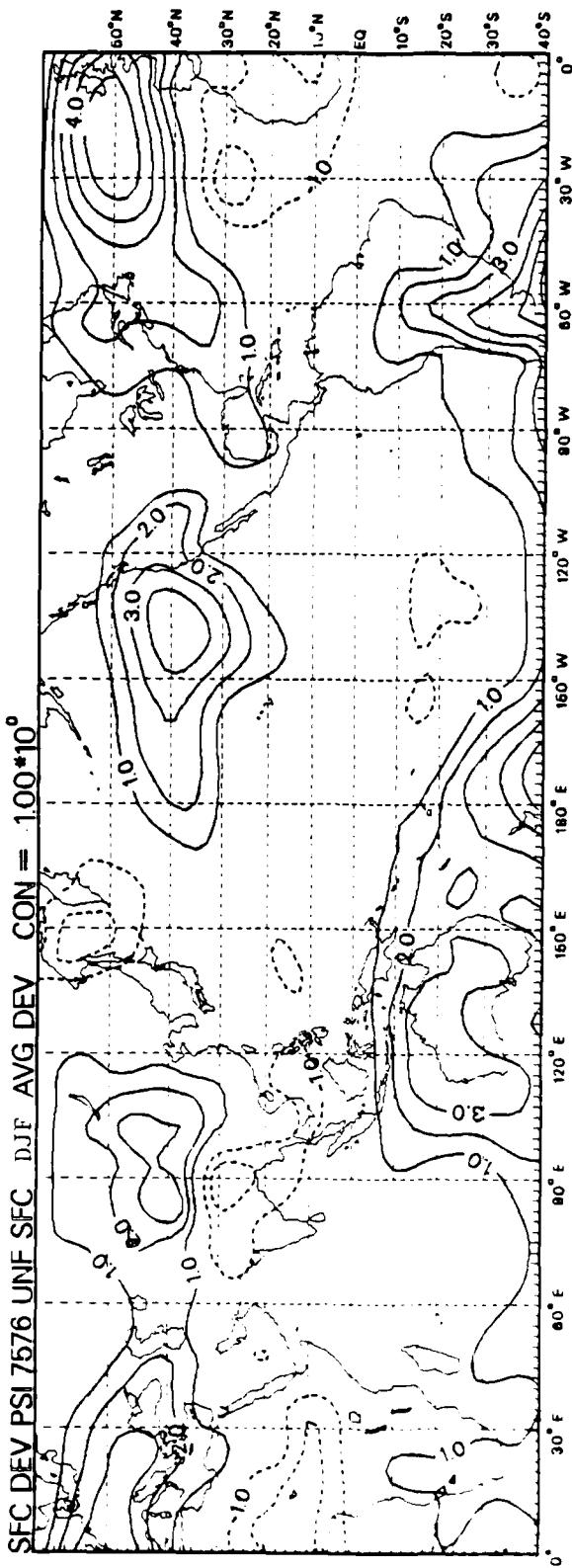
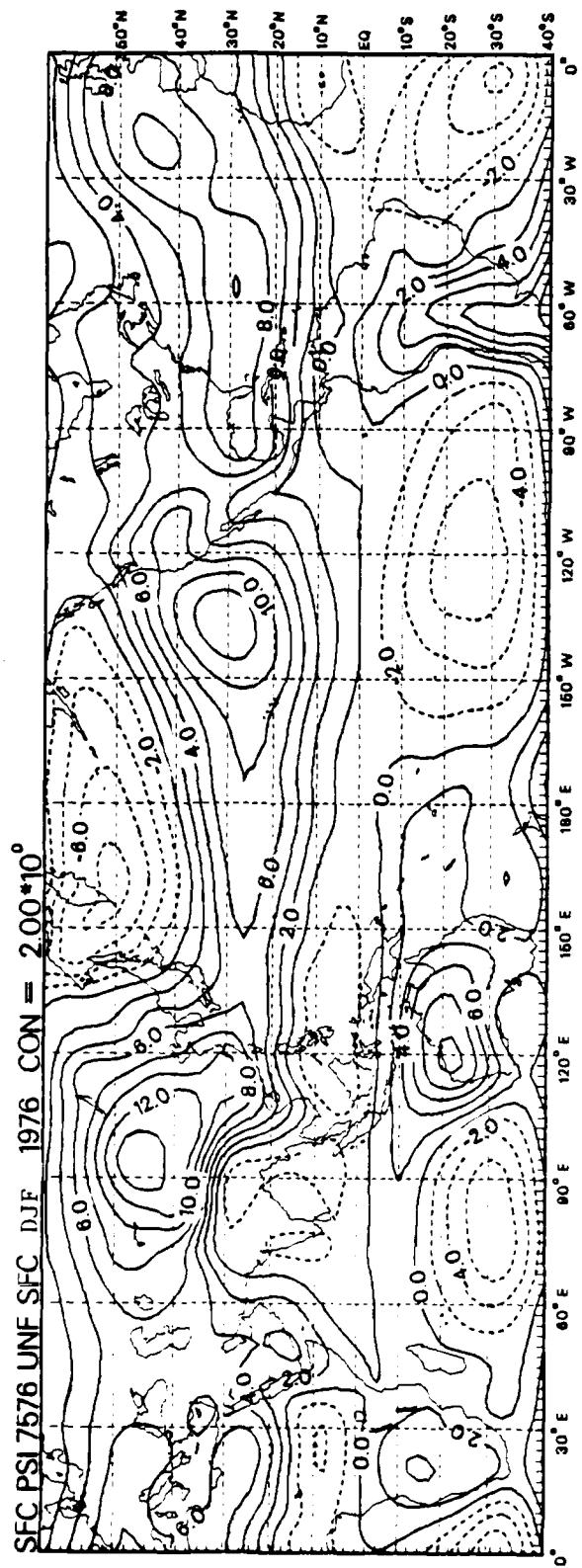


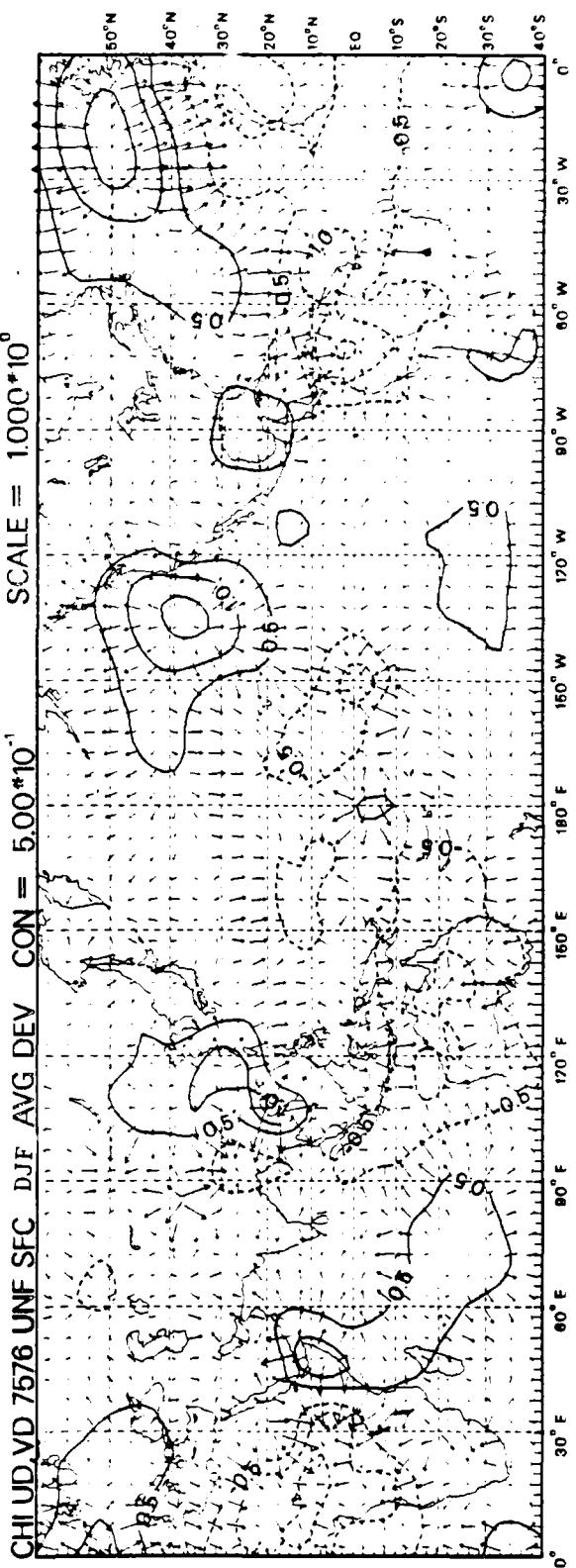
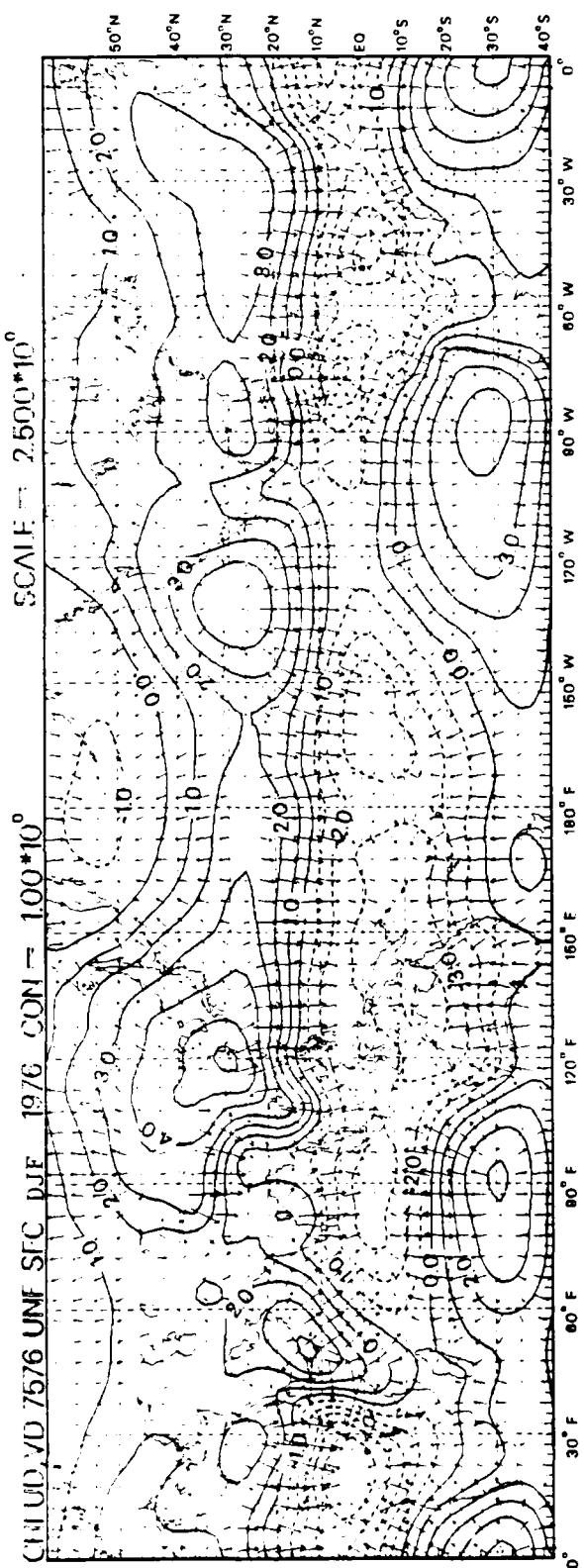
B3

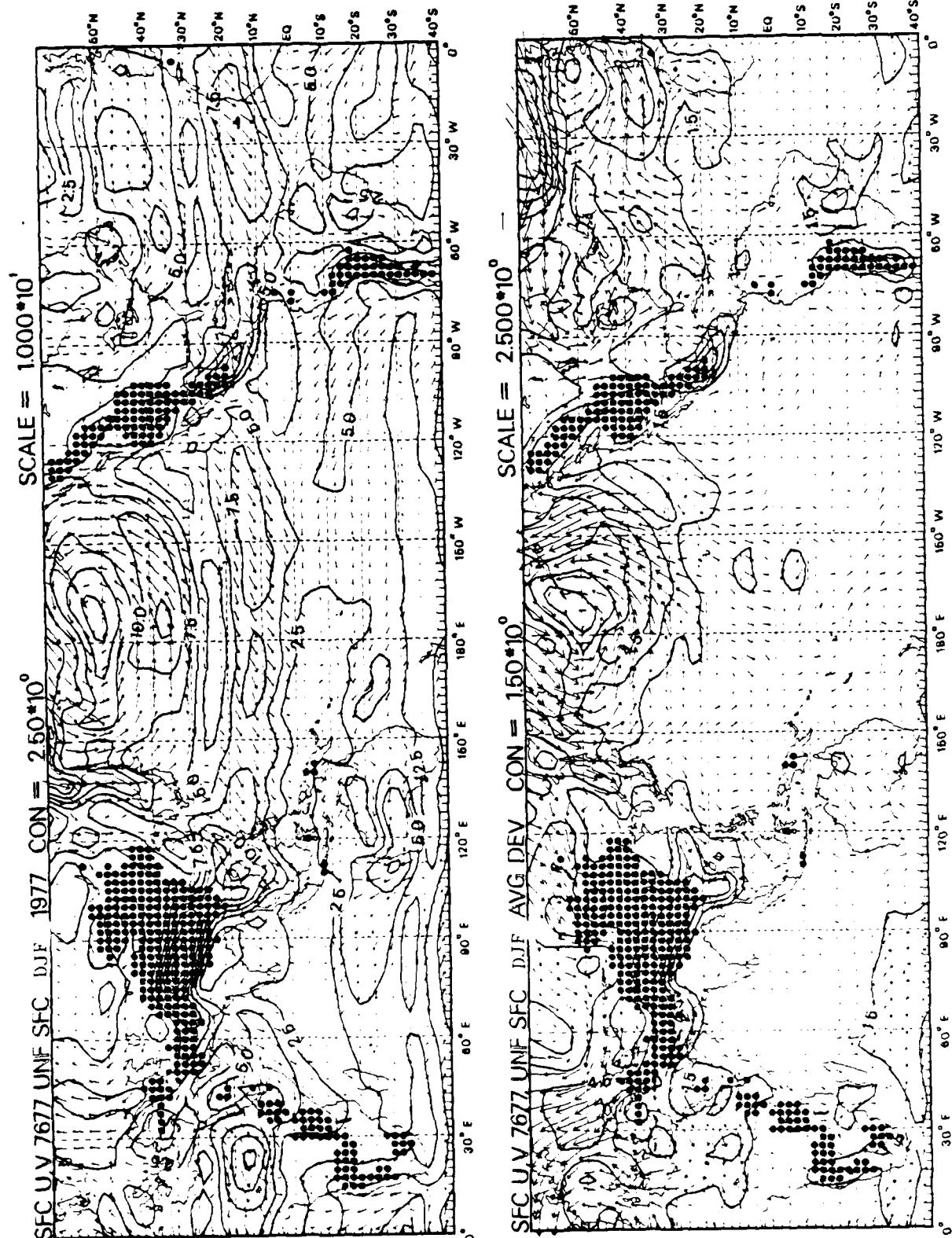


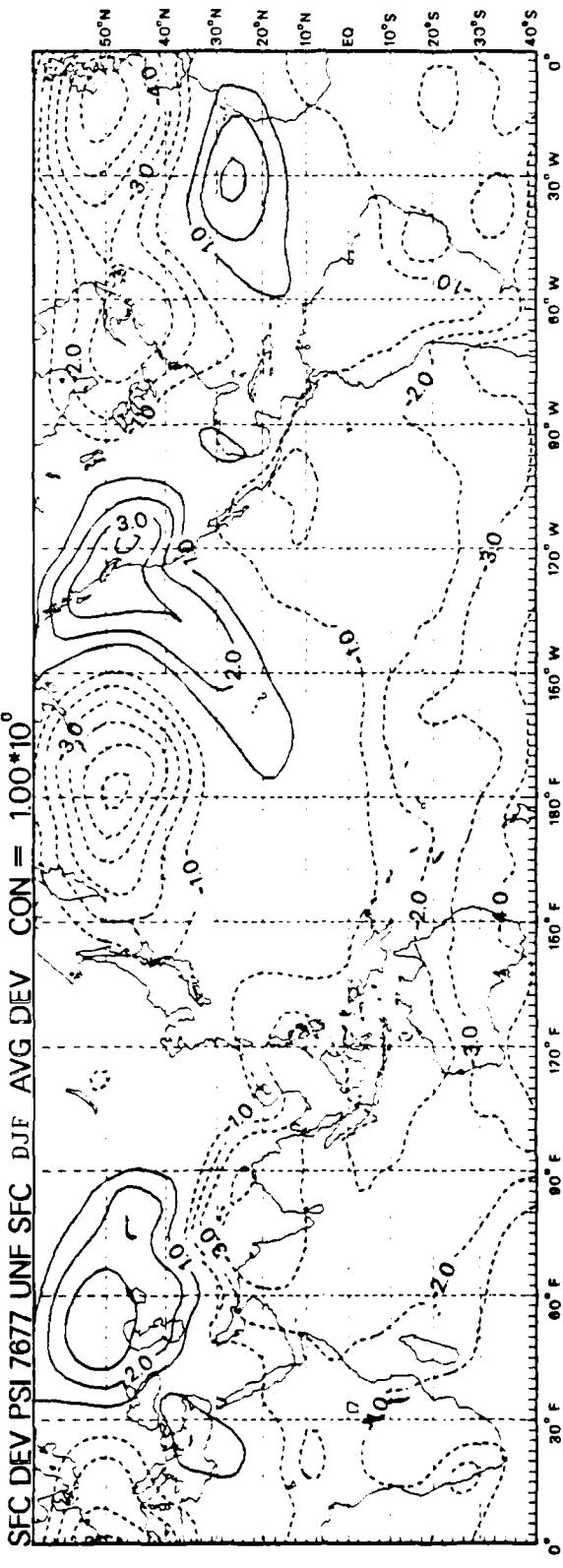
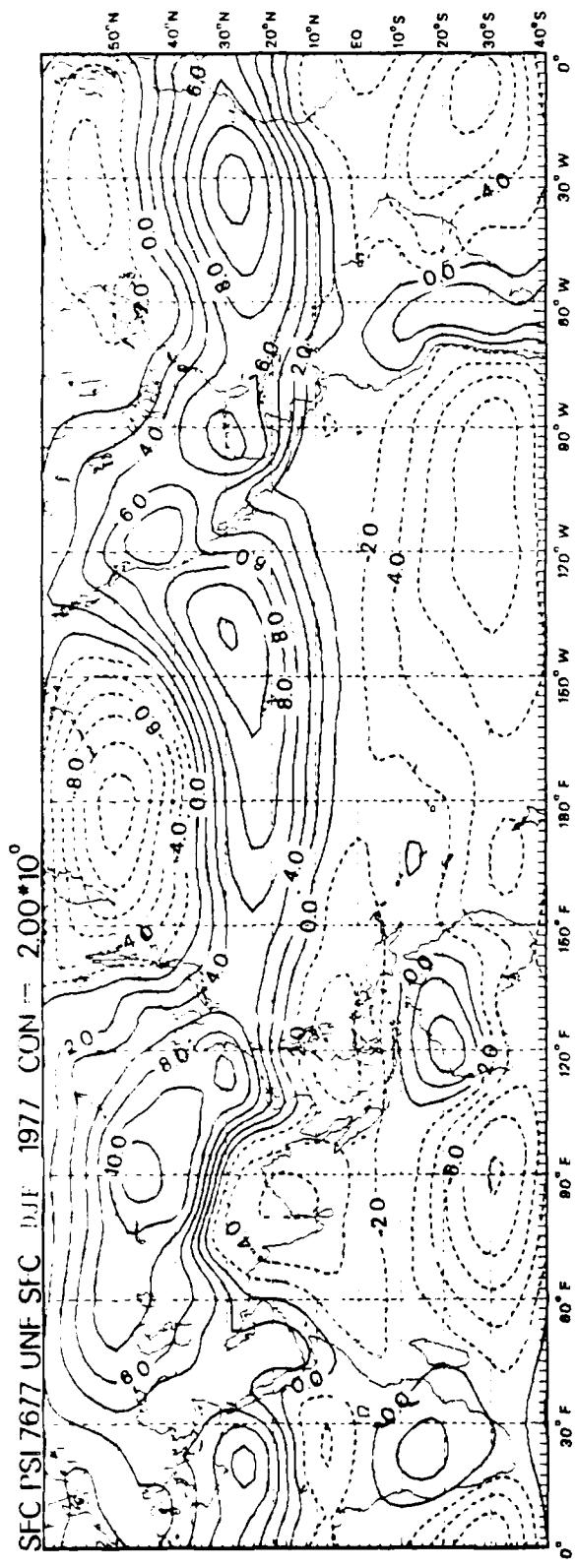


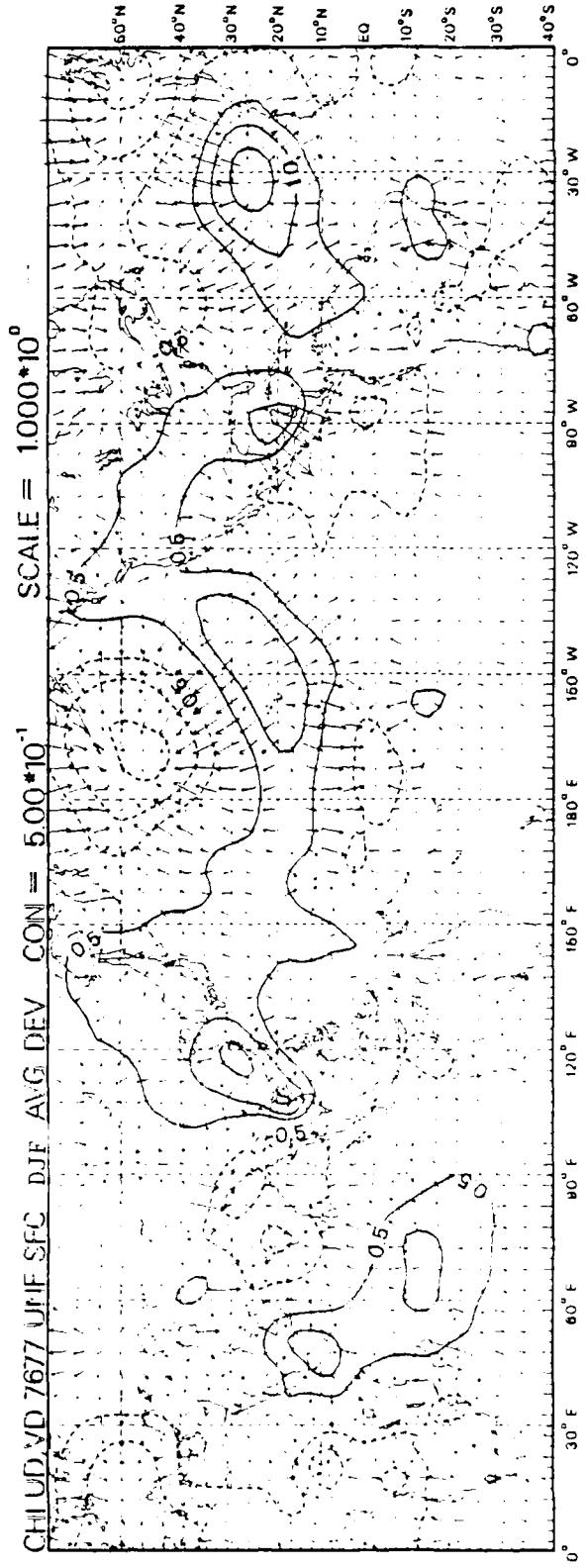
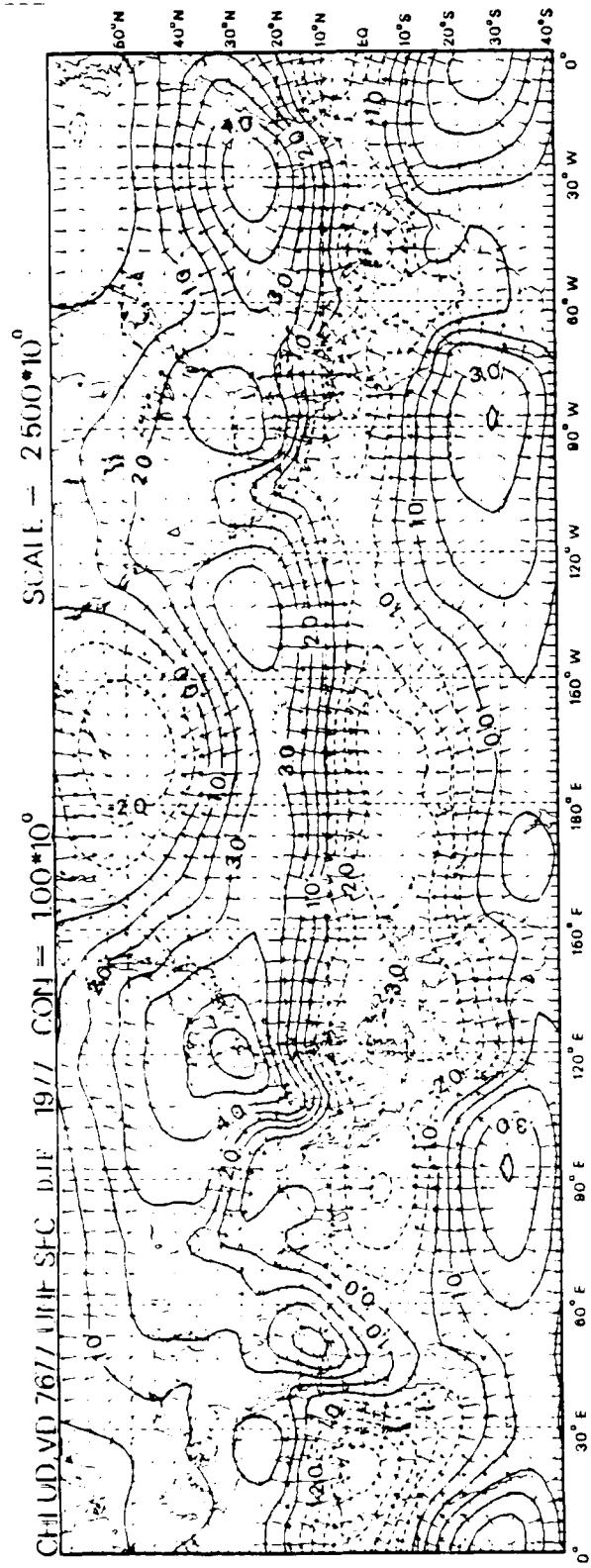
B5

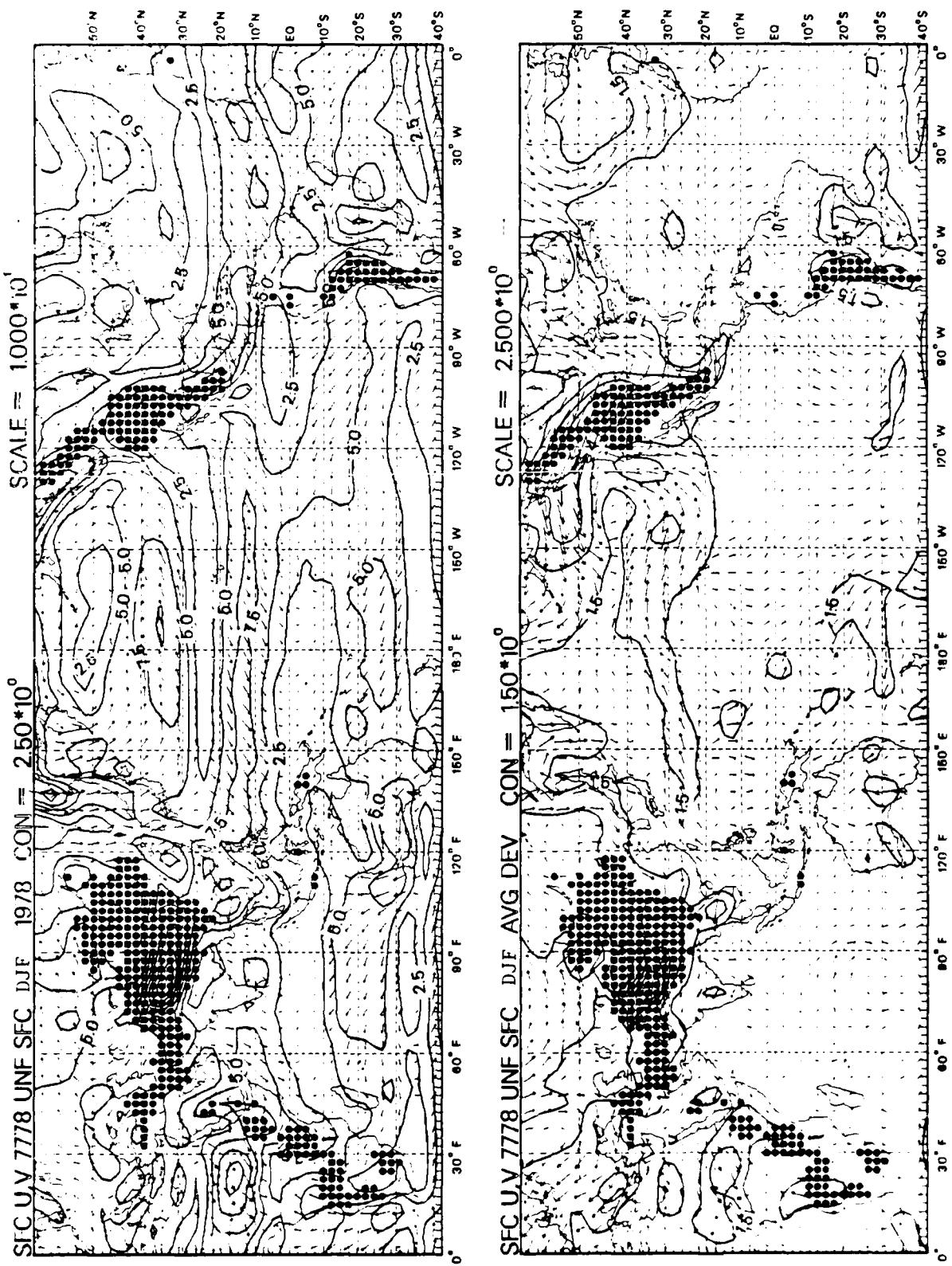




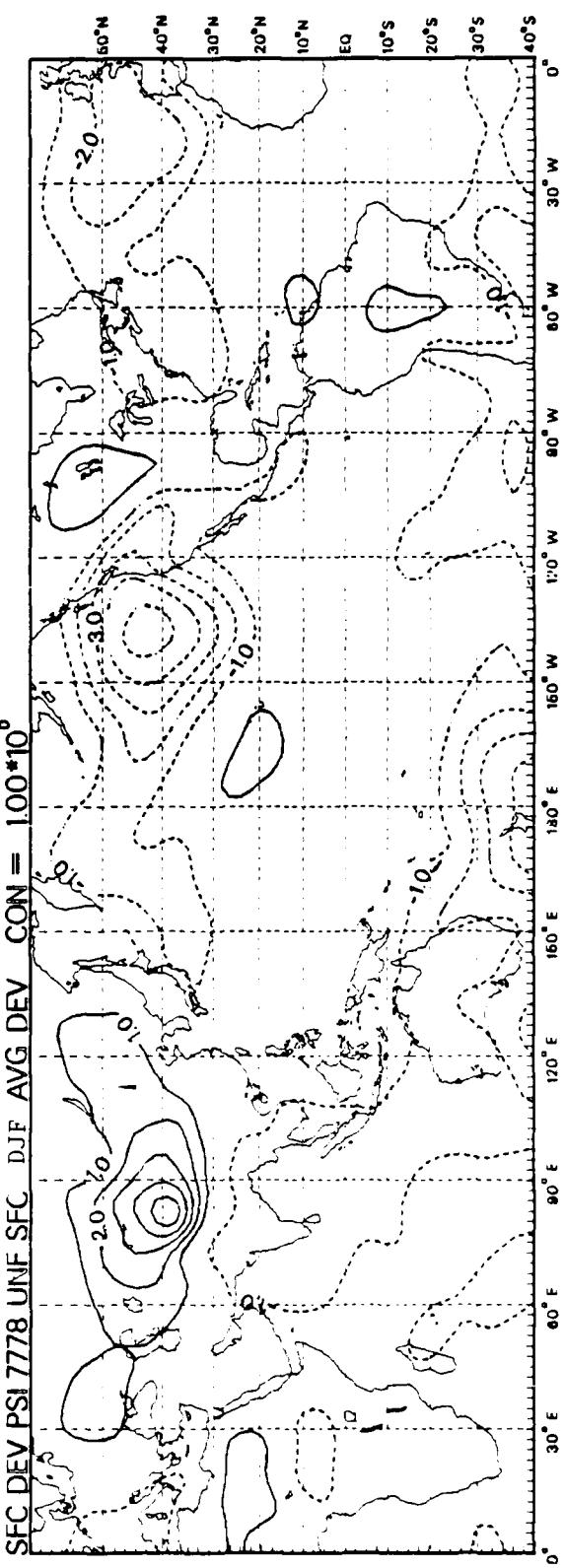
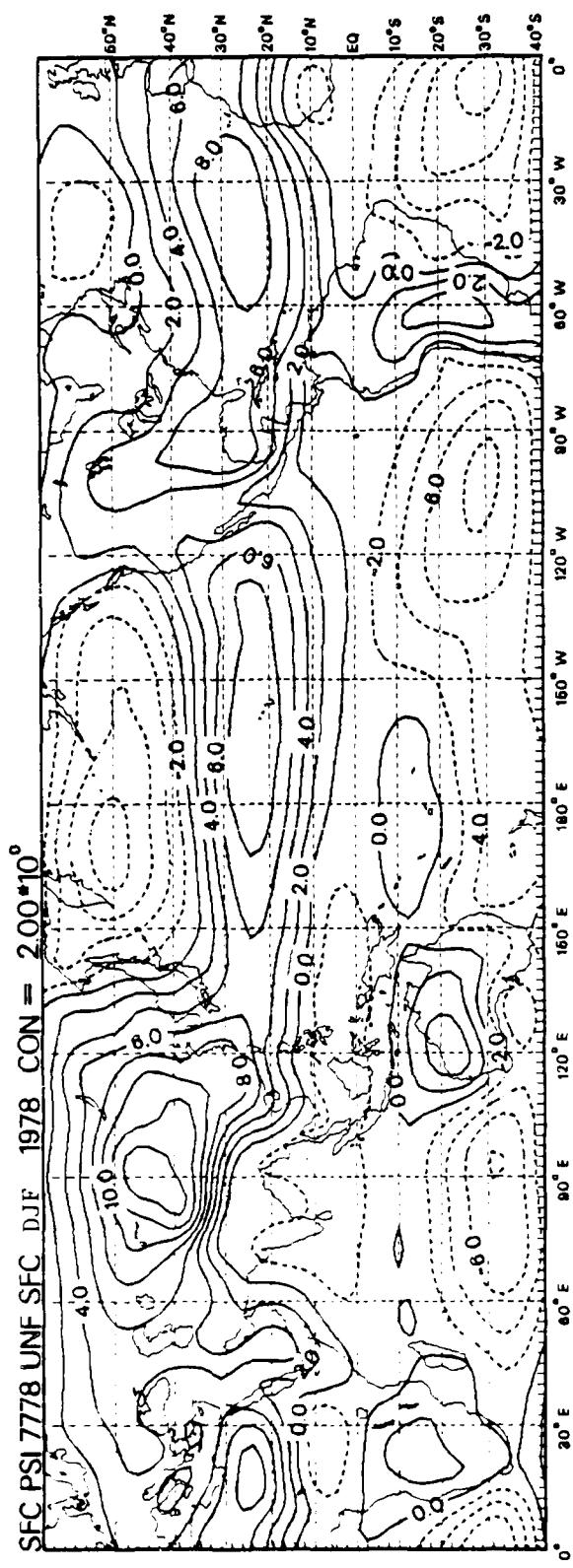




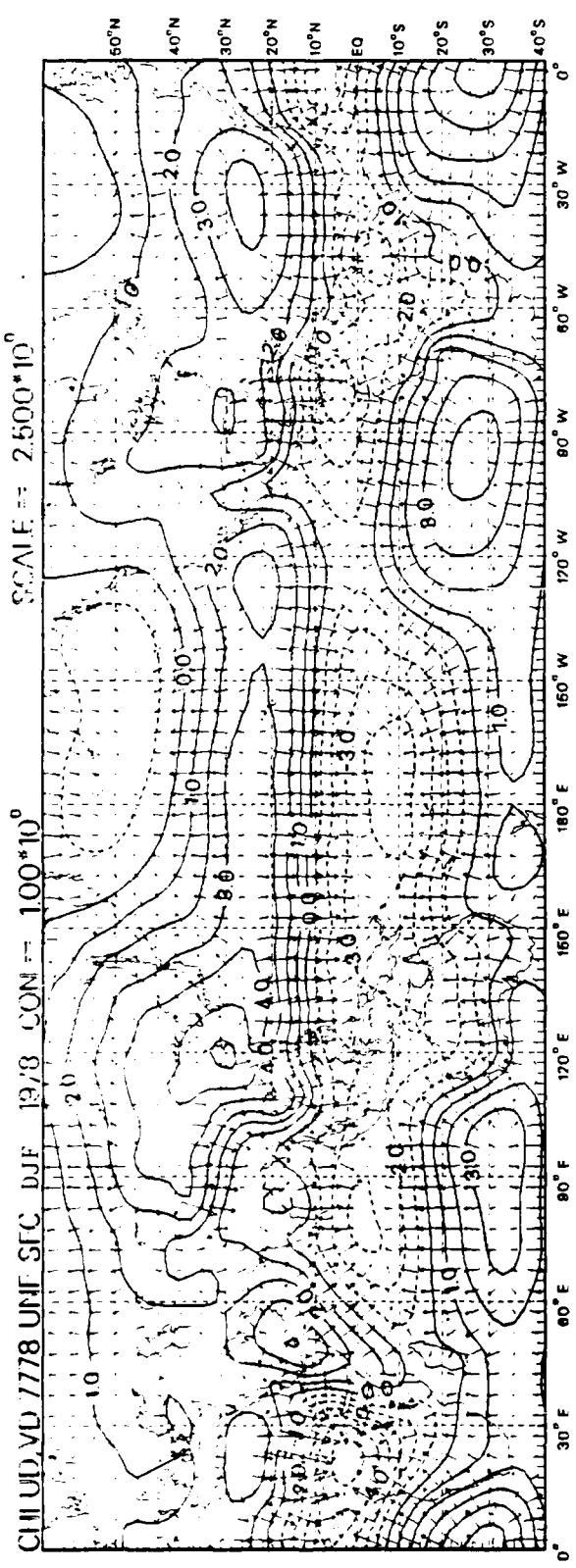


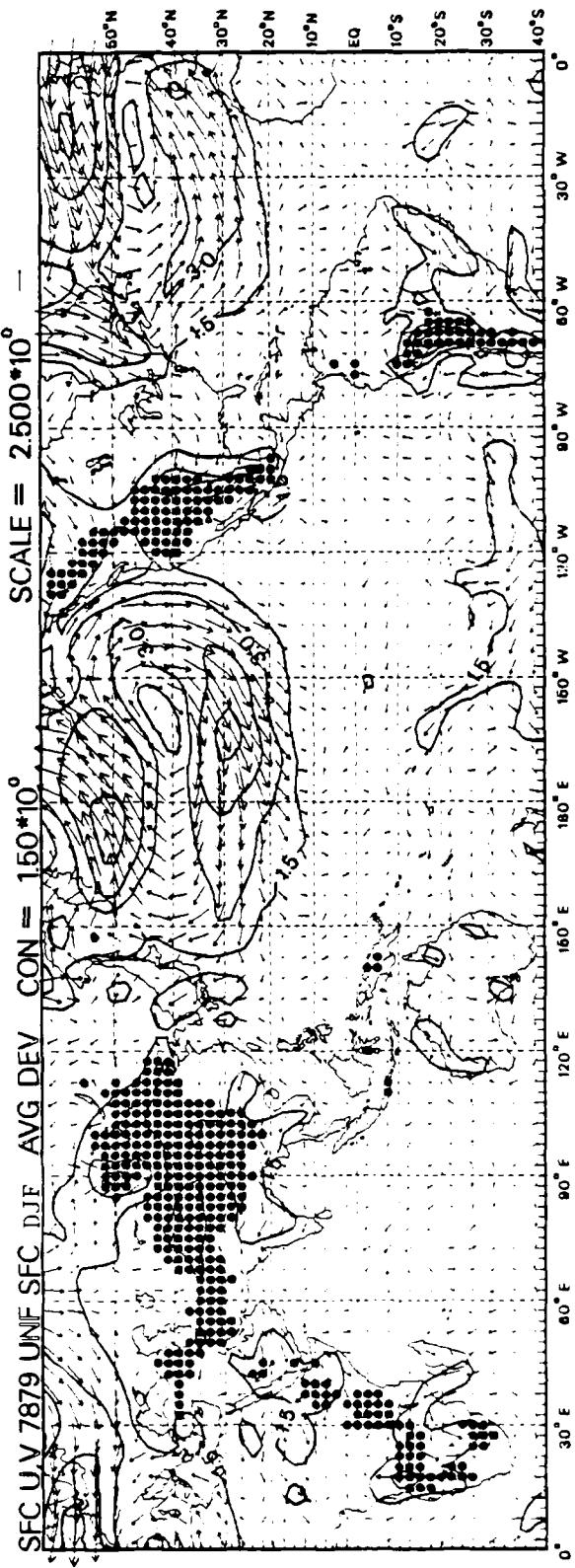
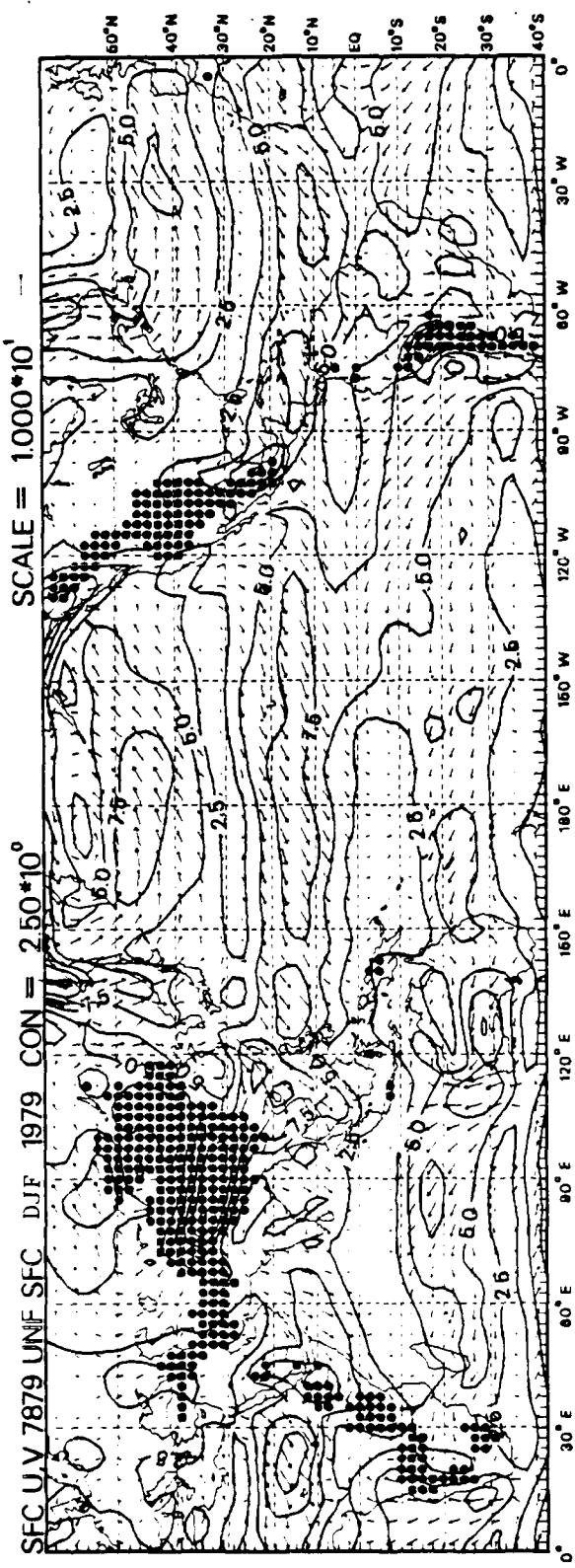


B11



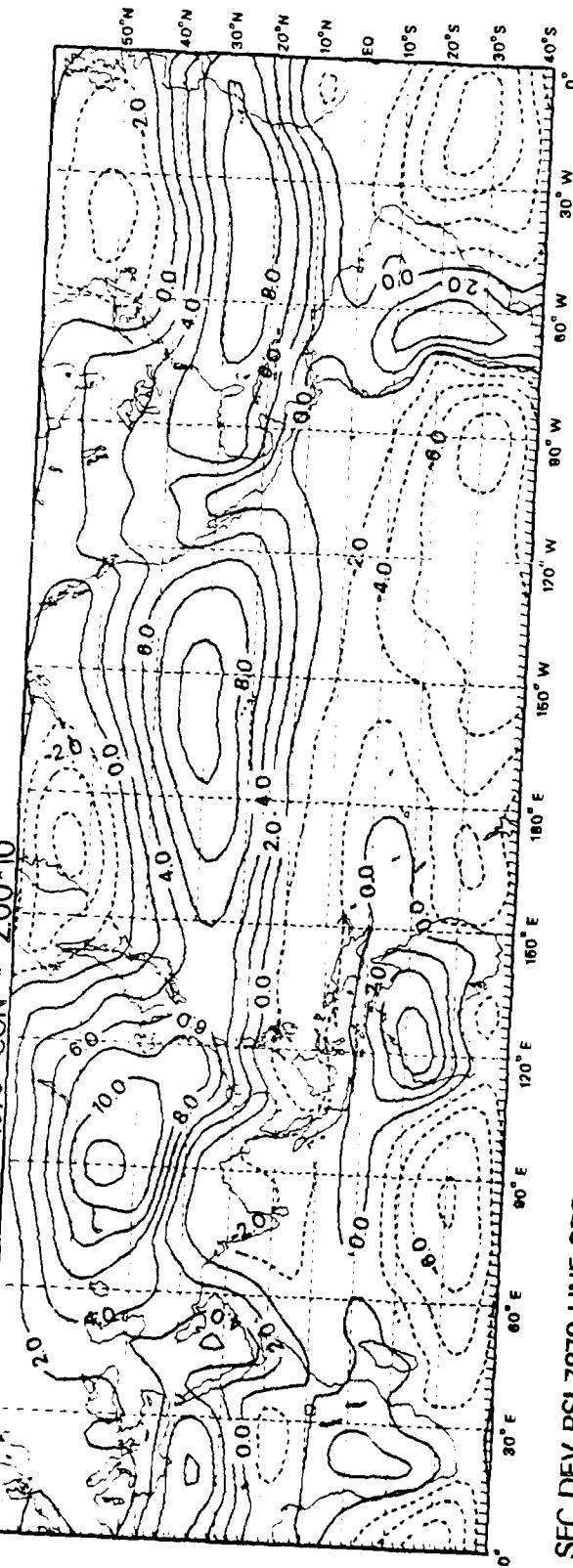
B12



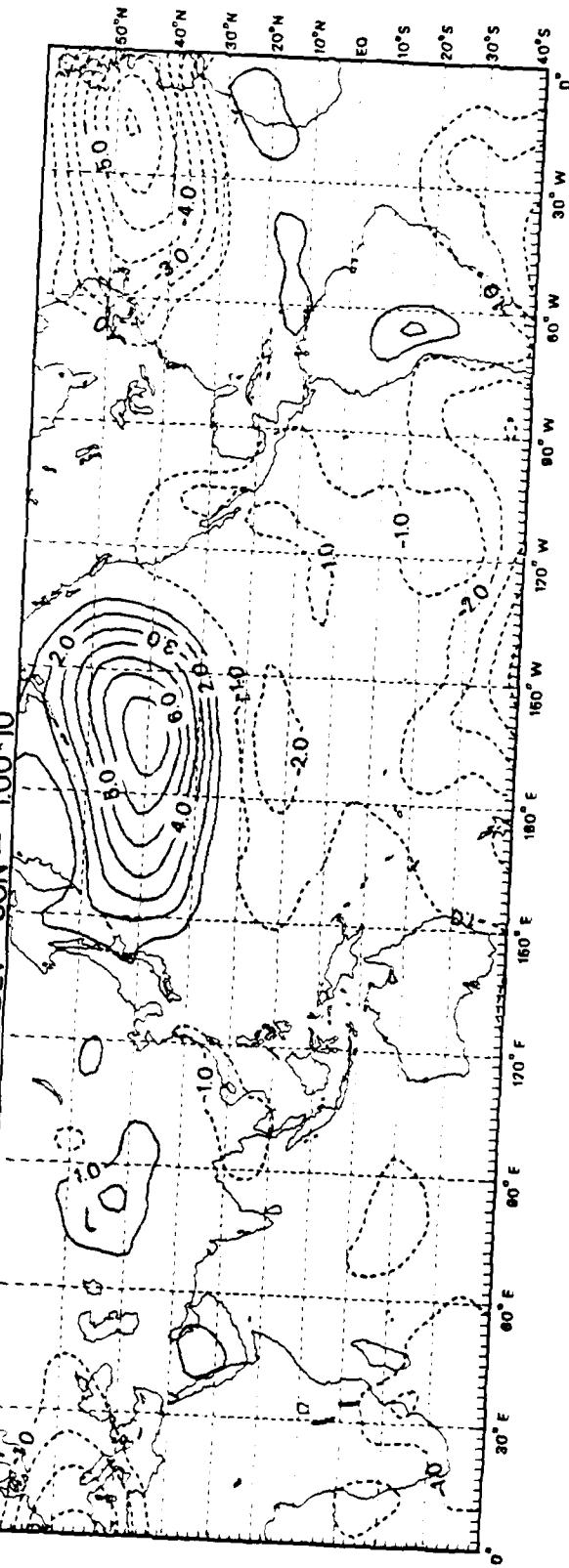


B14

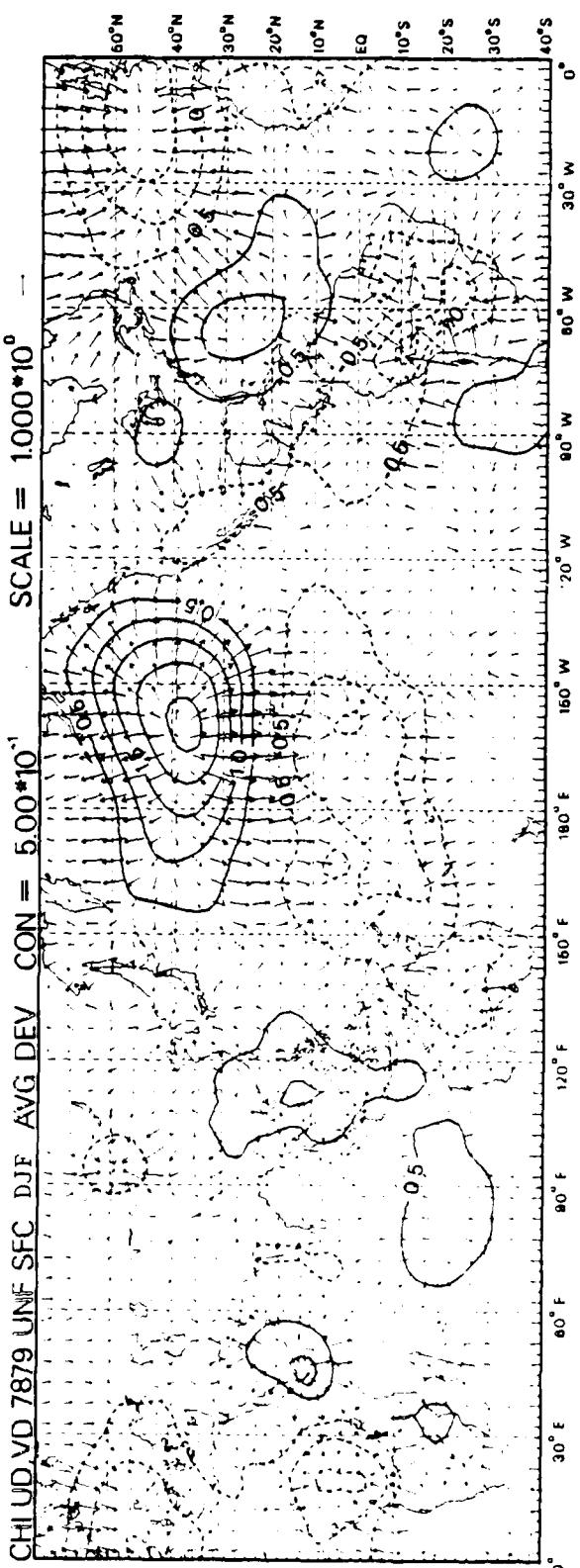
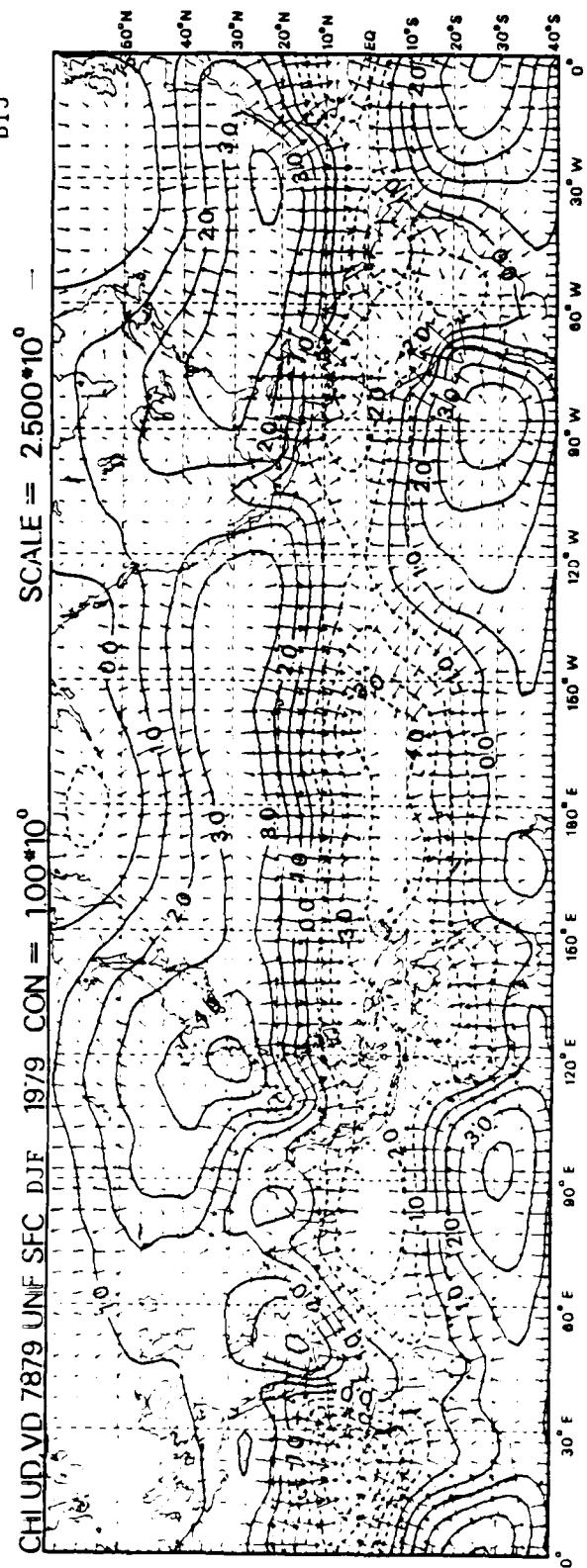
SFC PSI 7879 UNF SFC DJF 1979 CON = 2.00×10^0



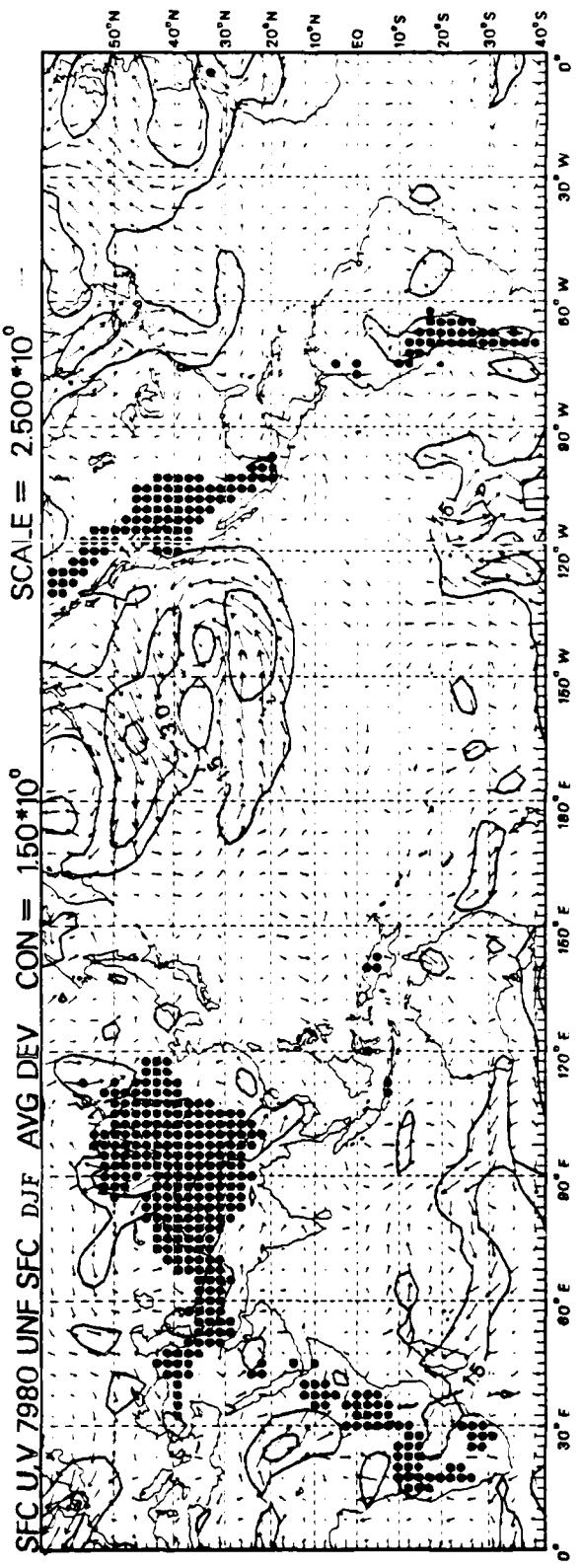
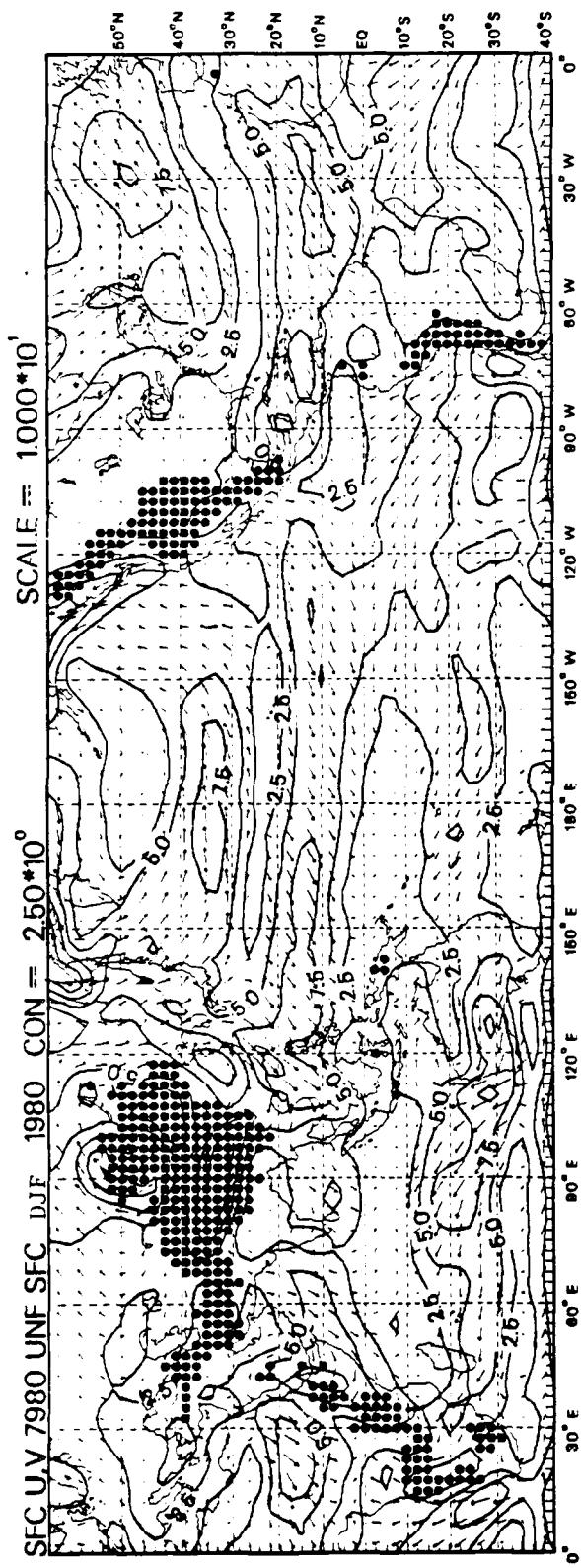
SFC DEV PSI 7879 UNF SFC DJF AVG DEV CON = 1.00×10^0

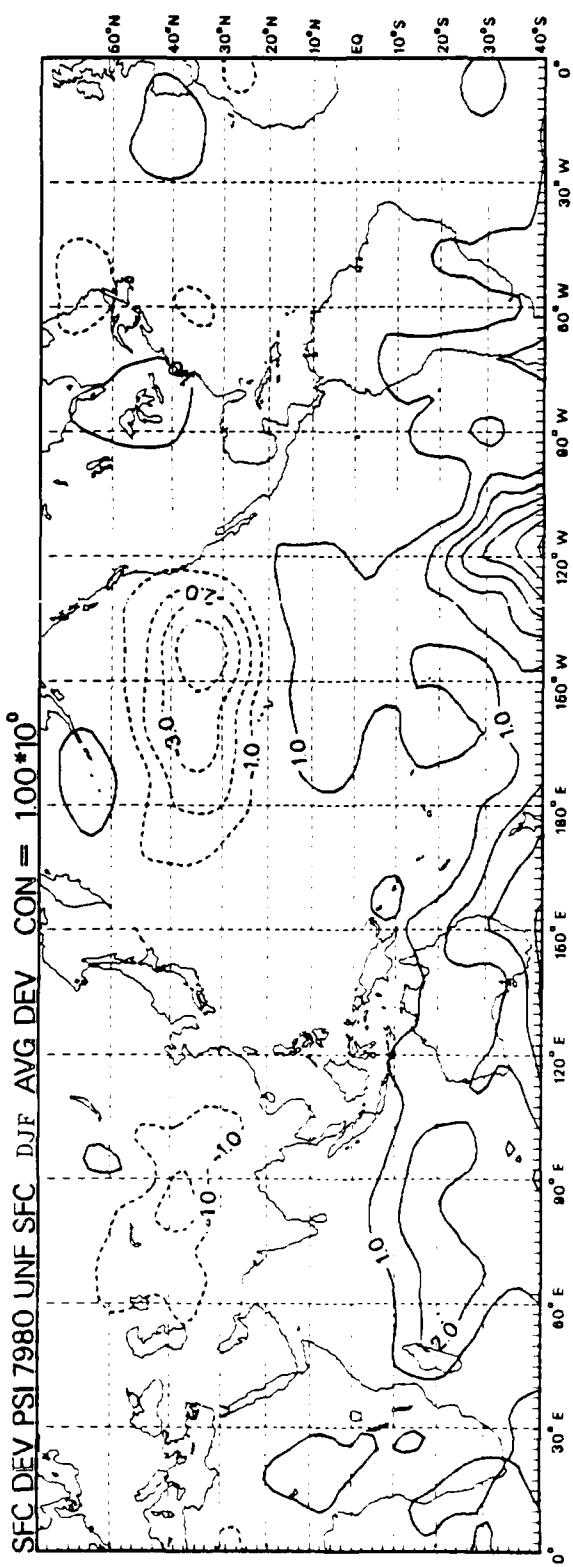
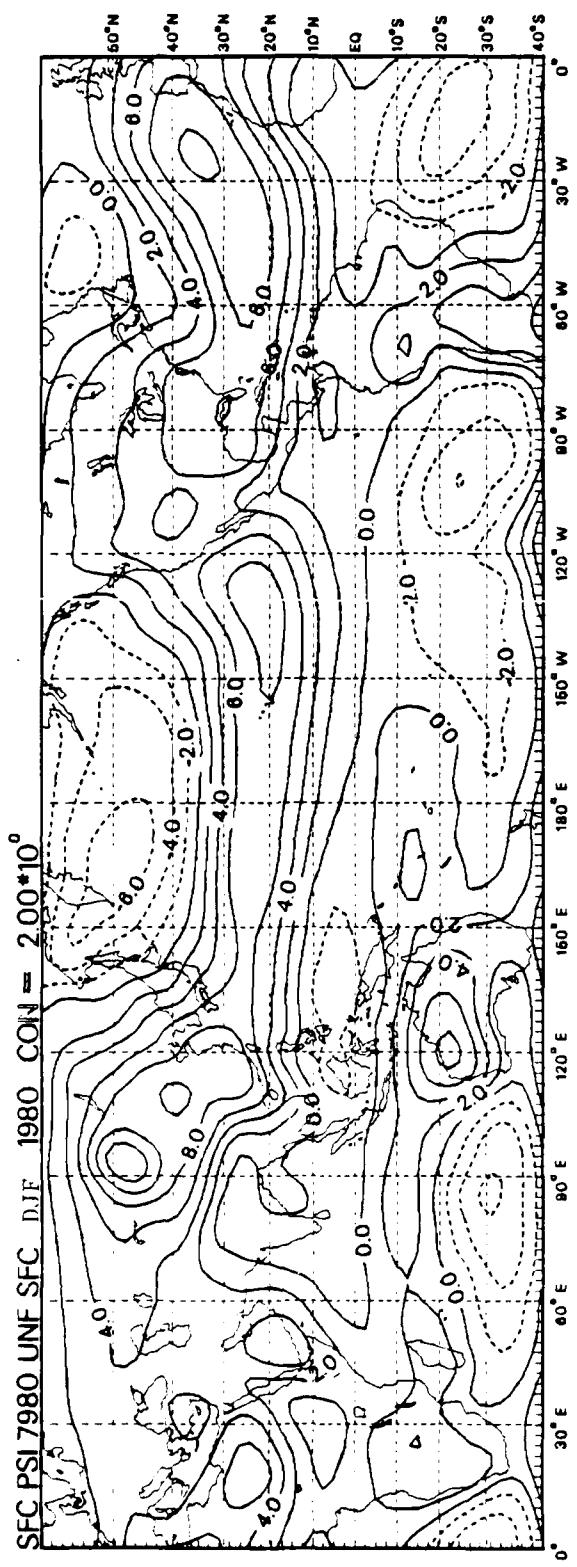


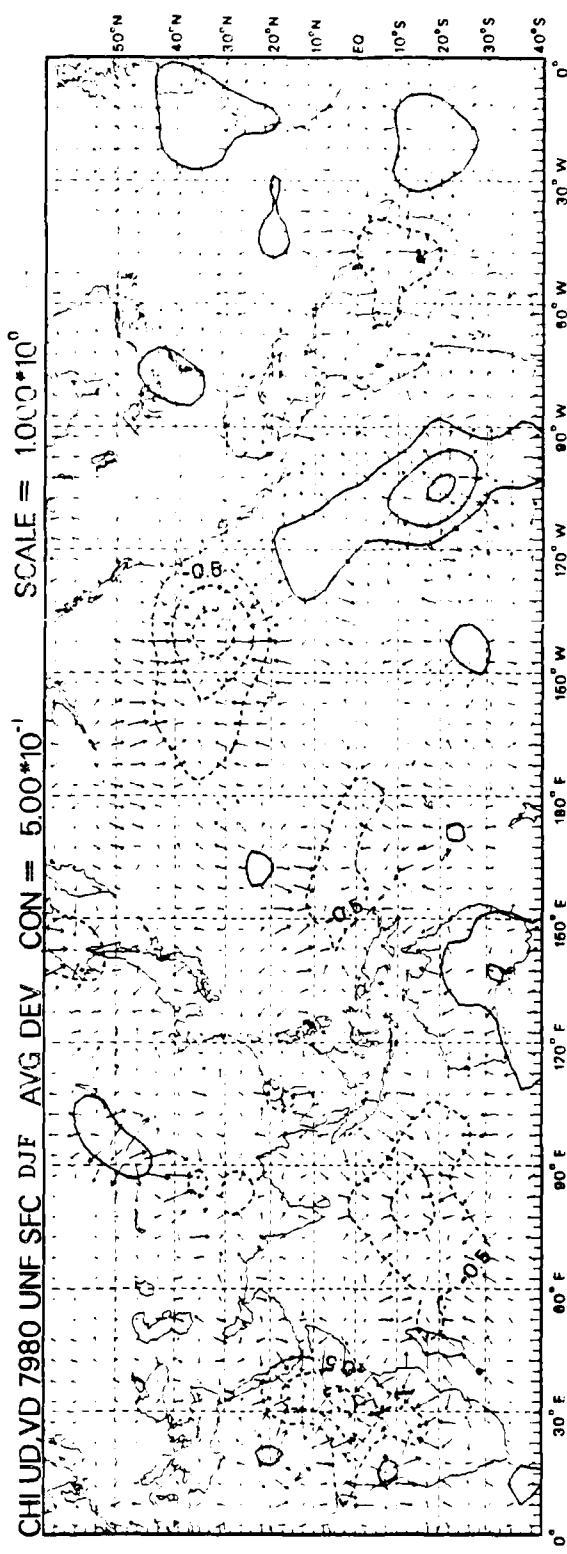
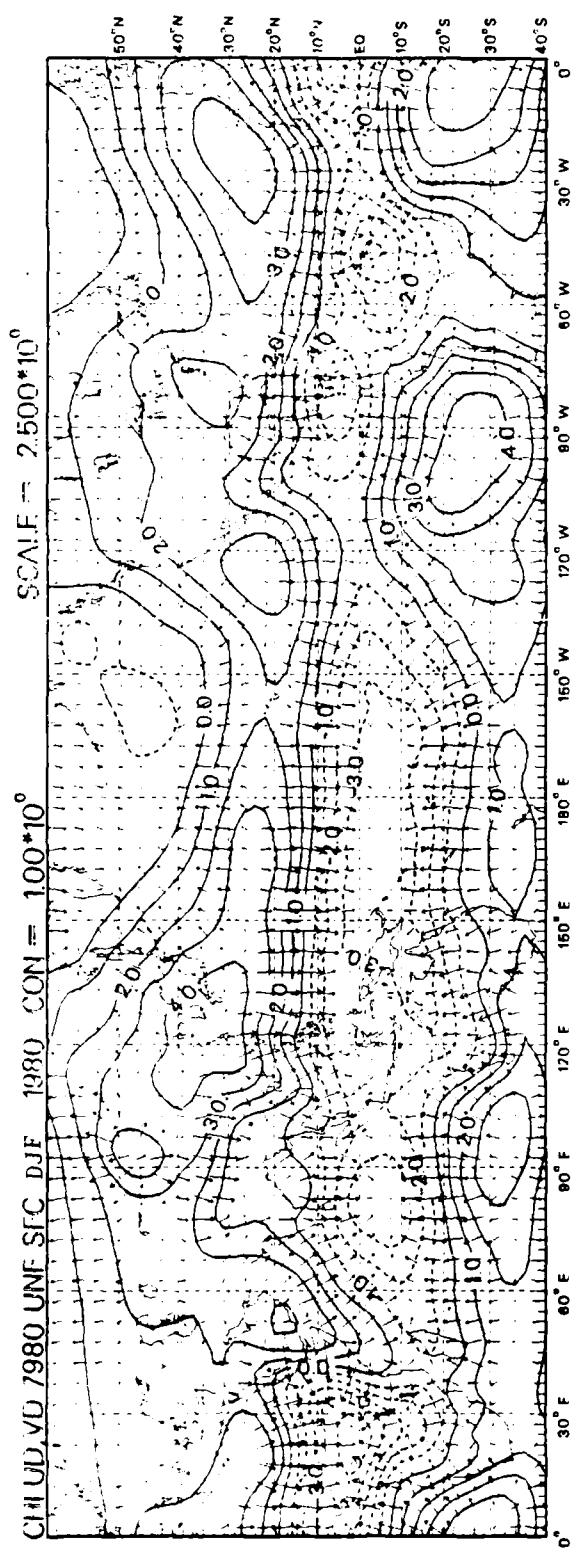
B15



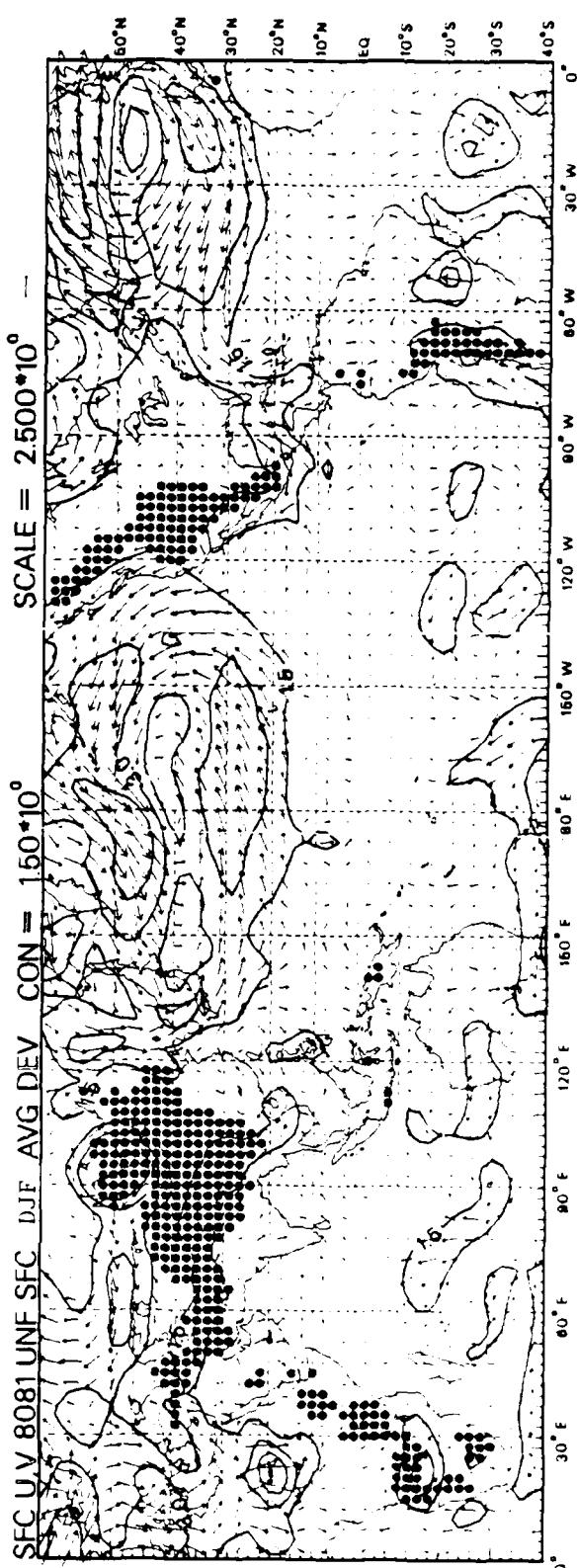
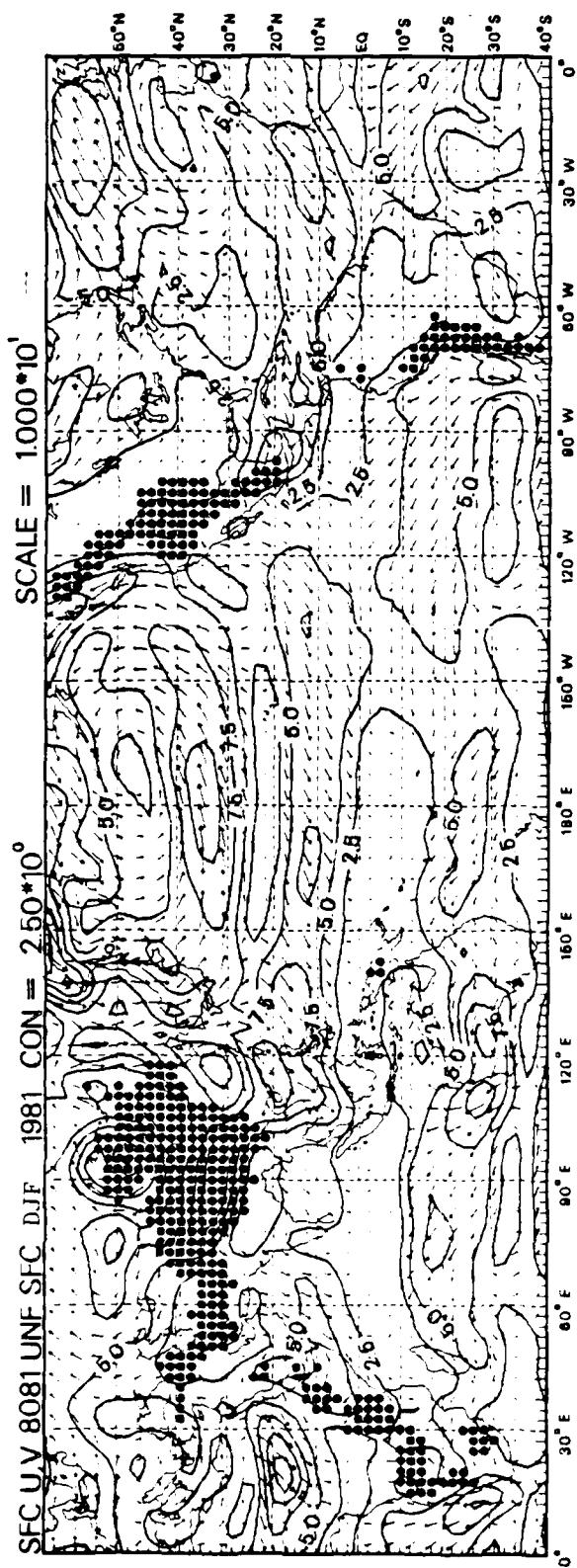
B16

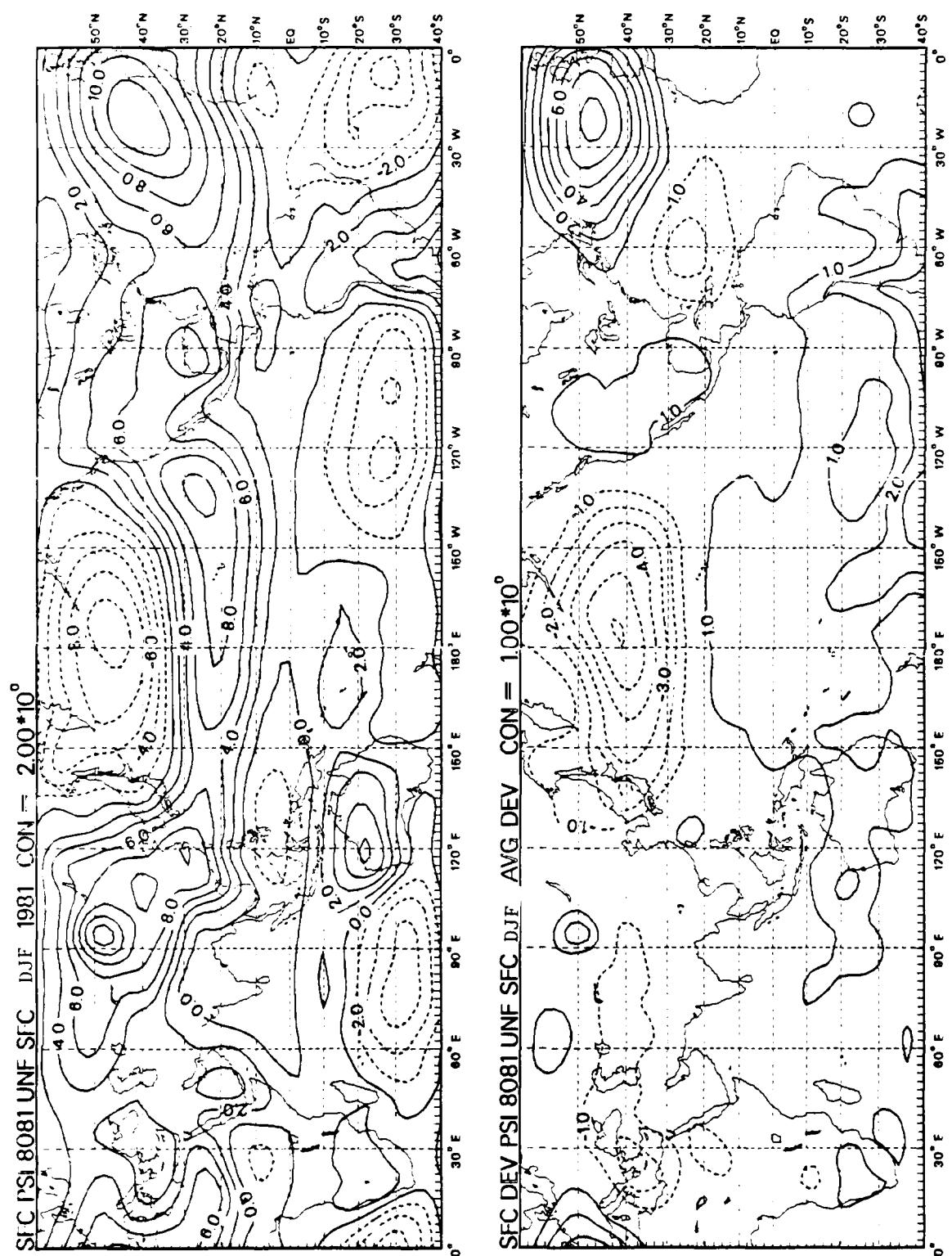




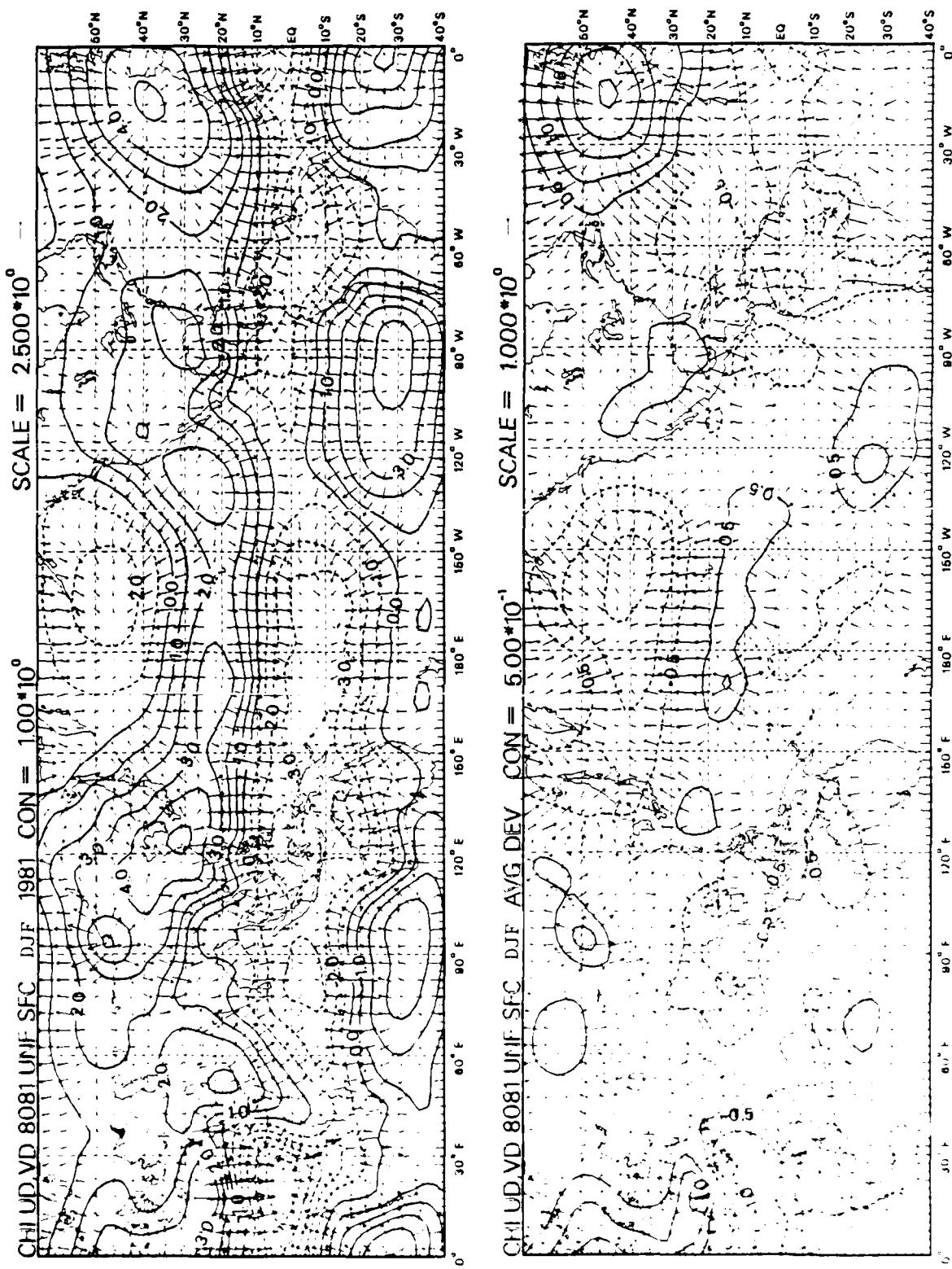


B19

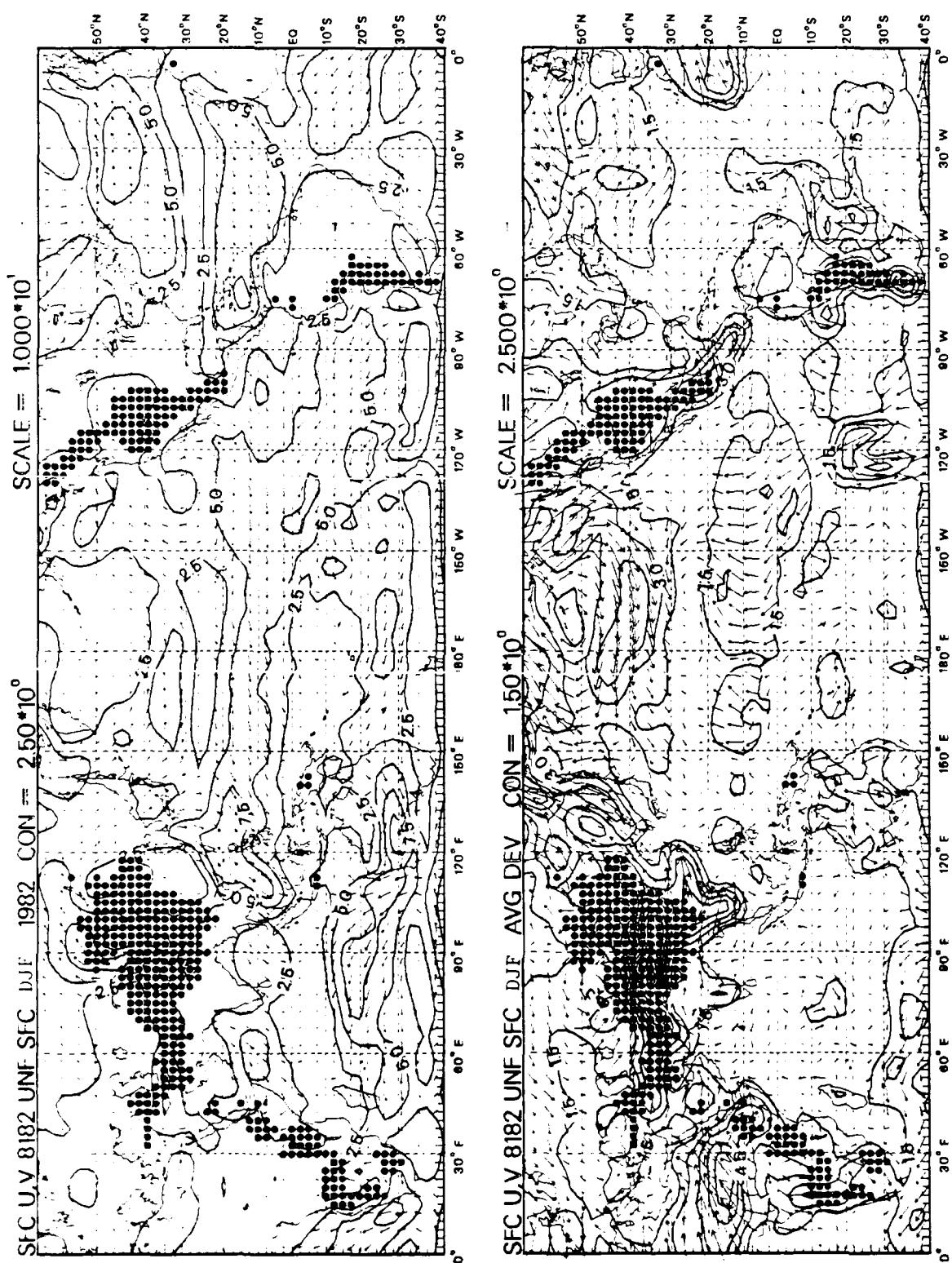




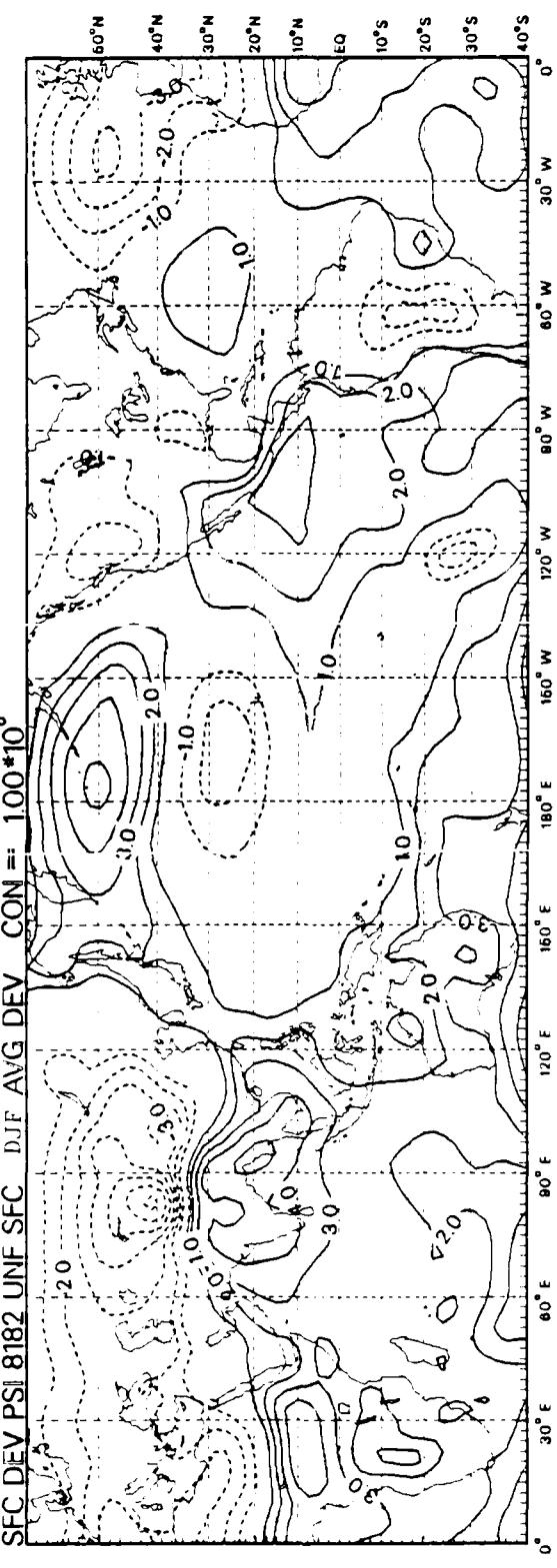
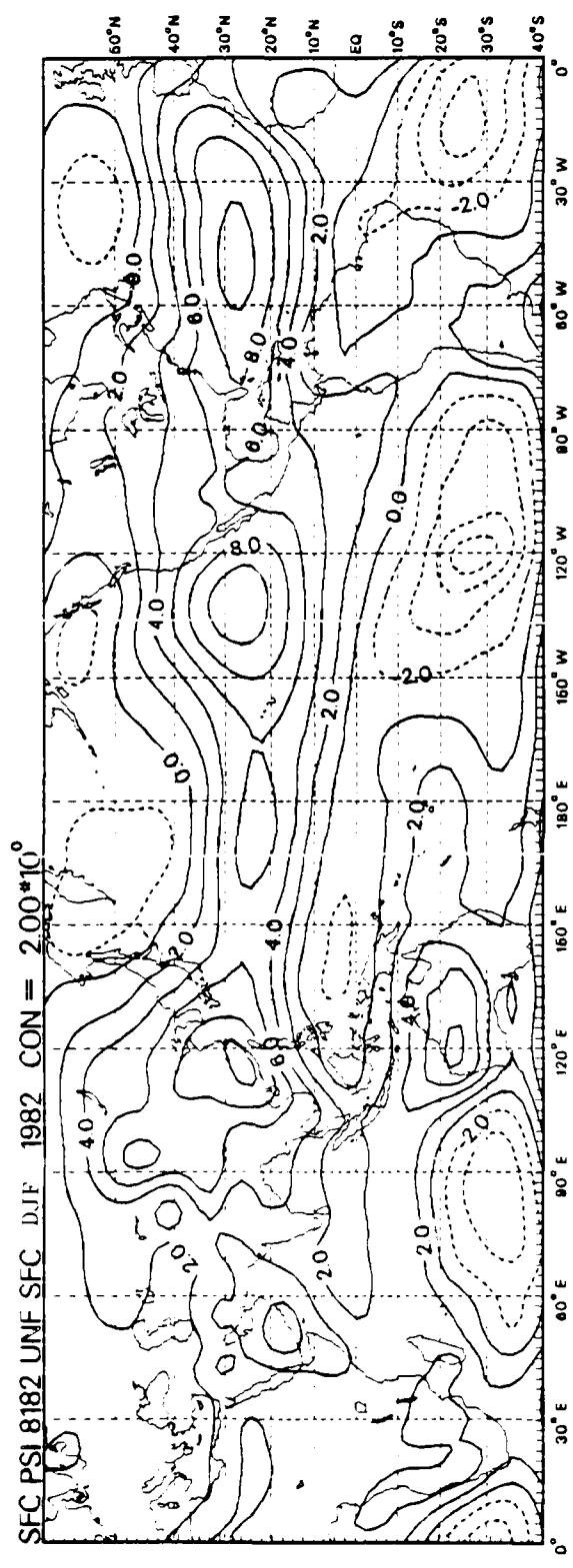
B21

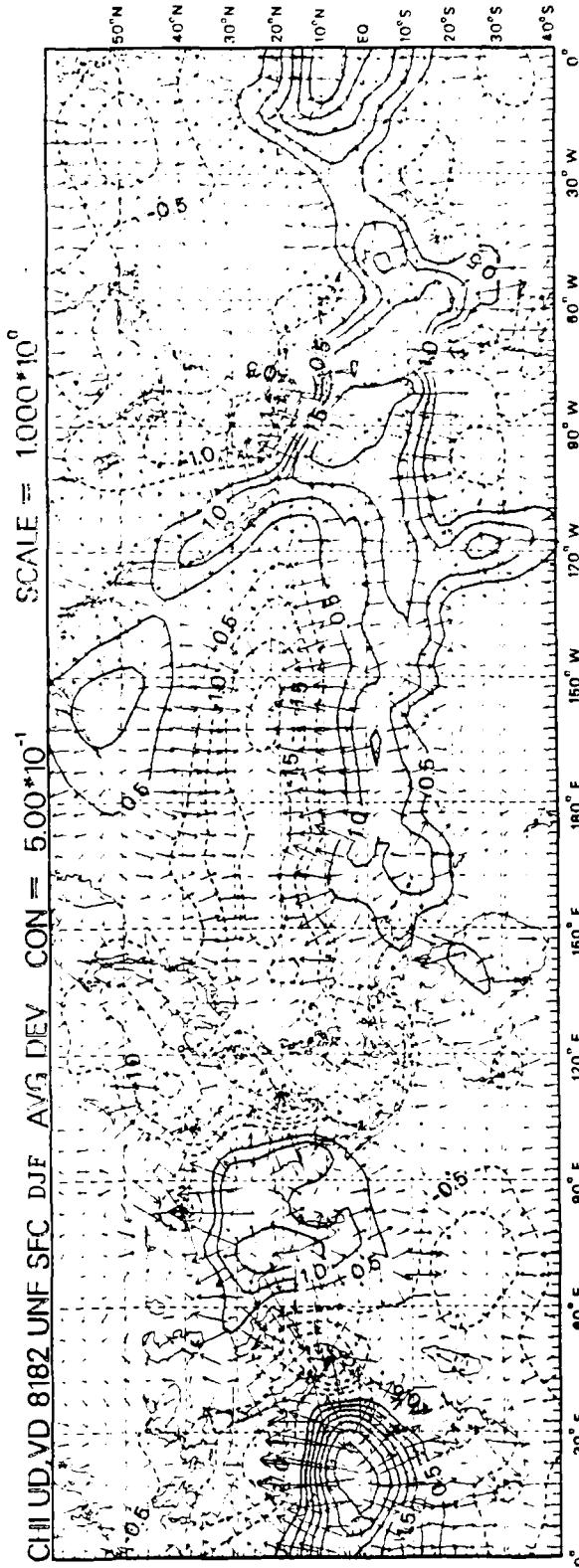
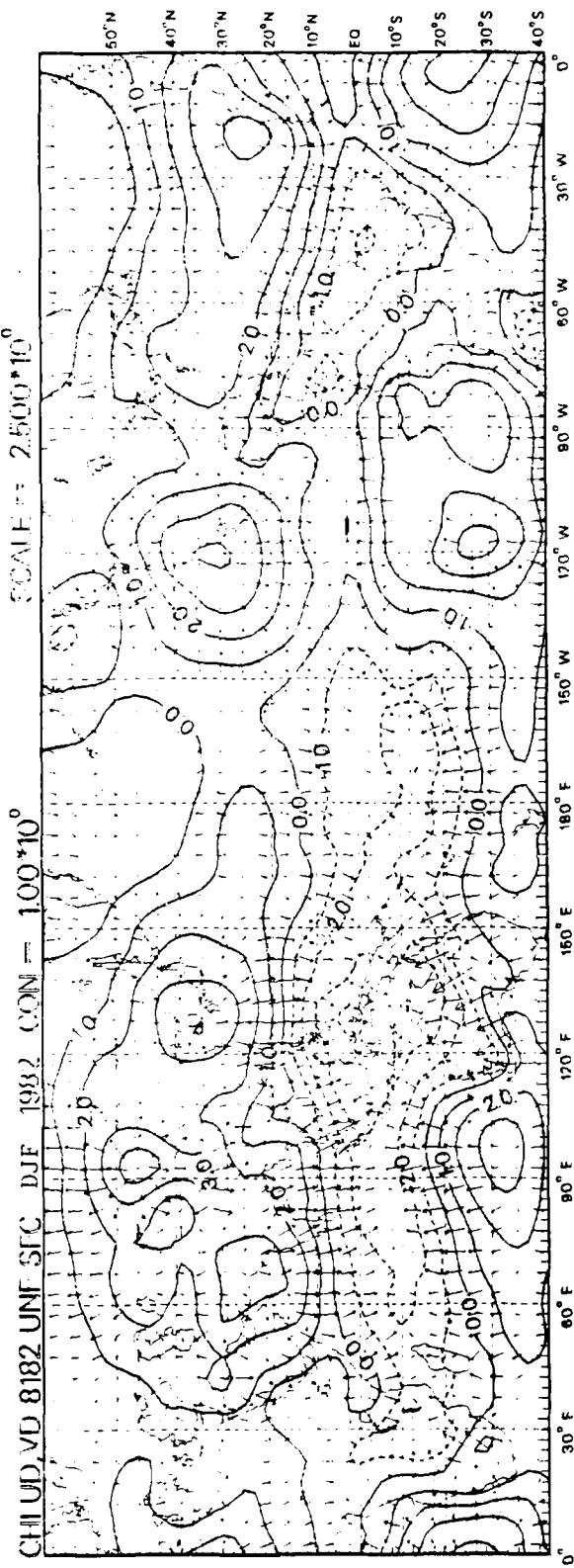


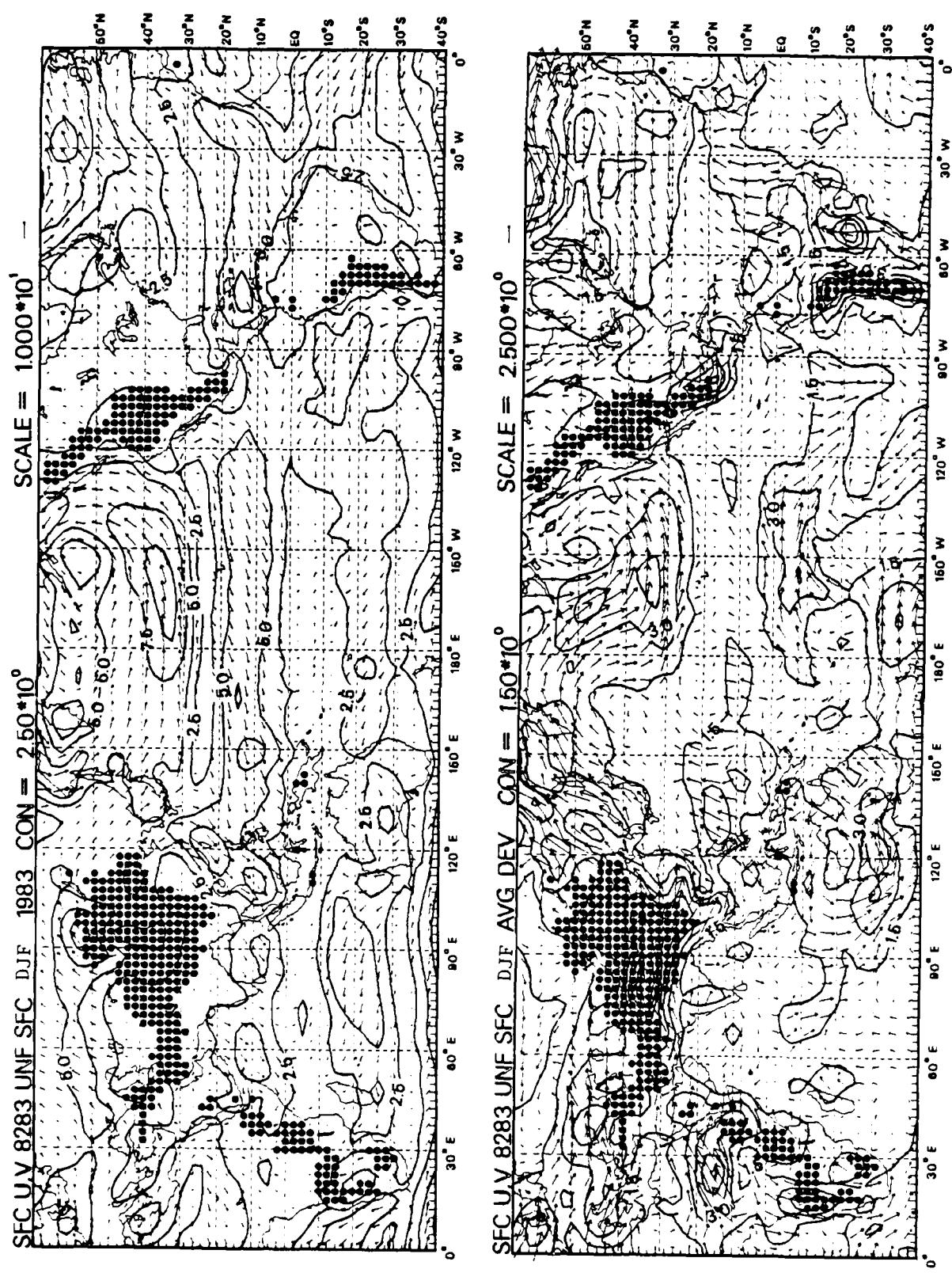
B22

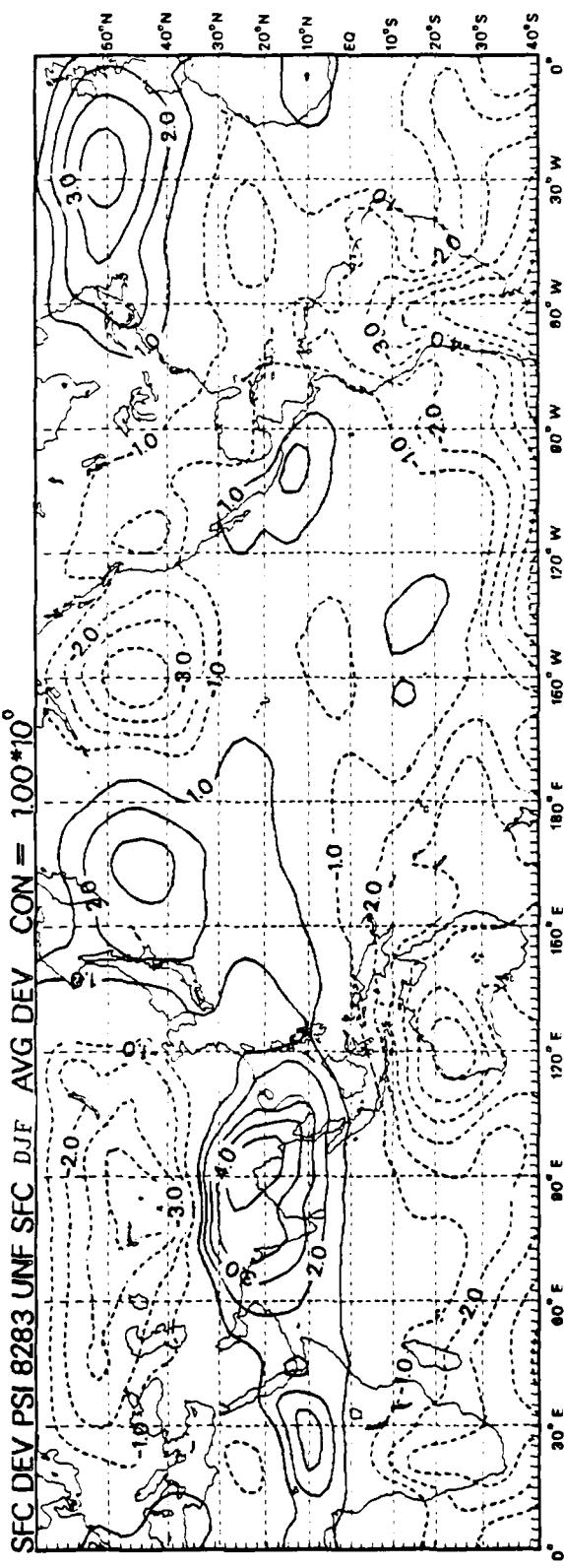
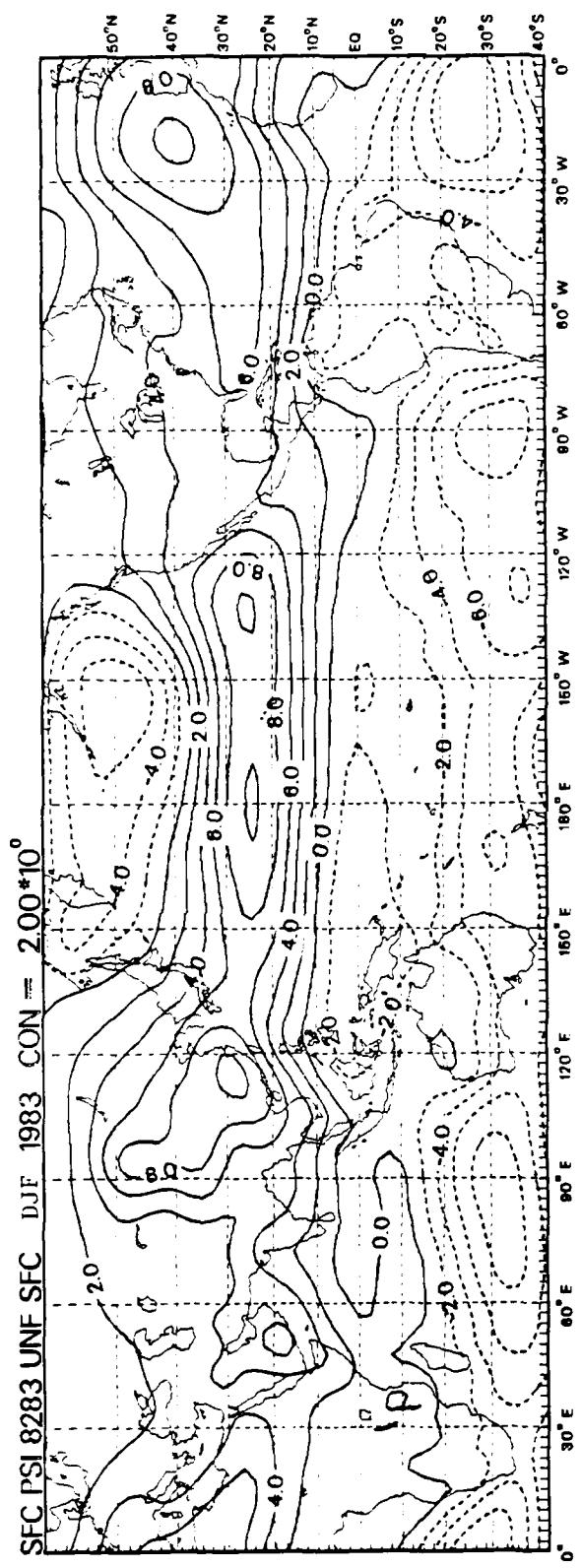


823

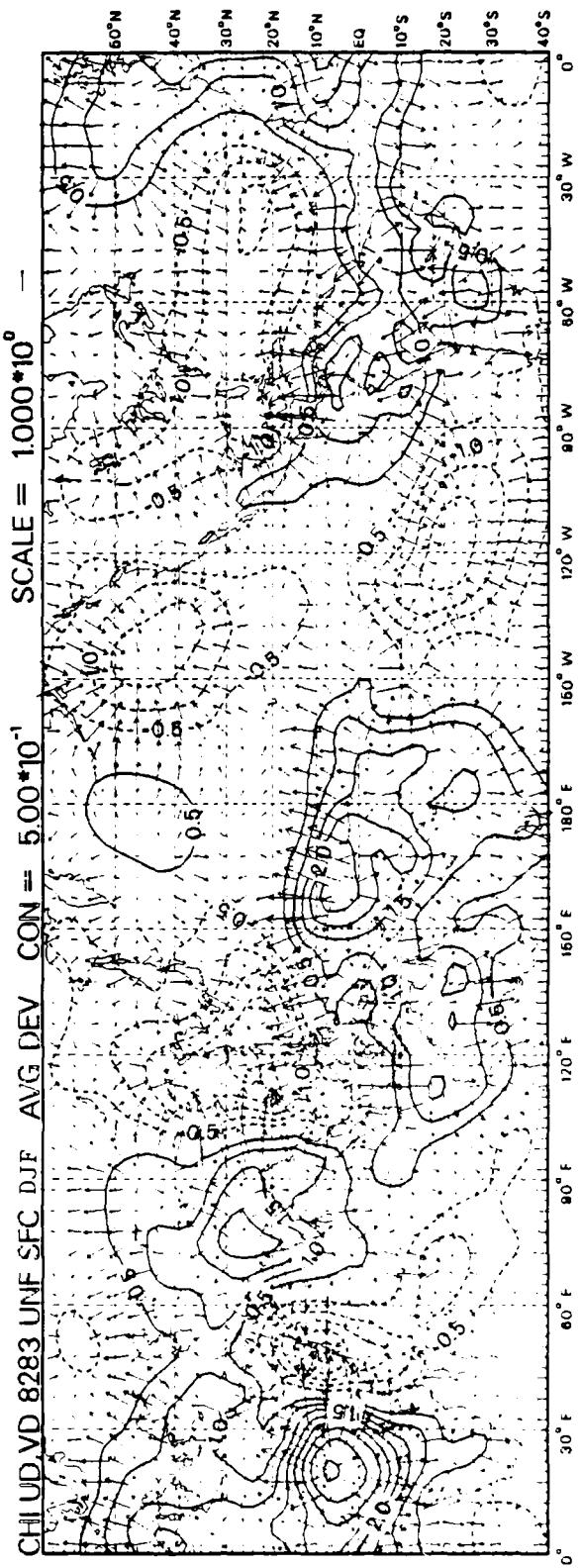
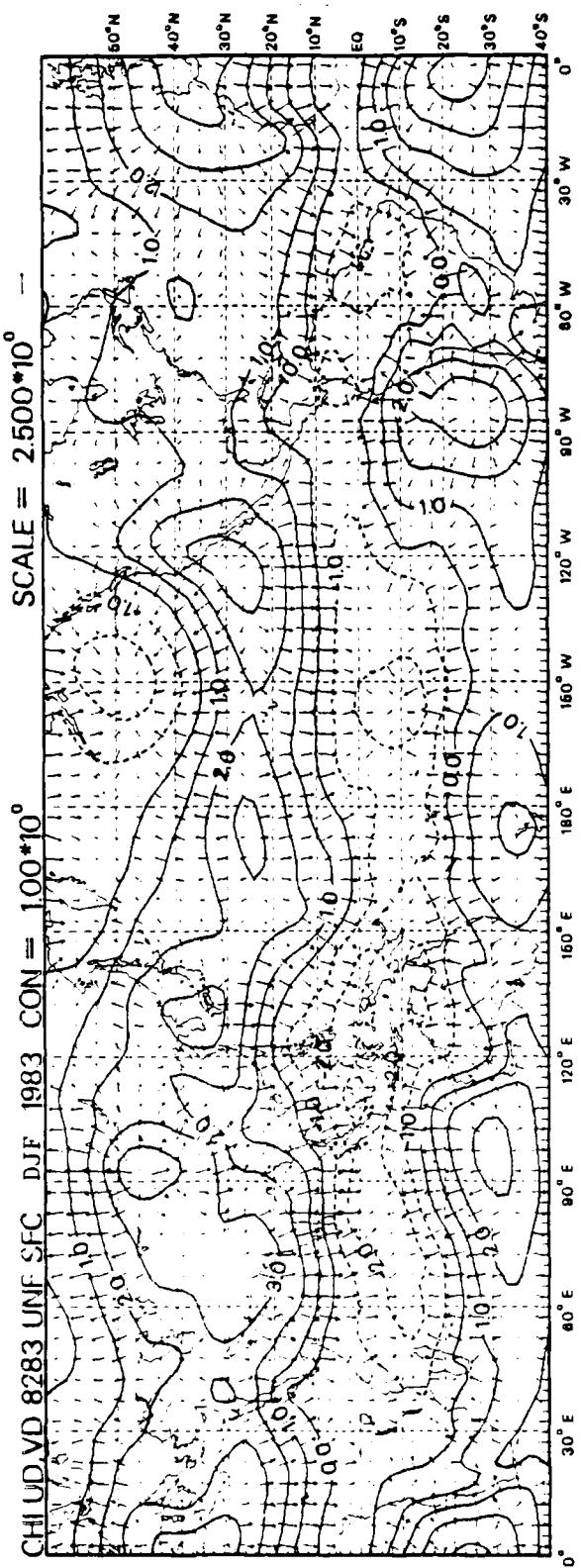


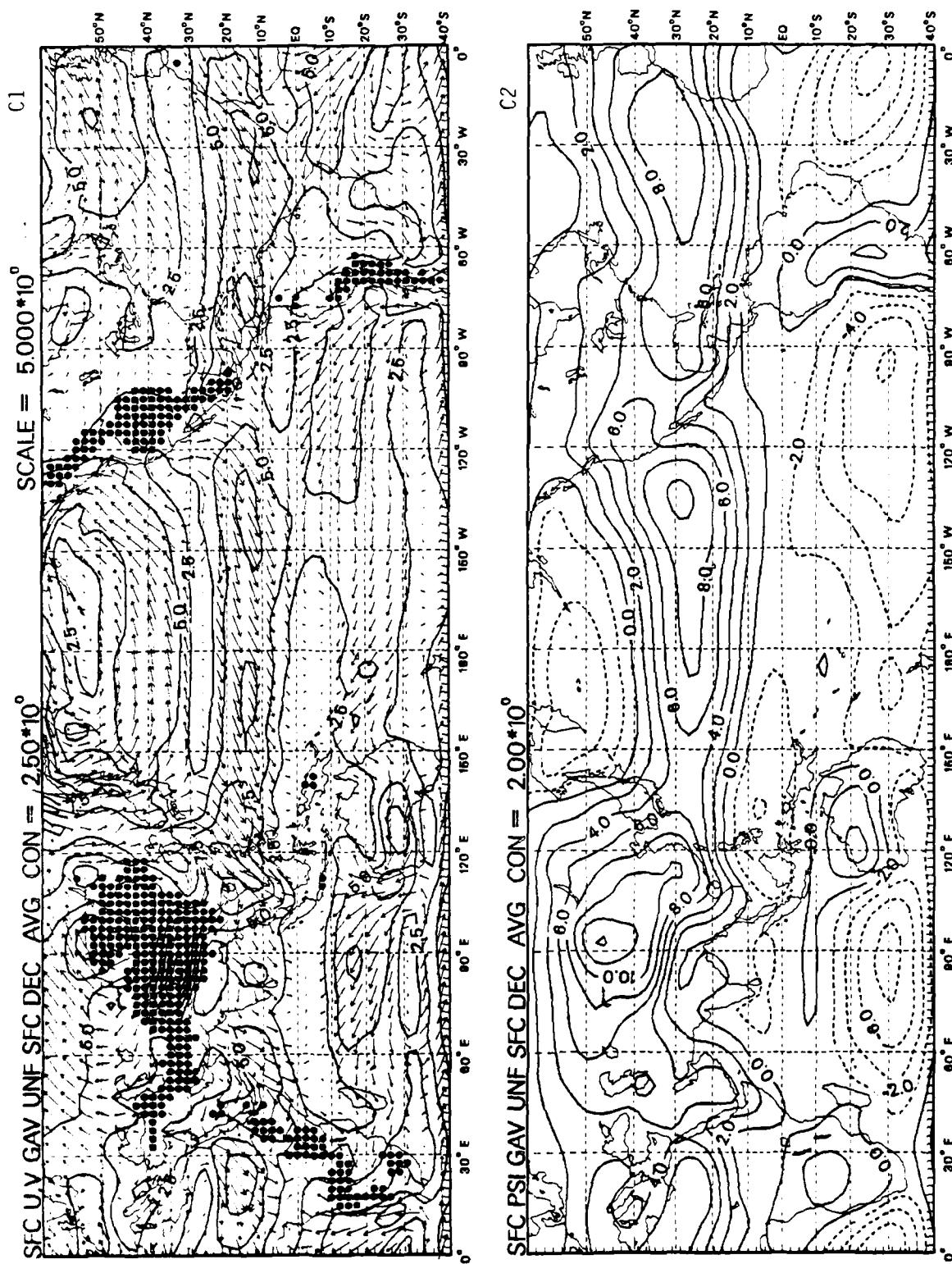


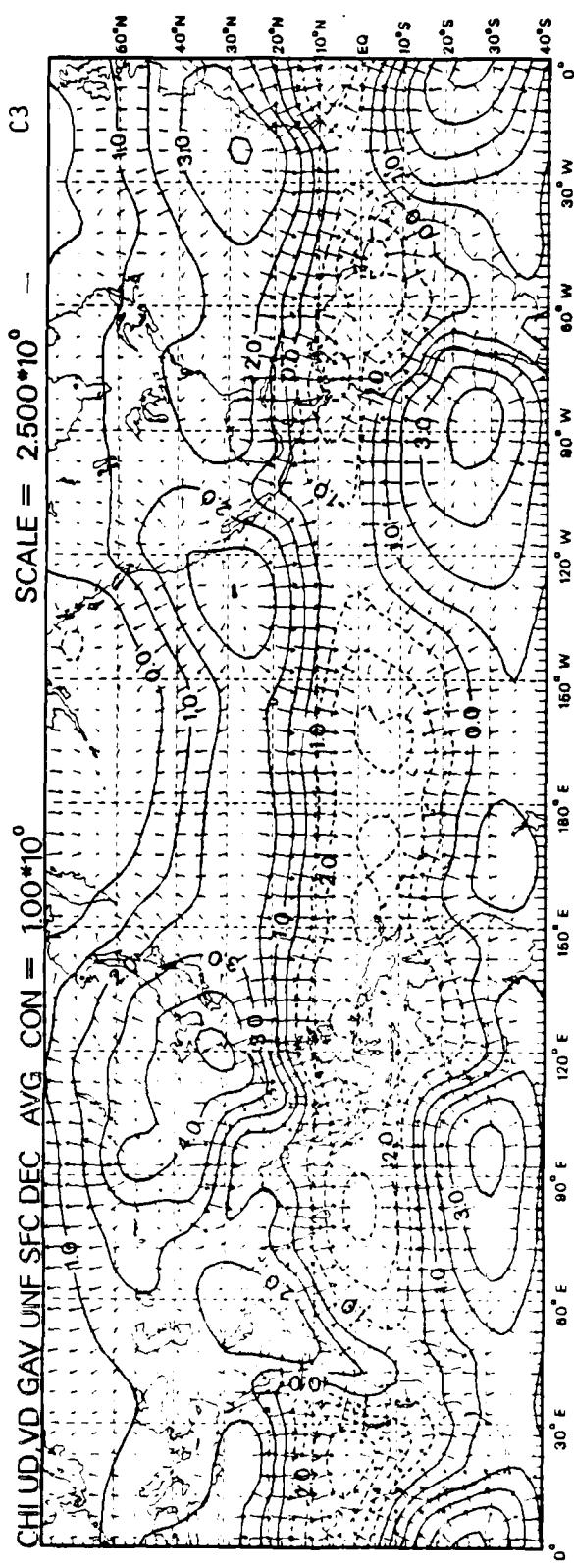


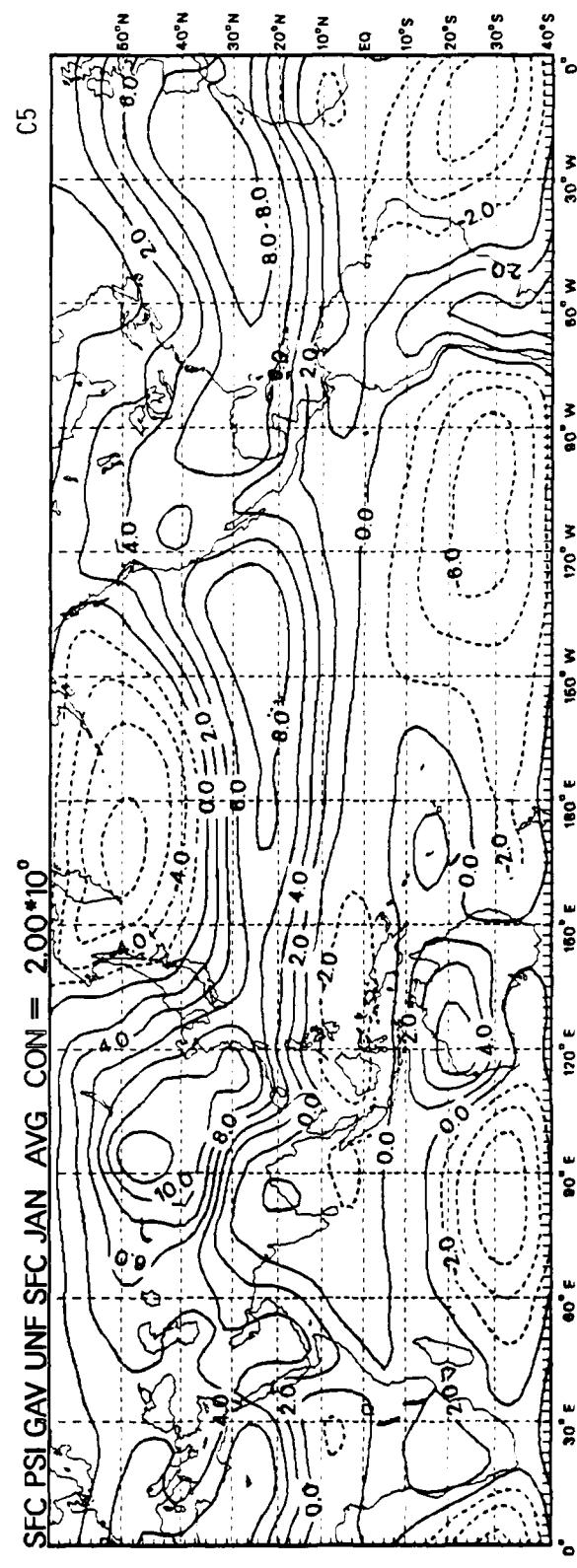
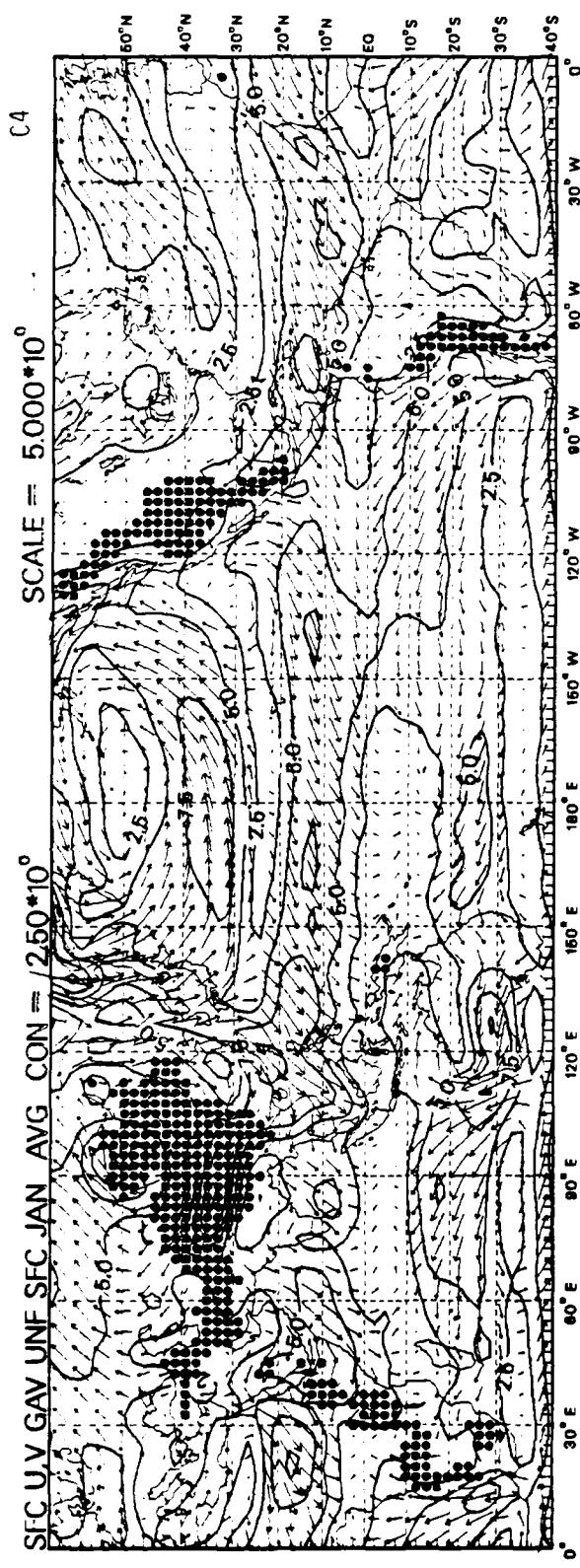


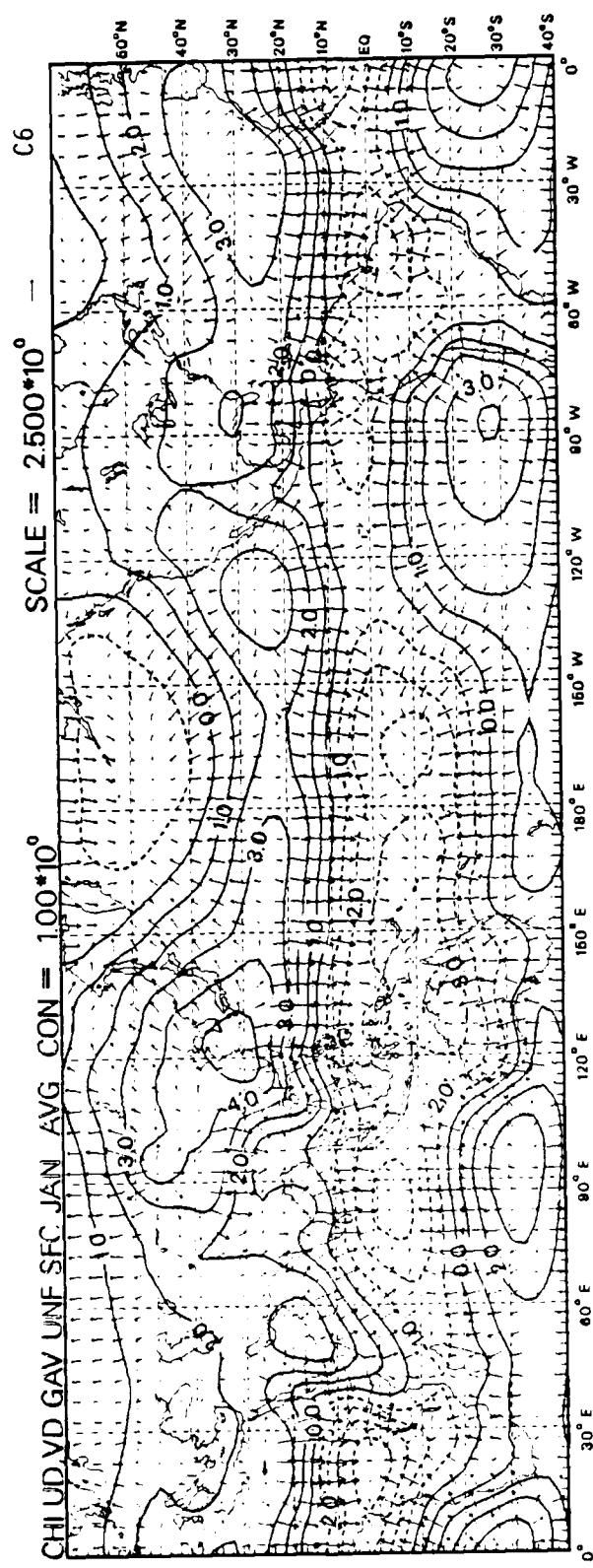
B27

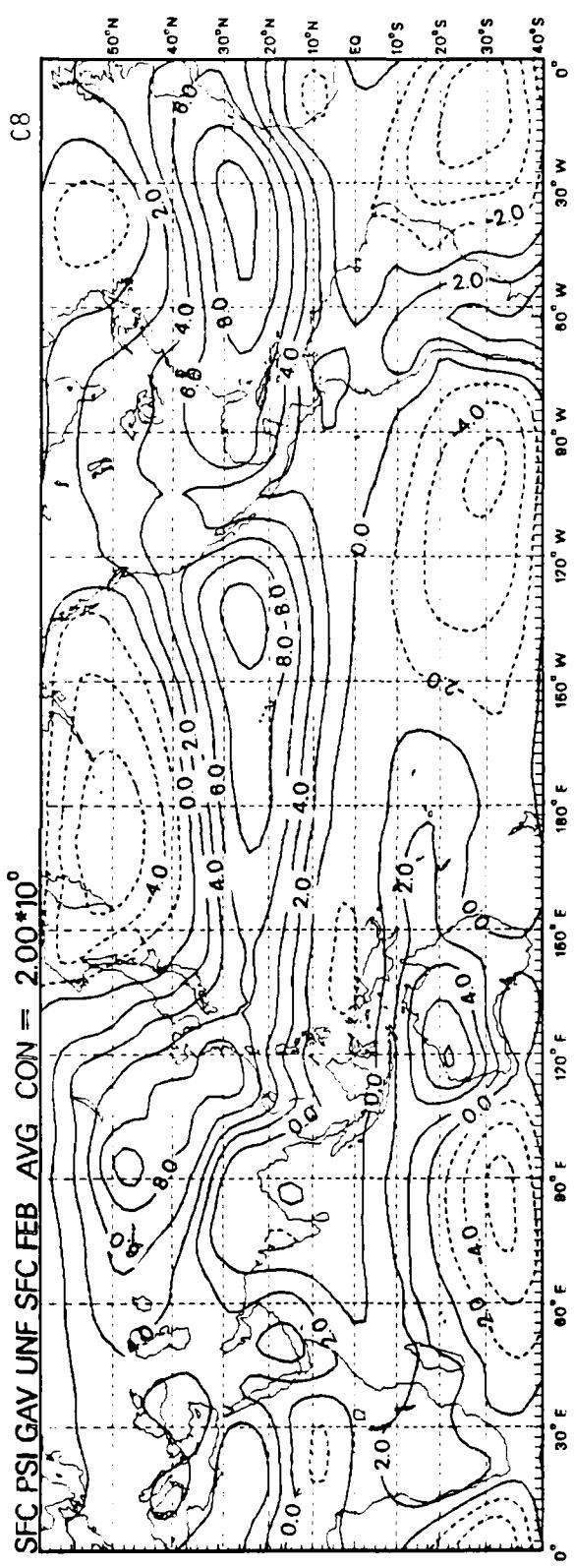
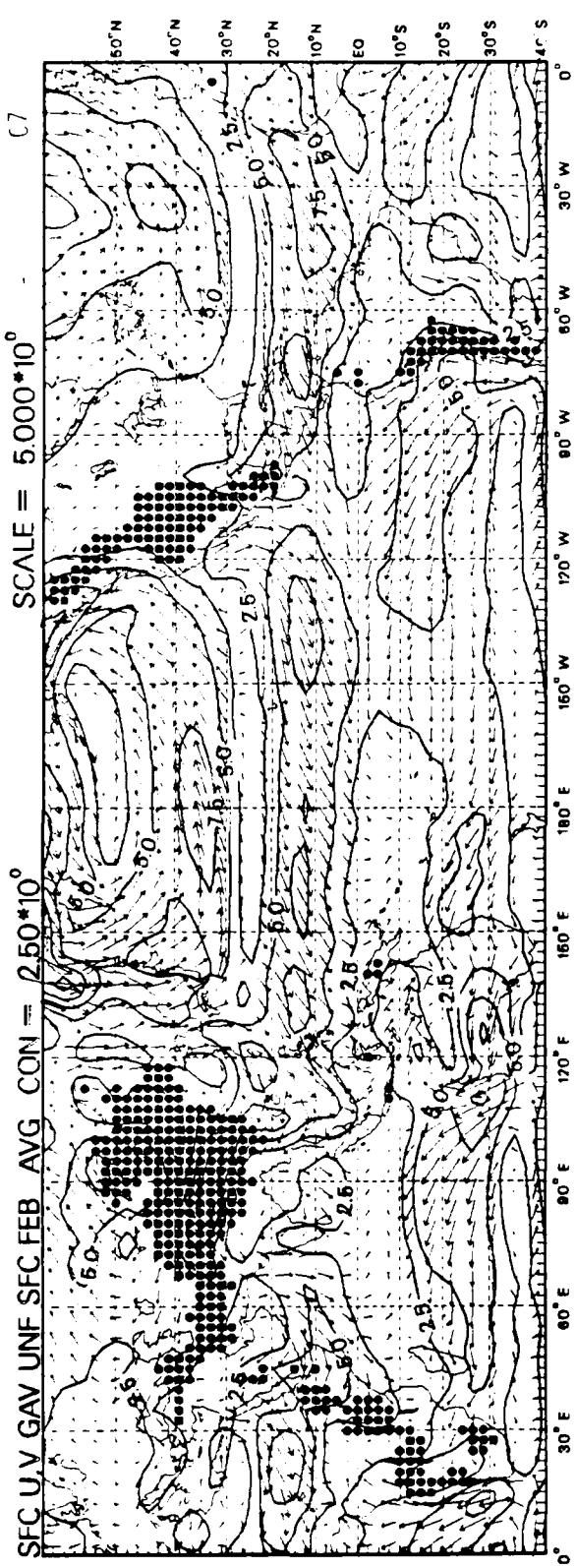


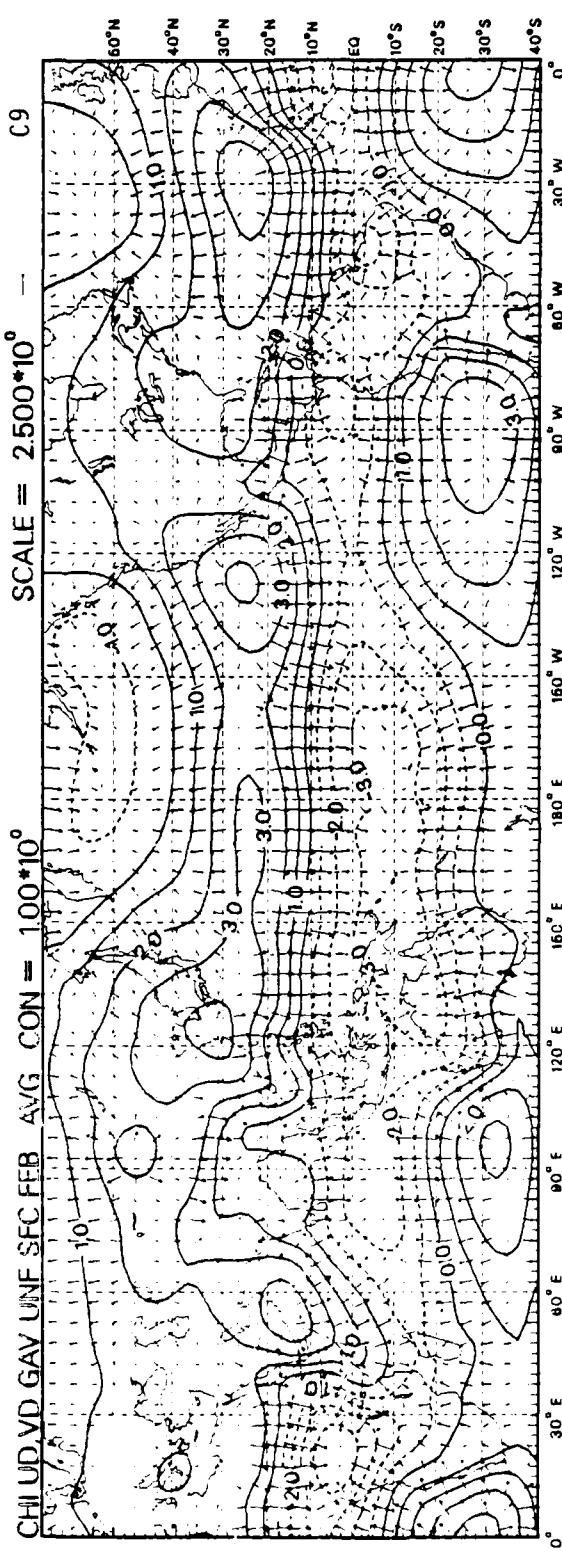




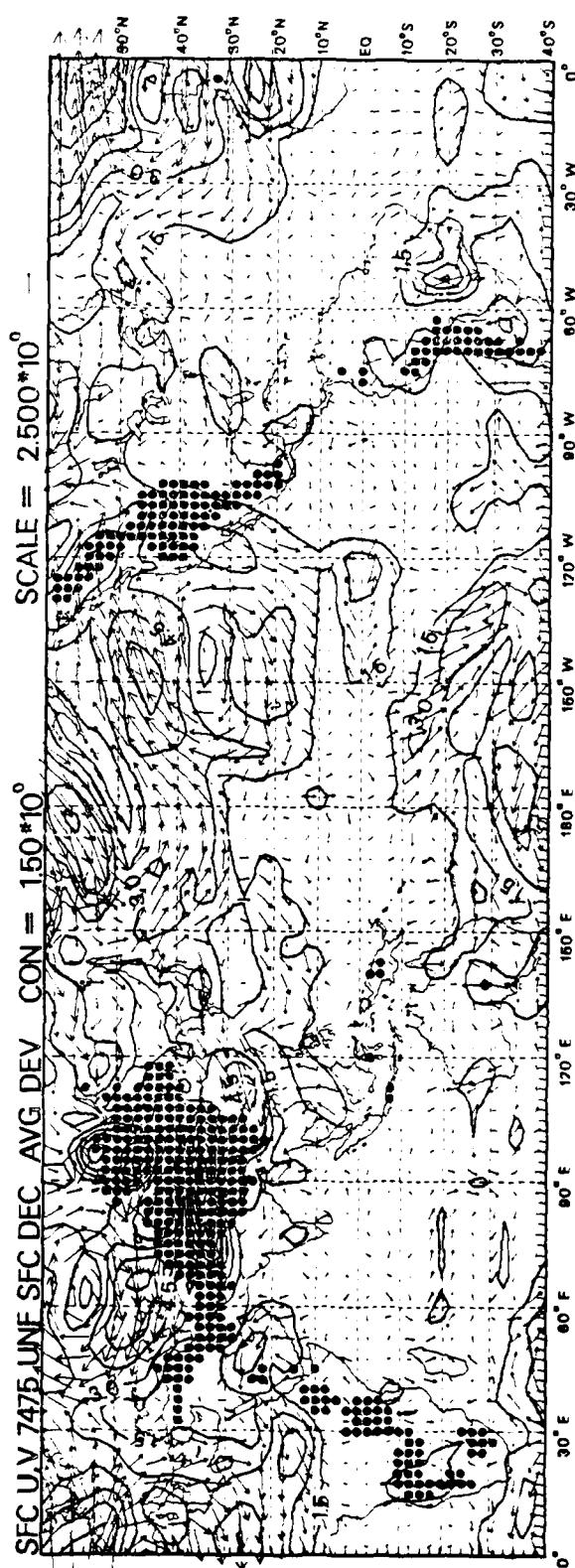
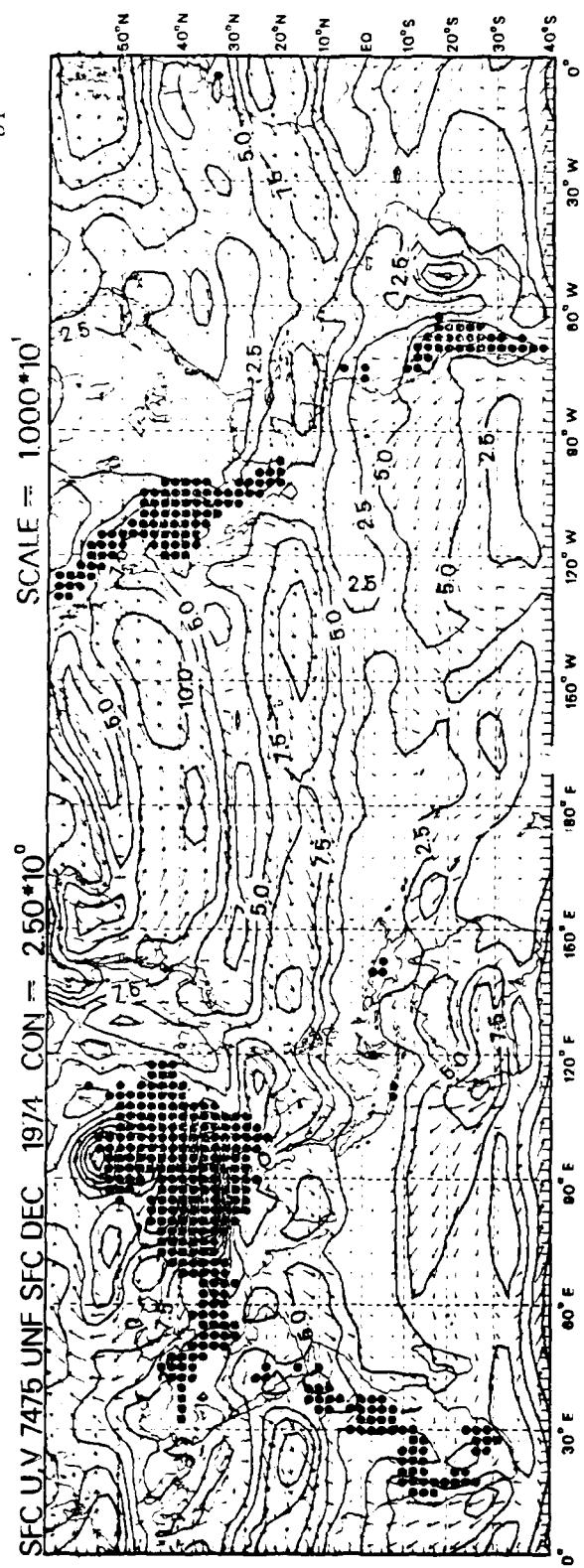




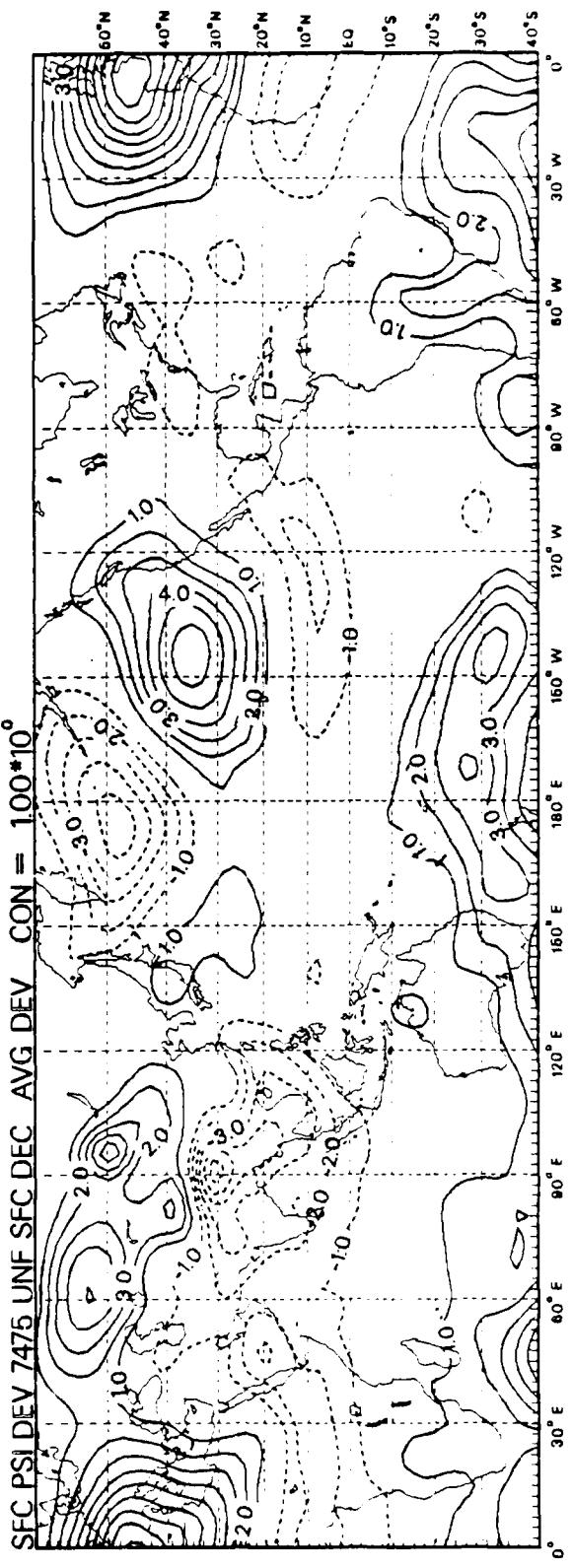
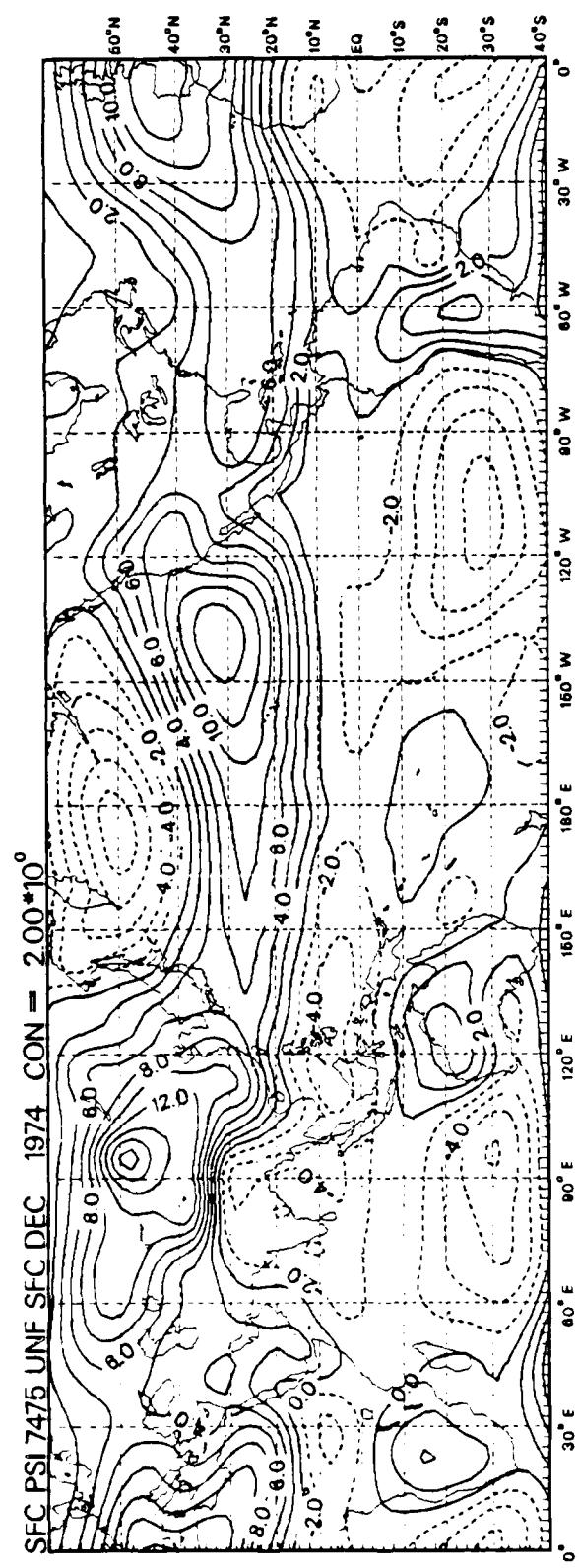




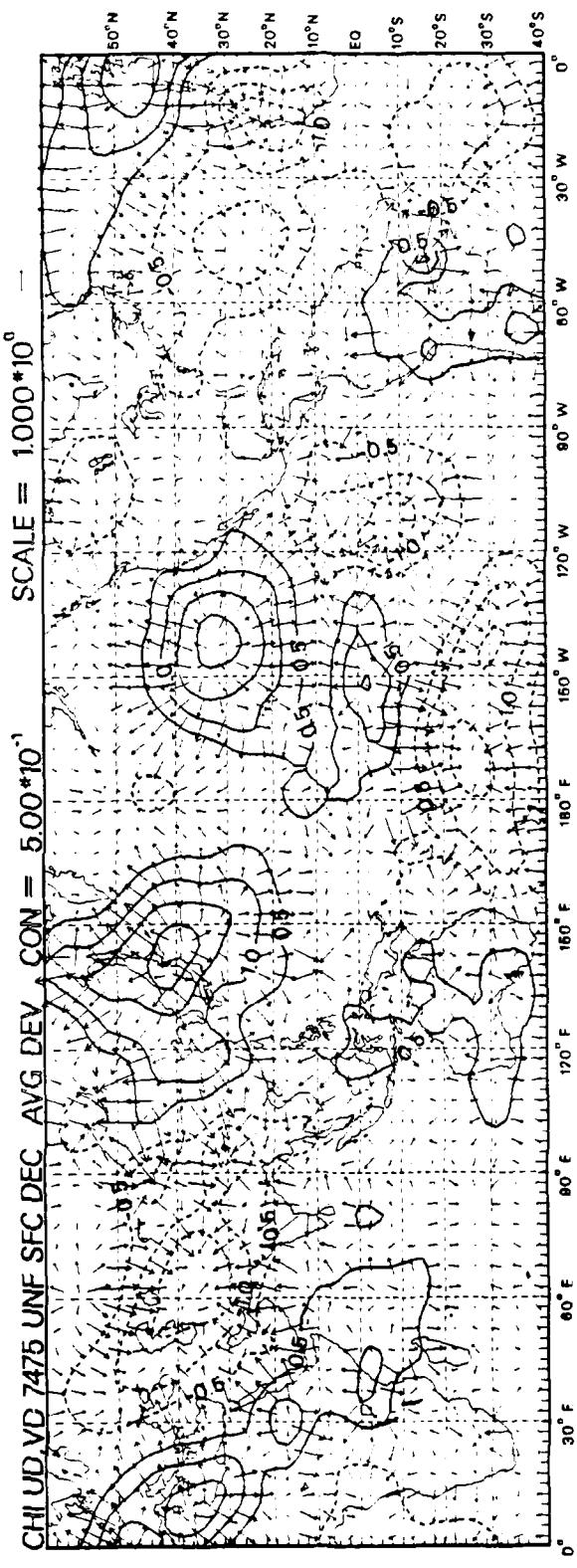
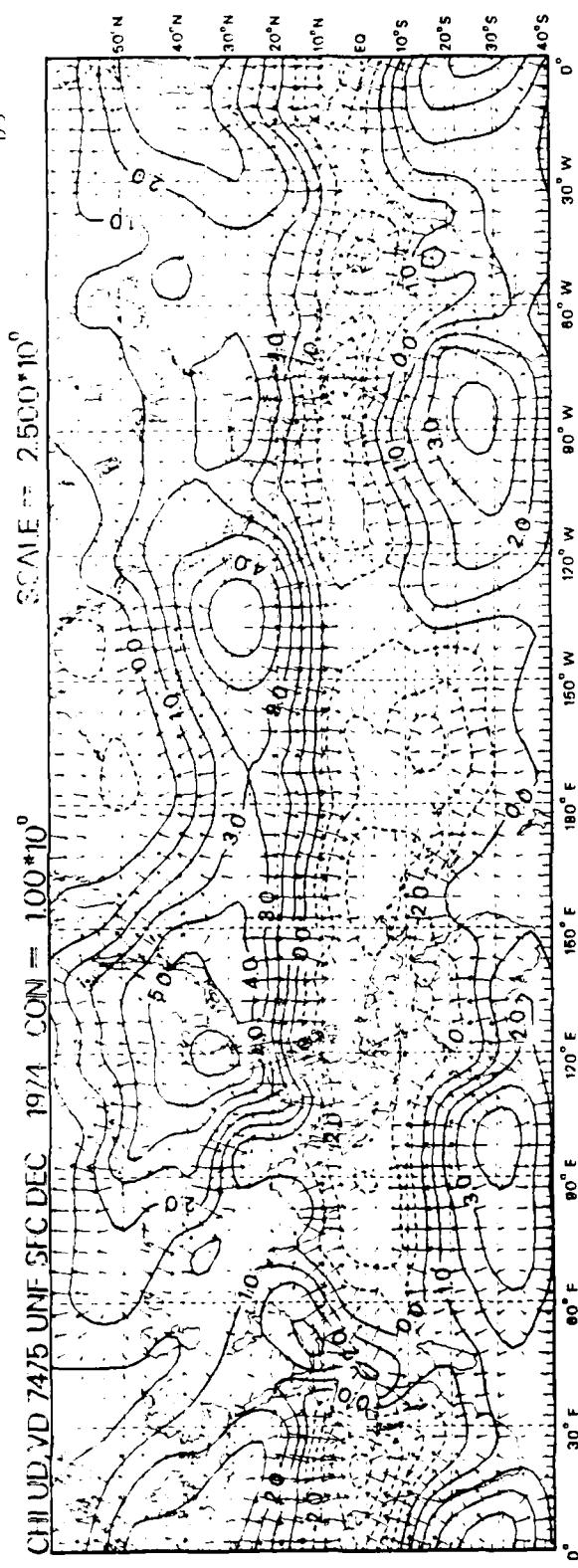
D1



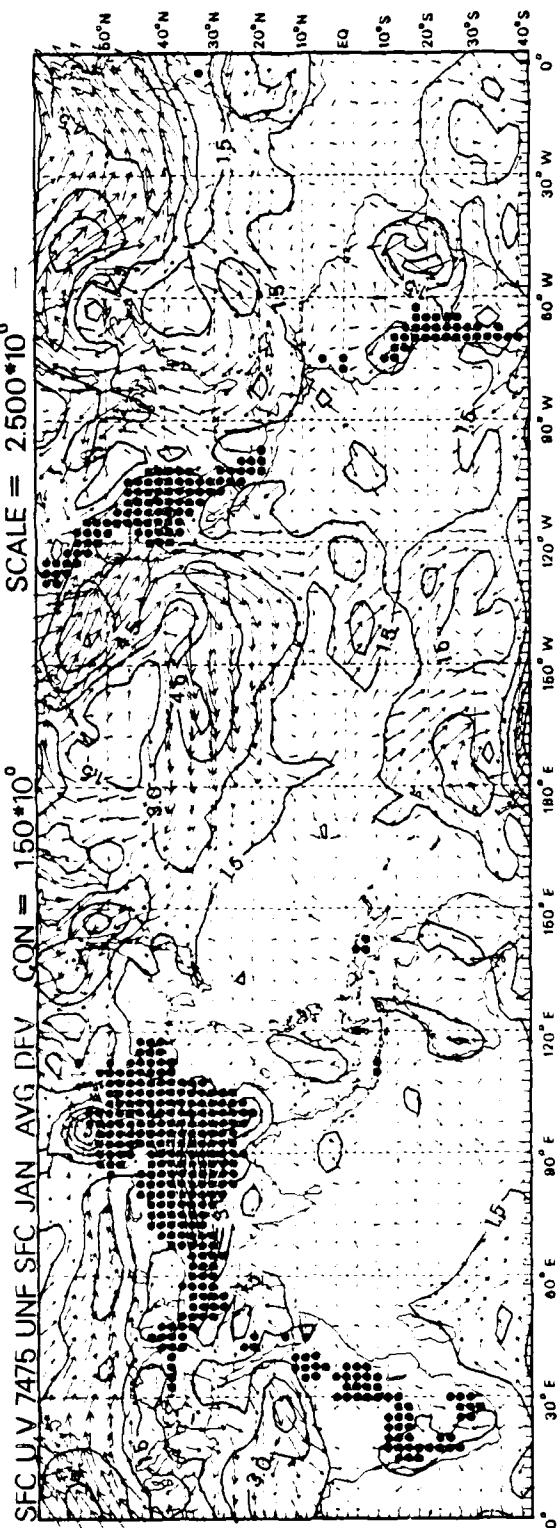
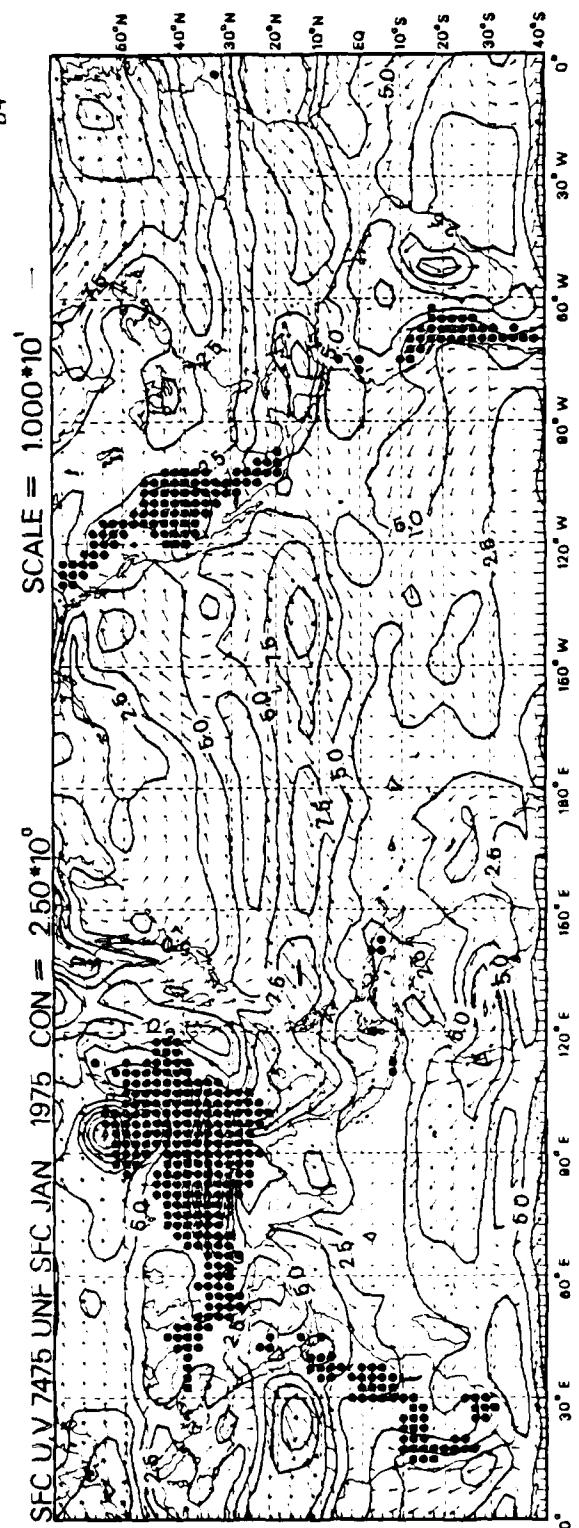
D2



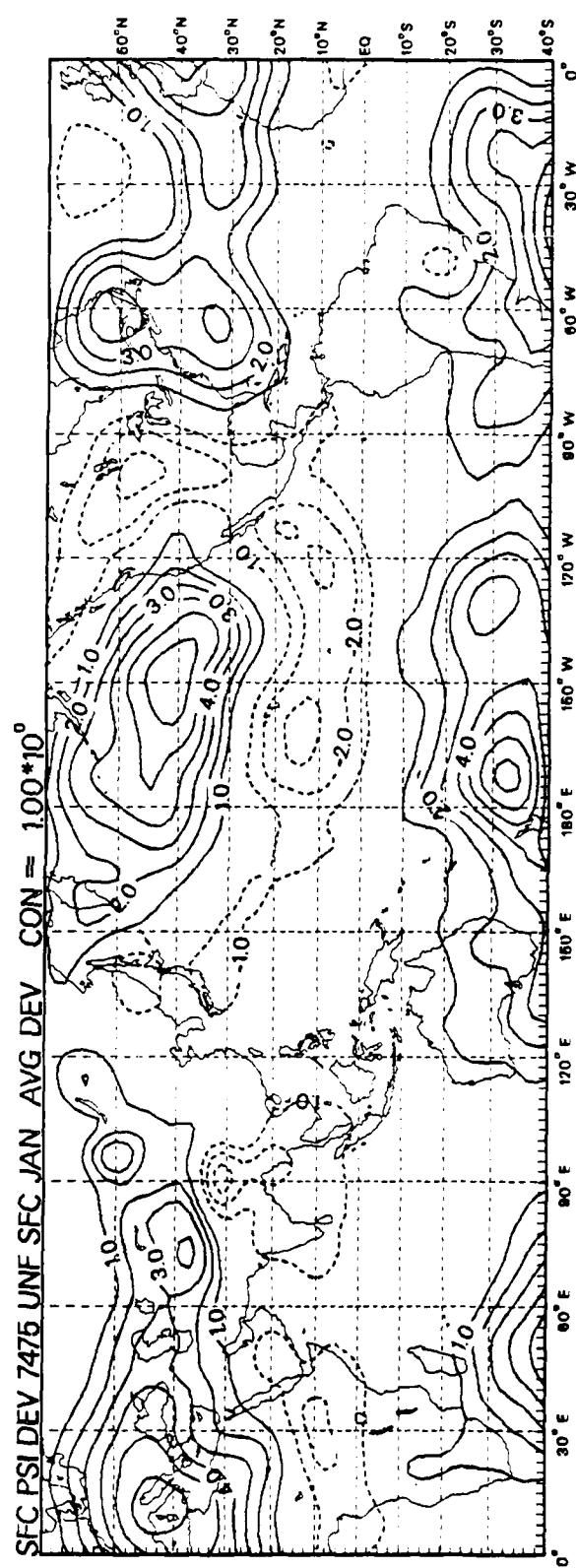
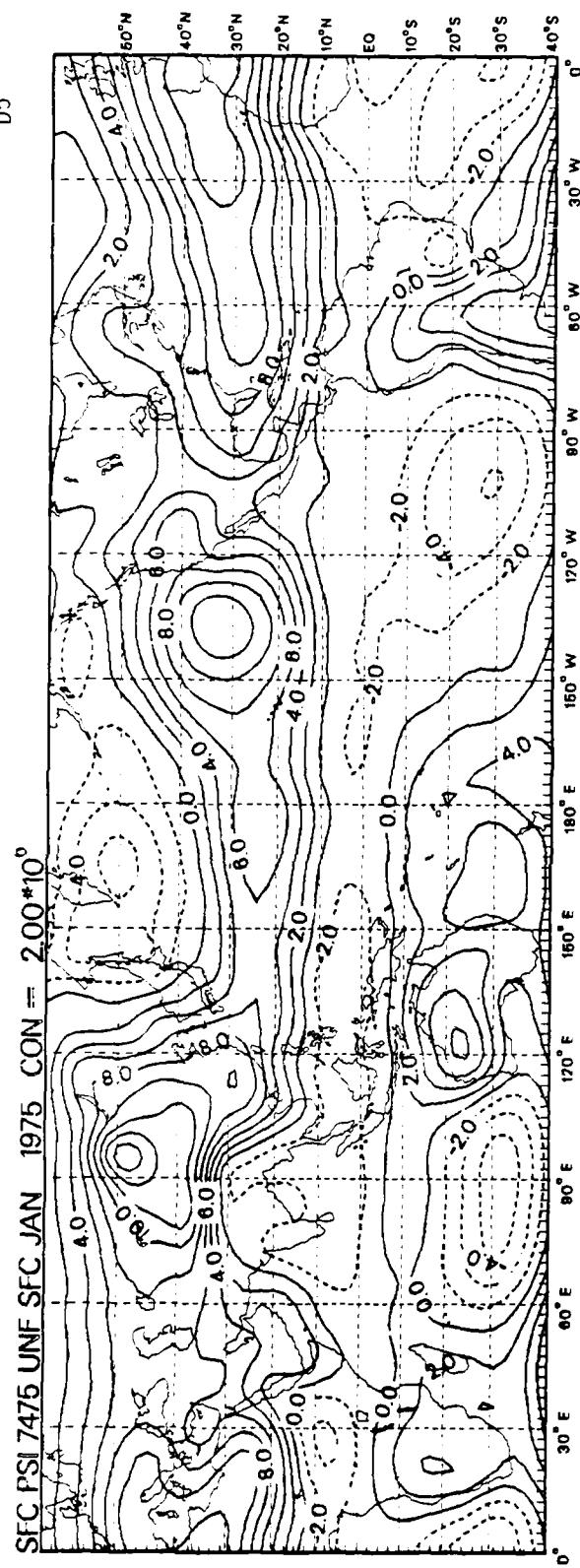
13



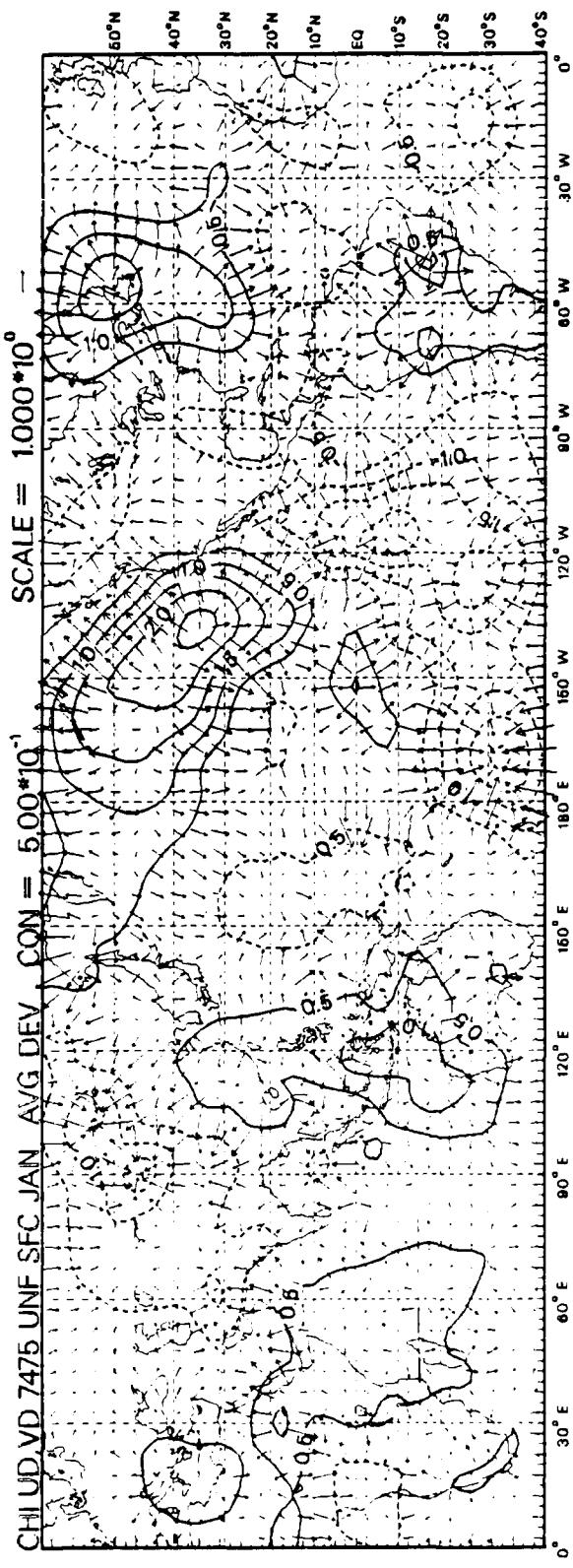
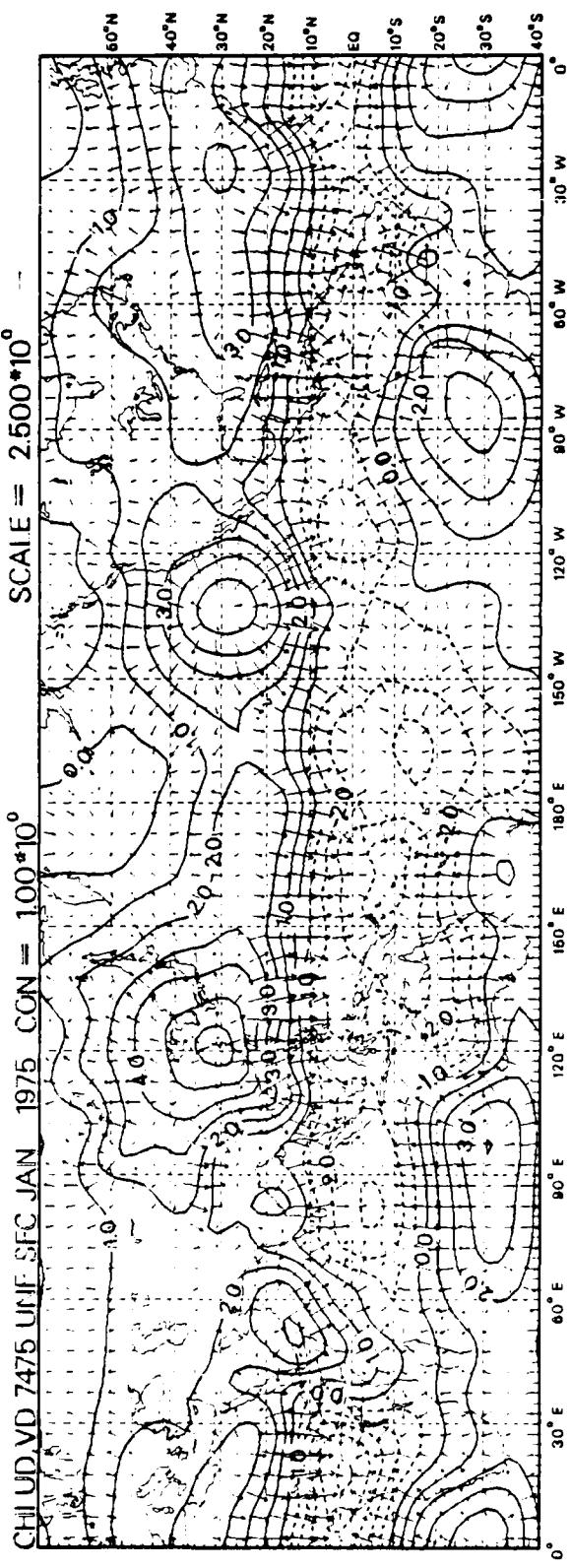
D4



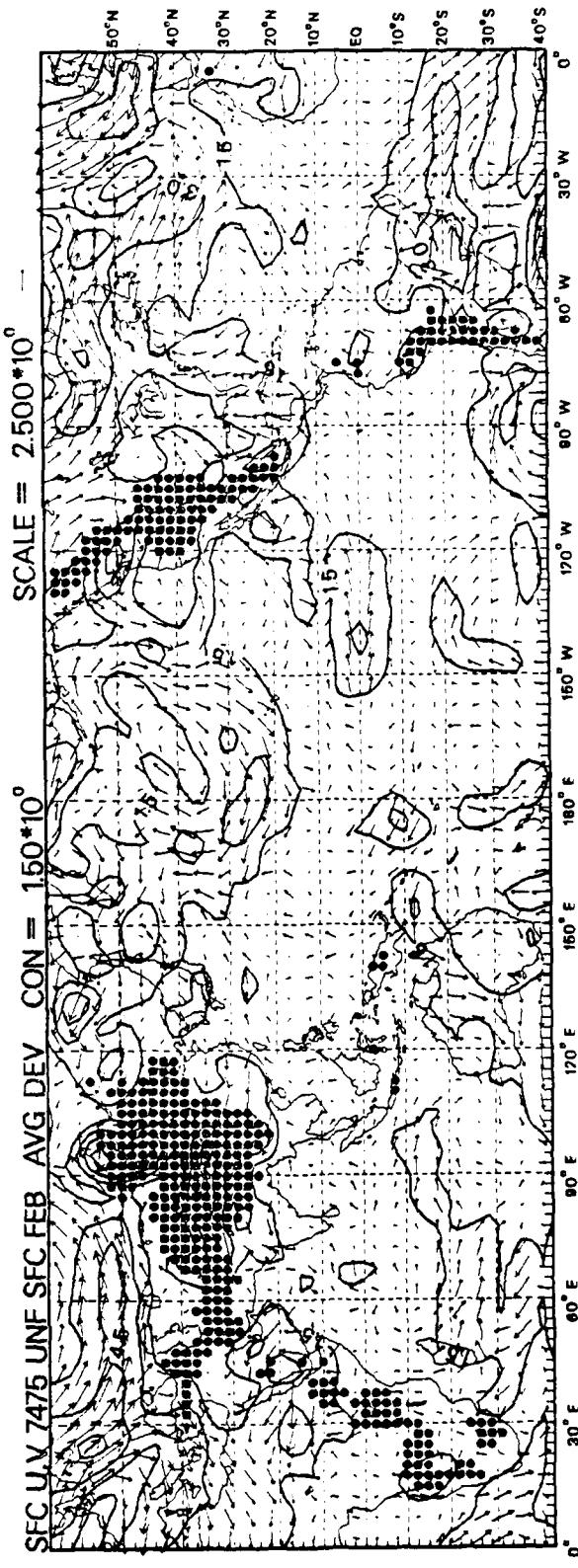
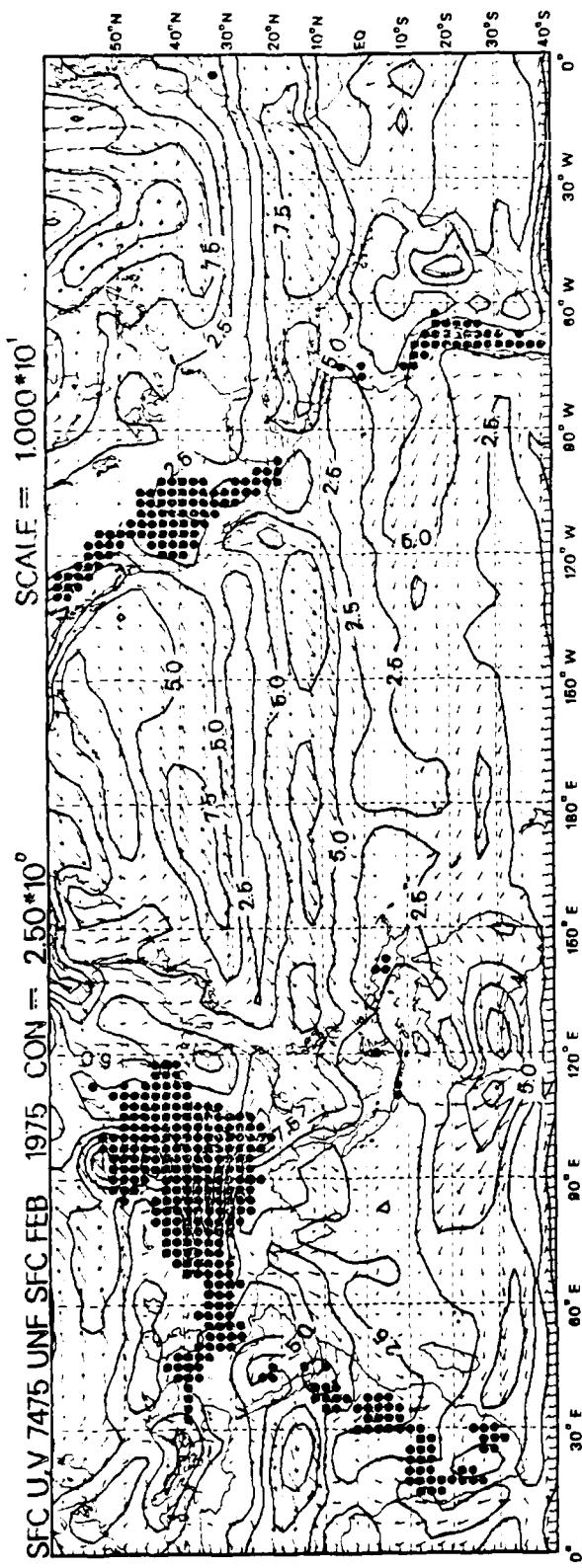
D5



06

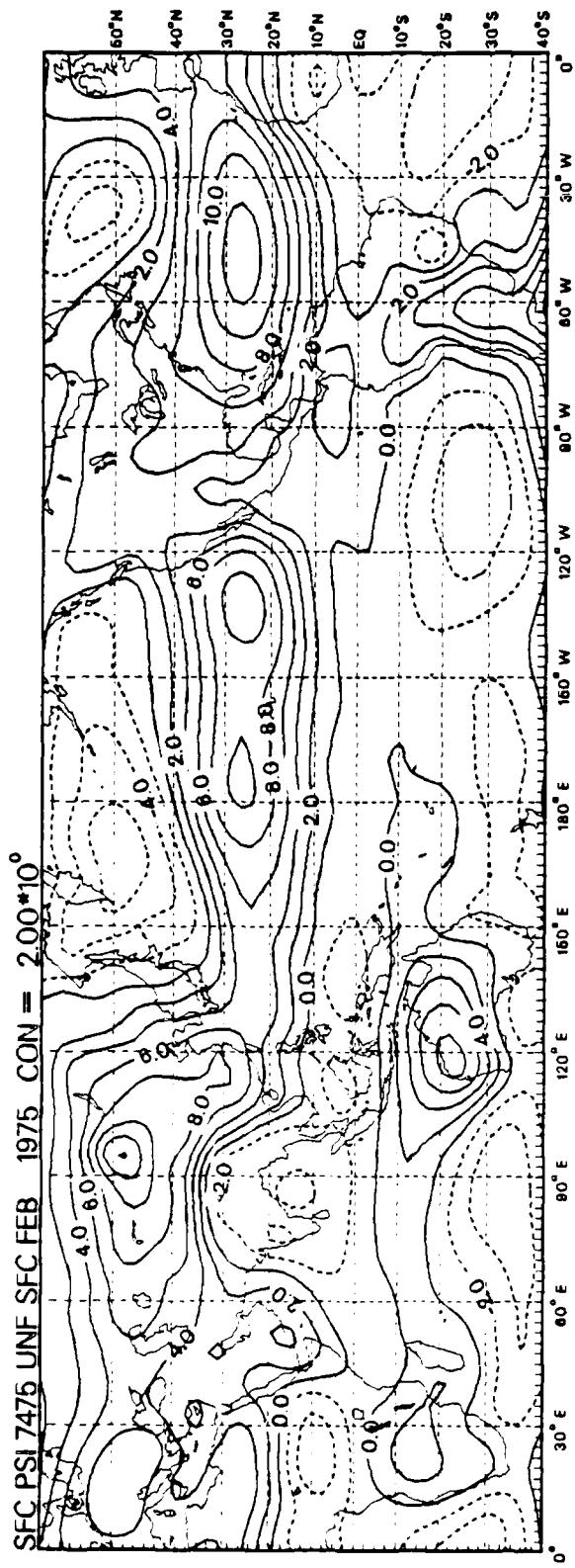


07

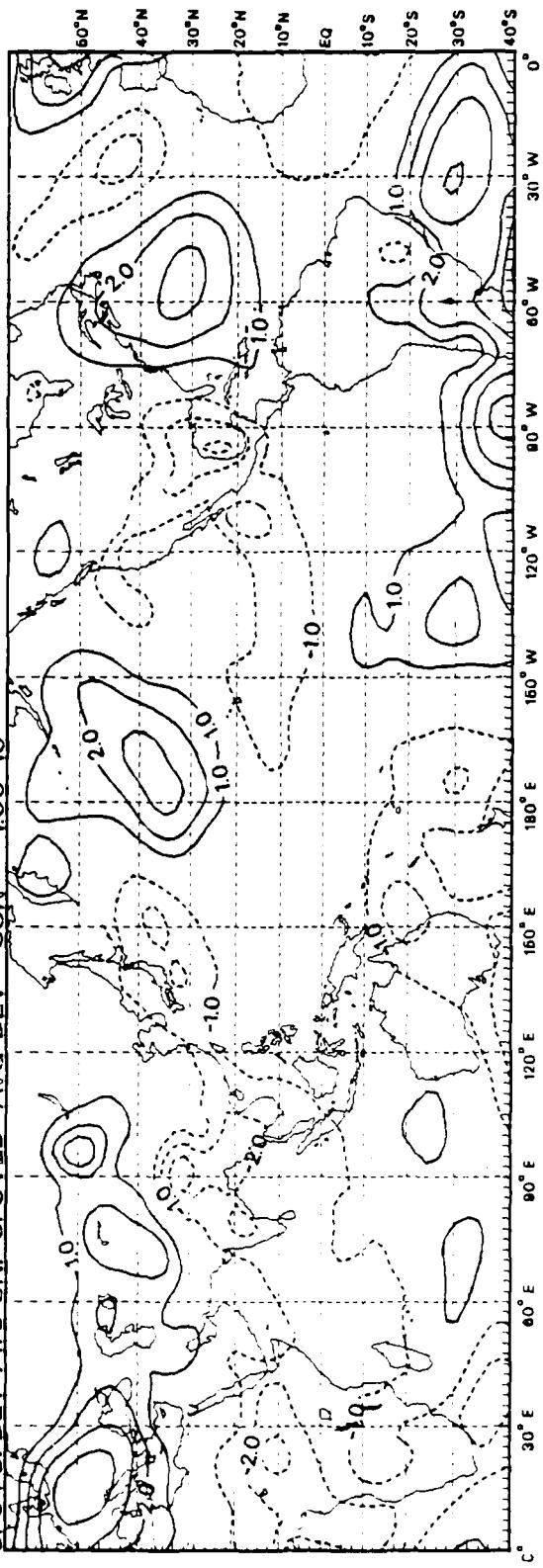


66

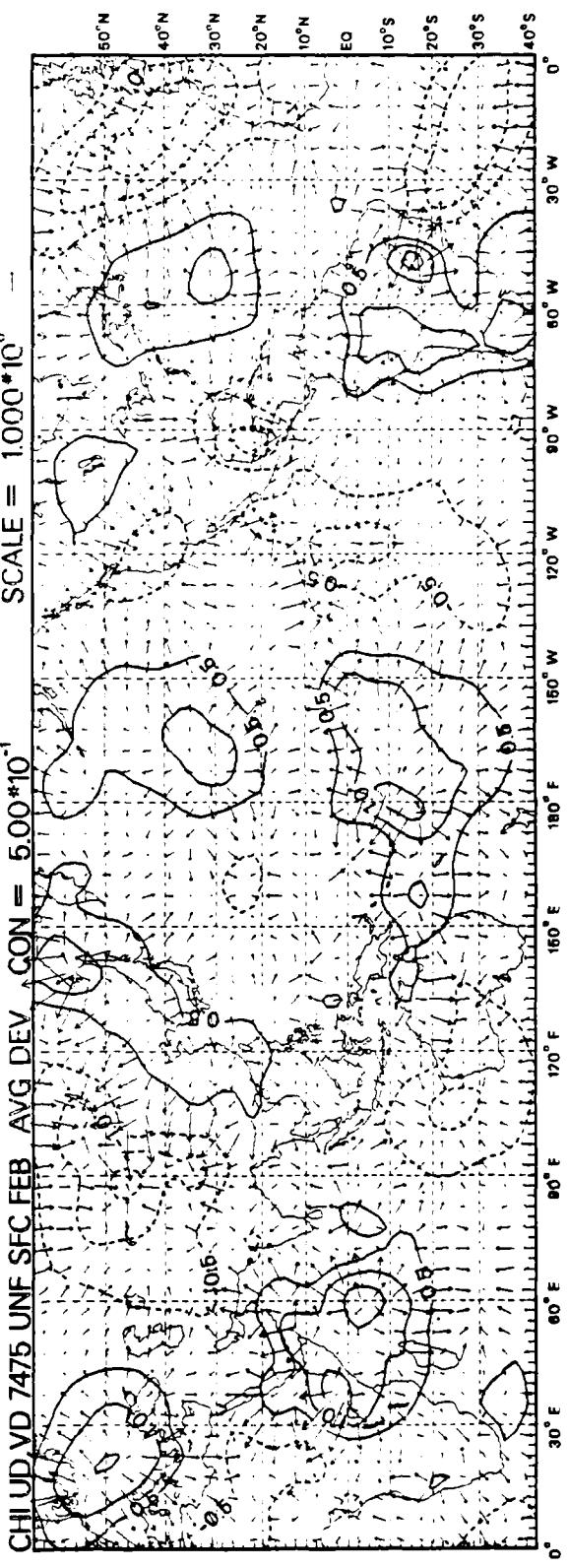
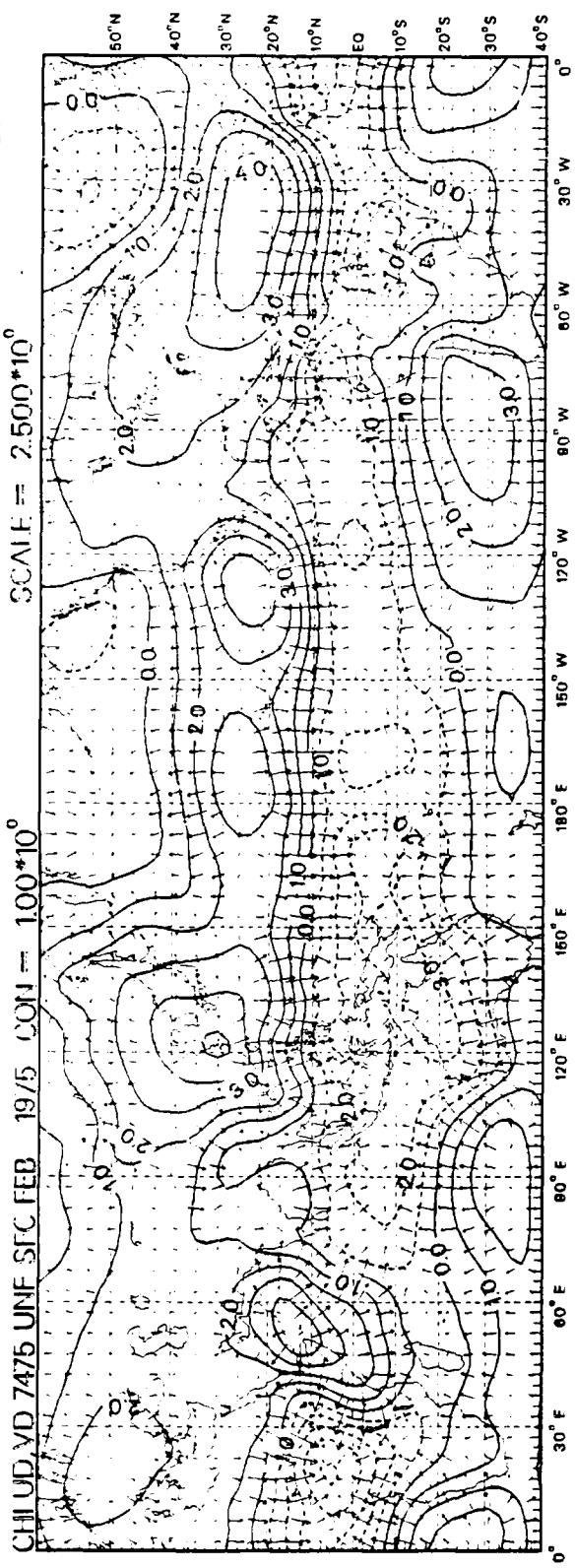
D8



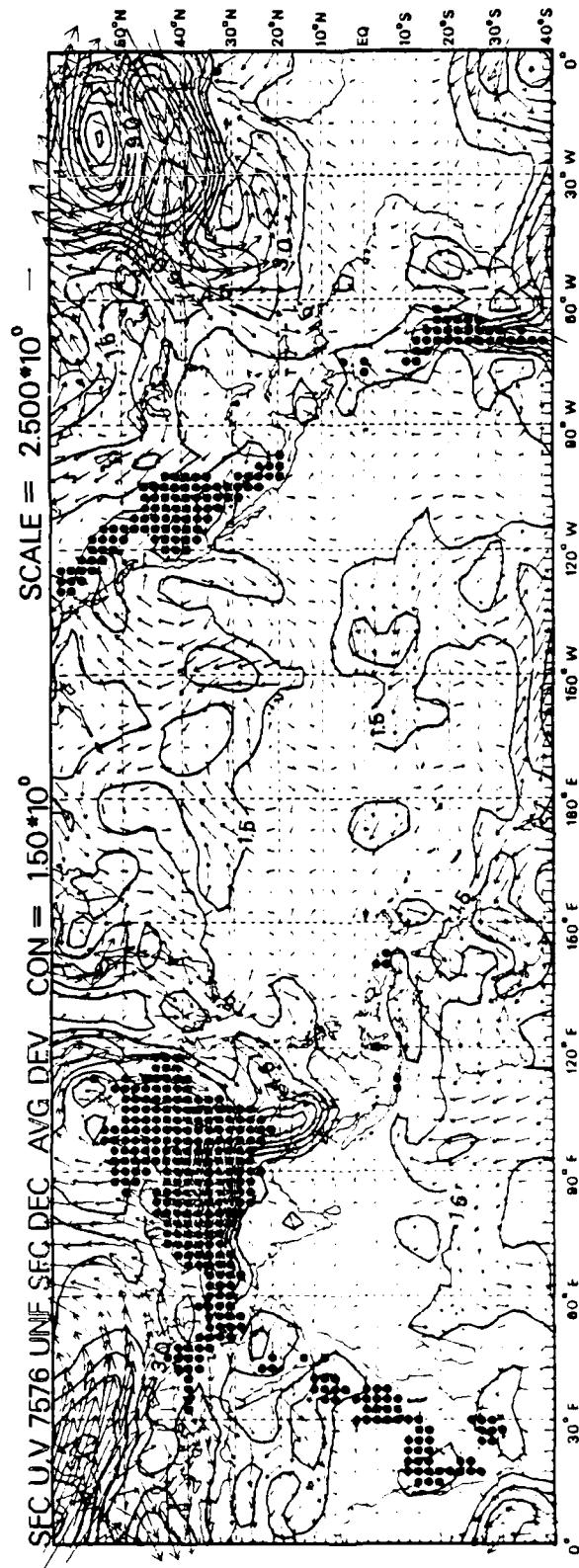
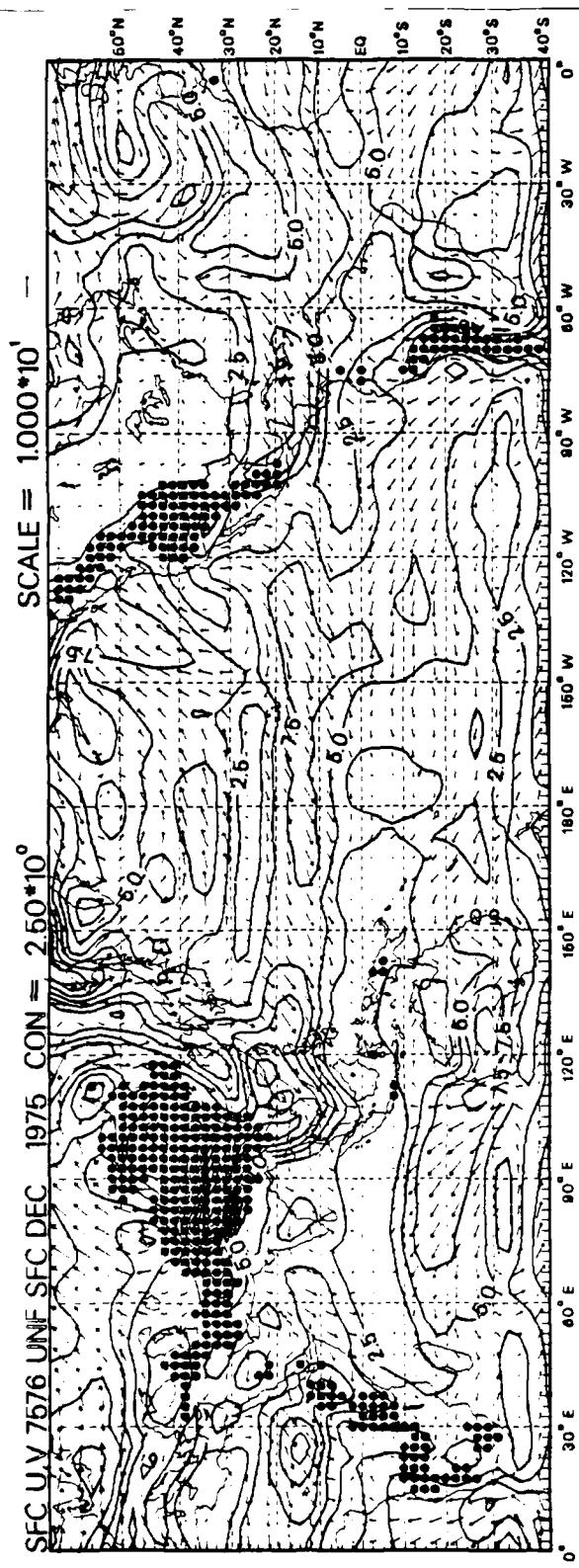
SFC PSI 7475 UNF SFC FEB AVG DEV CON = $1.00 \cdot 10^6$



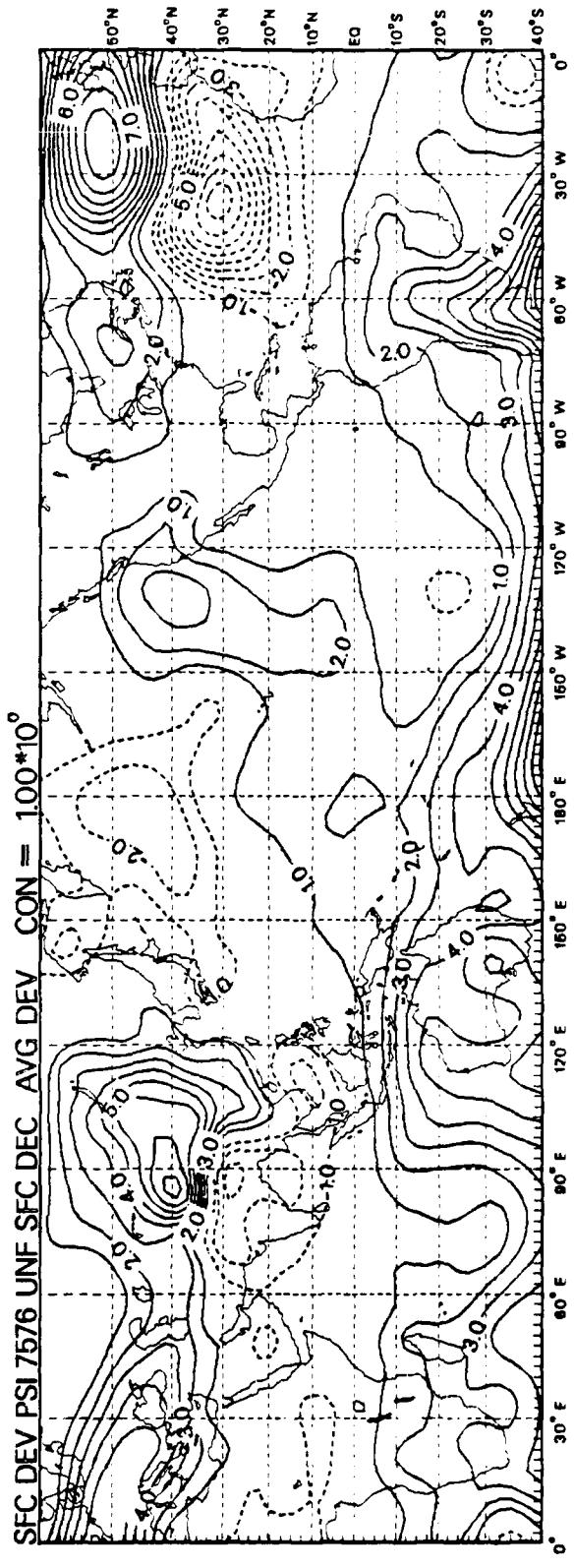
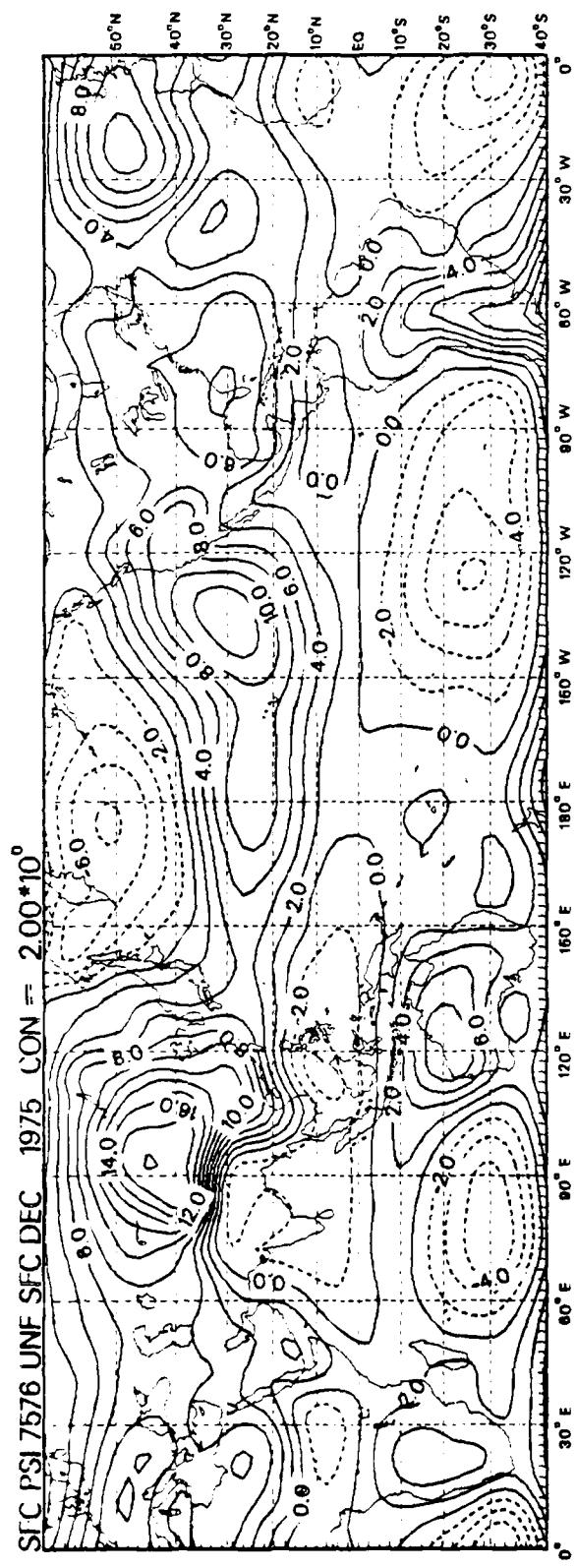
D9



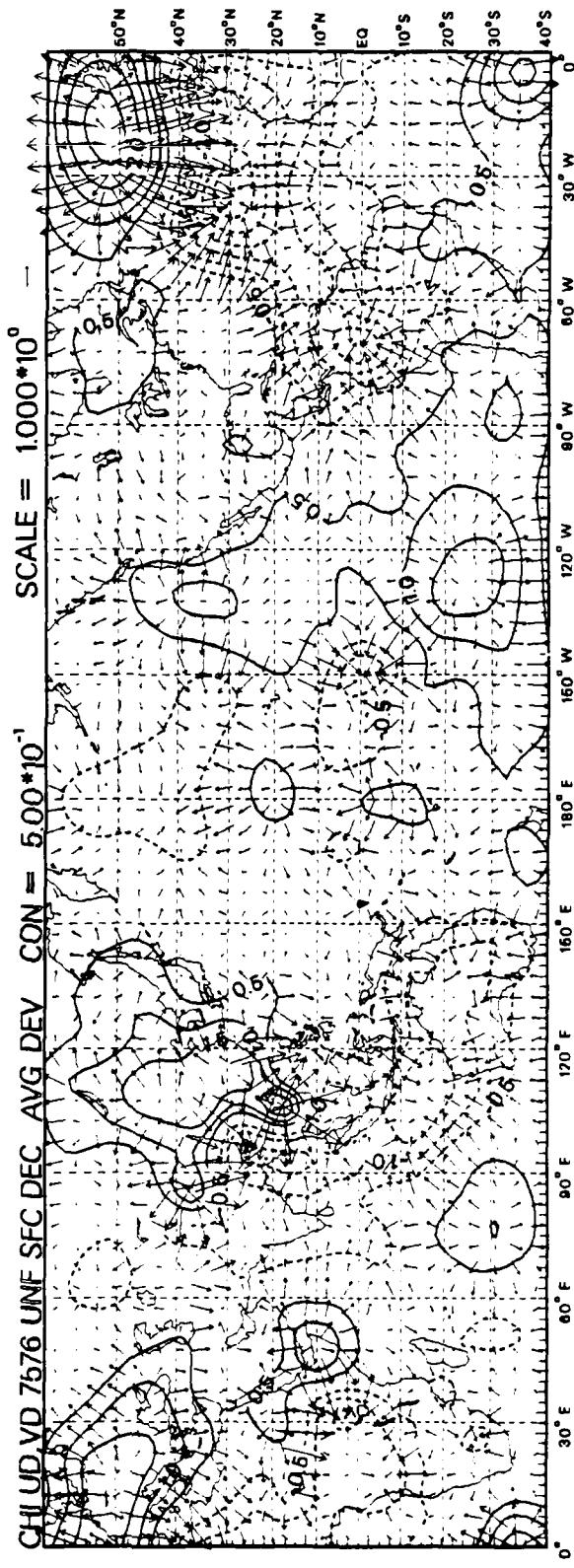
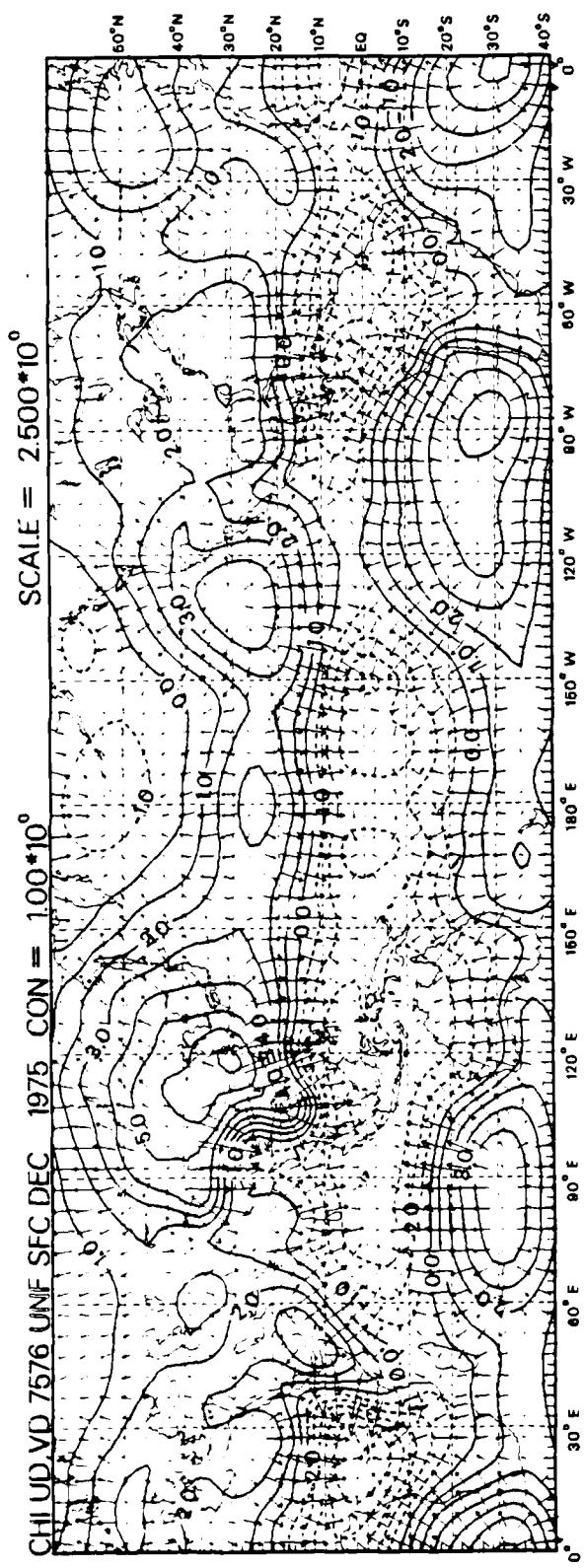
D10



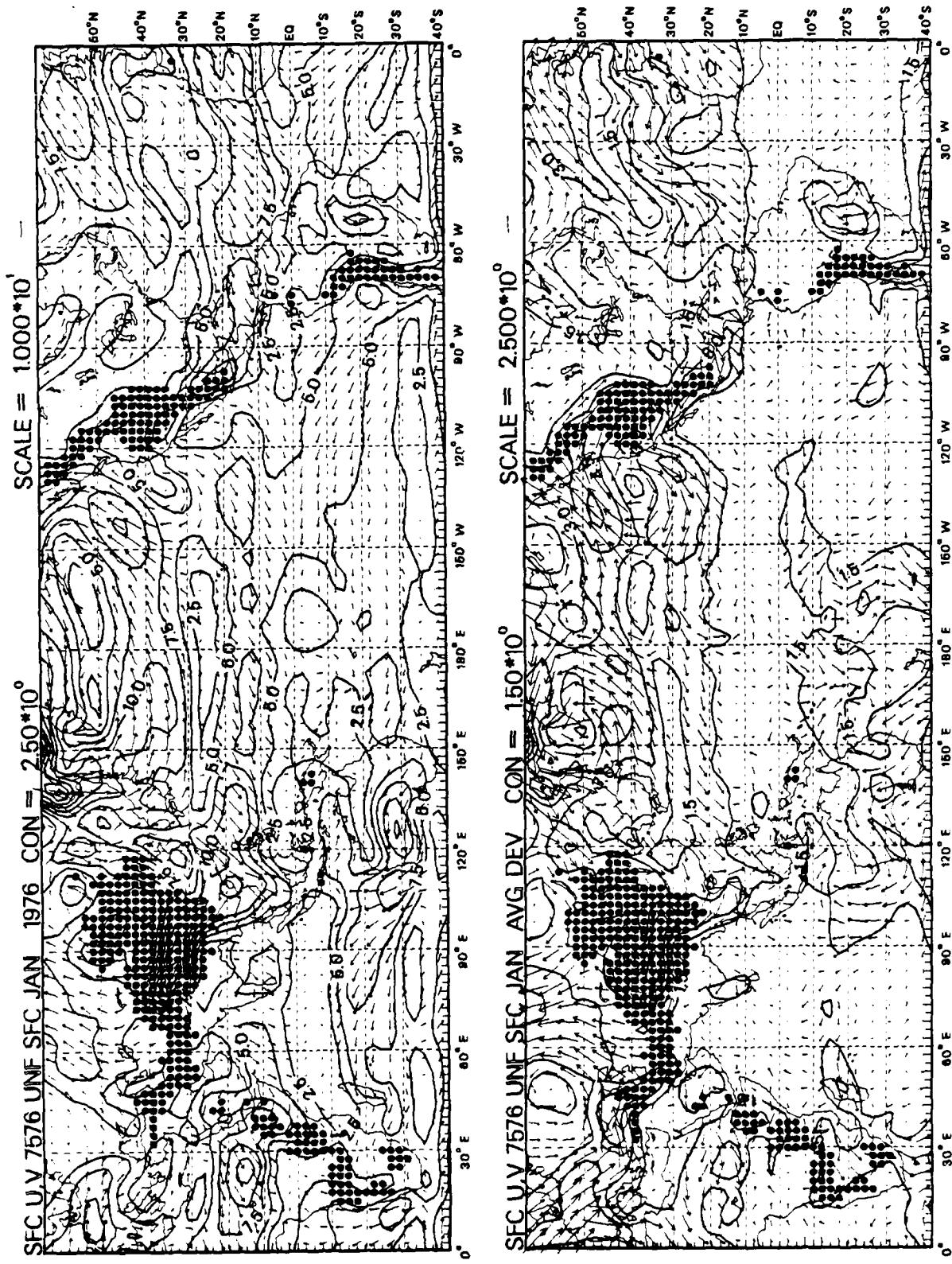
D11

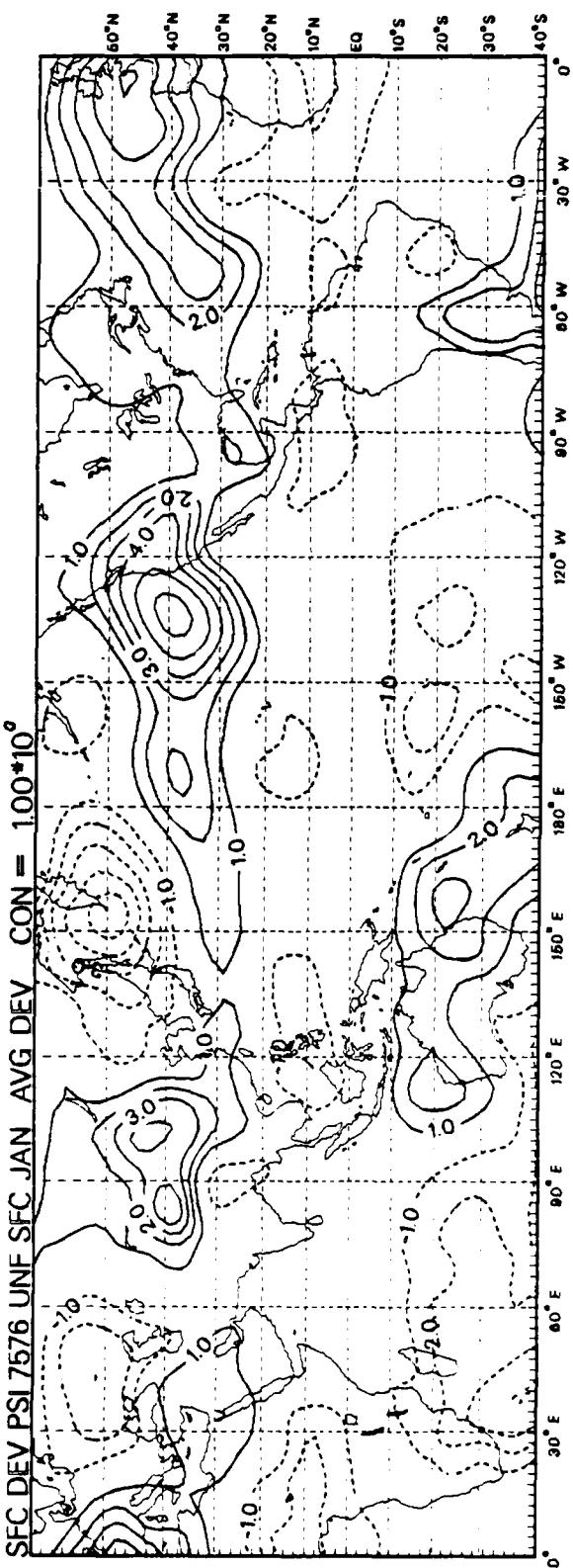
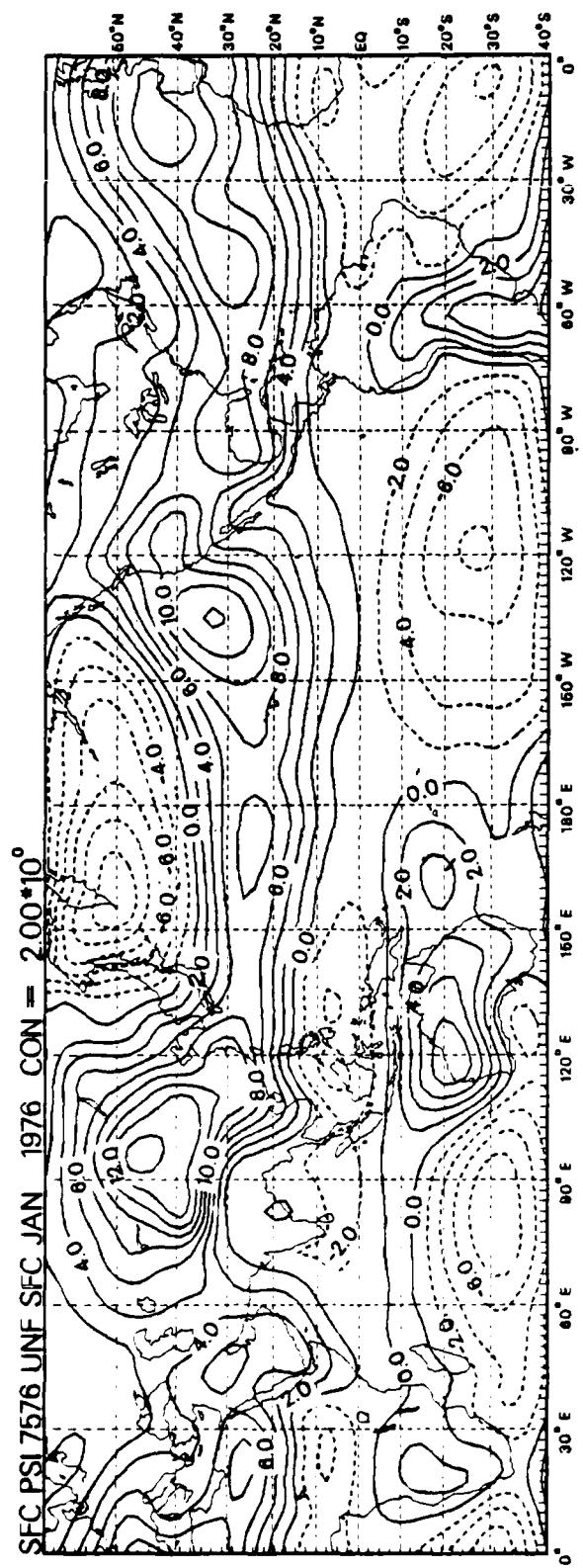


D12

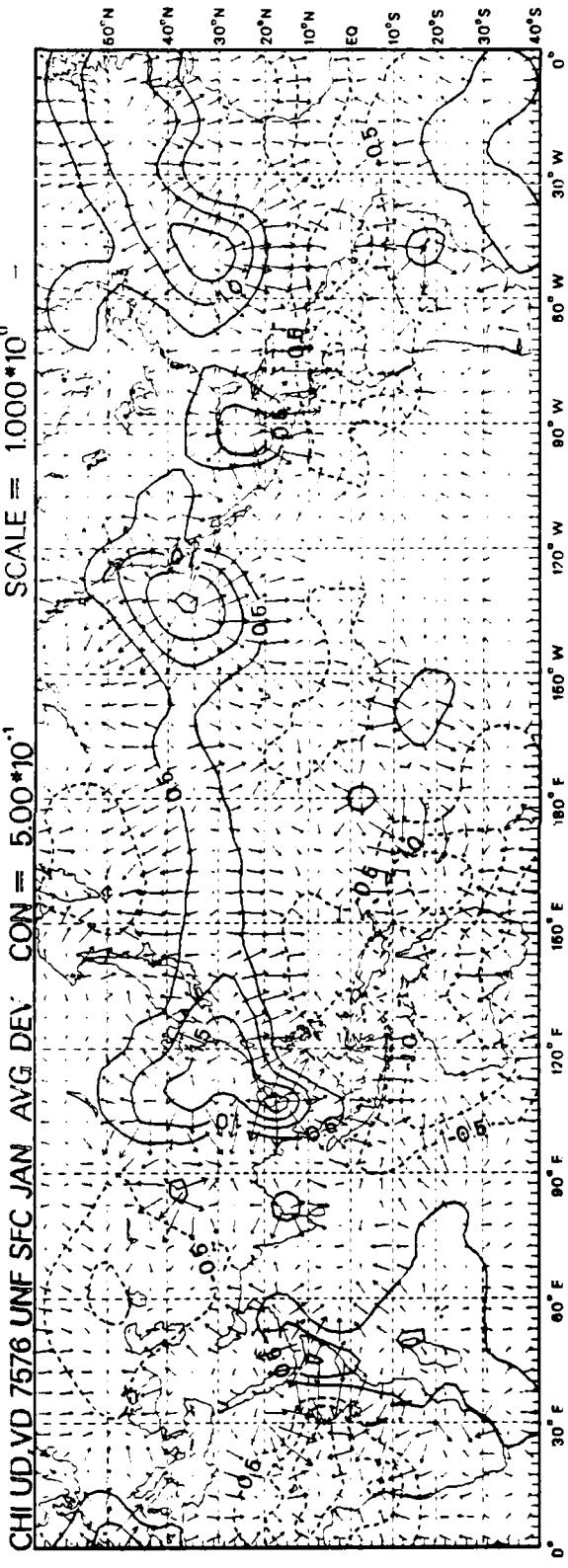
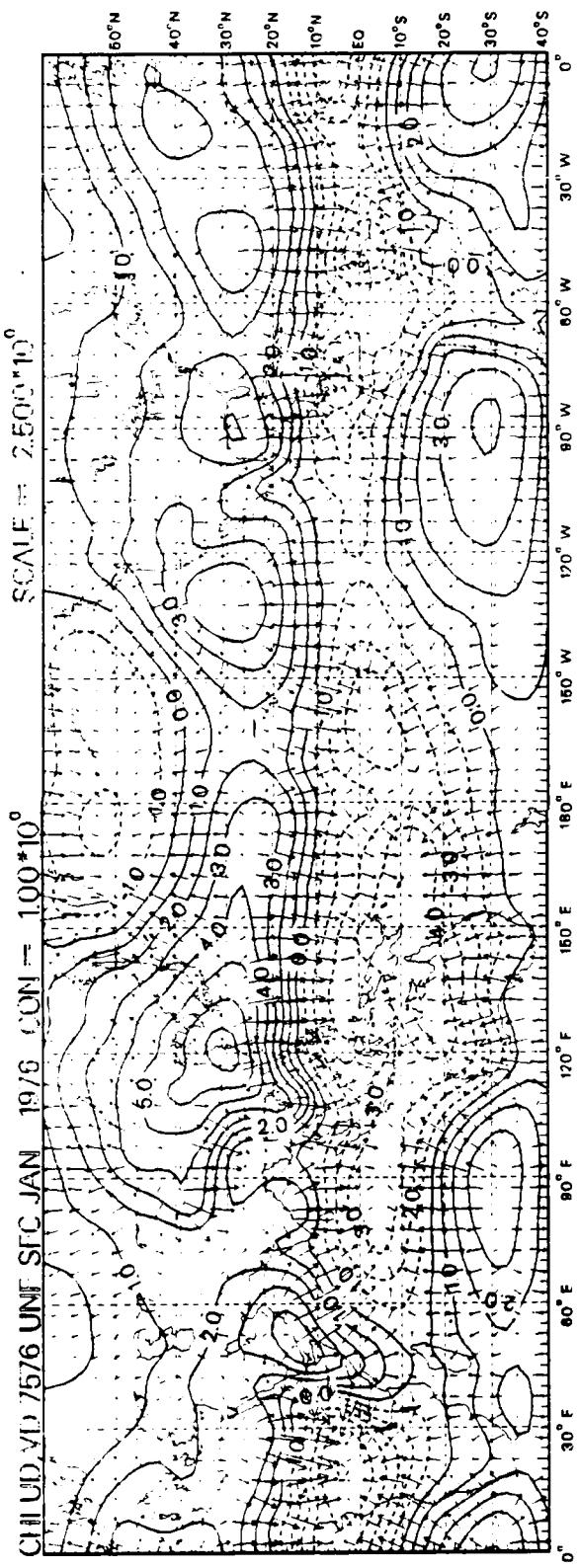


D13

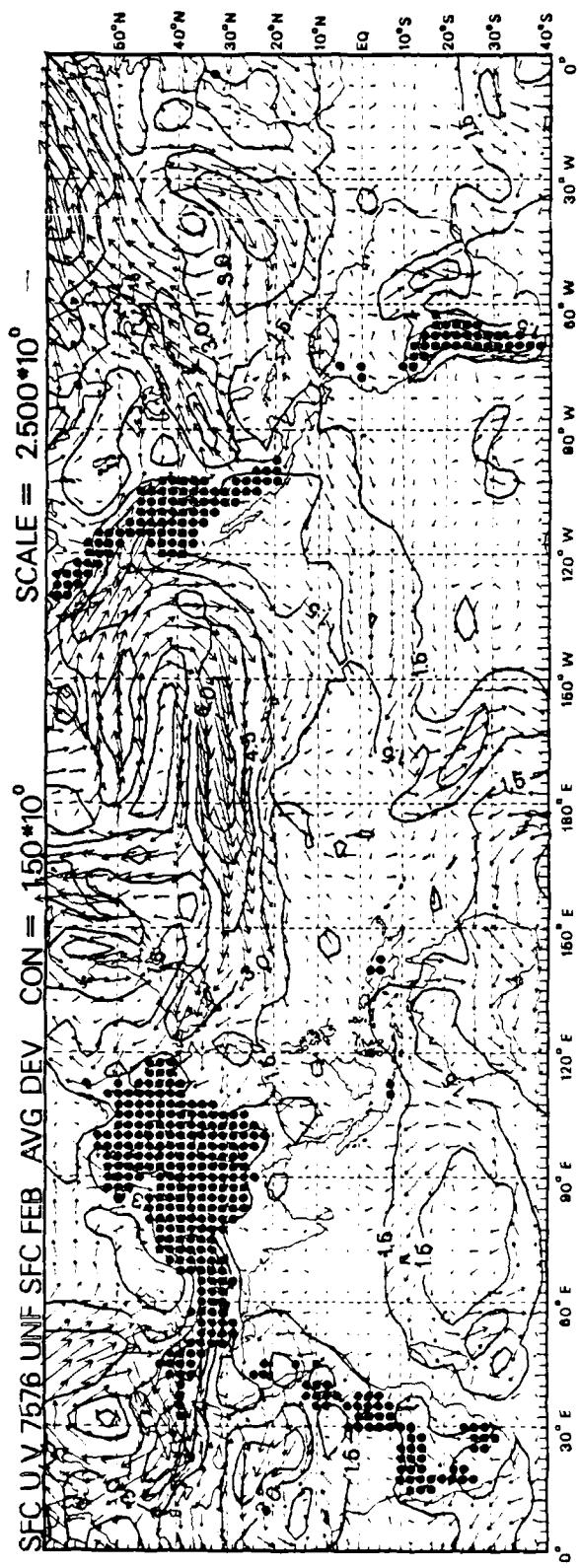
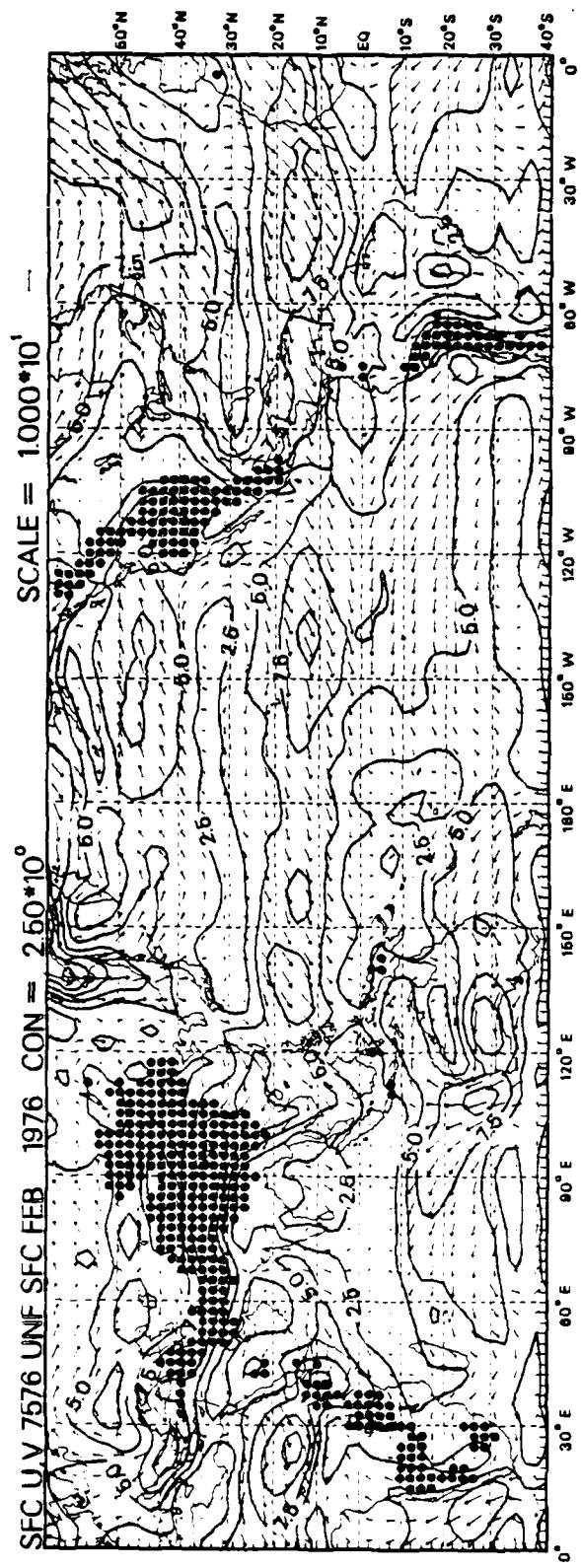


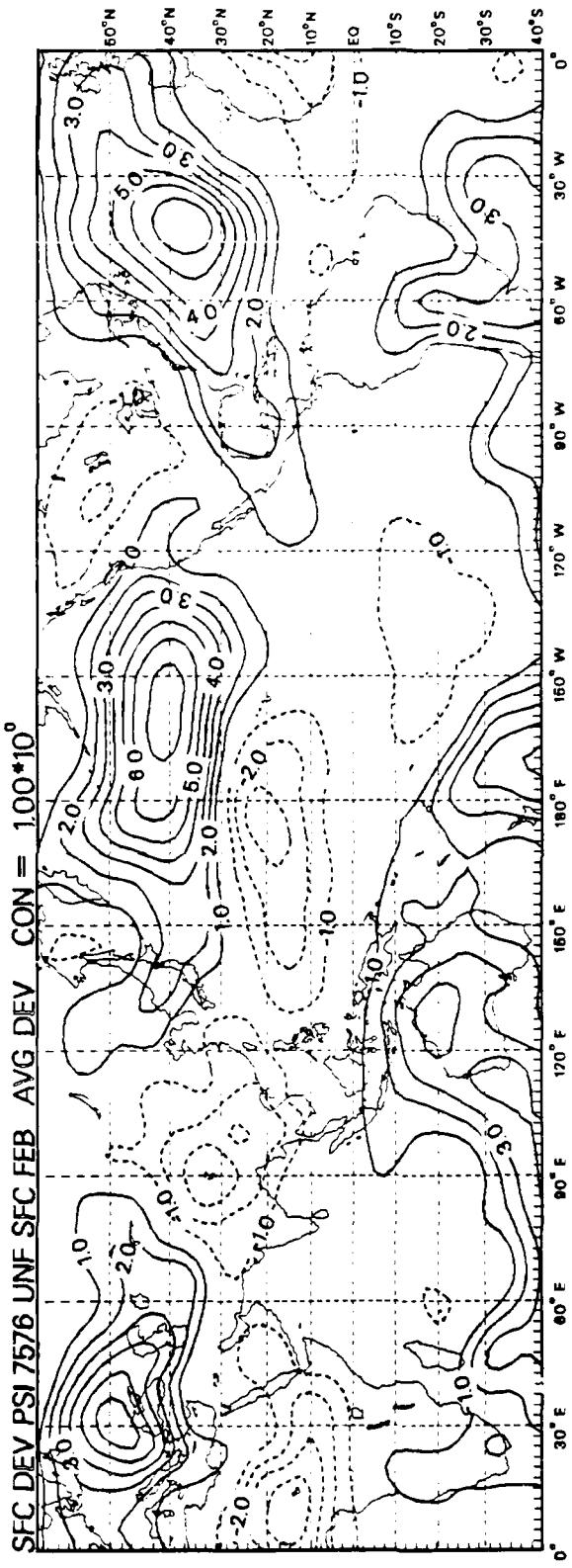
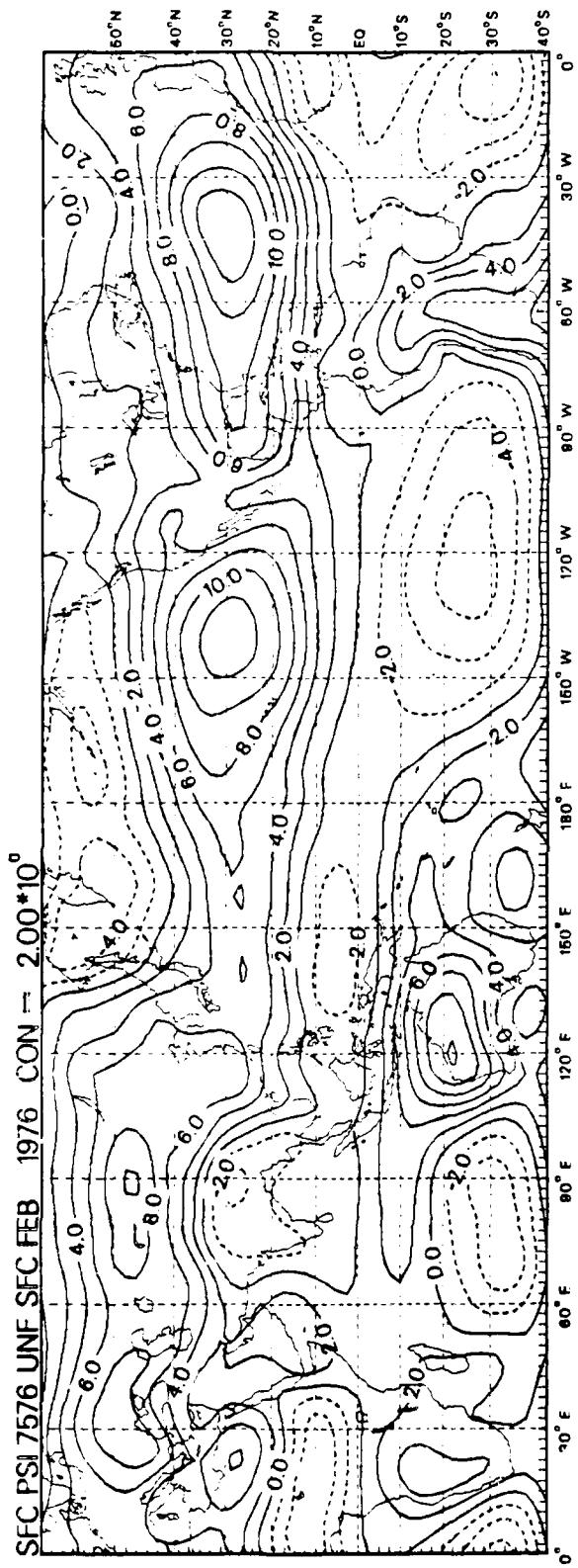


D15

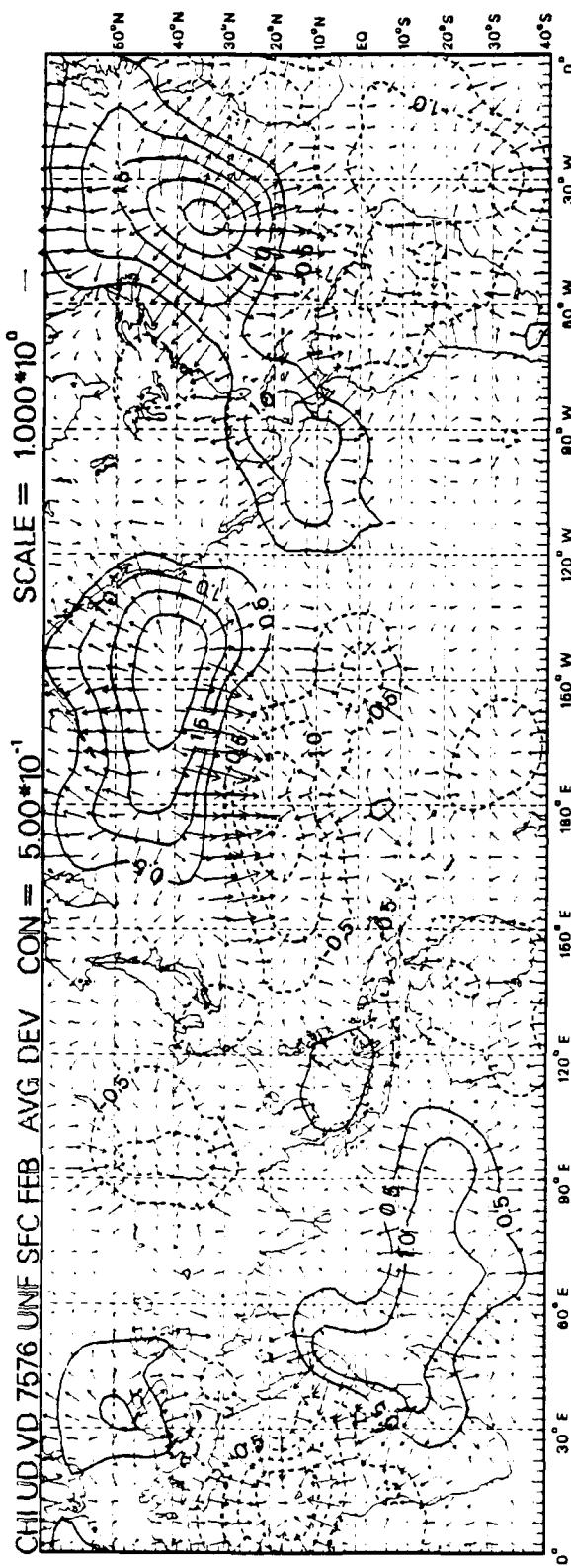
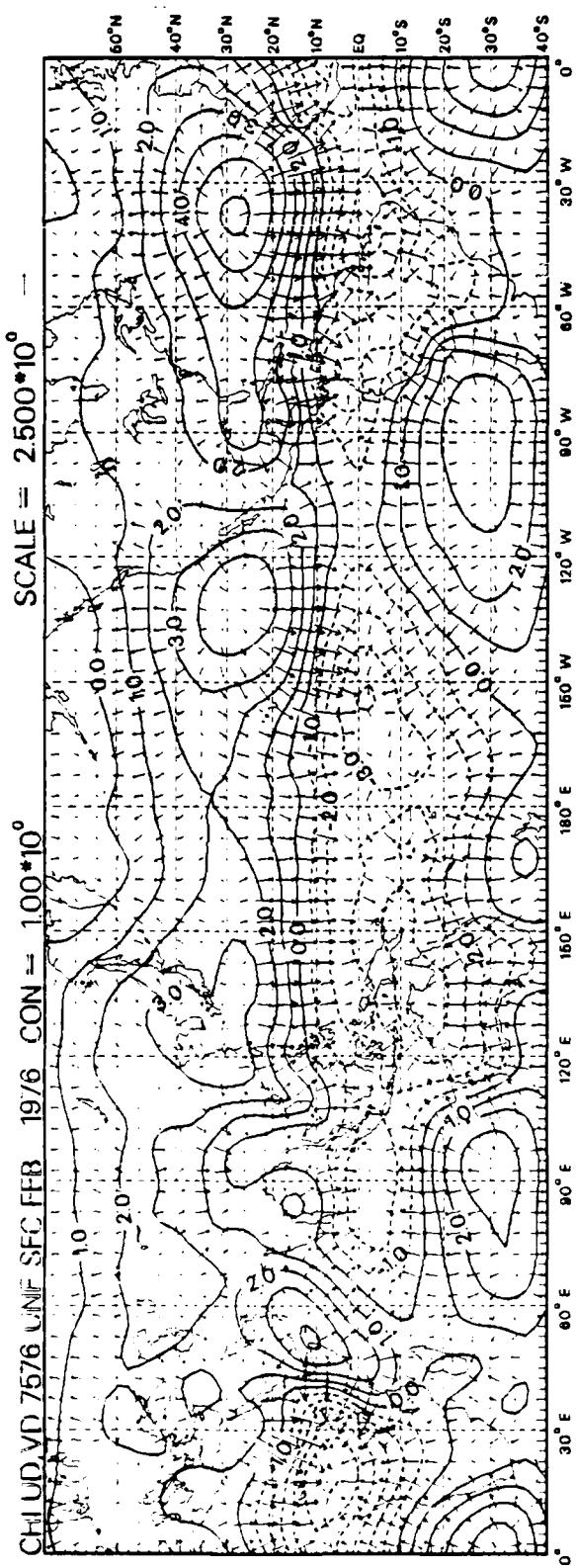


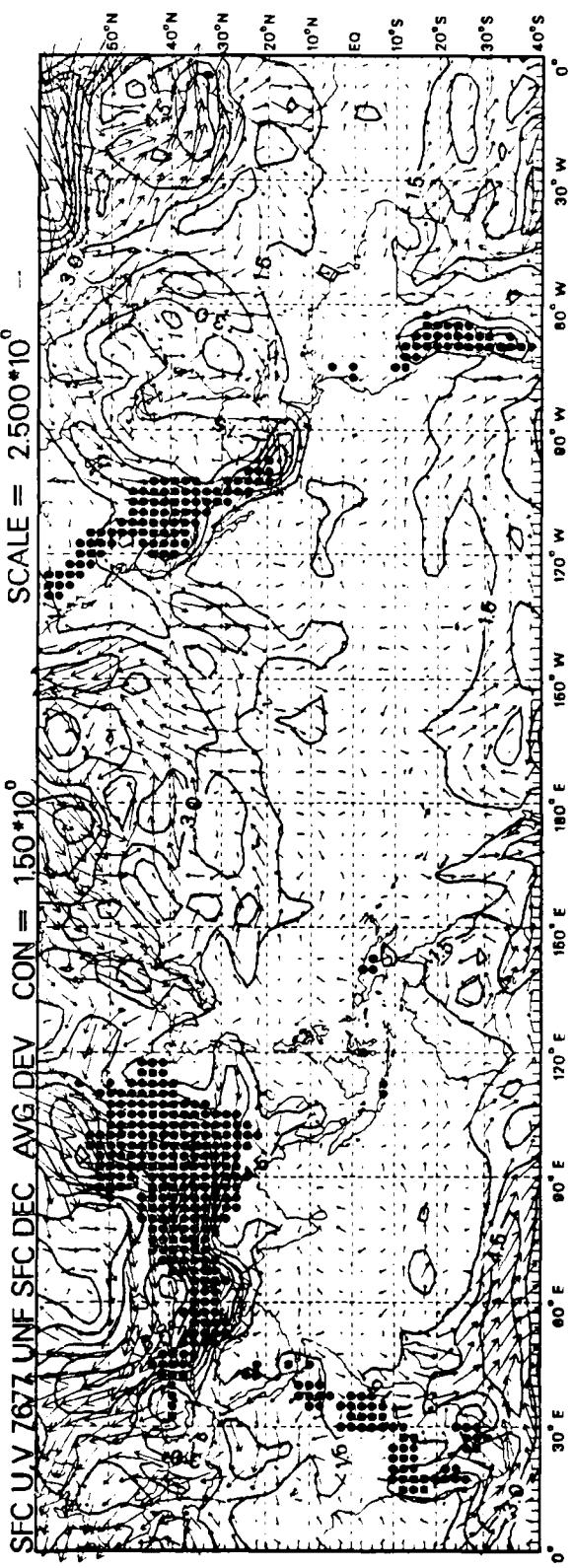
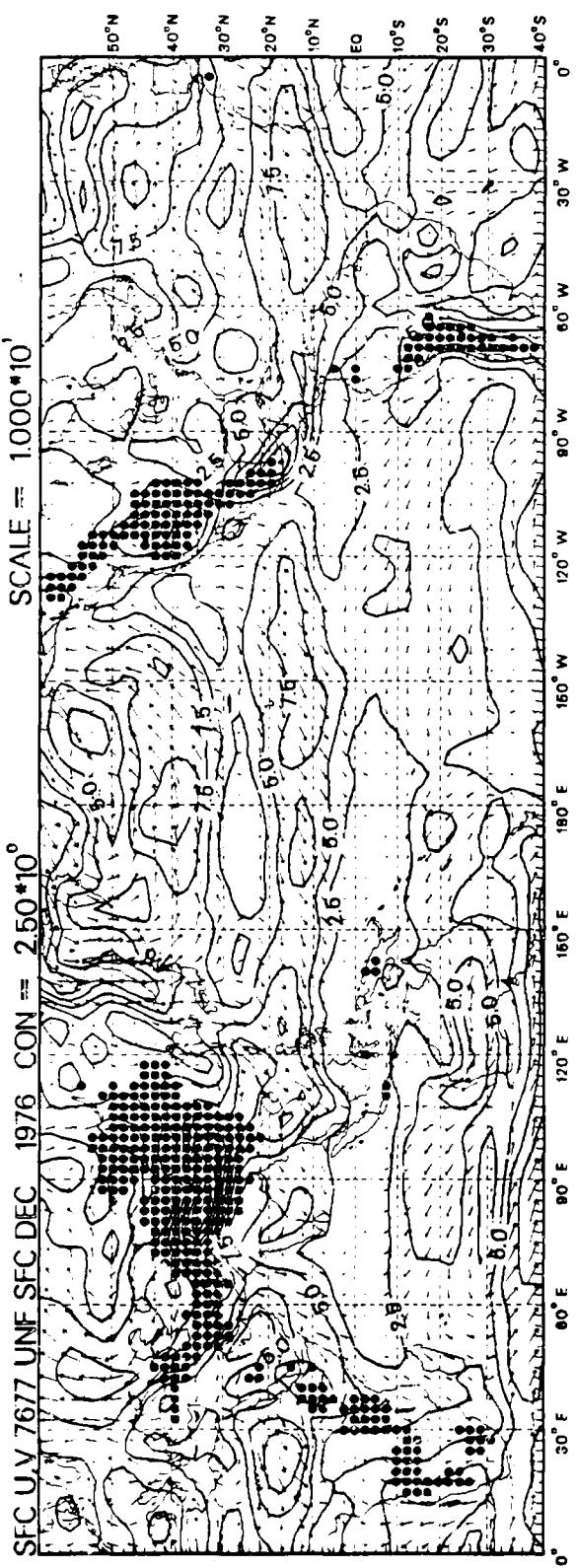
016



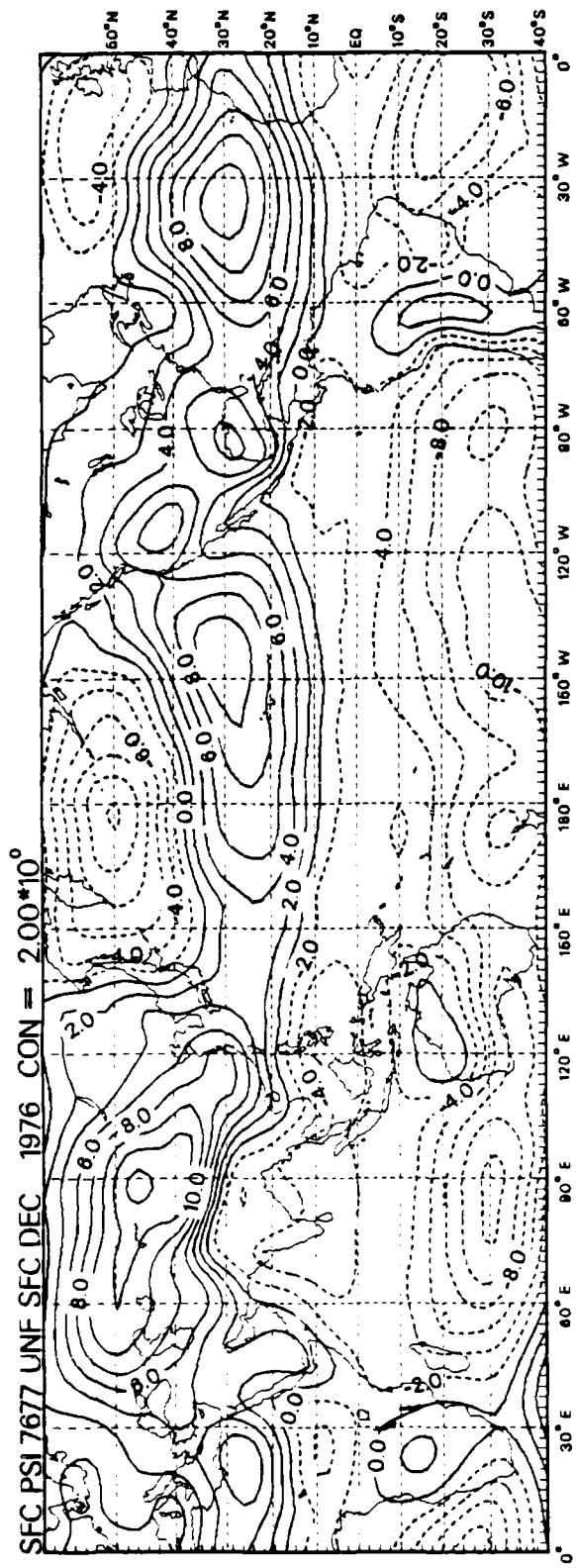


D18

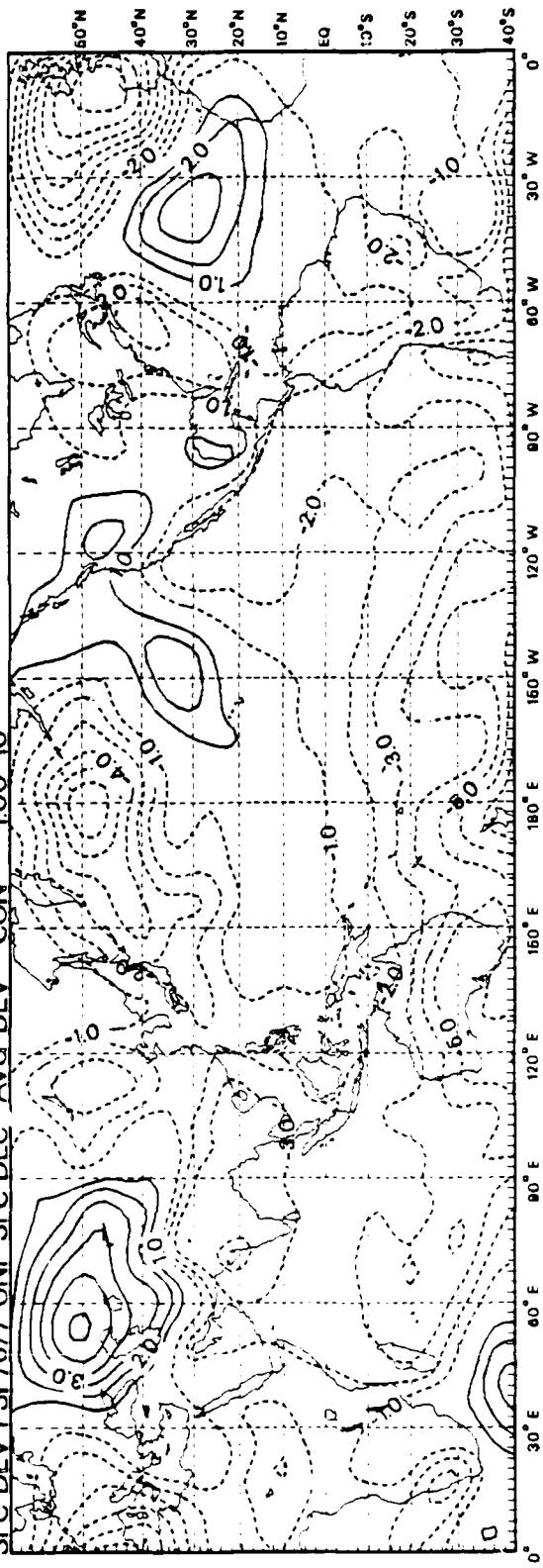




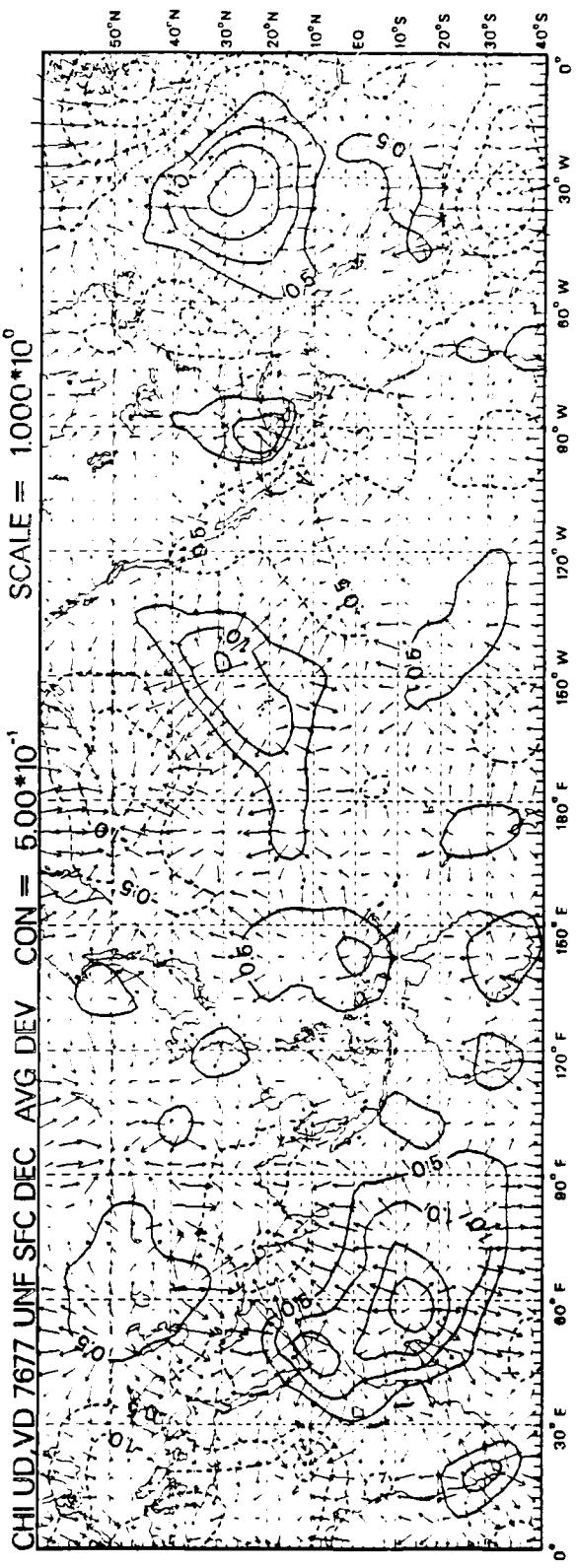
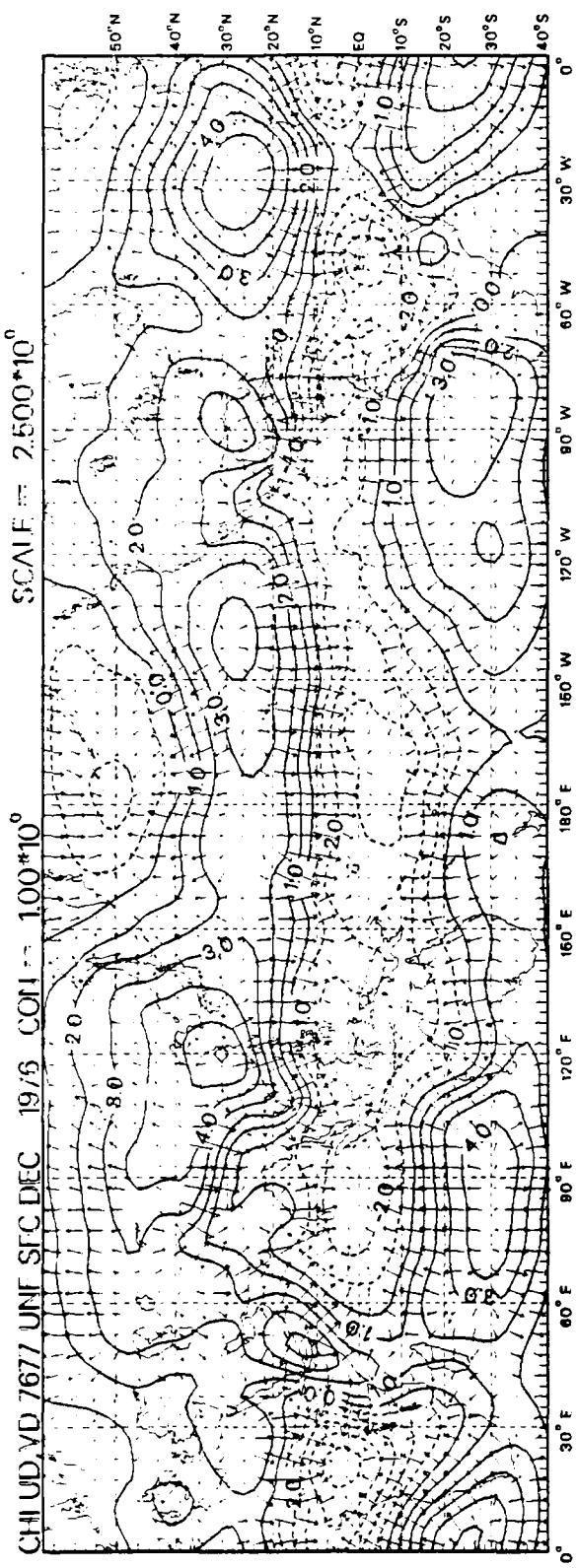
D20

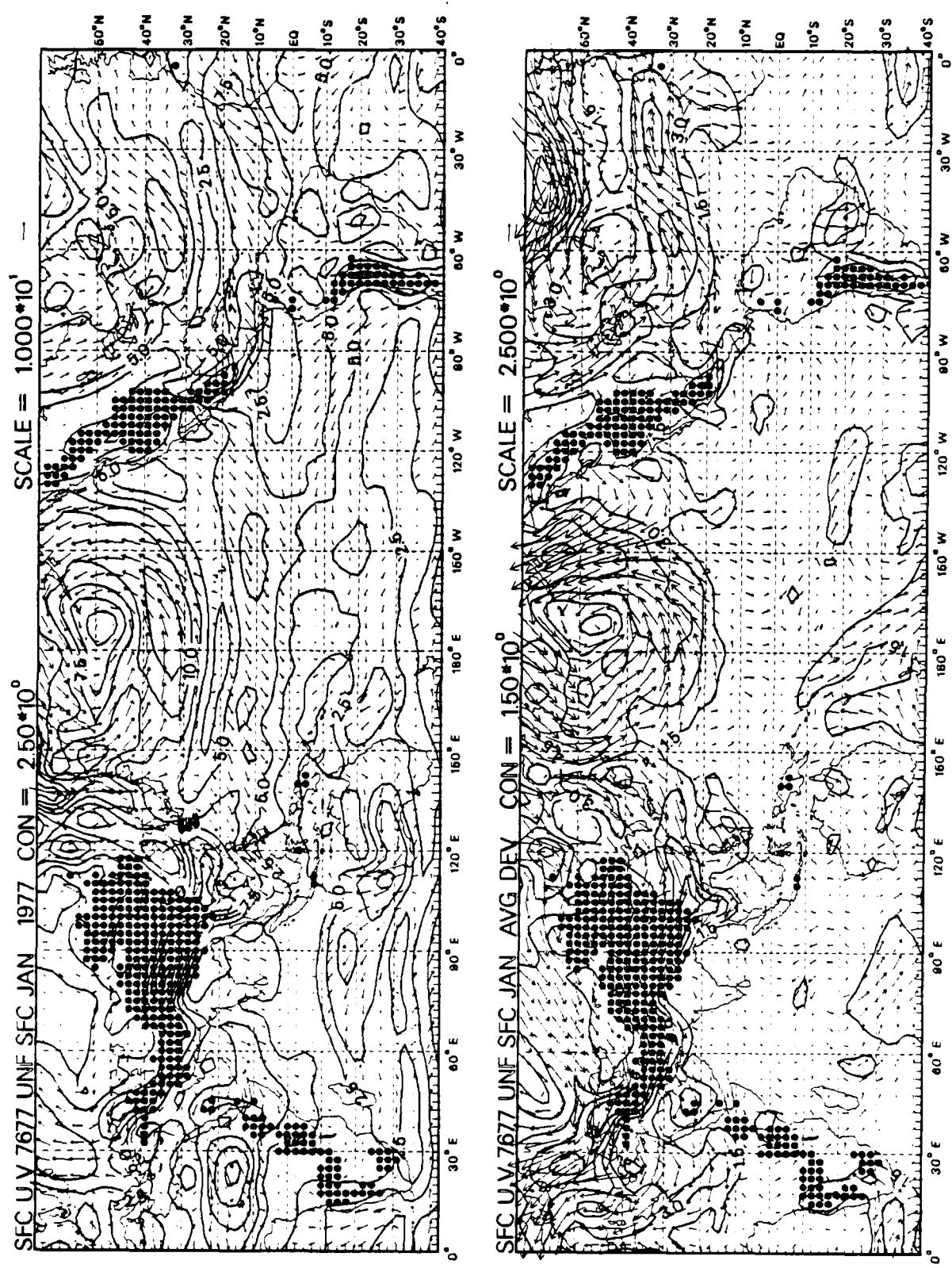


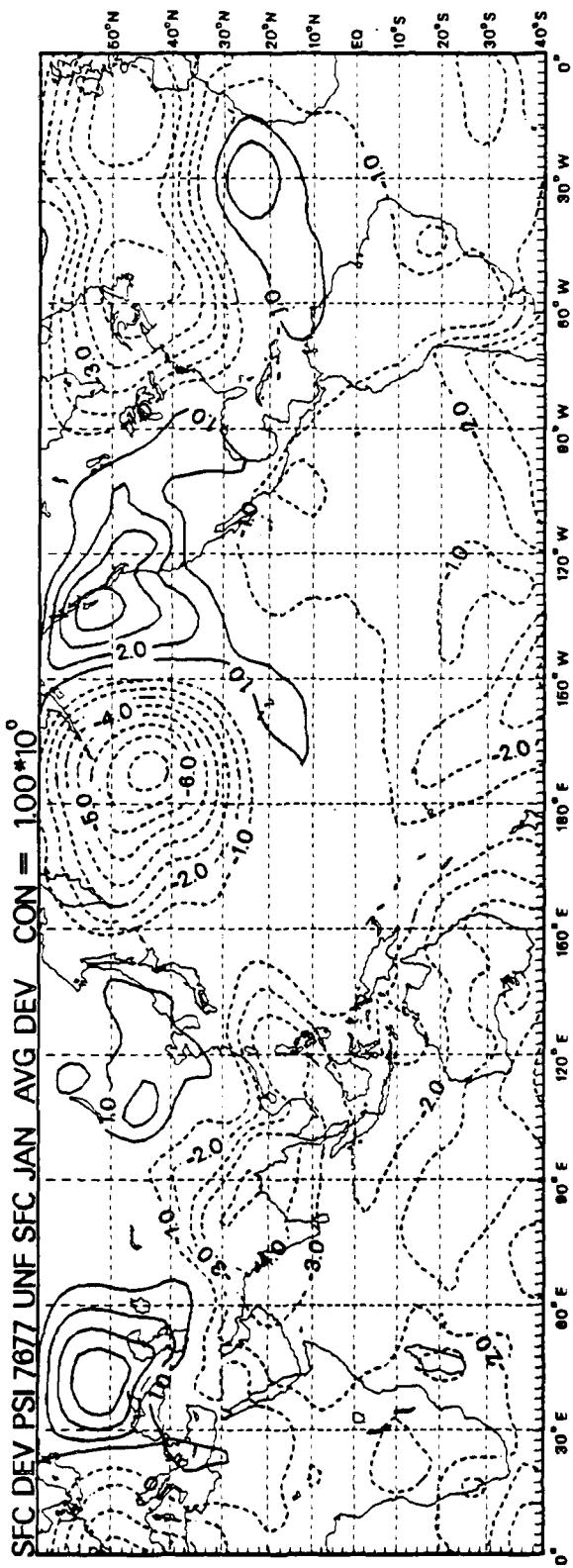
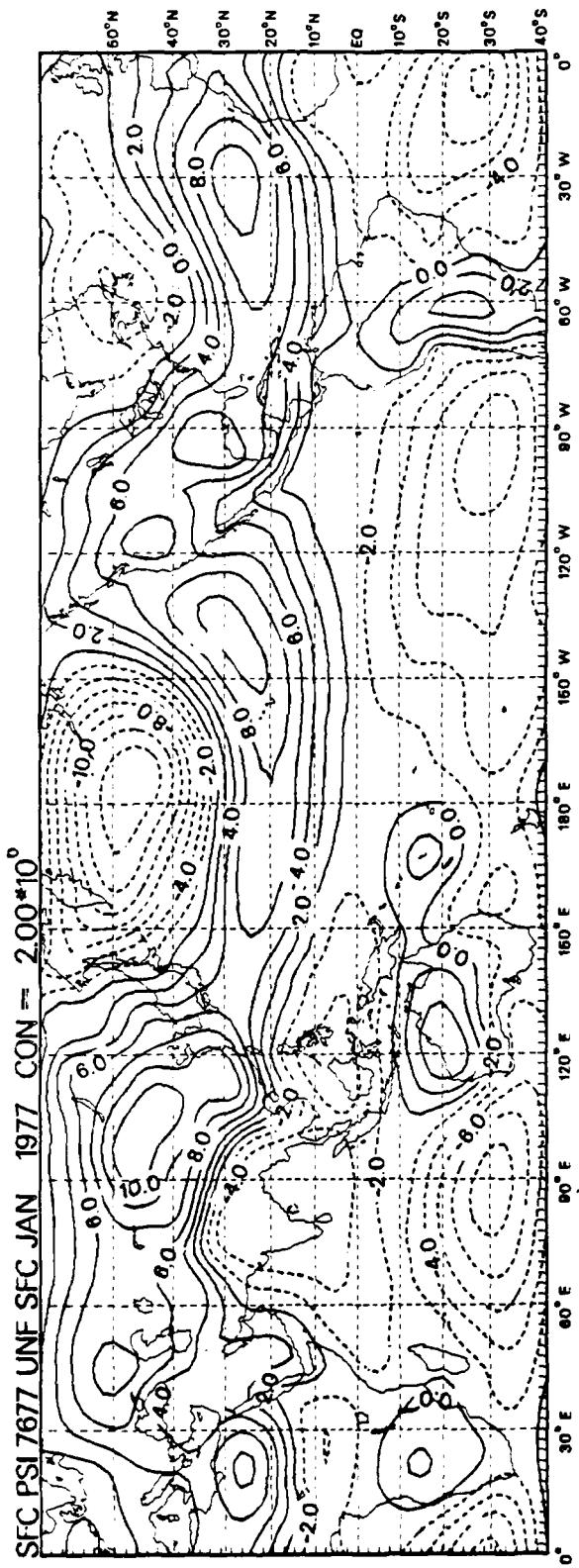
SFC DEV PSI 7677 UNF SFC DEC AVG DEV CON = 100*10⁰



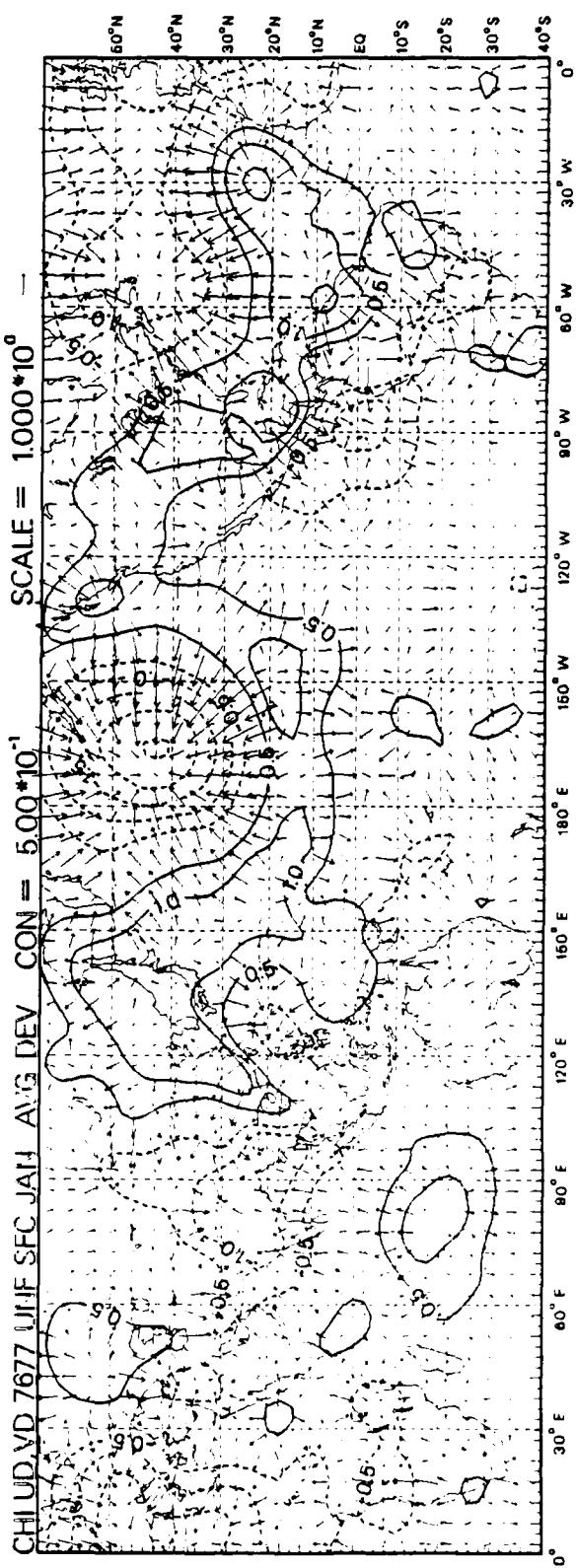
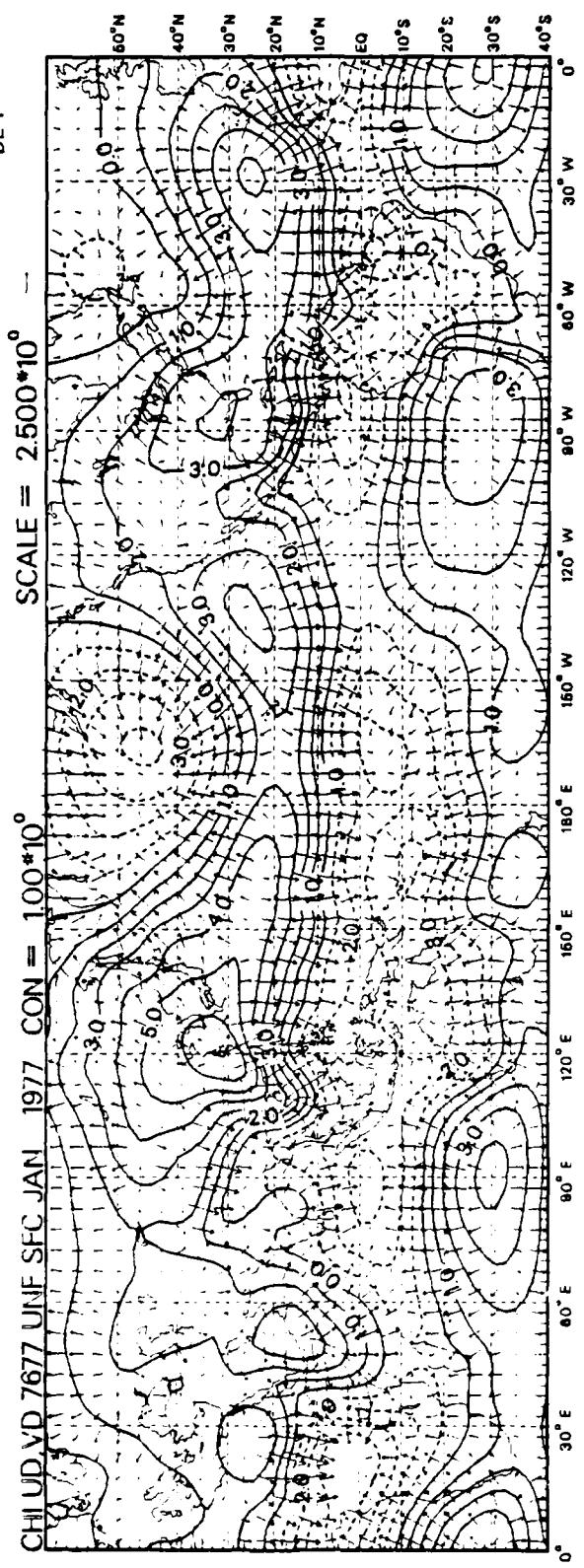
D21



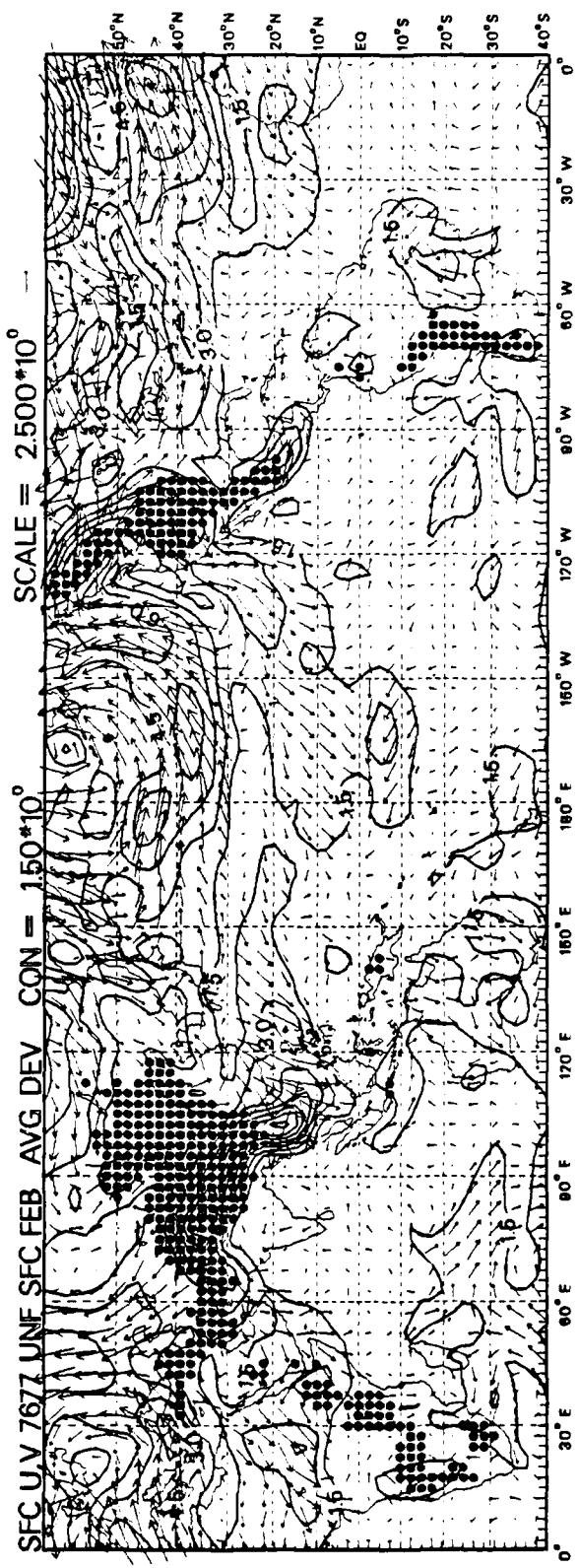
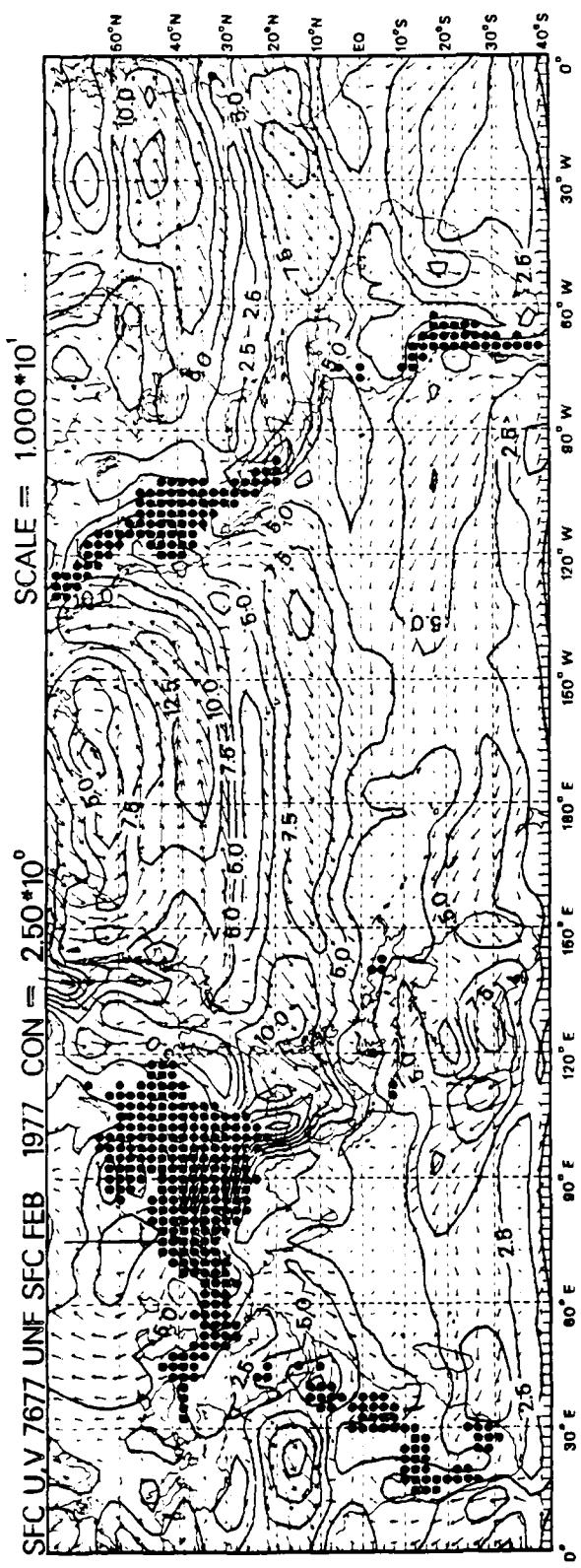




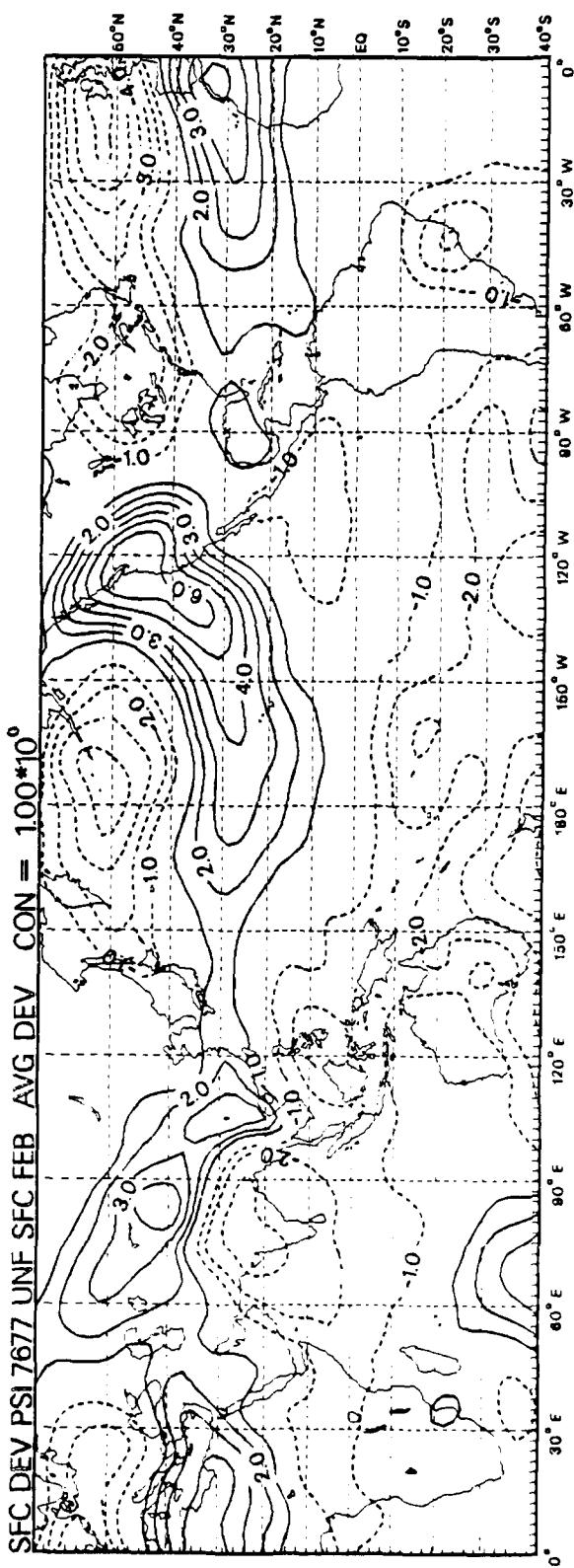
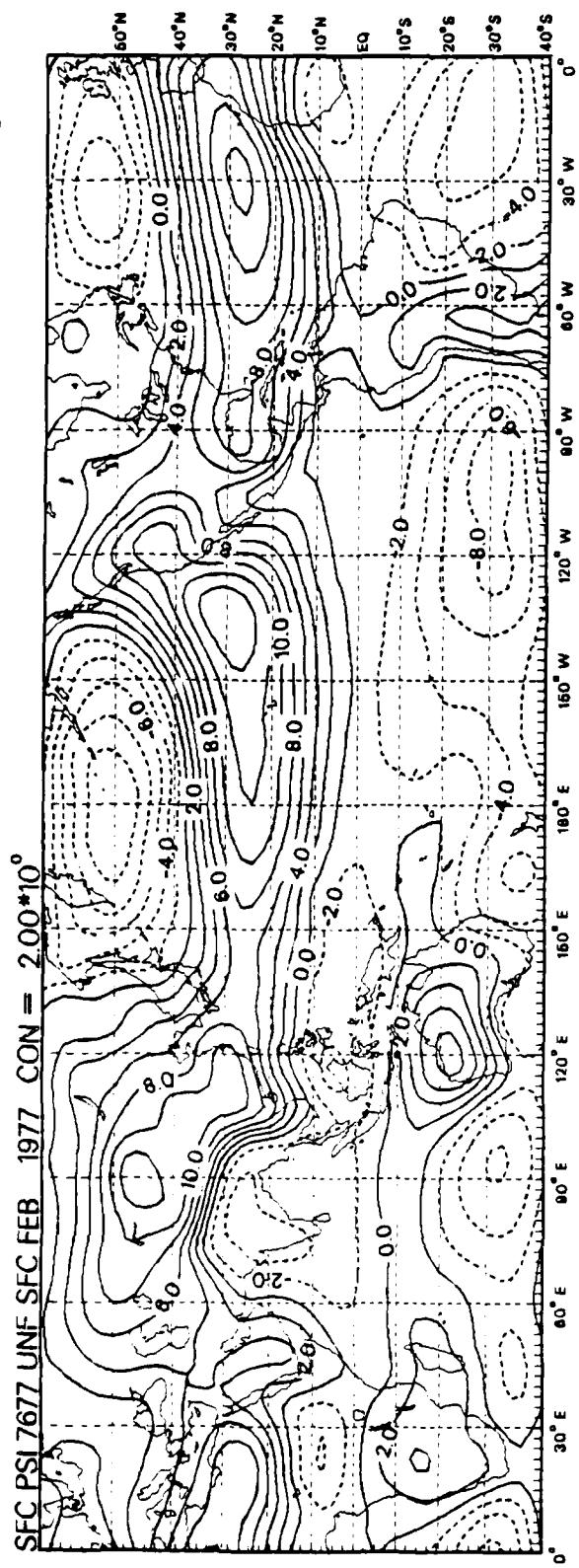
D24



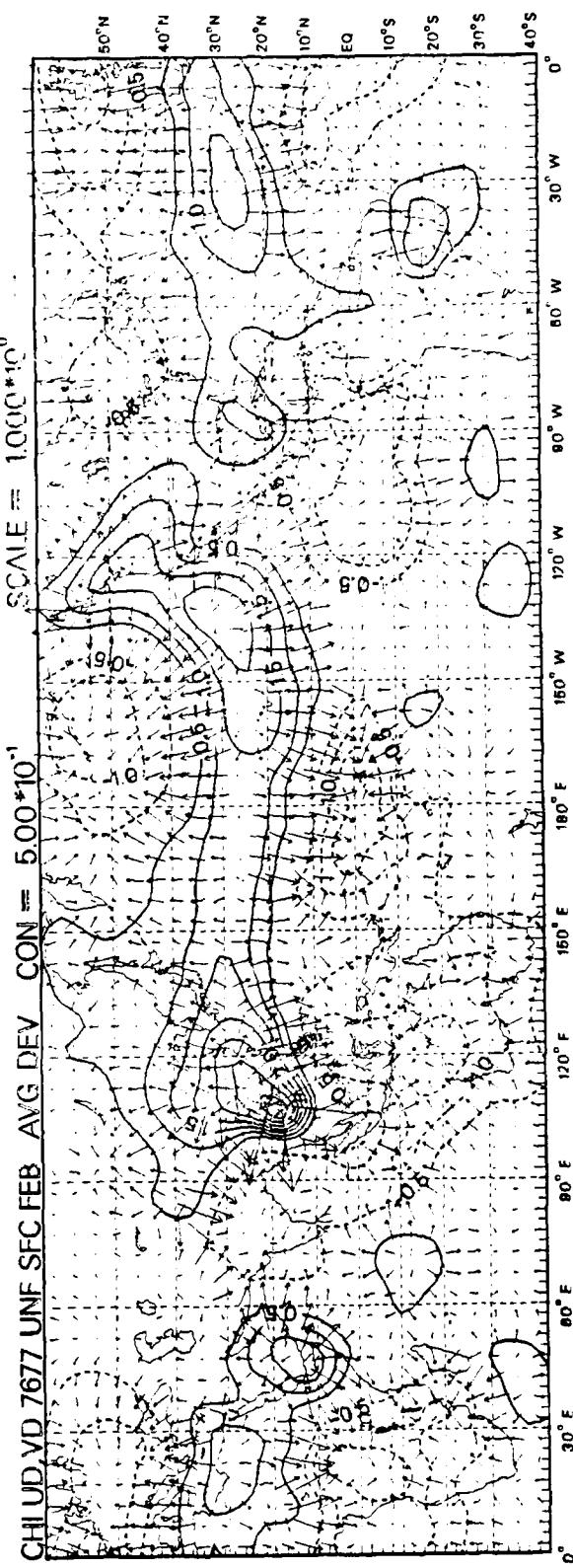
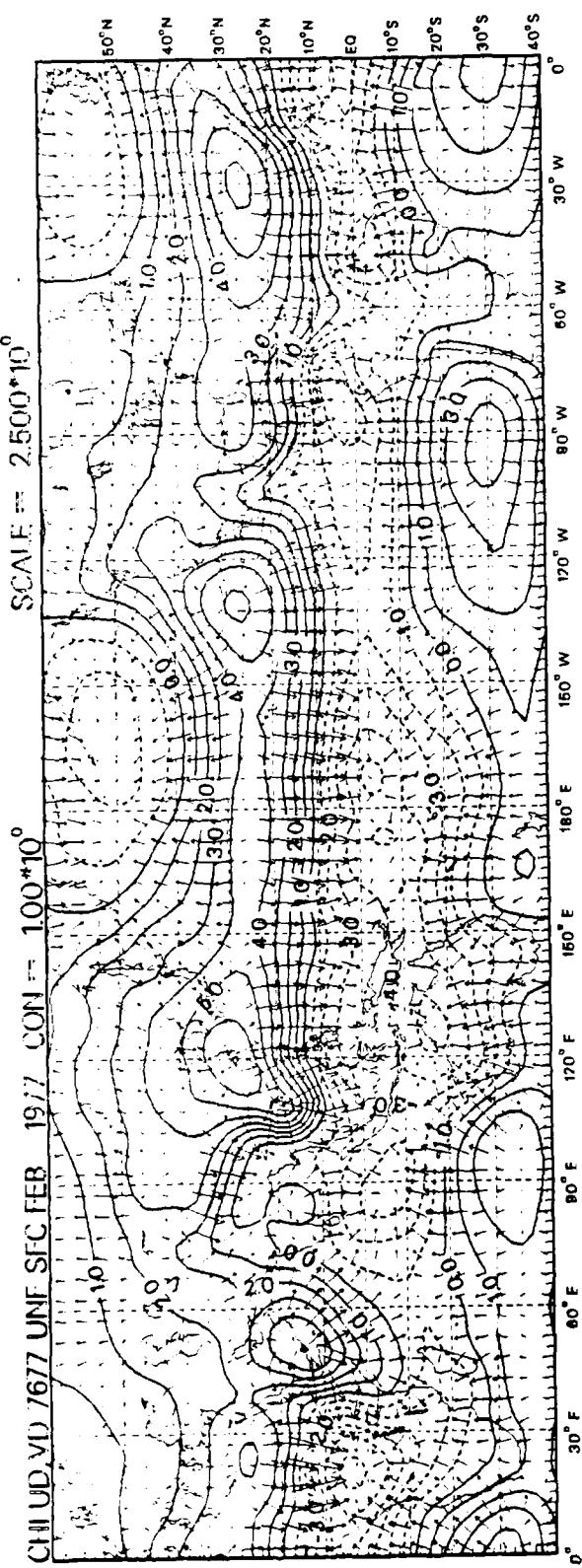
D25



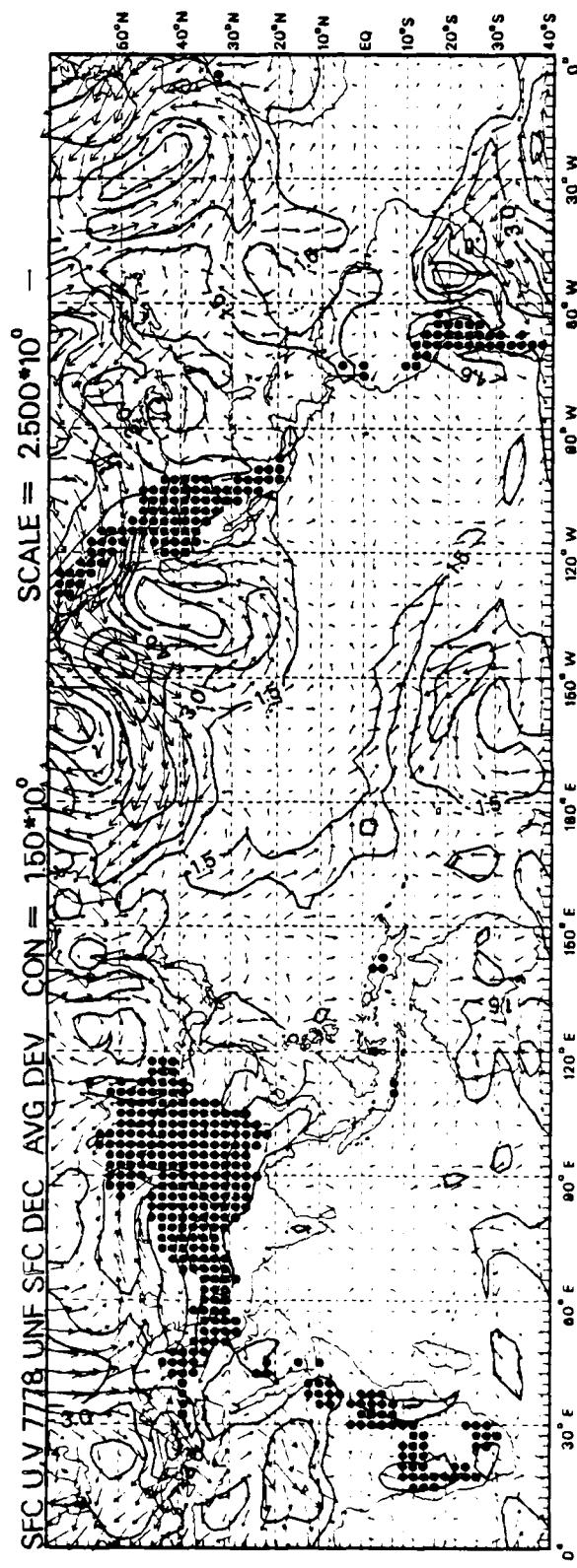
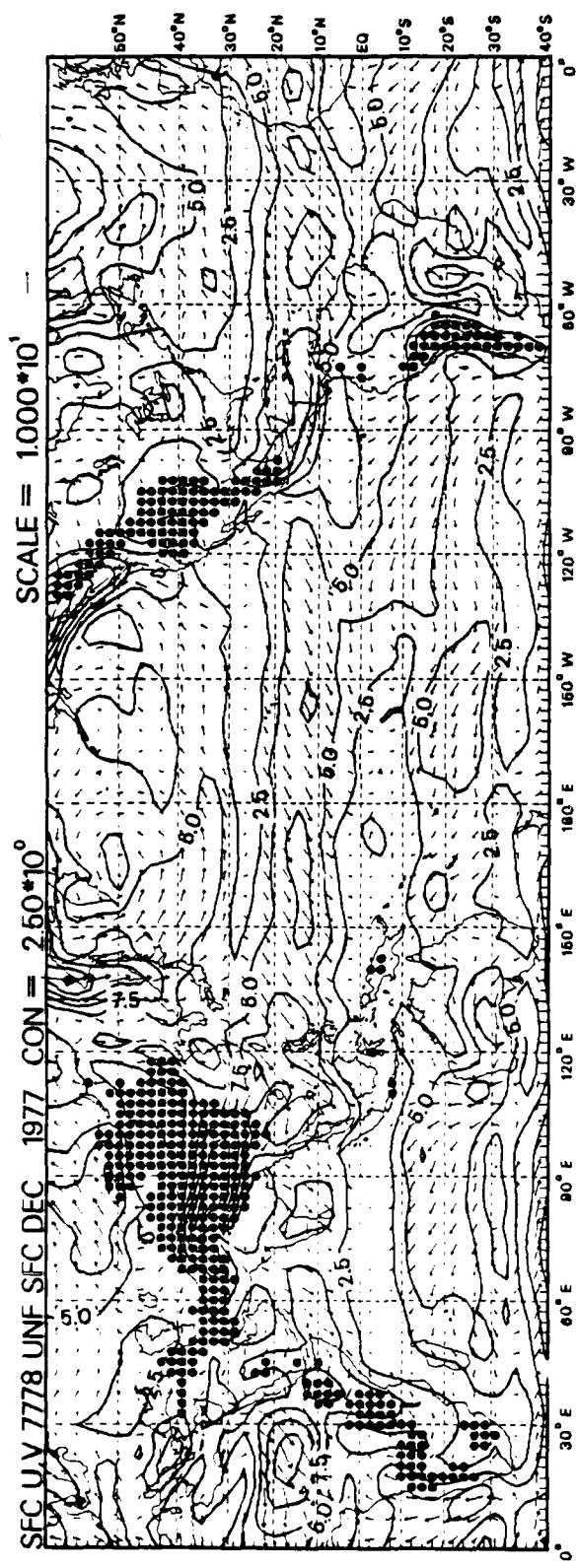
D26



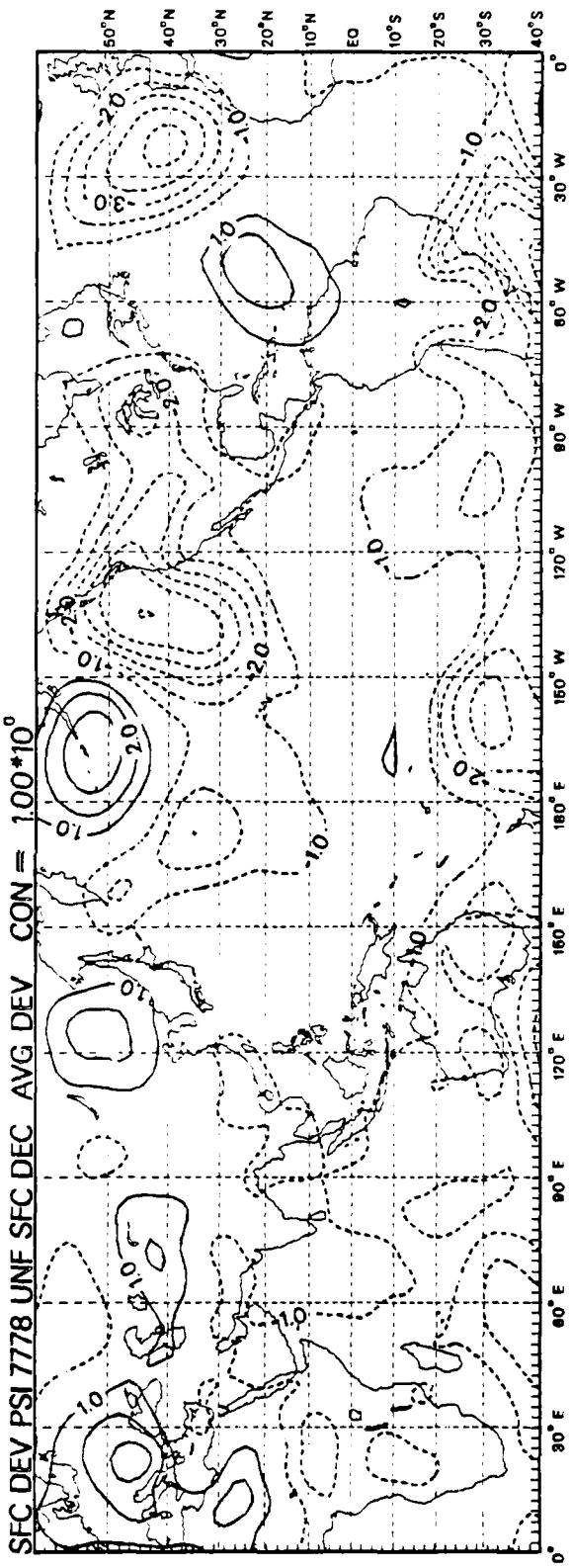
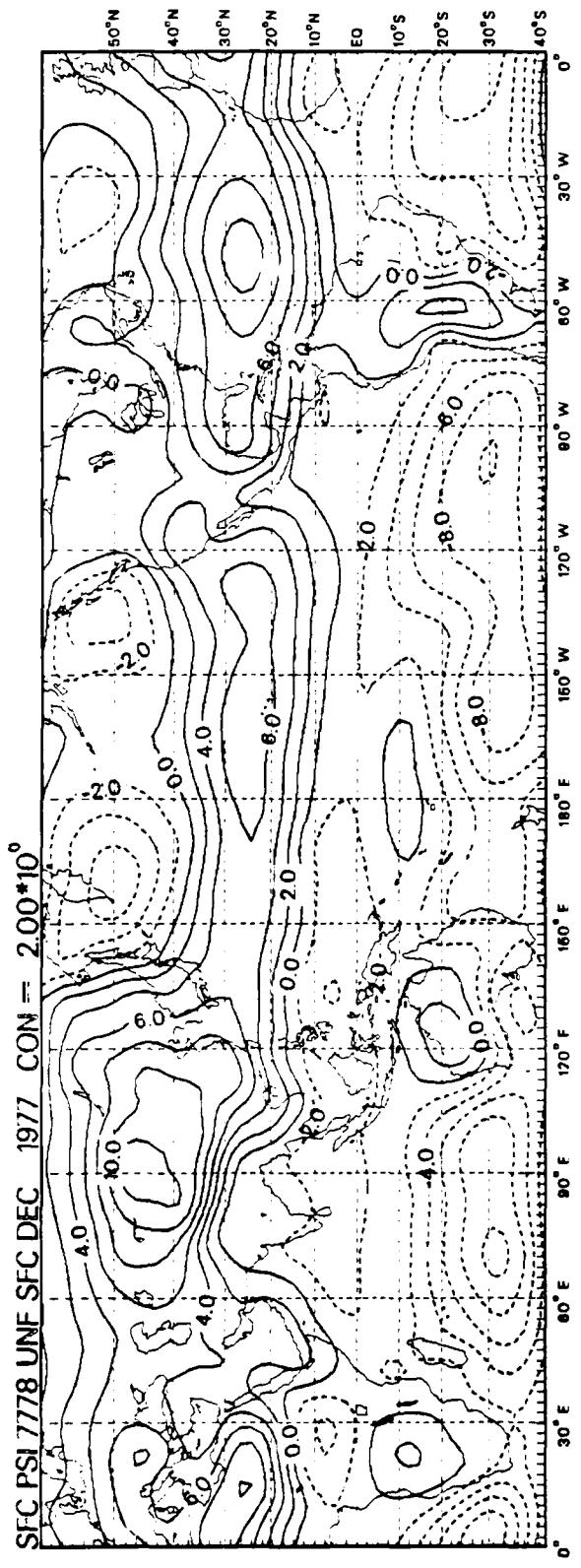
D27



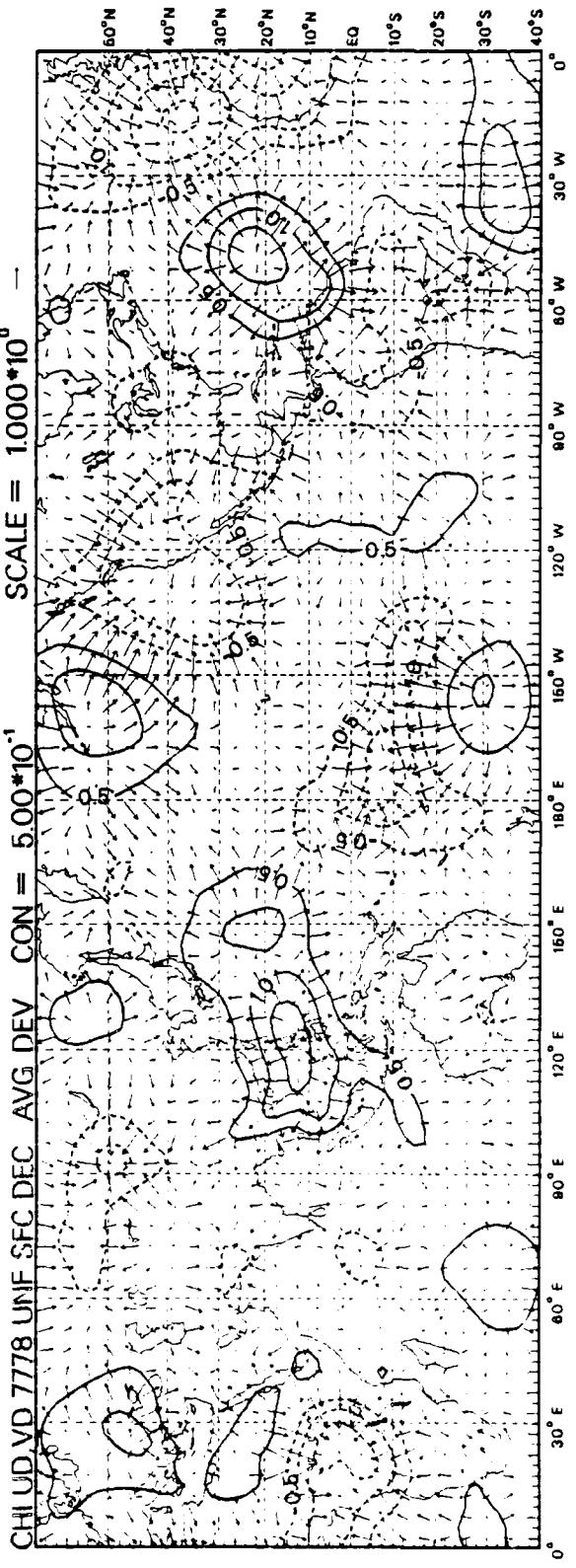
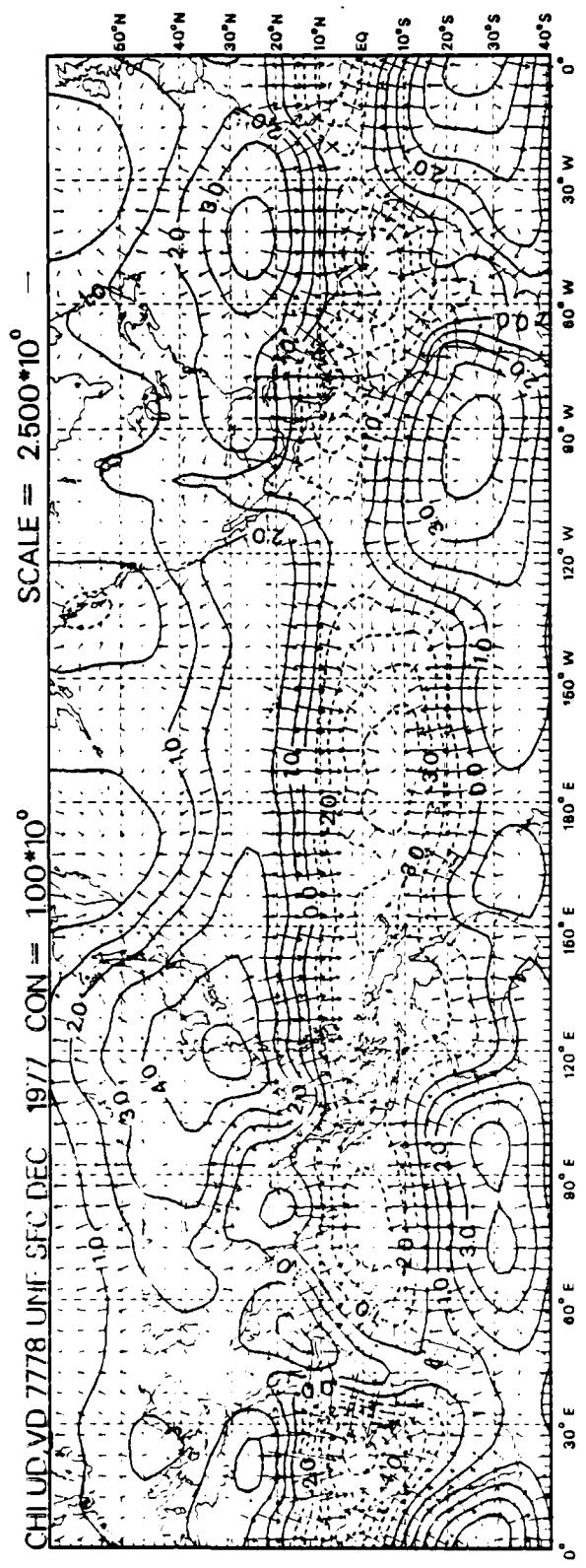
D28

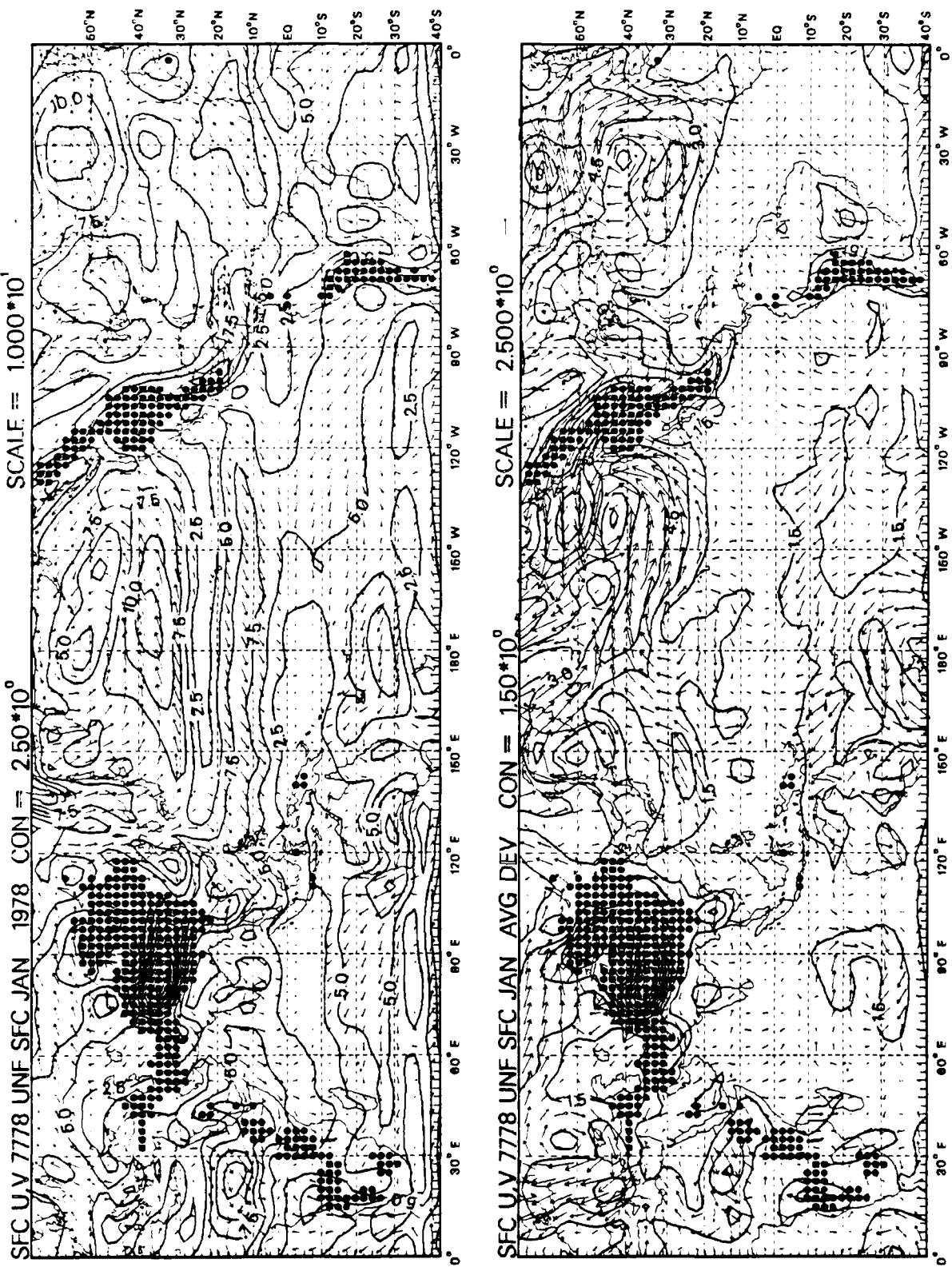


D29

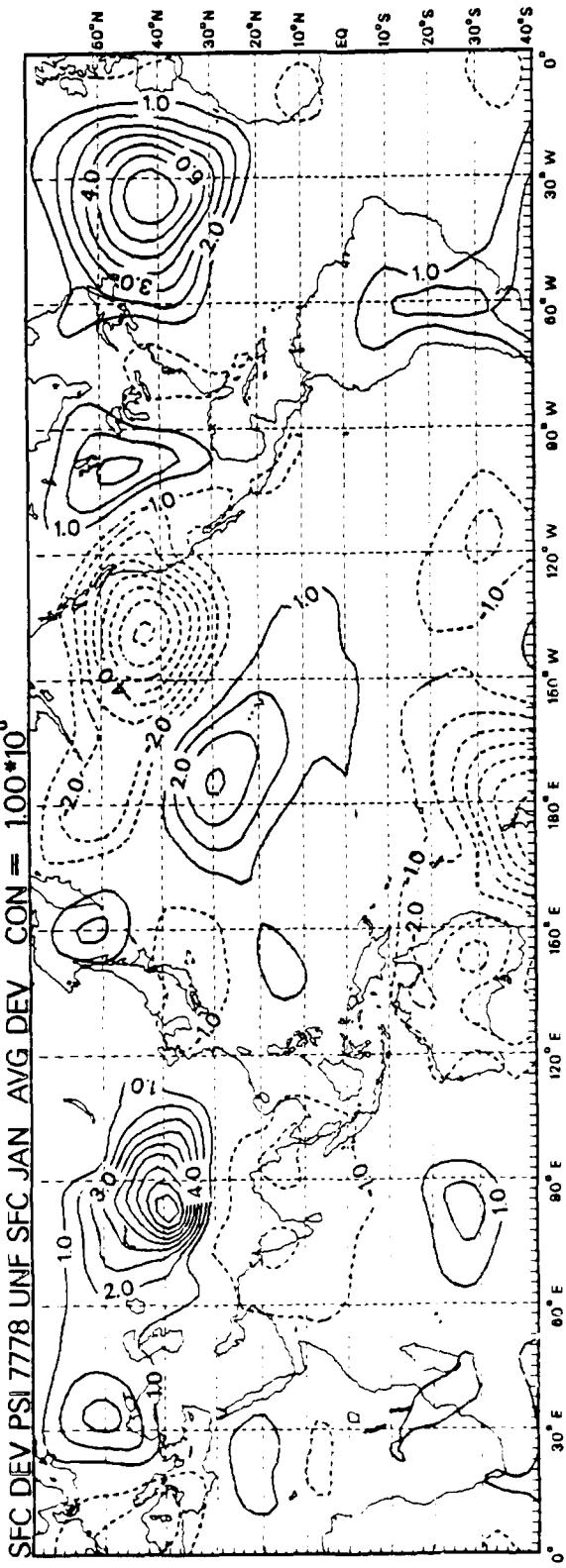
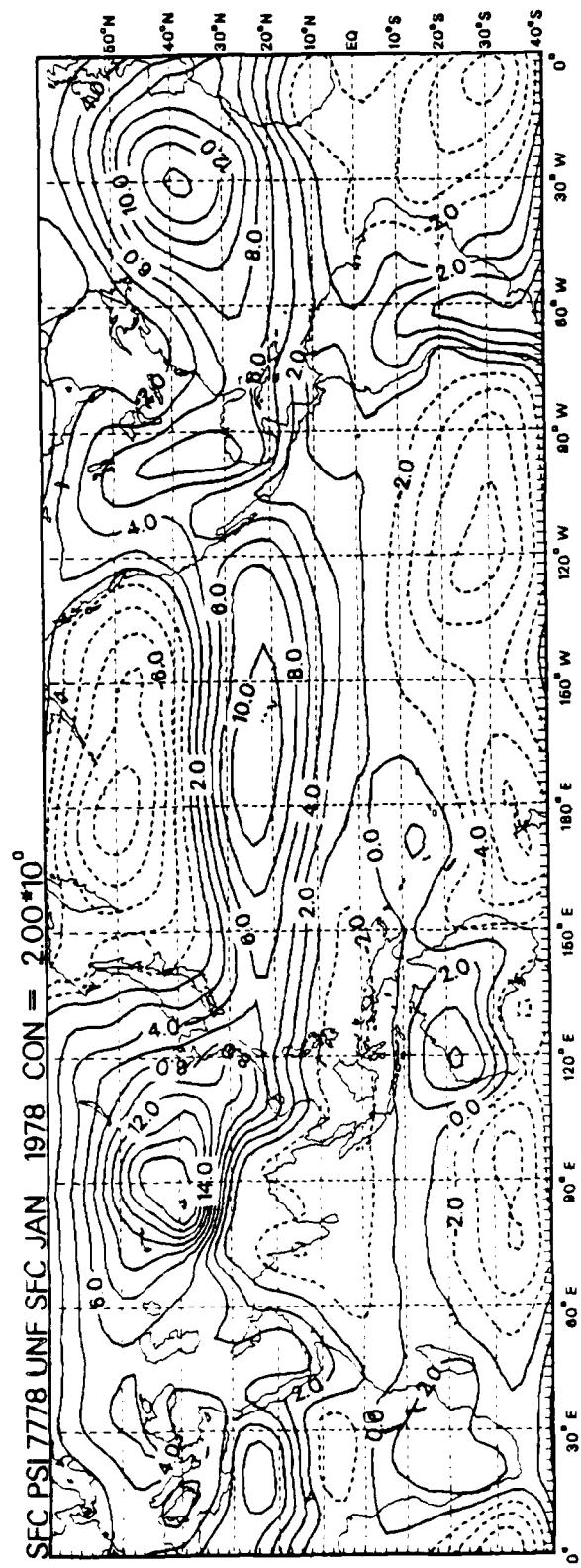


D30





D32

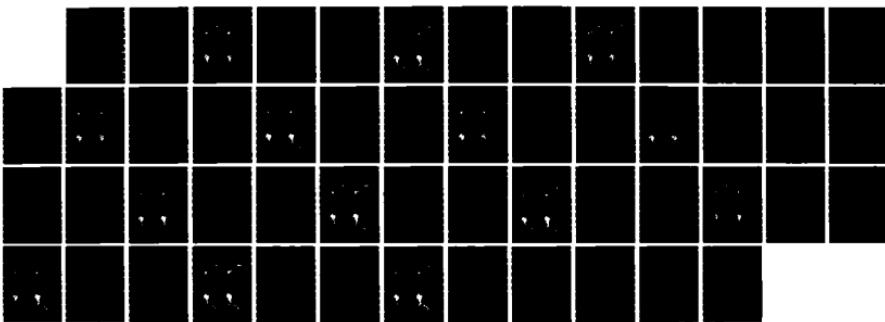


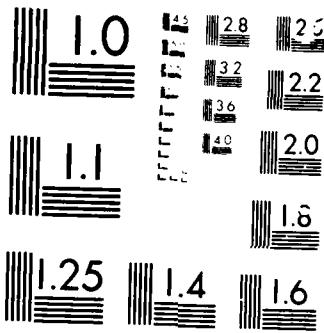
RD-A168 852 MONTHLY AND SEASONAL CLIMATOLOGY OF THE NORTHERN WINTER 2/2
OVER THE GLOBAL T. (U) NAVAL POSTGRADUATE SCHOOL
MONTEREY CA J S BOYLE ET AL. MAY 86

UNCLASSIFIED NPS-63-86-002-VOL-3

F/G 4/2

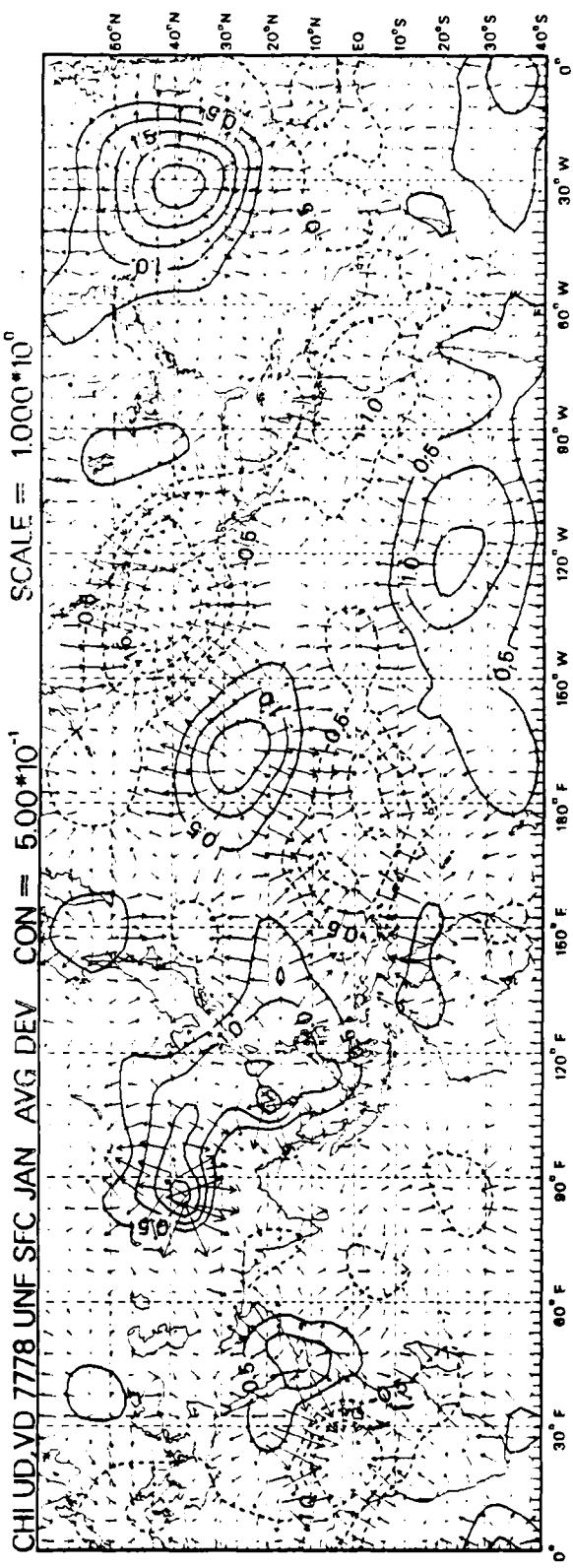
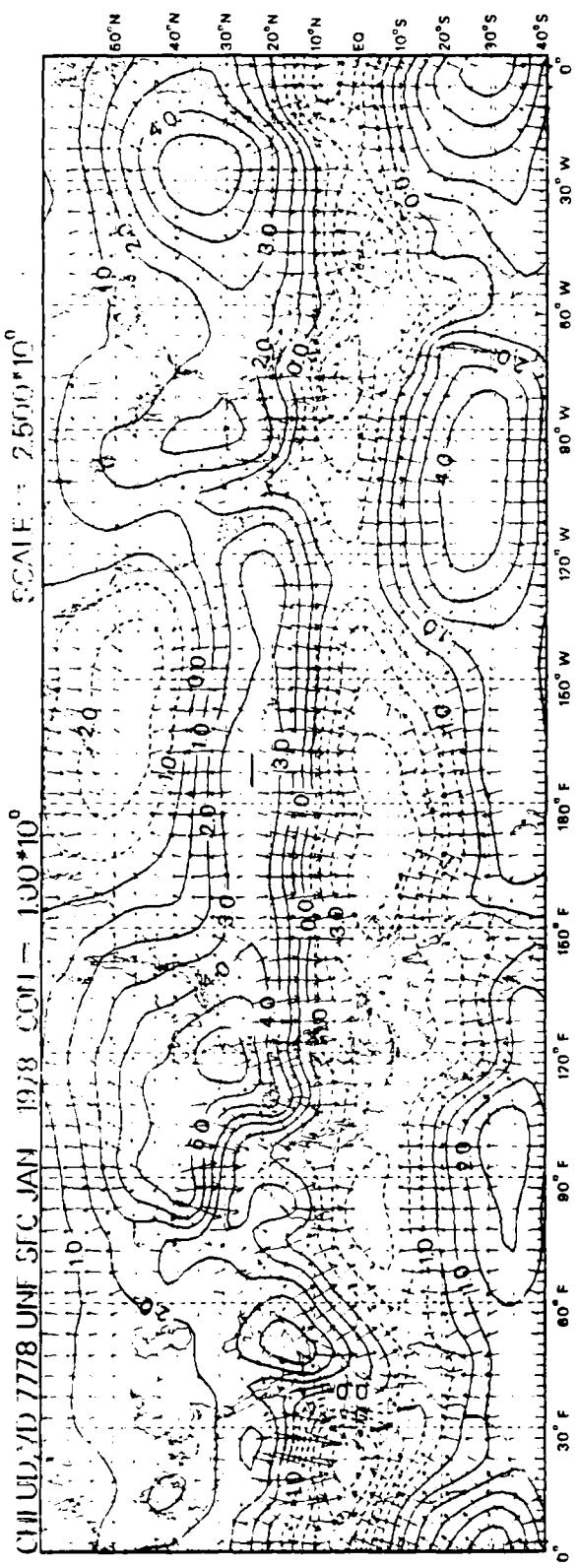
NL



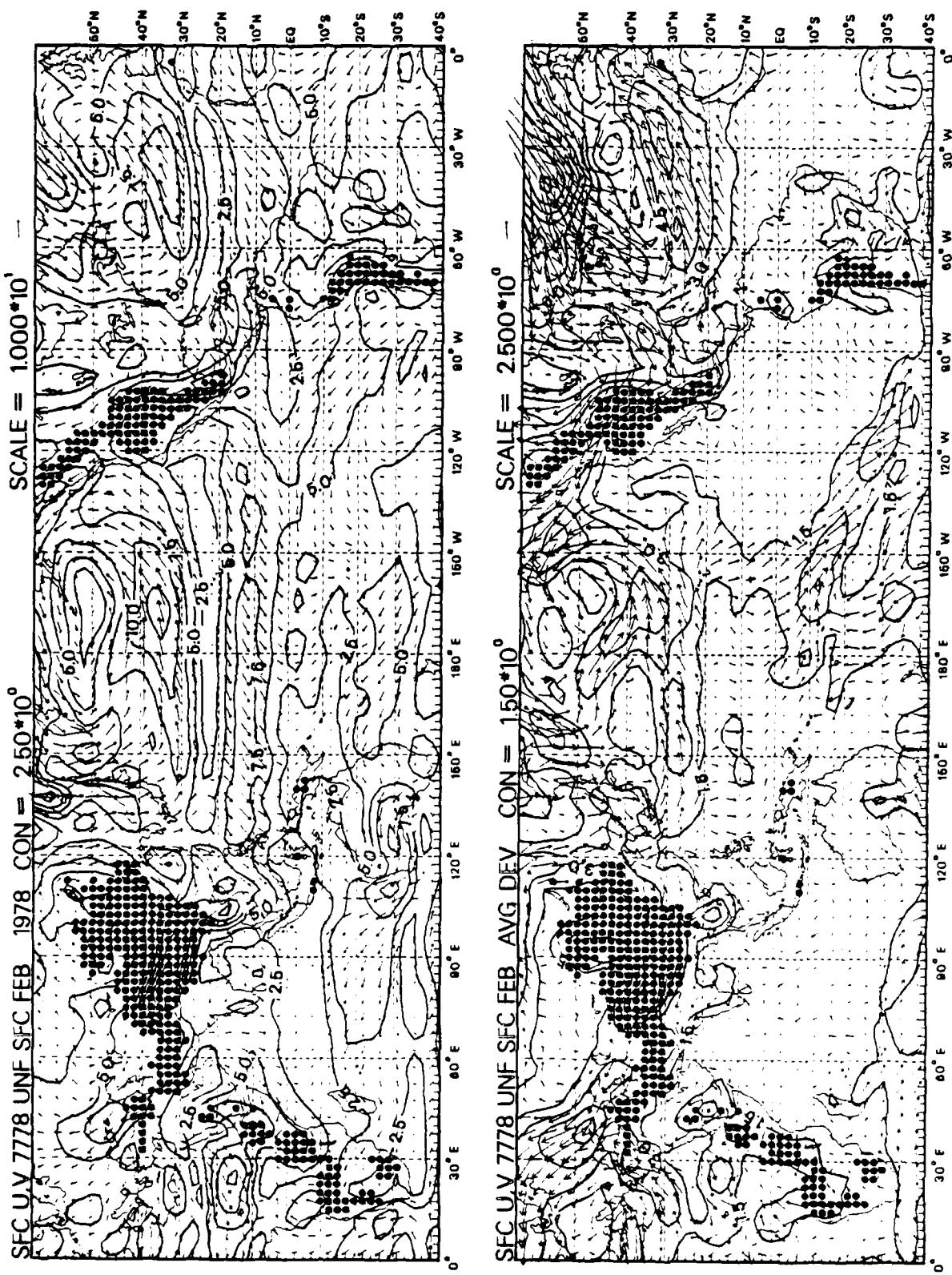


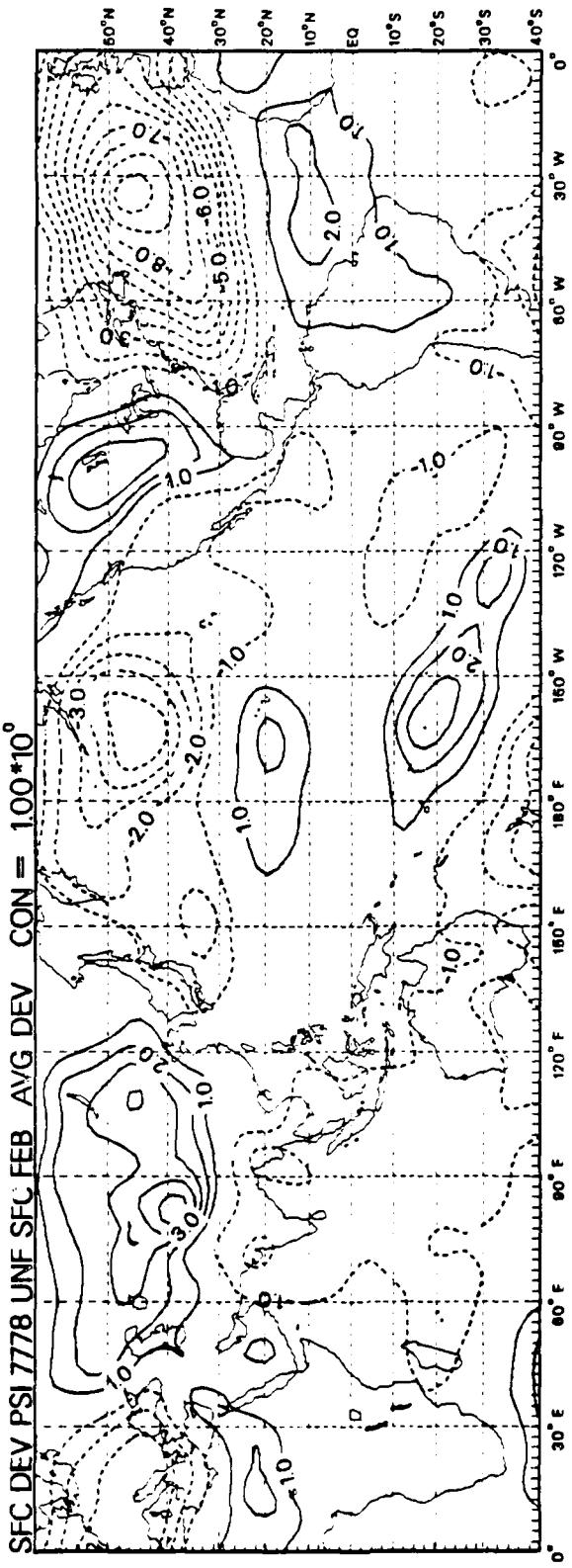
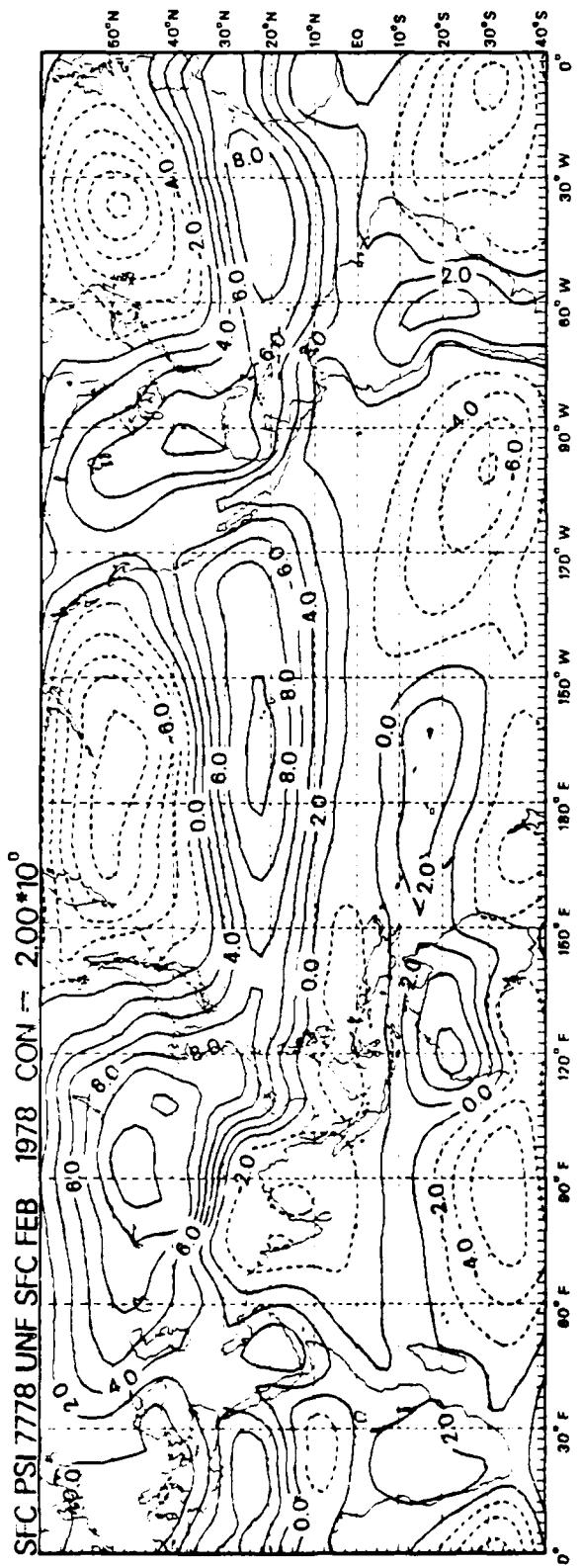
M 32-1000

033



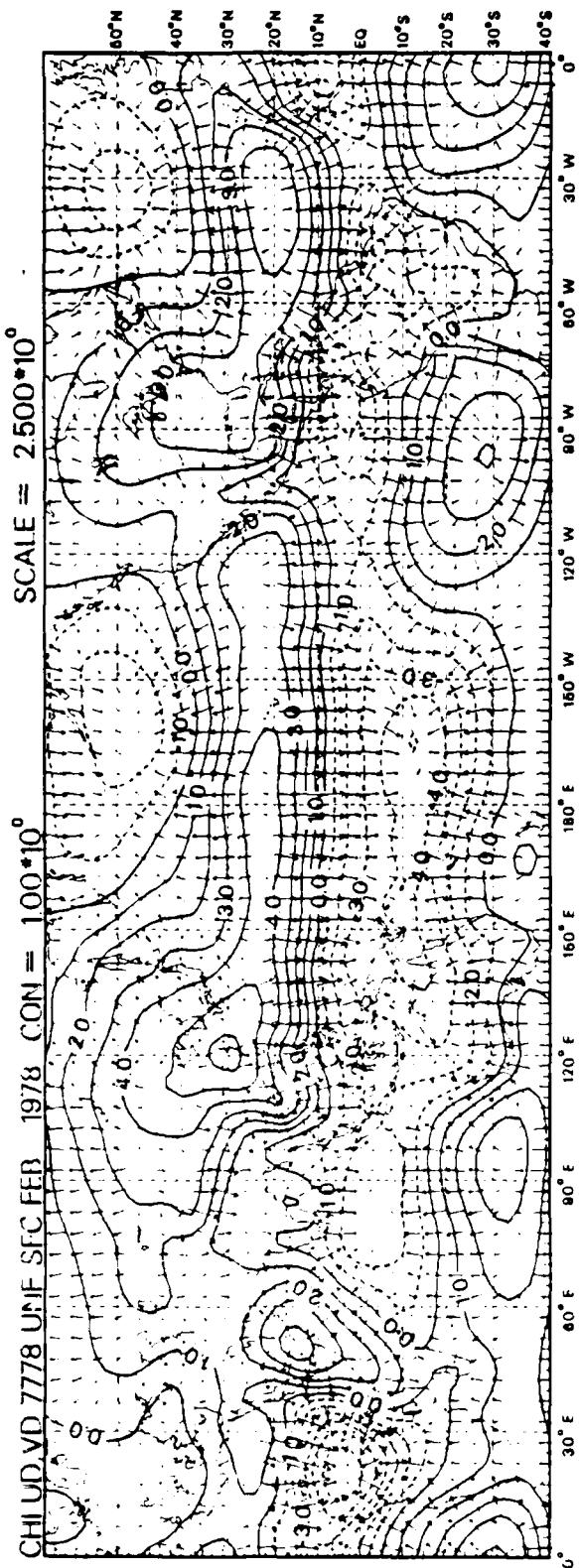
D34



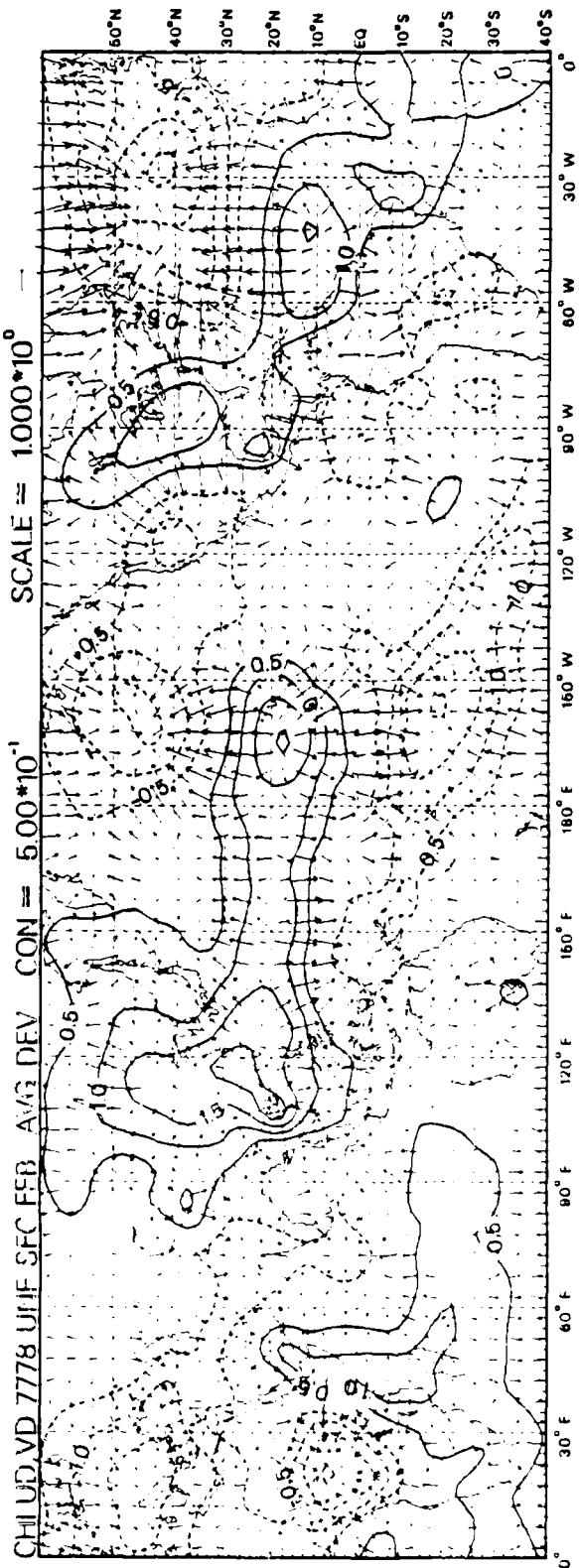


D36

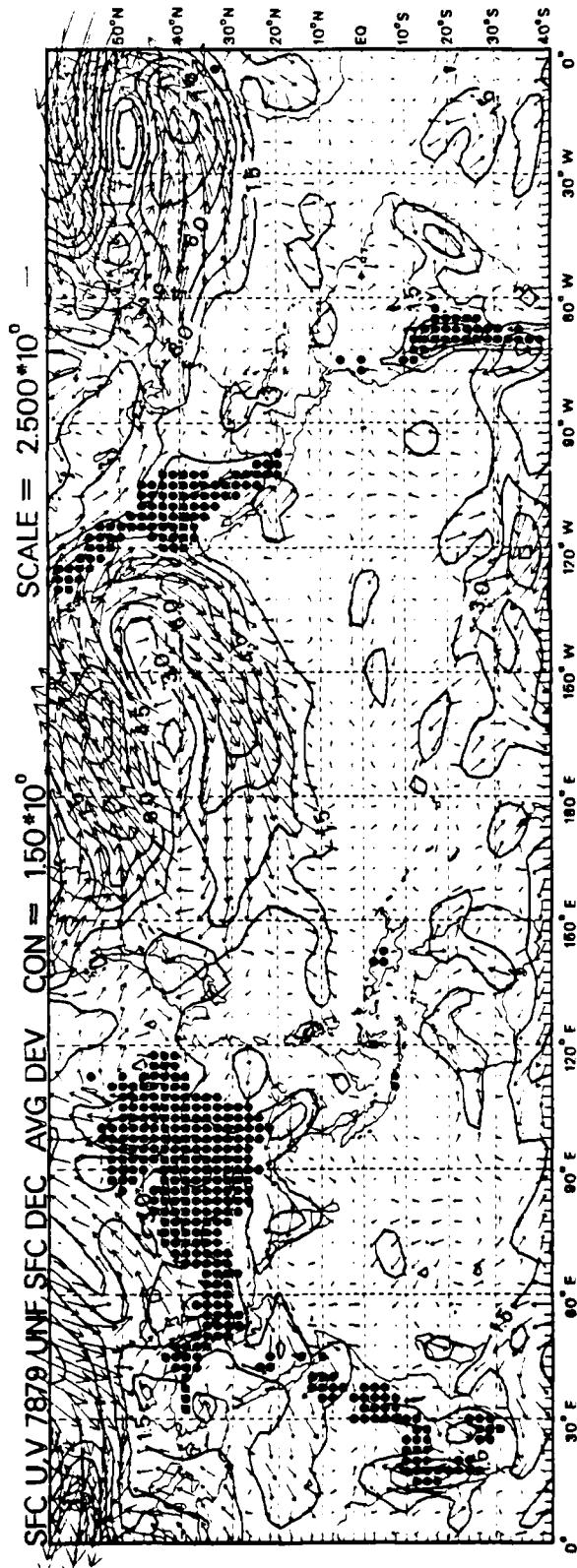
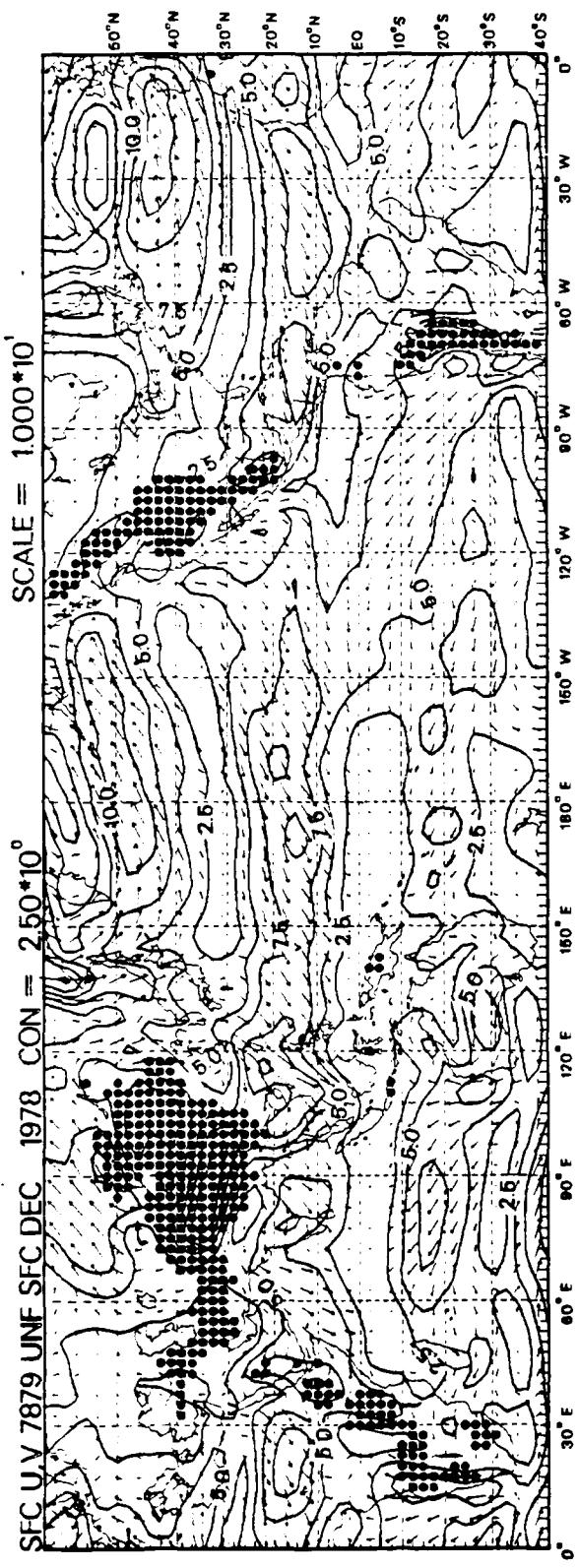
CHI UDV 7778 UNIF SFC FFR 1978 CON = $100 \cdot 10^0$



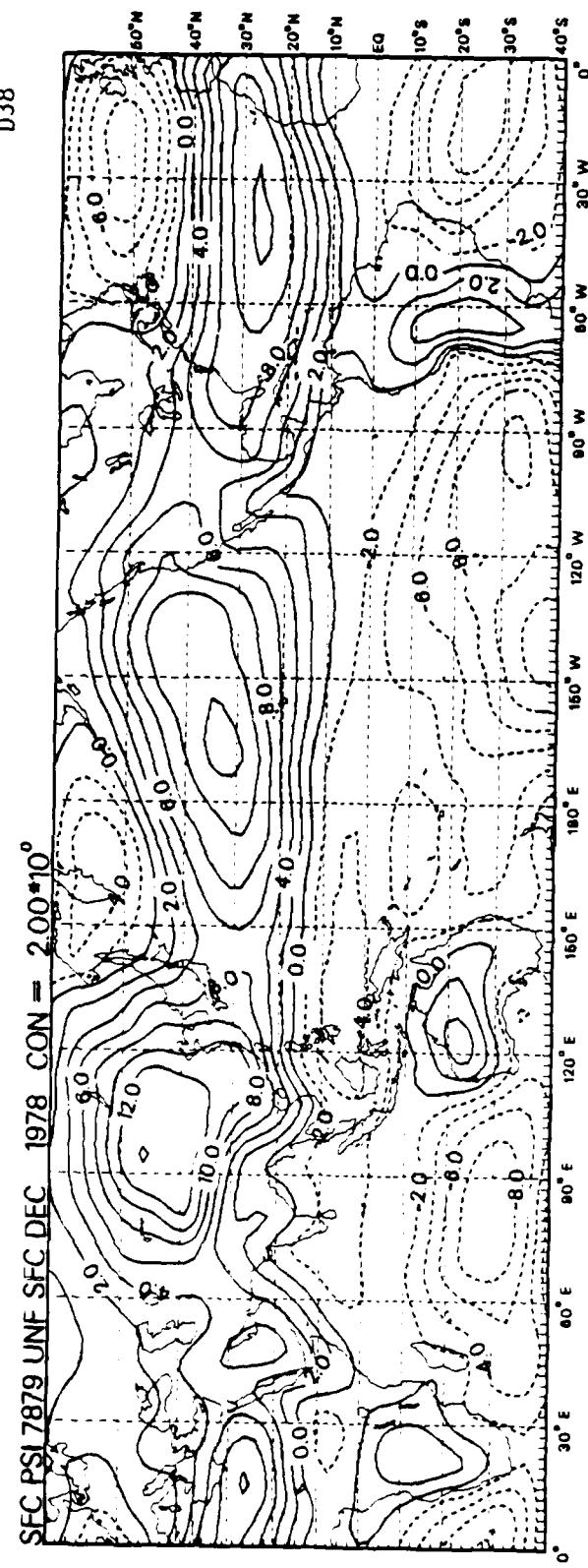
CHI UDV 7778 UNIF SFC FFB AVG DEV CON = $500 \cdot 10^{-1}$



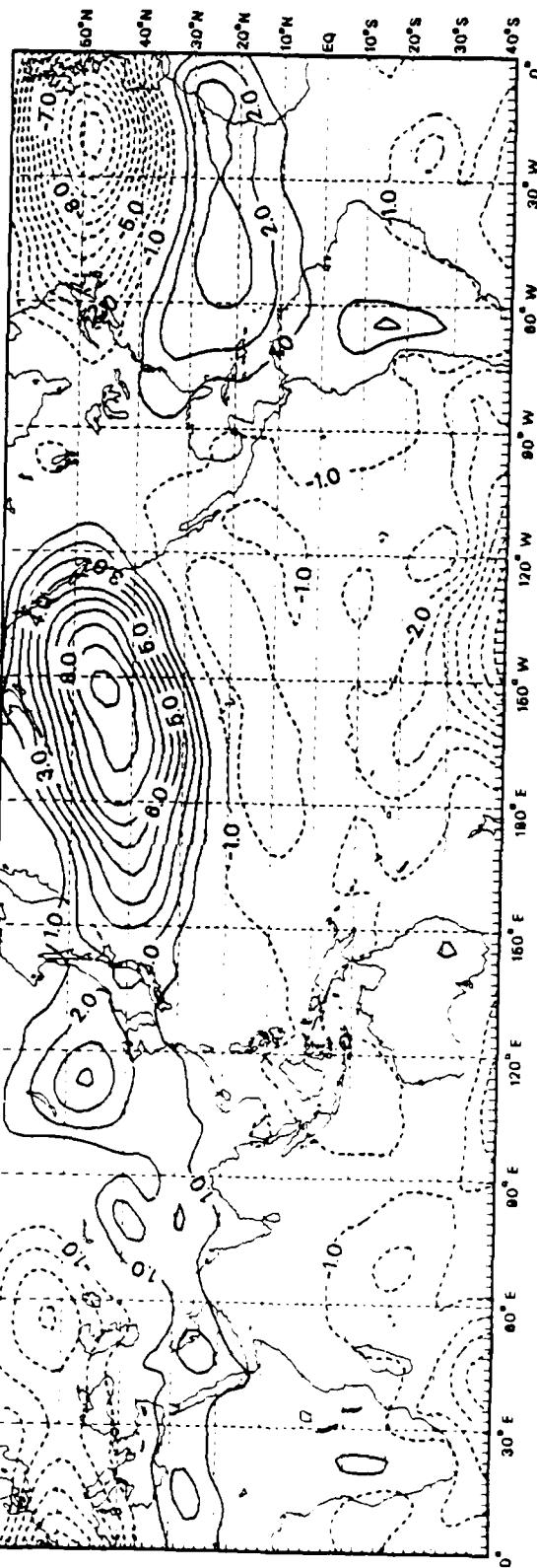
D37



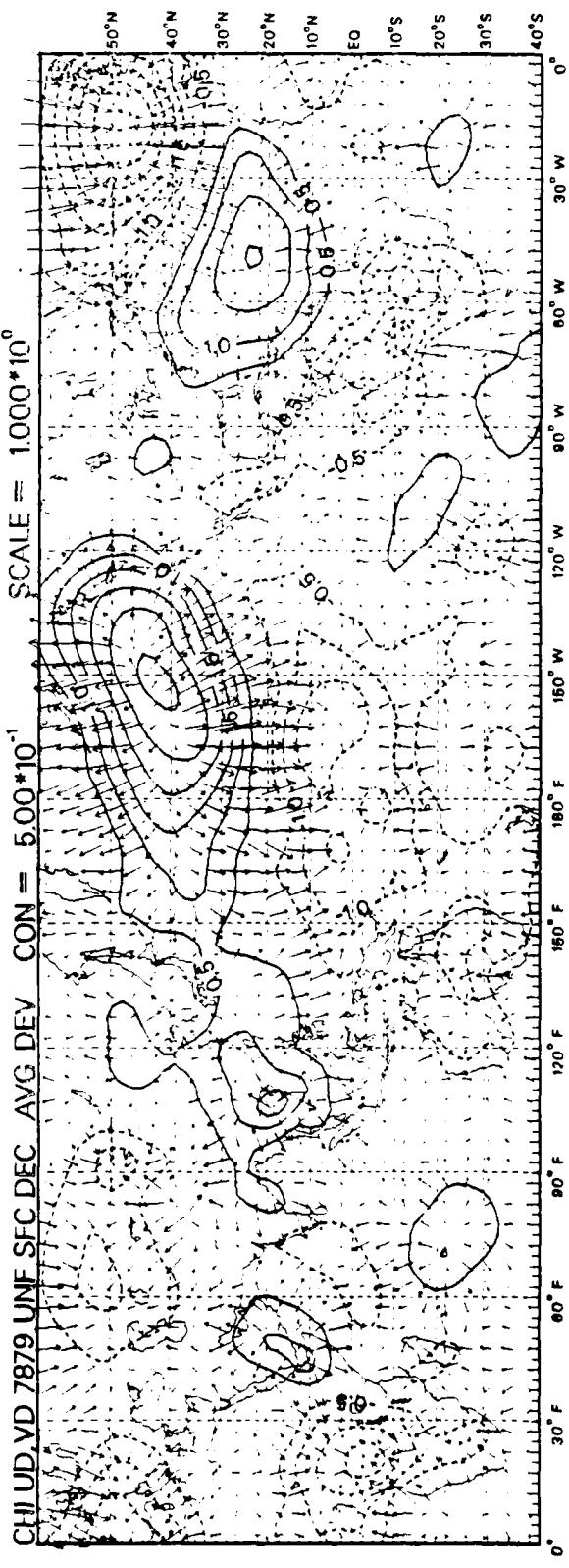
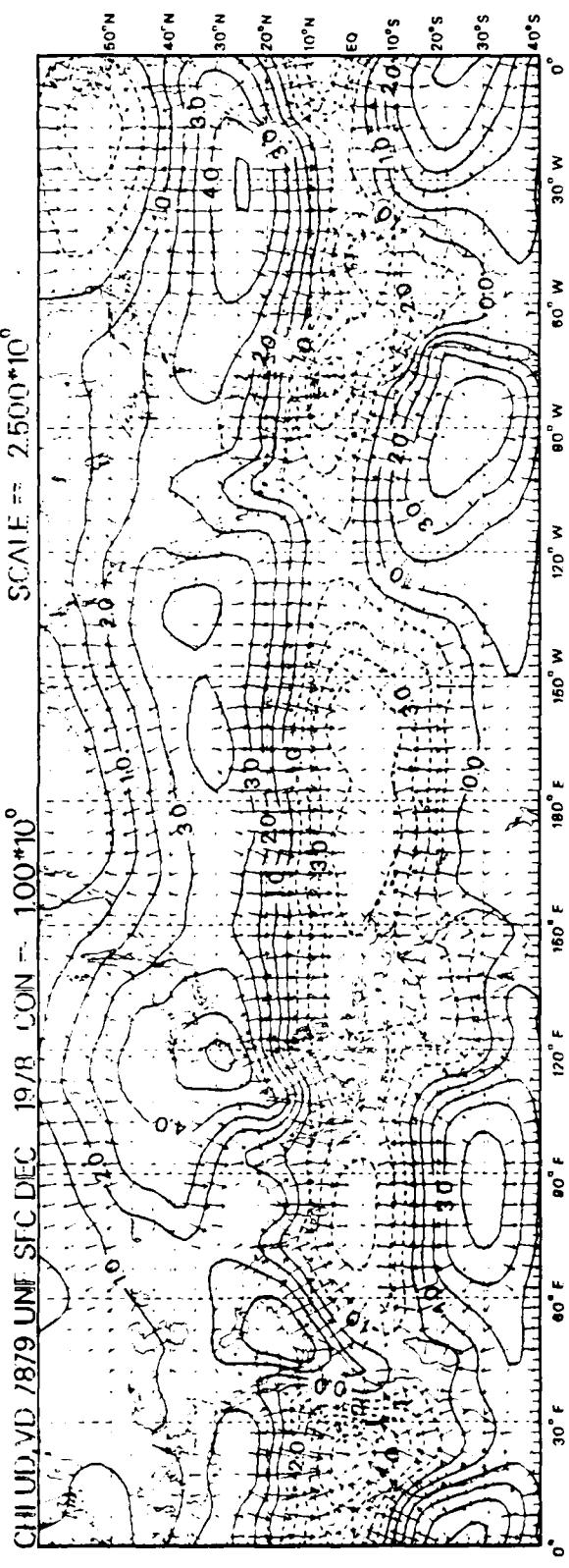
D38



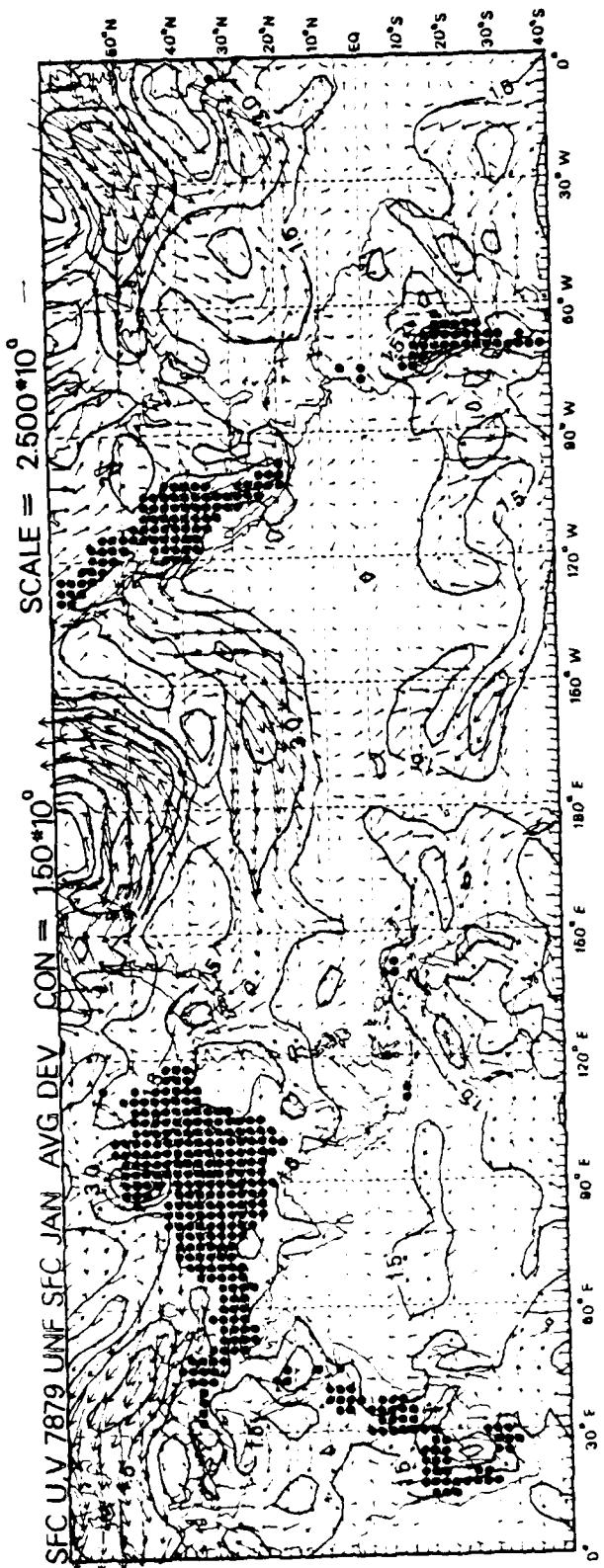
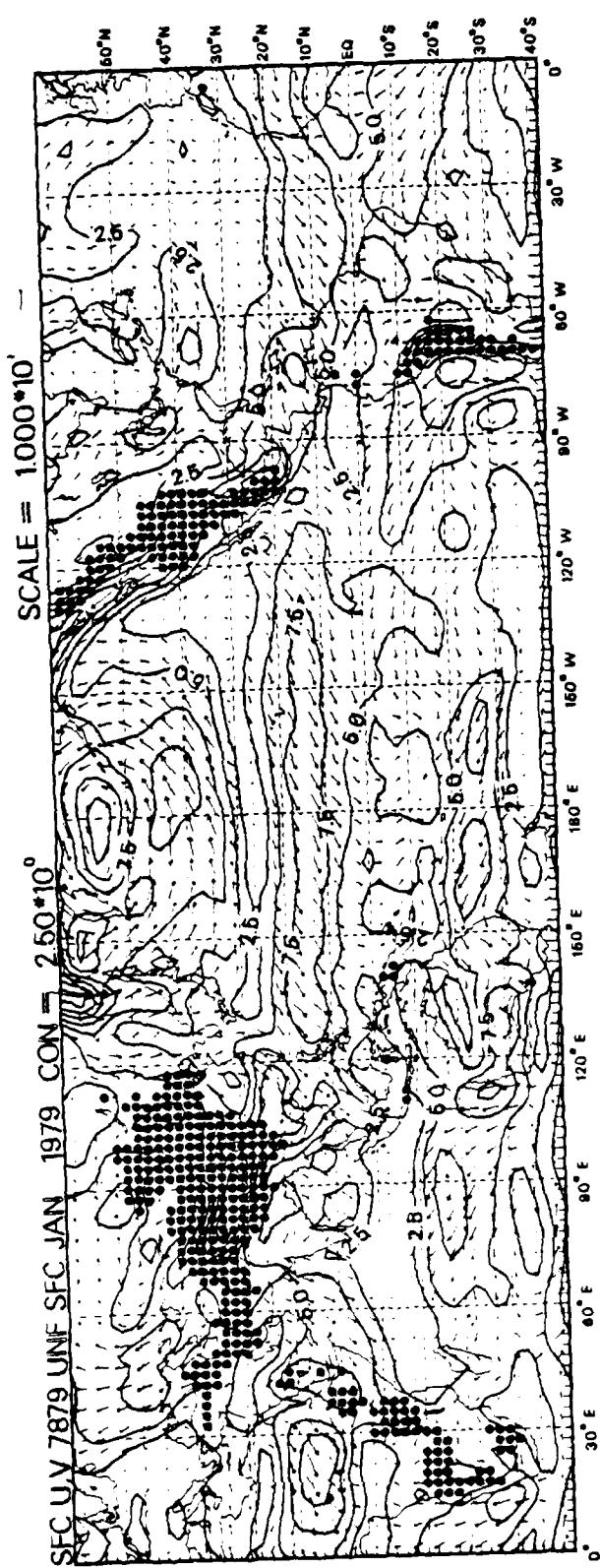
SFC DEV PSI 7879 UNF SFC DEC AVG DEV CON = 100*10⁰



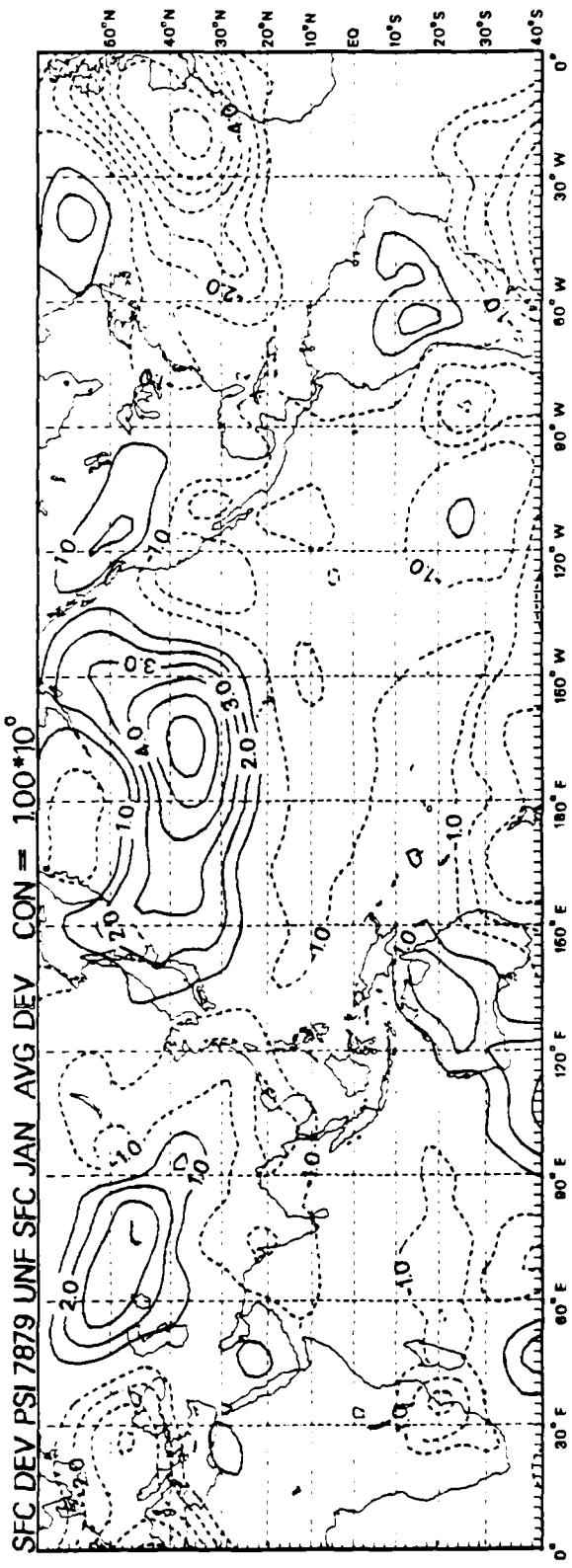
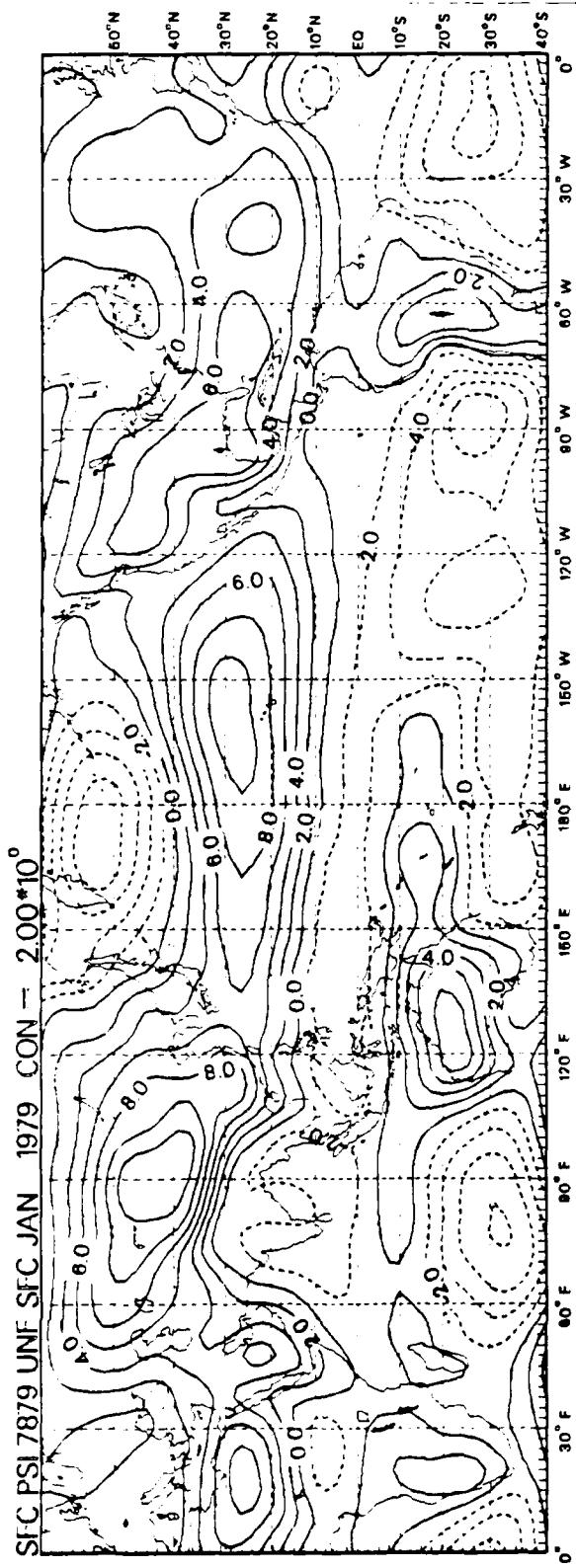
039



D40

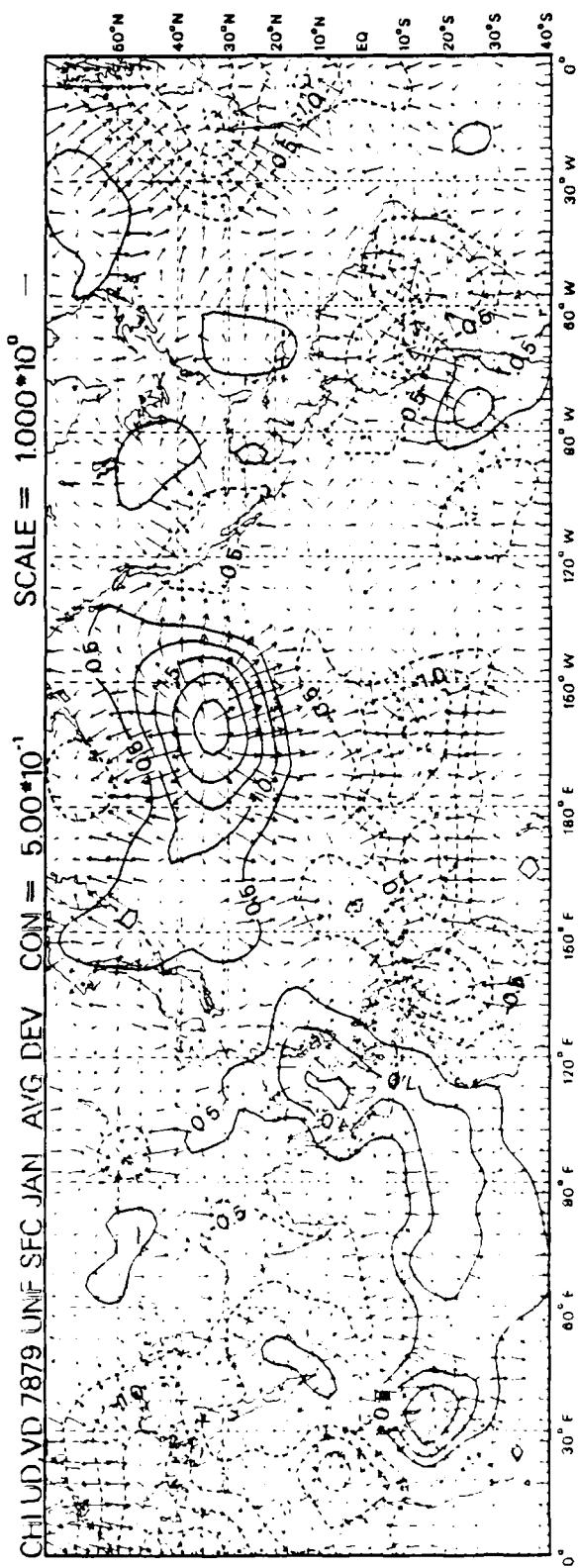
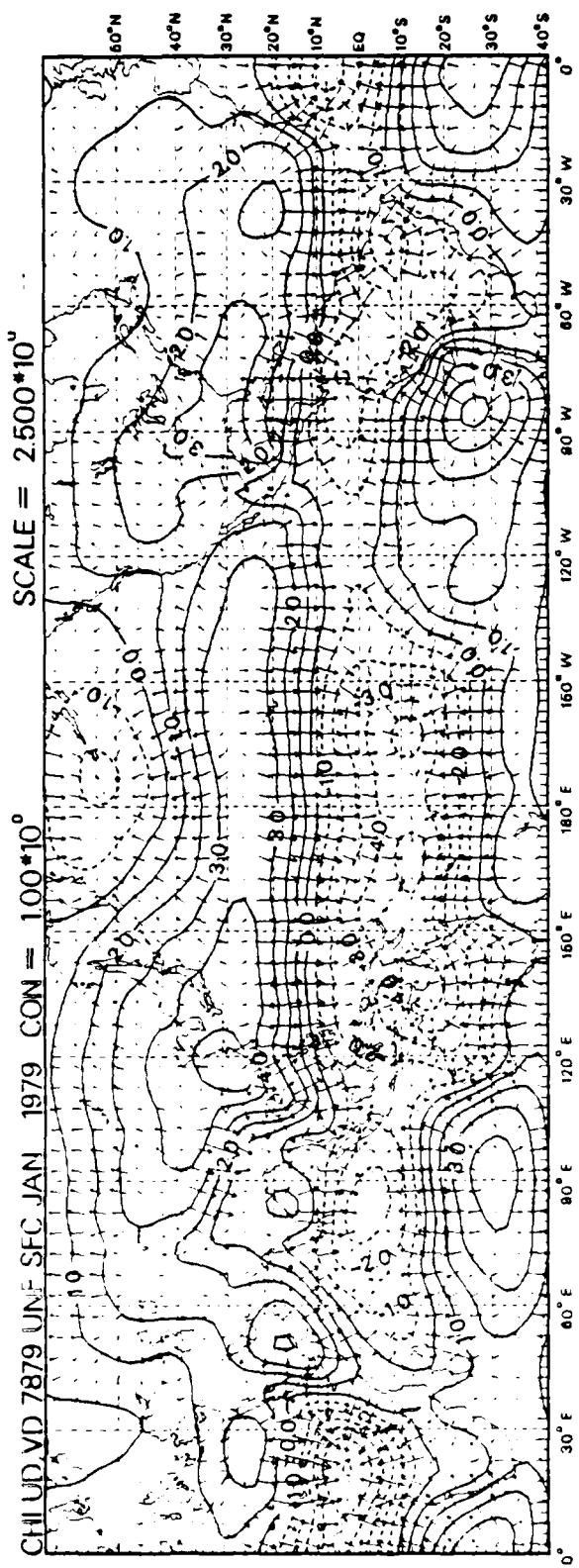


141

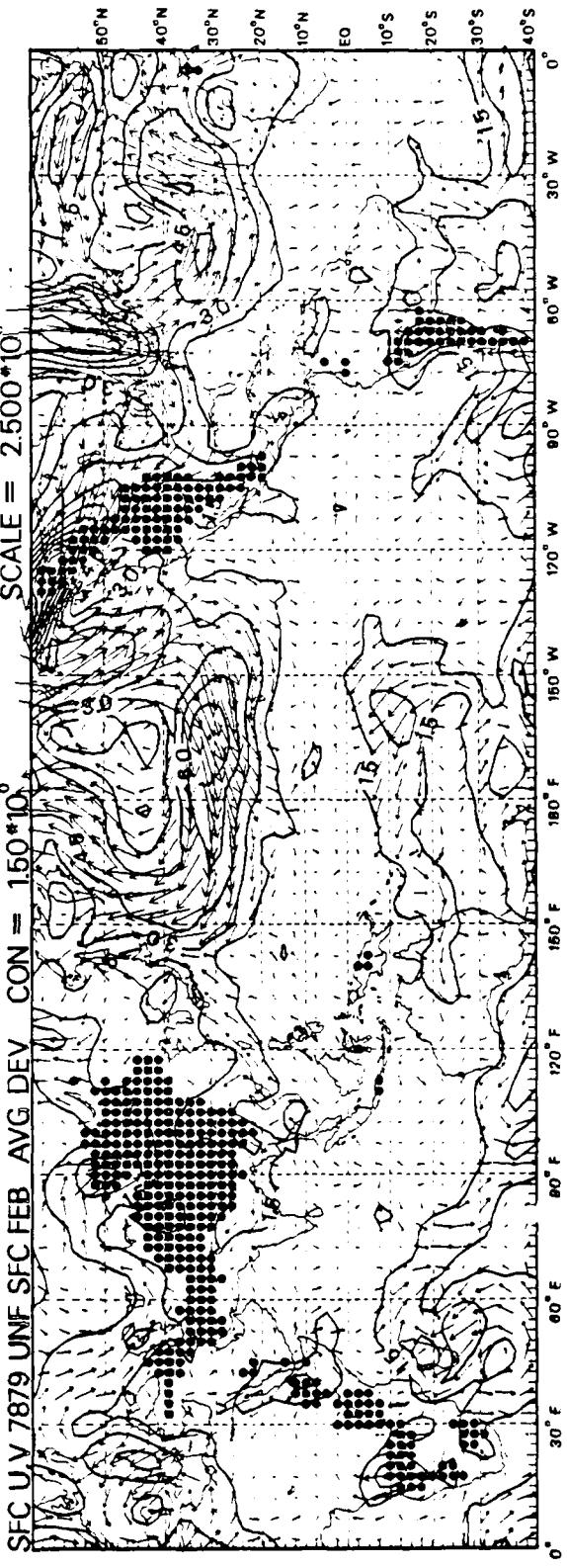
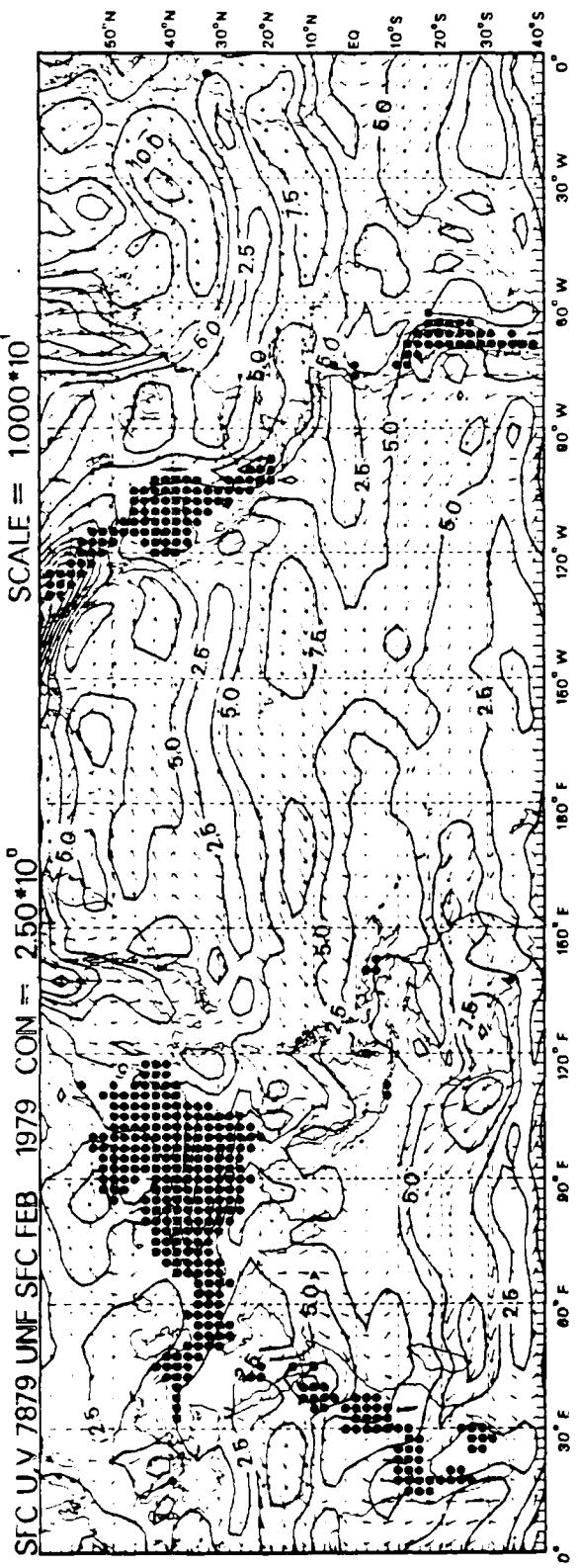


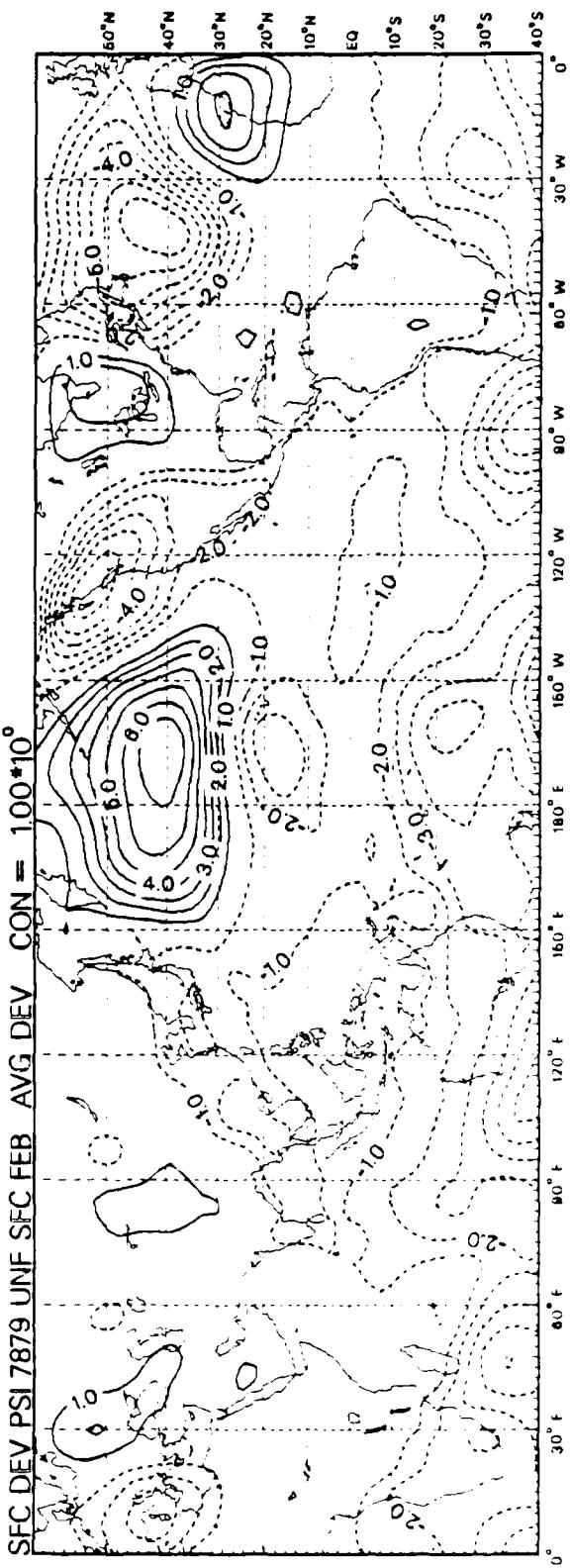
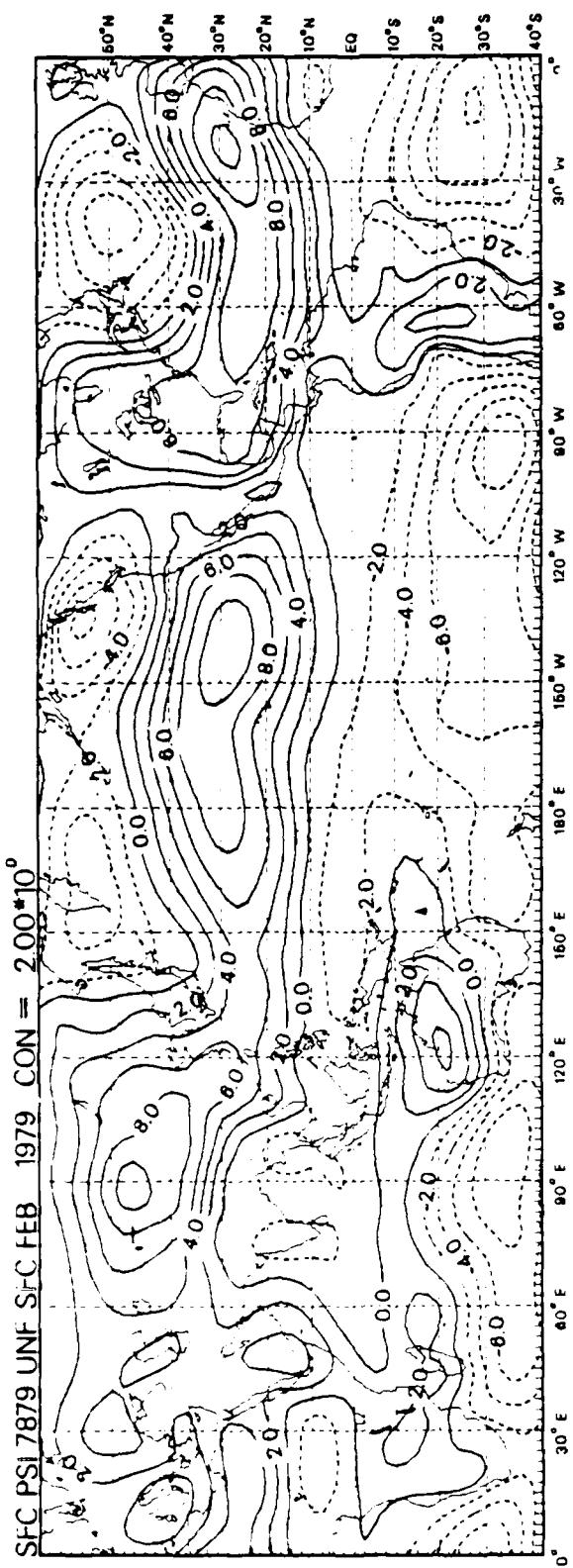
100

D42



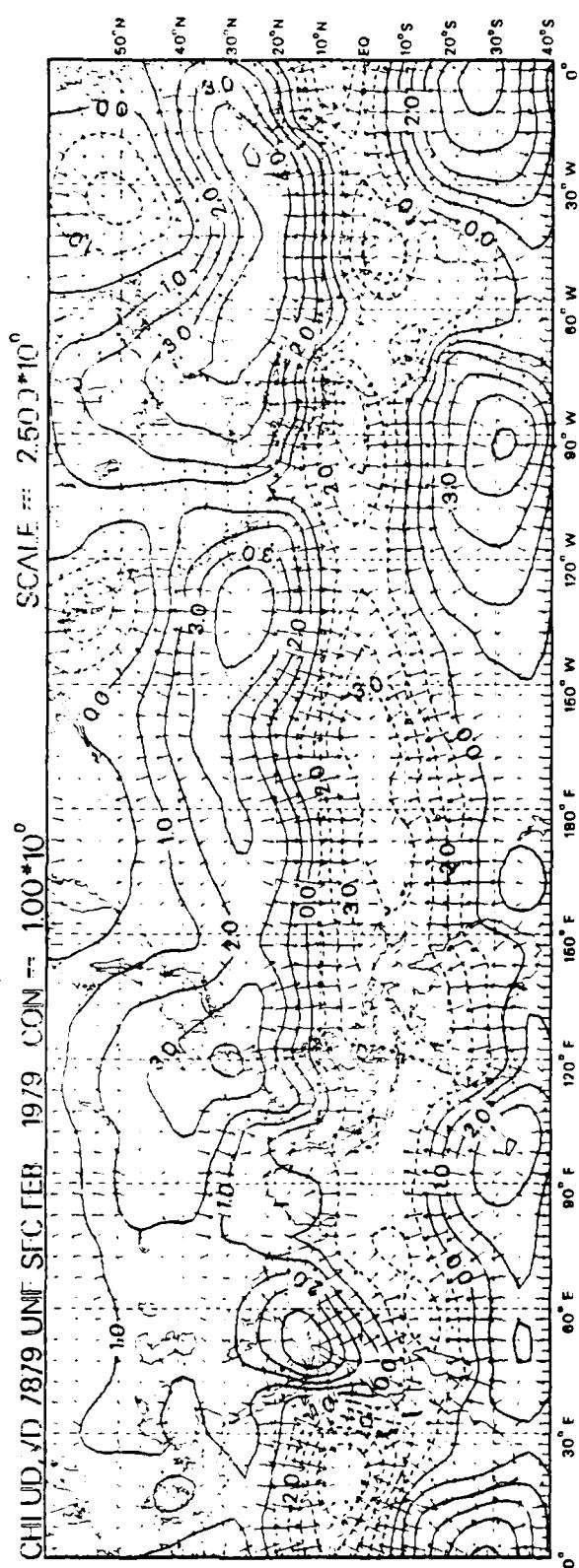
D43



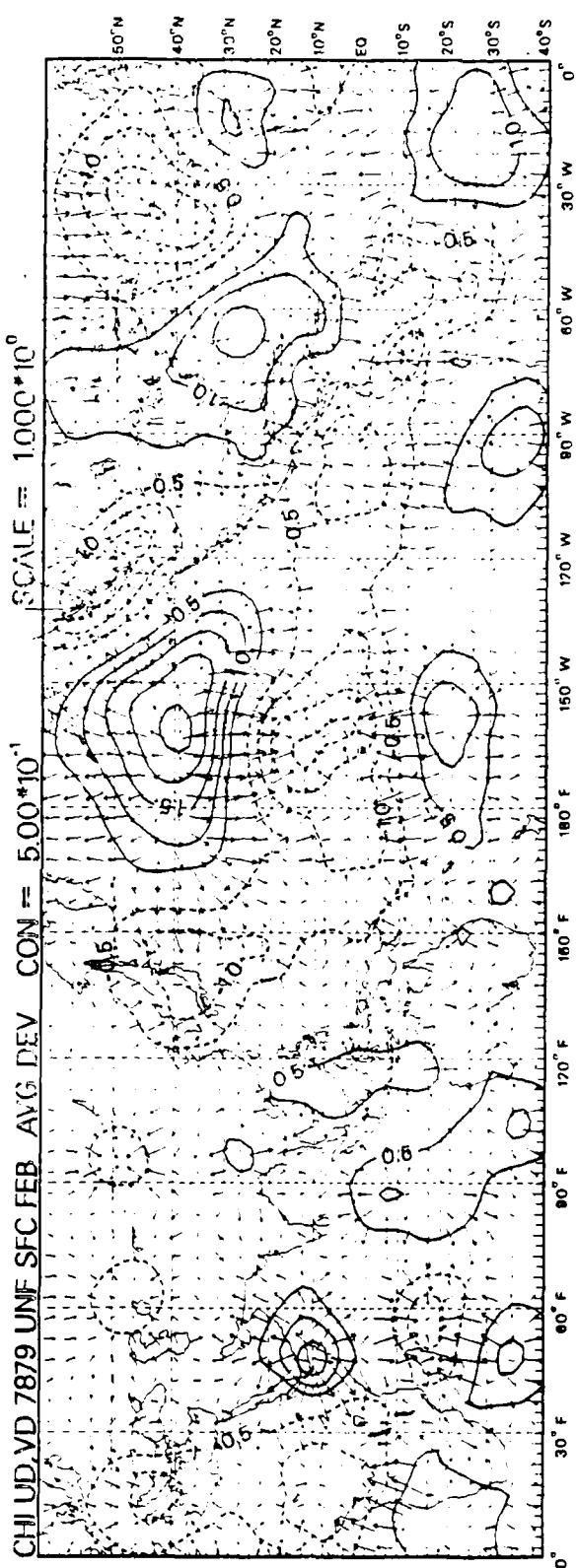


D45

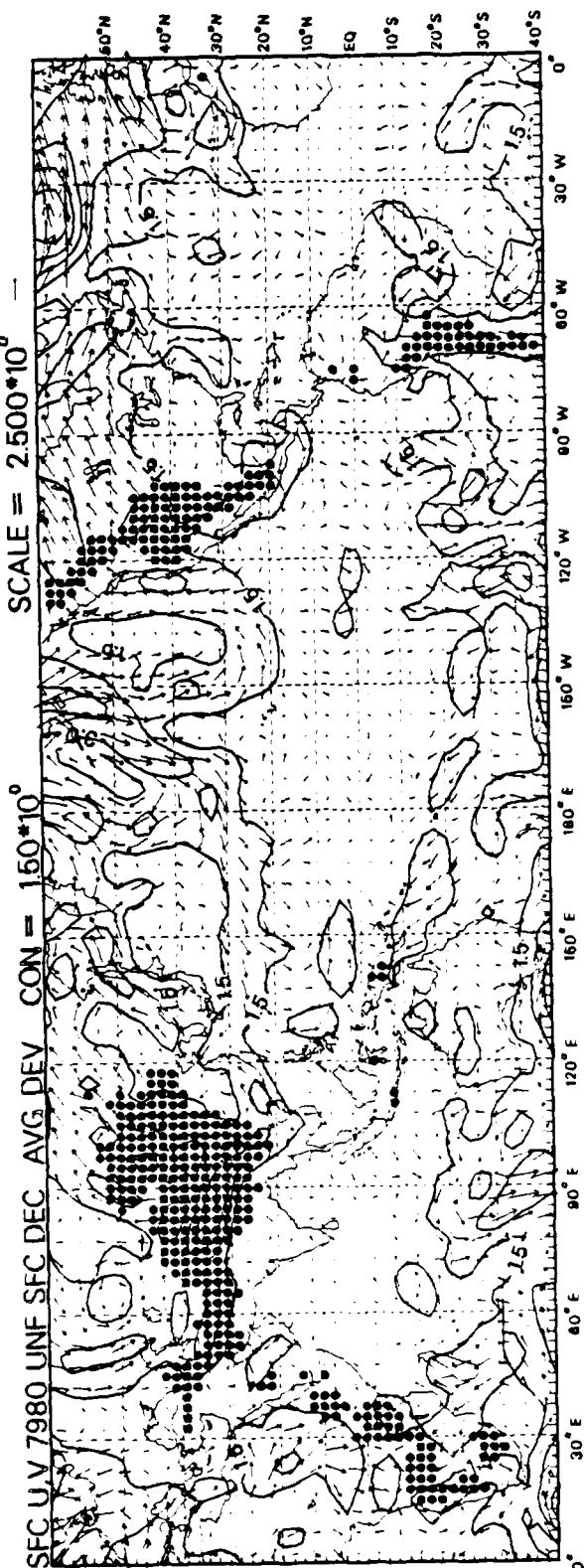
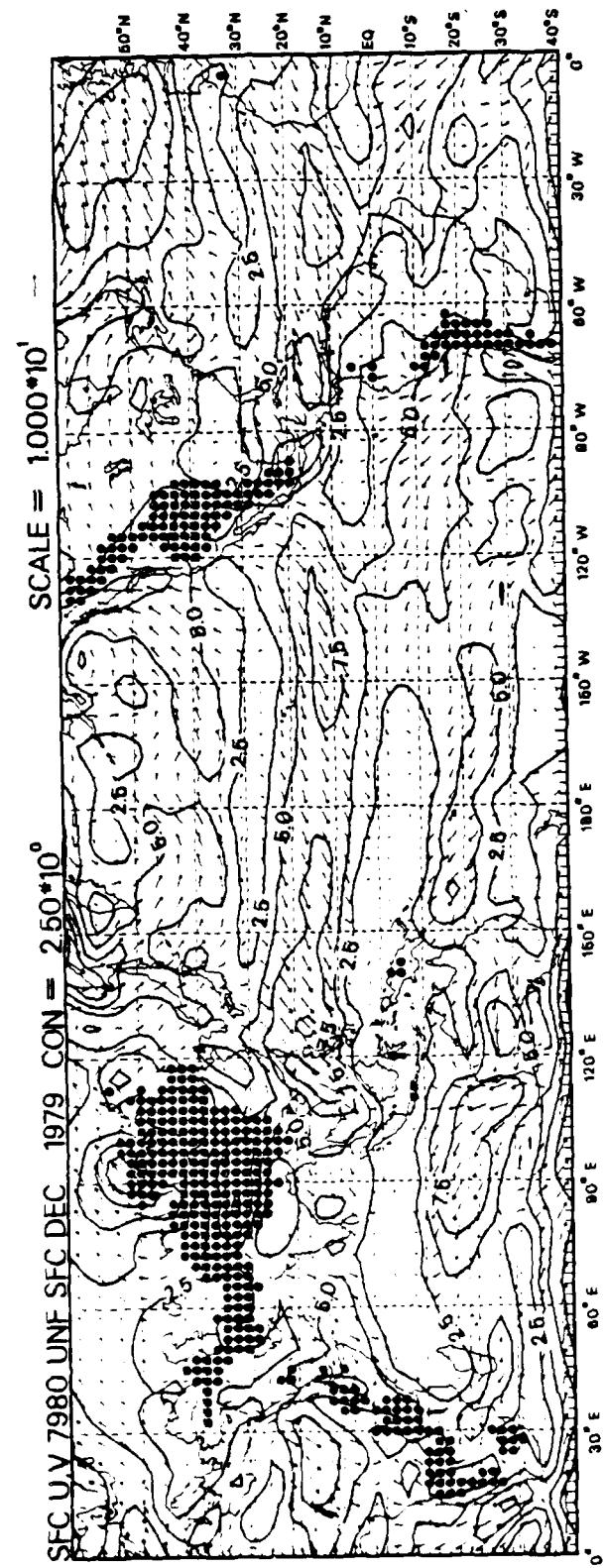
CHI UDV 7879 UNF SFC FEB 1979 CON = 1.00×10^0



CHI UDV 7879 UNF SFC FEB AVG DEV CON = 5.00×10^{-1}

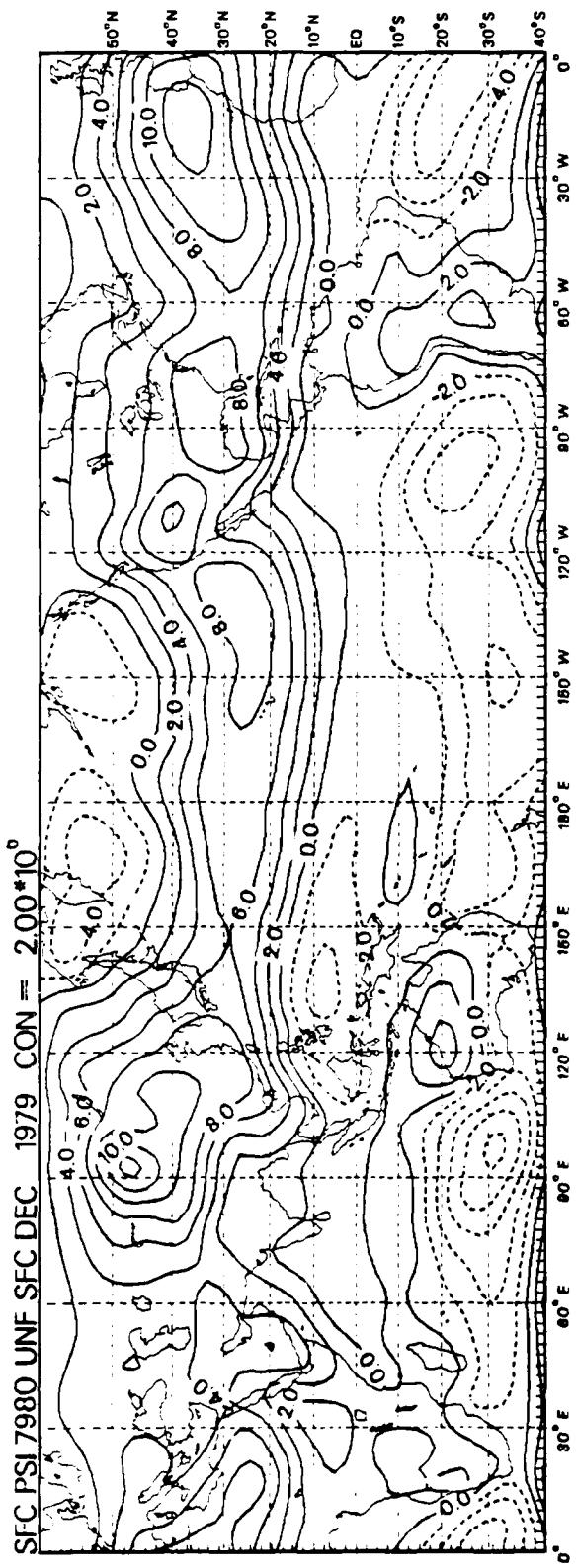


D46

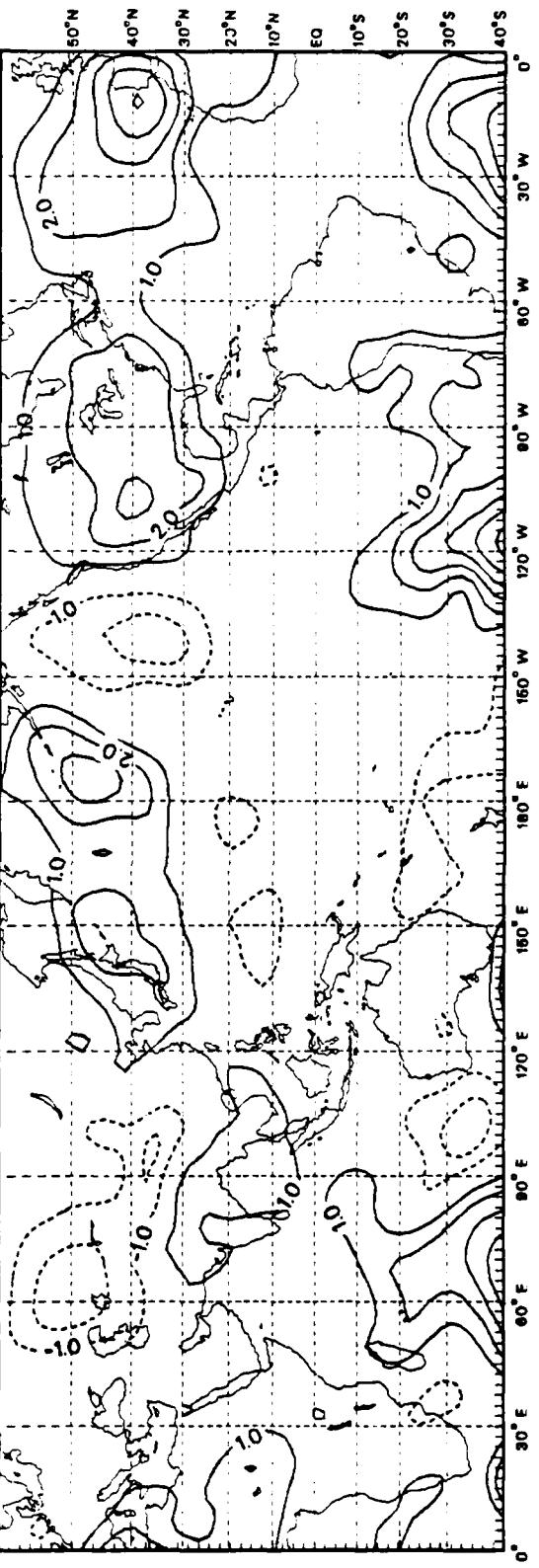


116

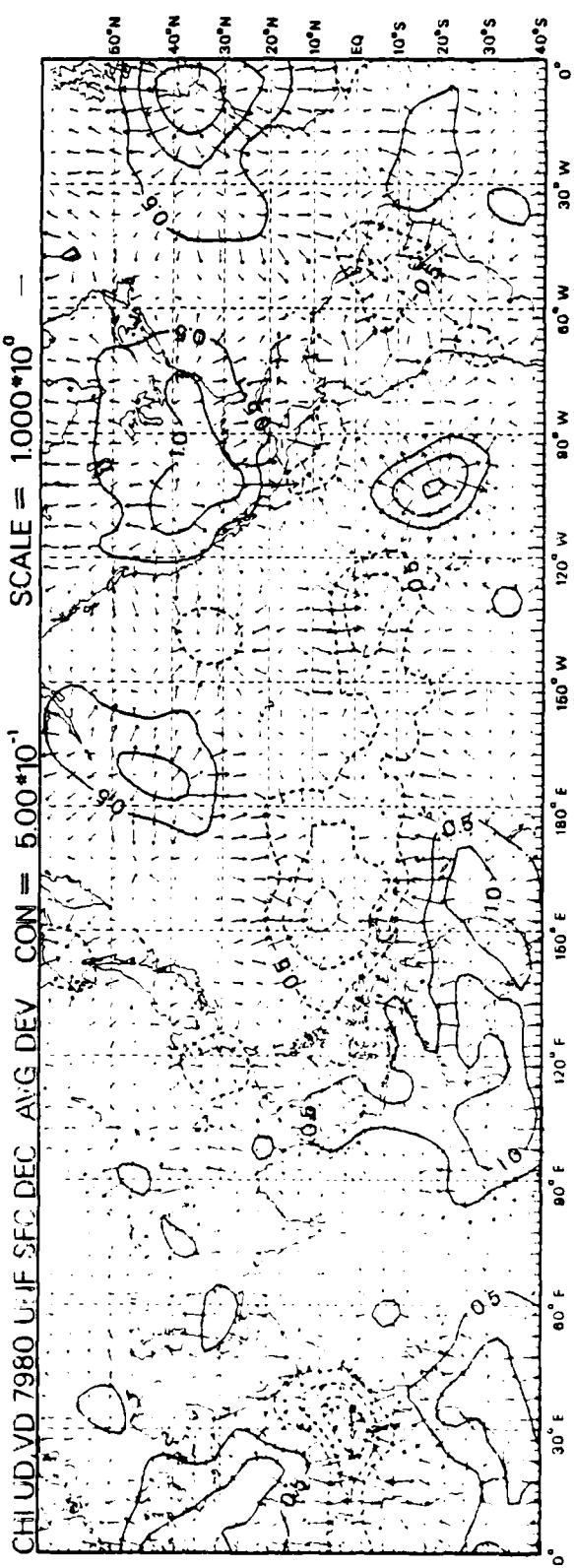
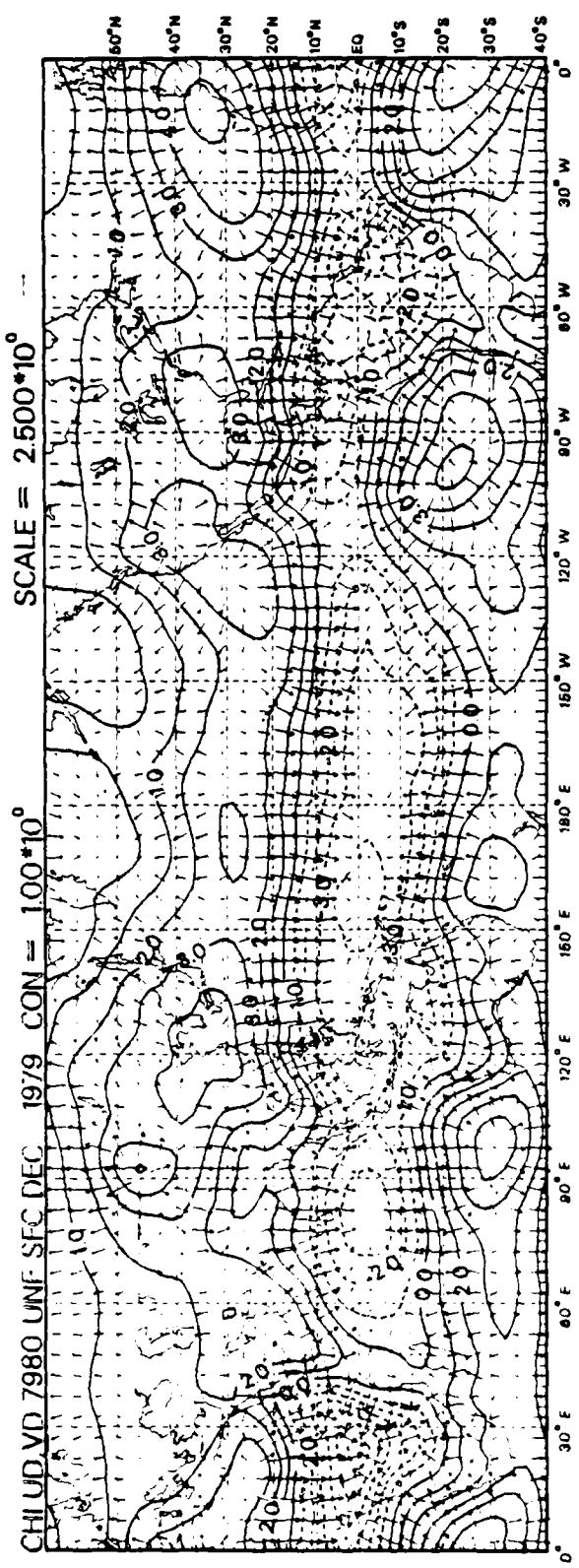
D47



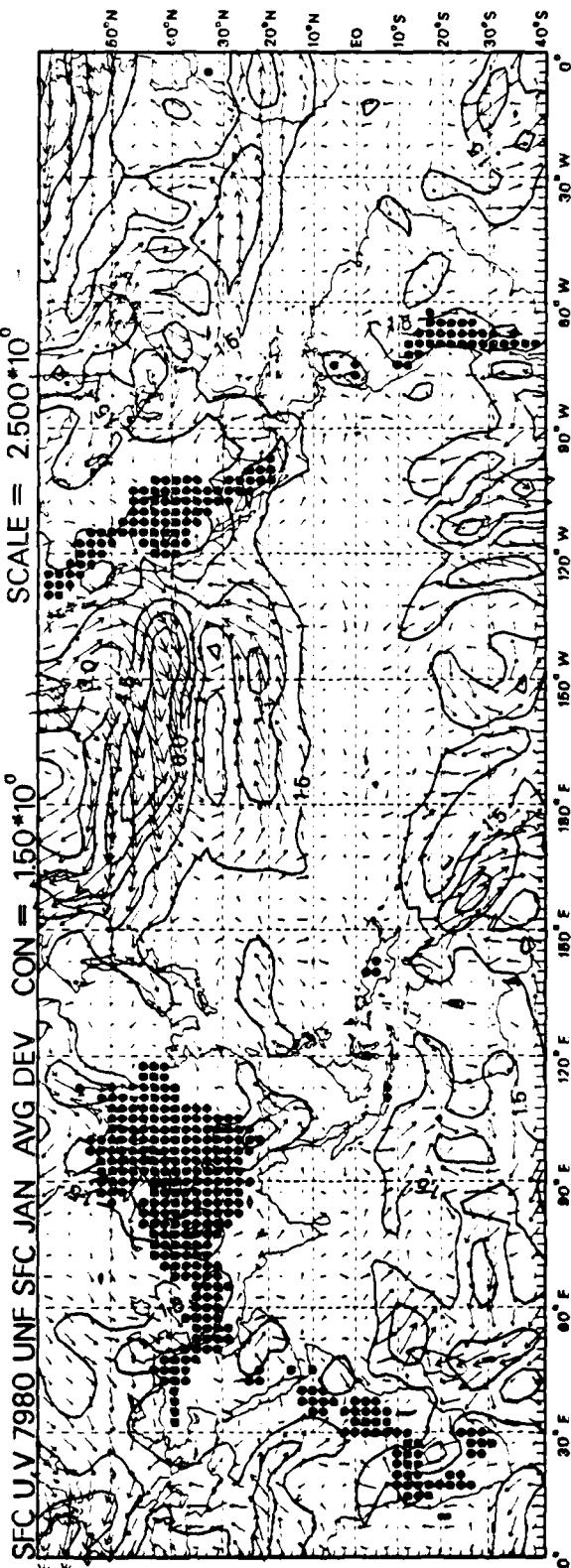
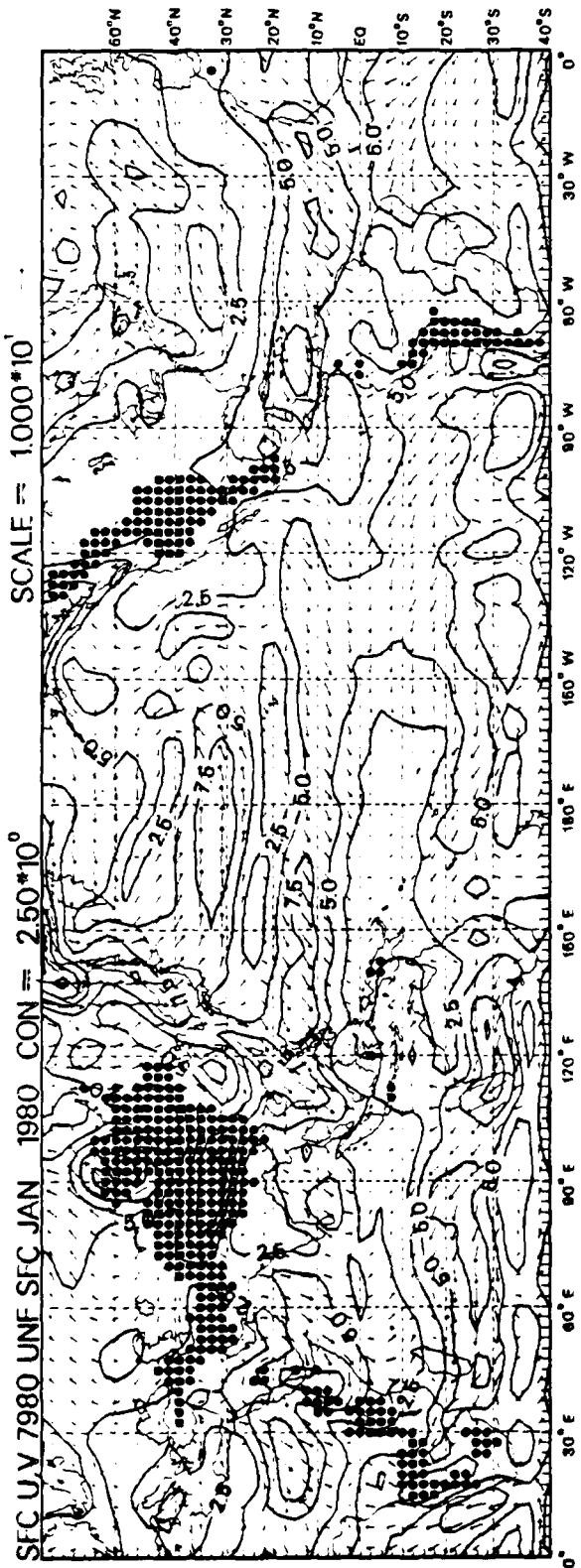
SFC DEV PSI 7980 UNF SFC DEC AVG DEV CON = $100 \cdot 10^6$



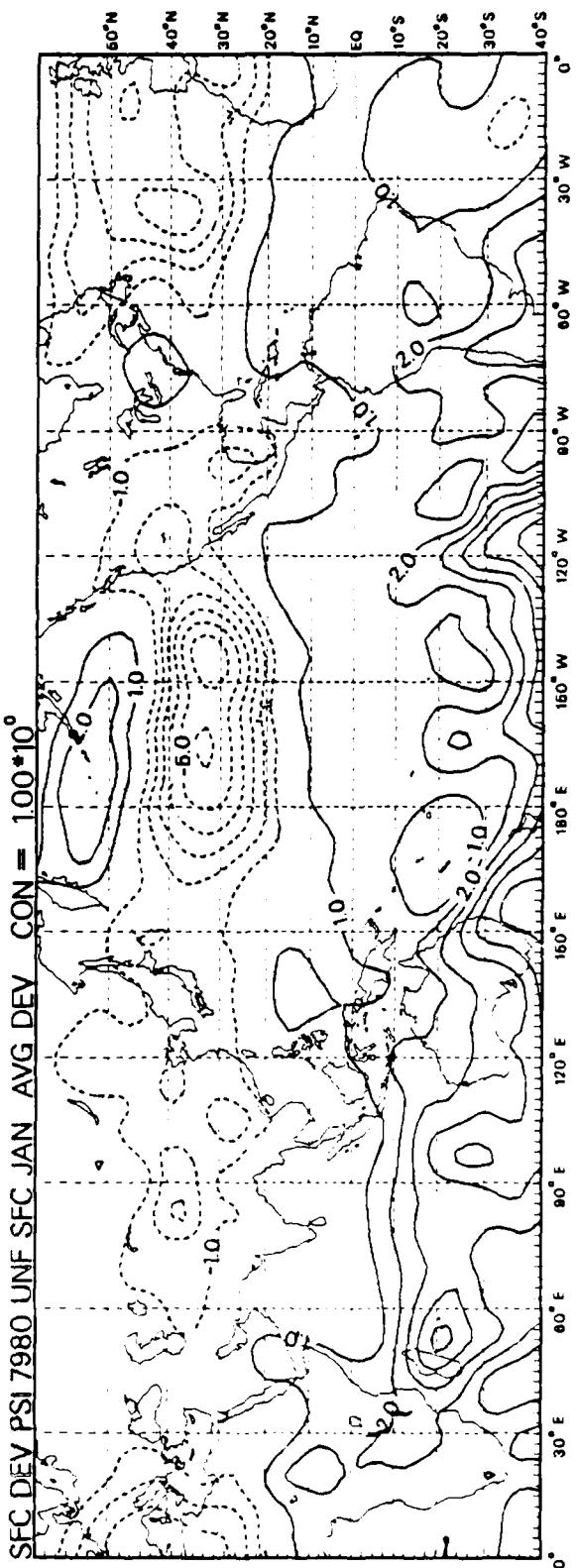
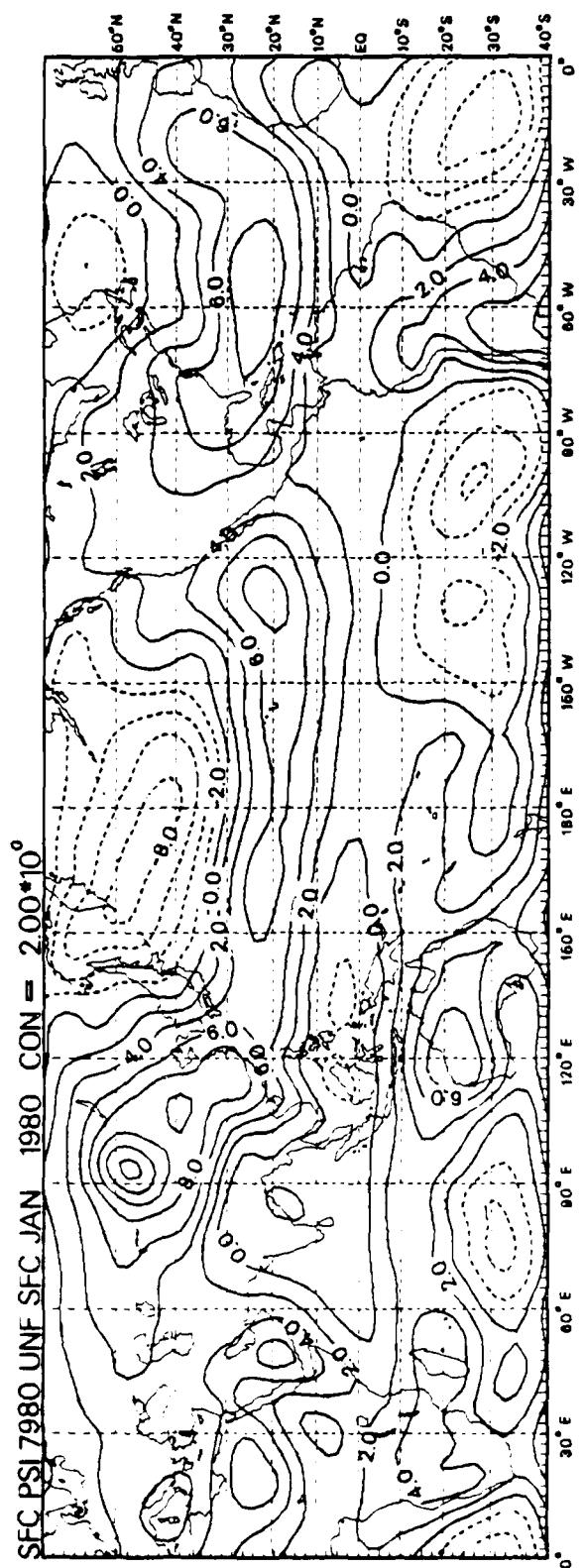
D48



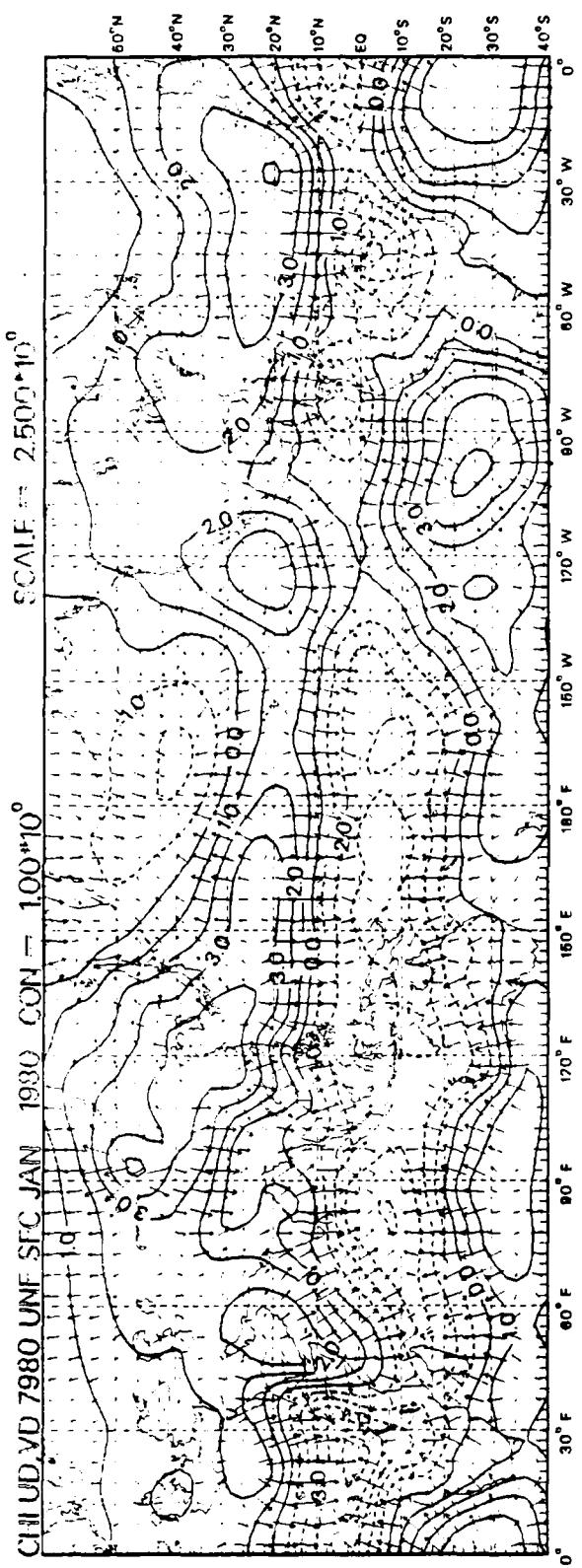
D49



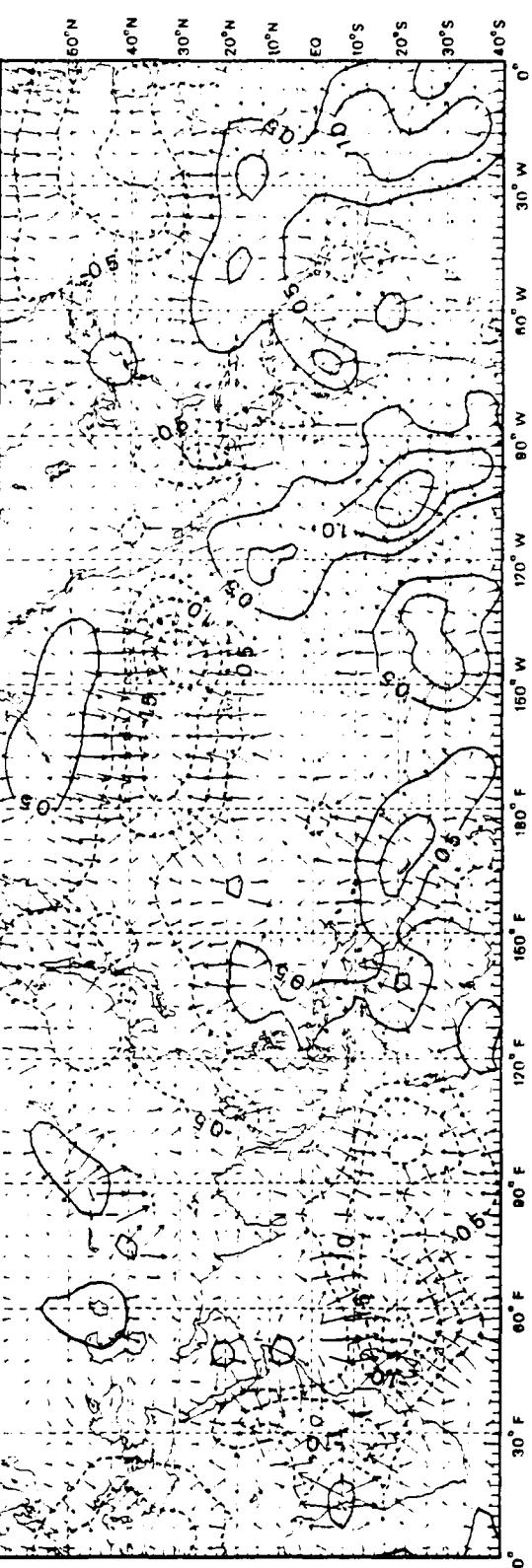
D50



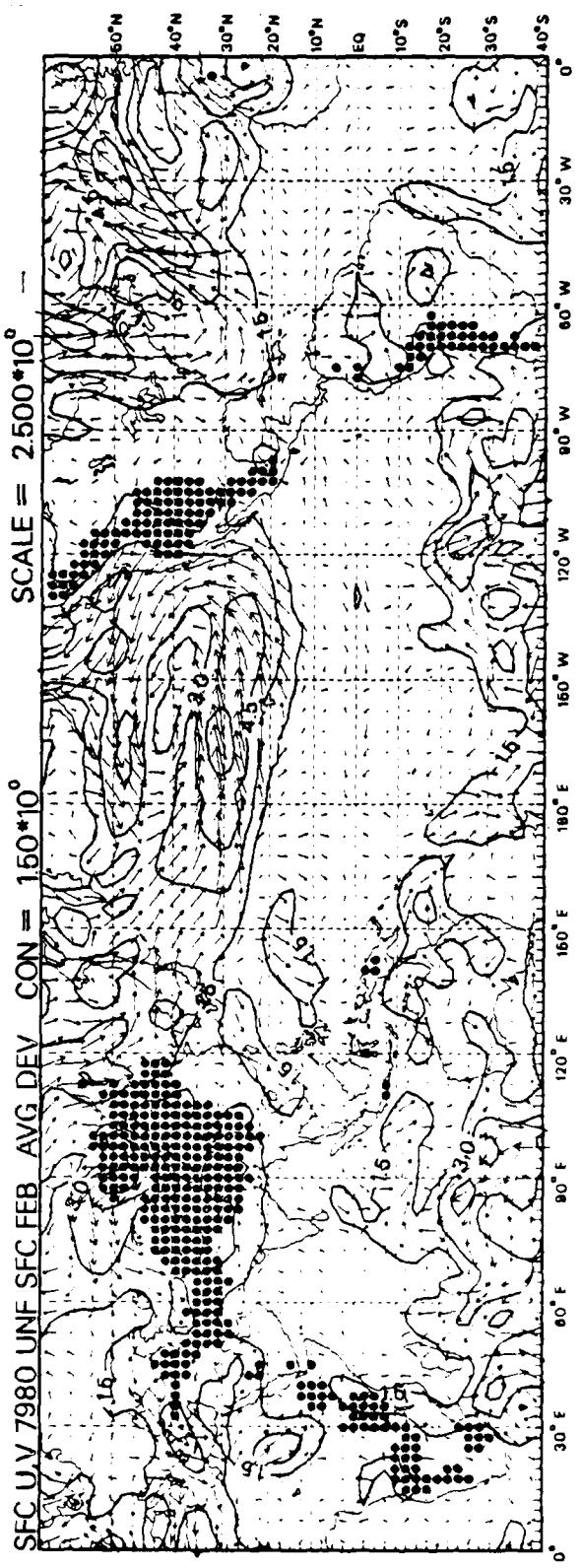
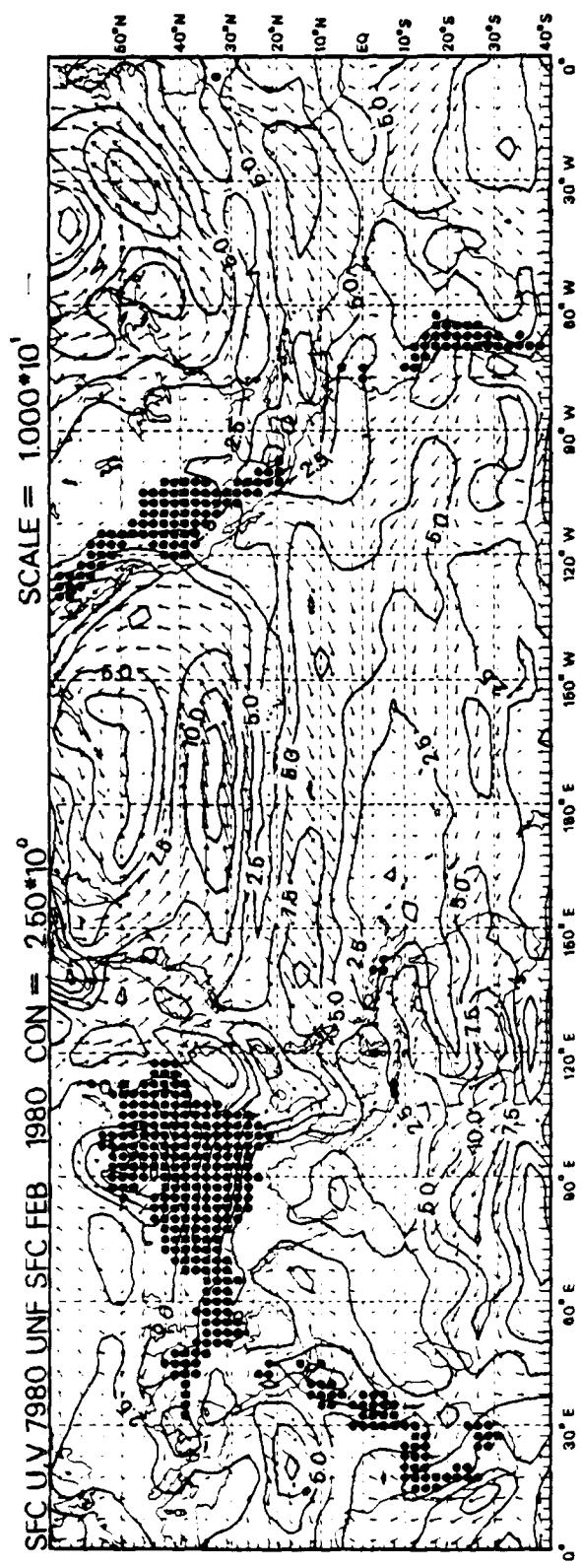
051



CHI UD VD 7980 UNF SFC JAN AVG DEV CON = $5,00 \cdot 10^1$

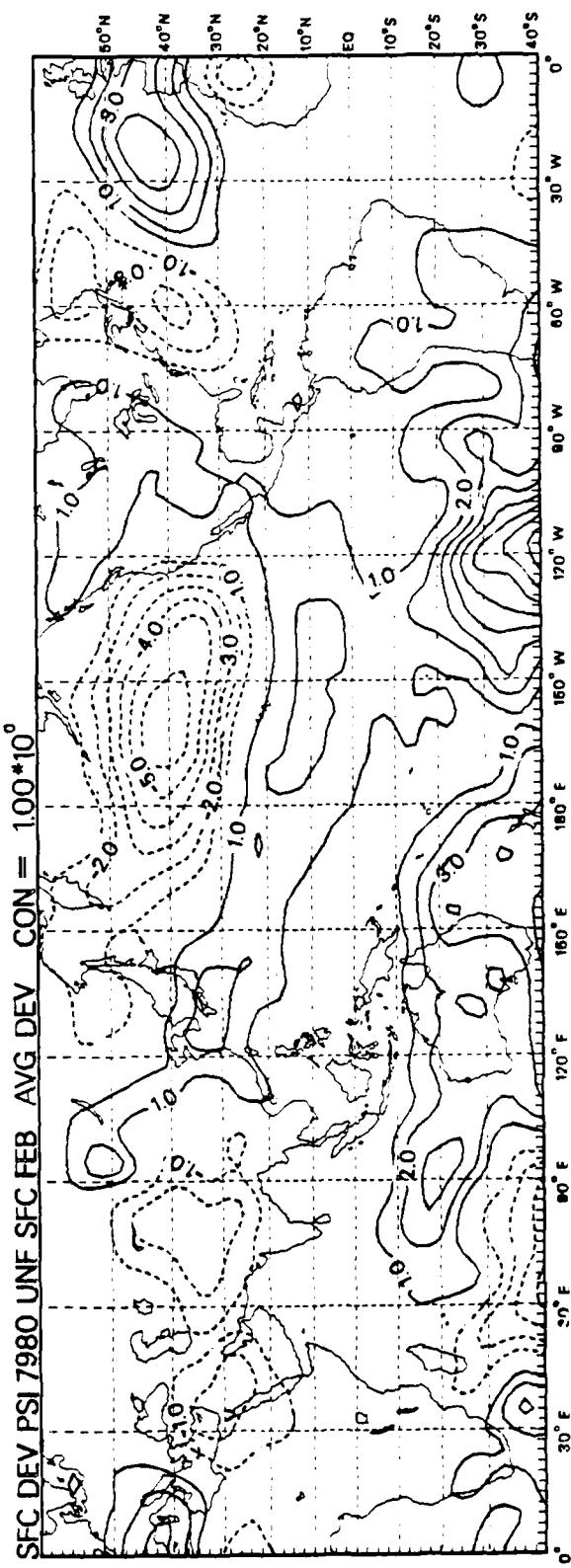
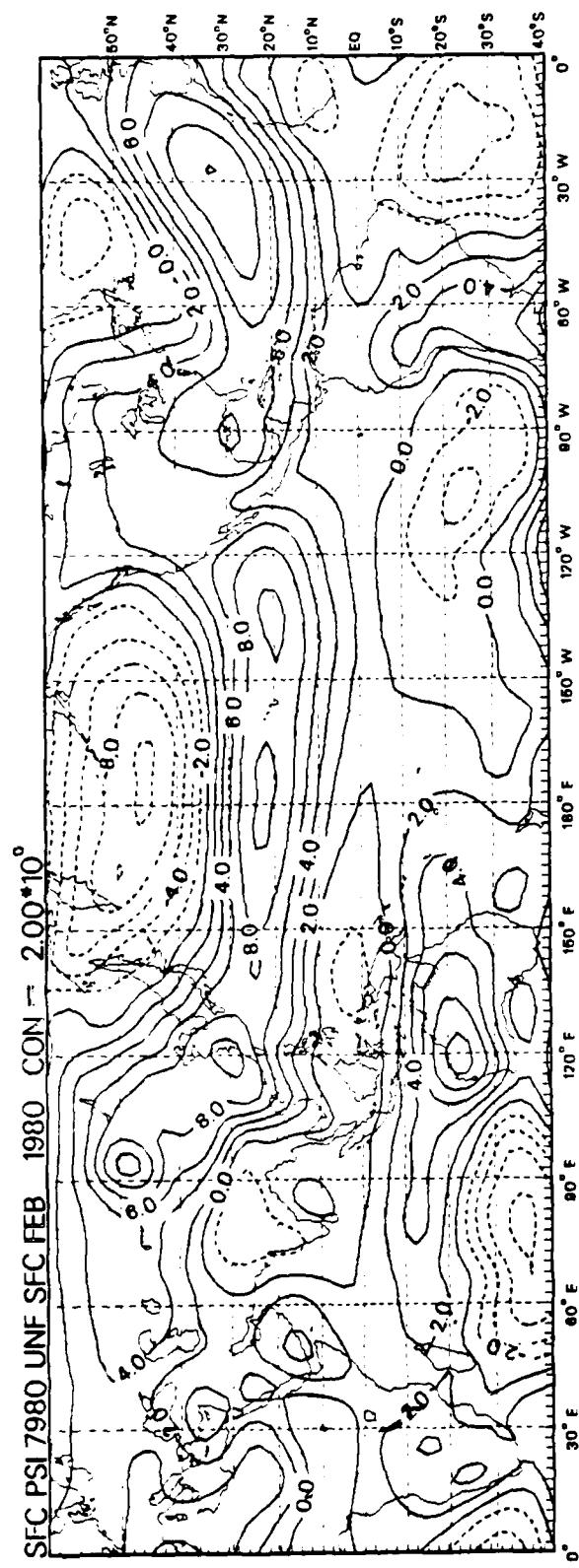


052



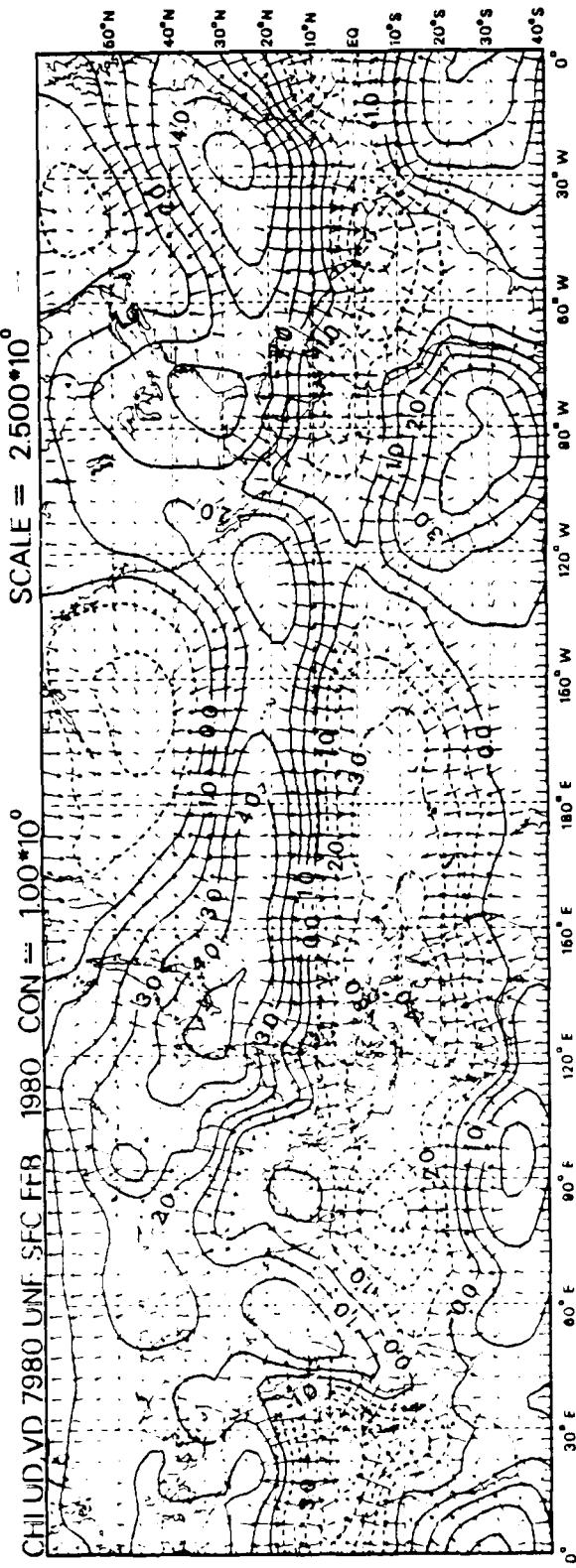
1111

D53

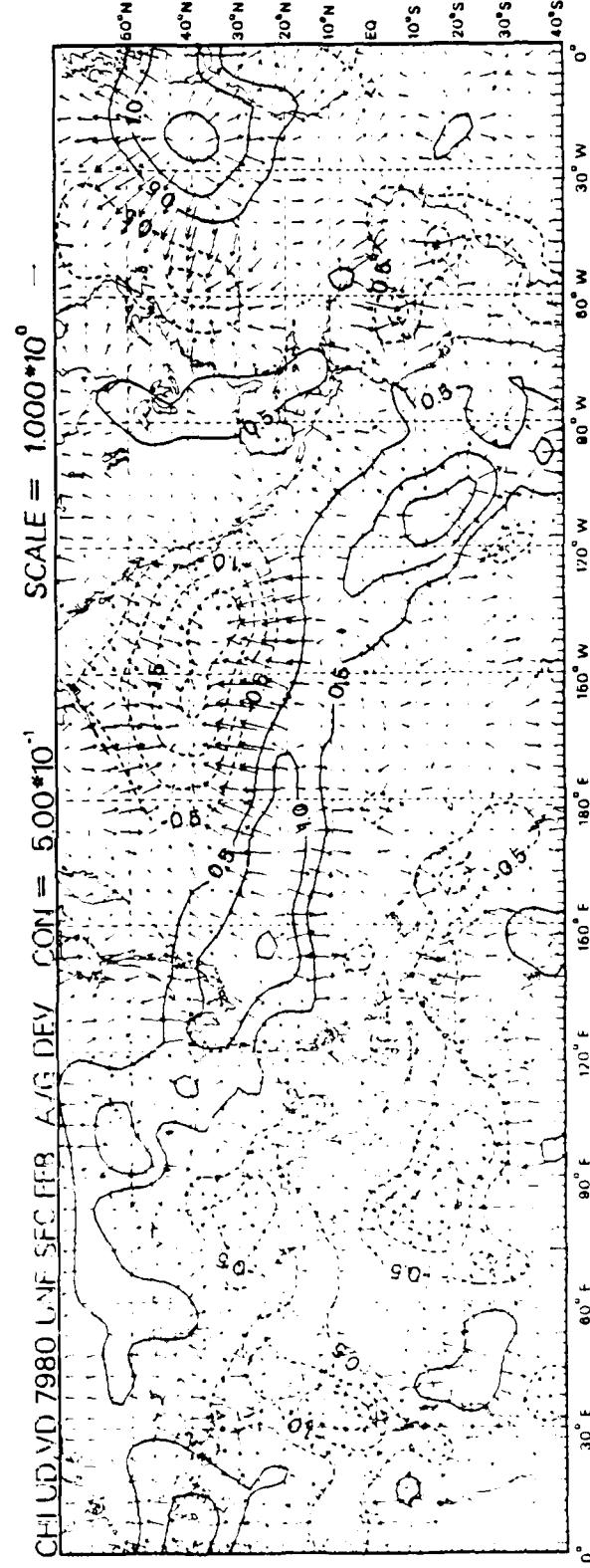


D54

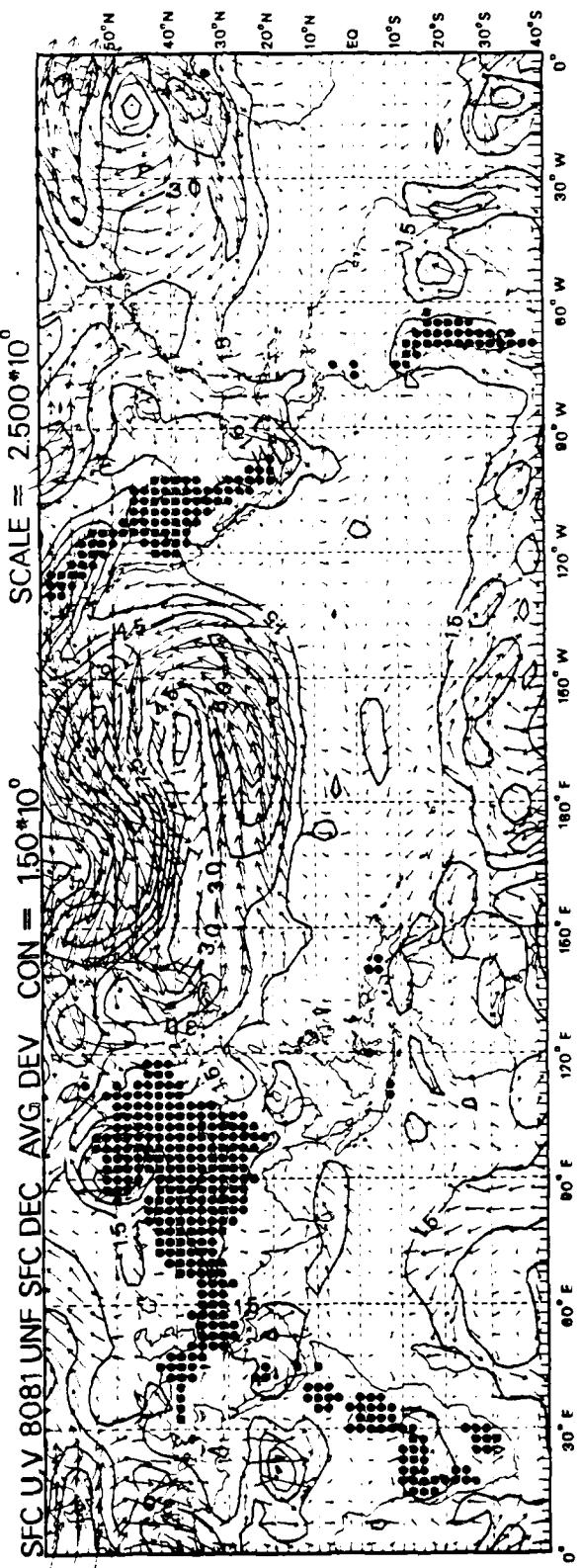
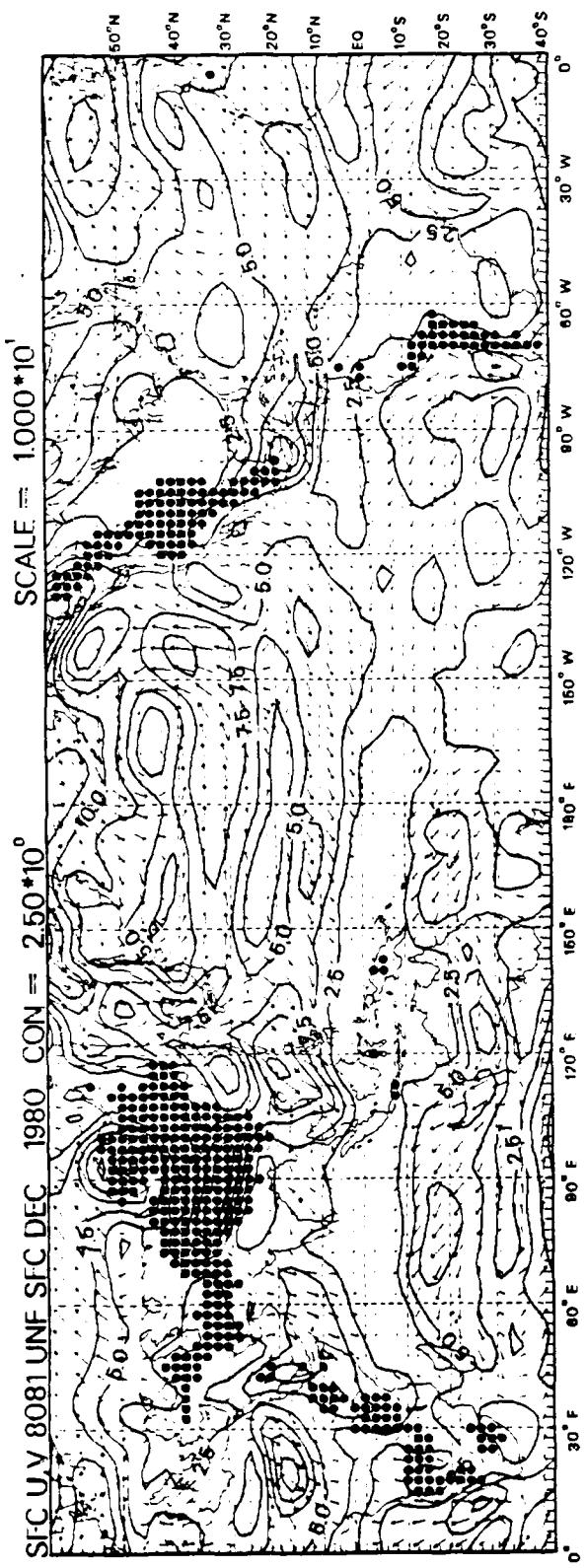
CHI LUD VD 7980 LNF SFC FFB 1980 CON = $100 * 10^6$



CHI LUD VD 7980 LNF SFC FFB A/G DEV CON = $5.00 * 10^6$

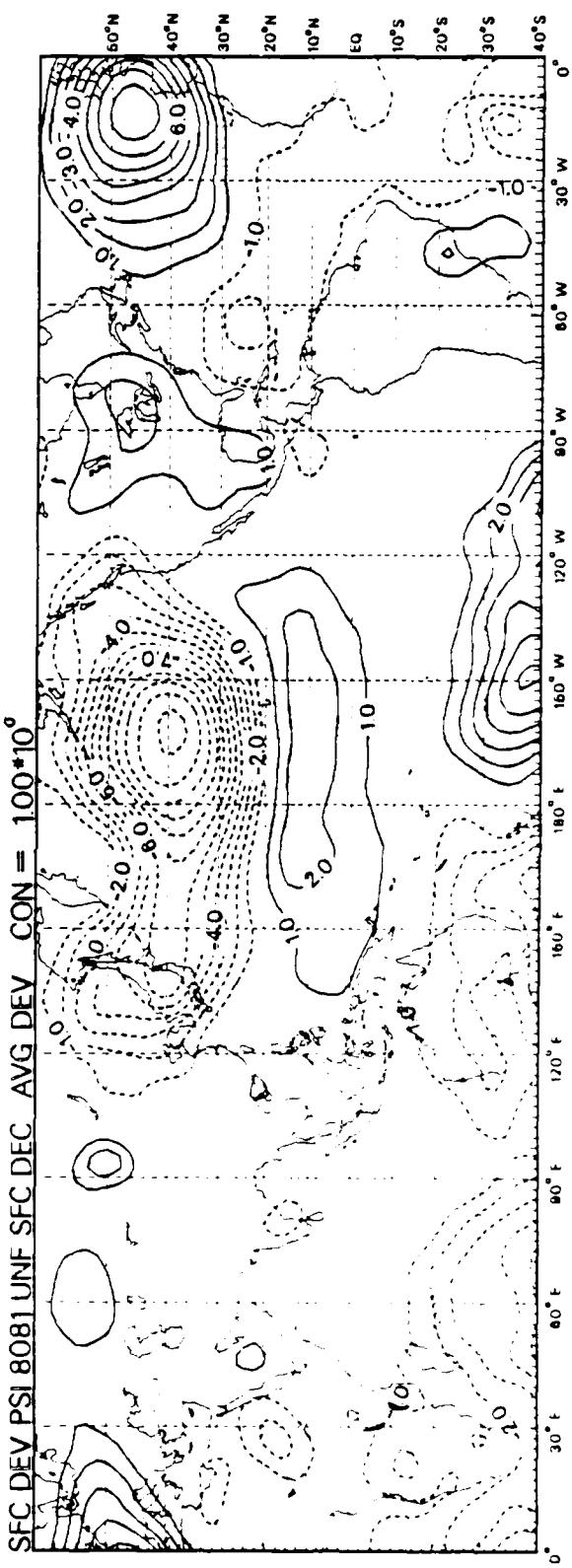
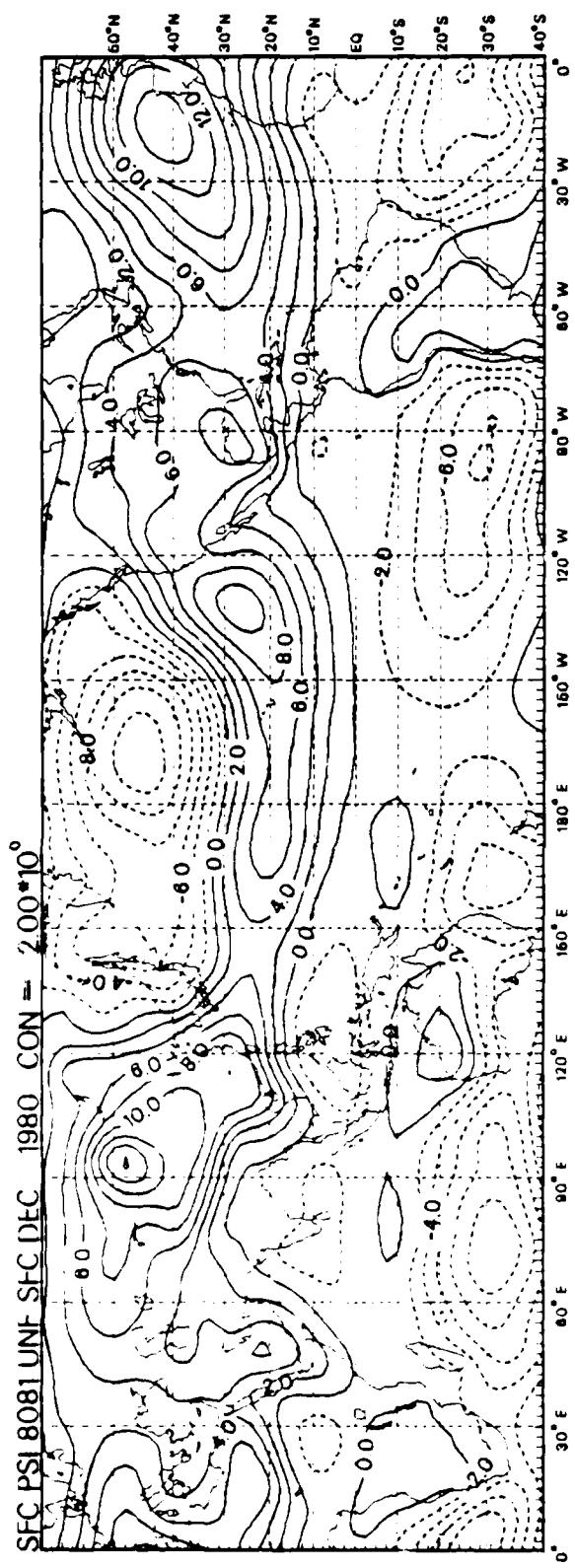


055

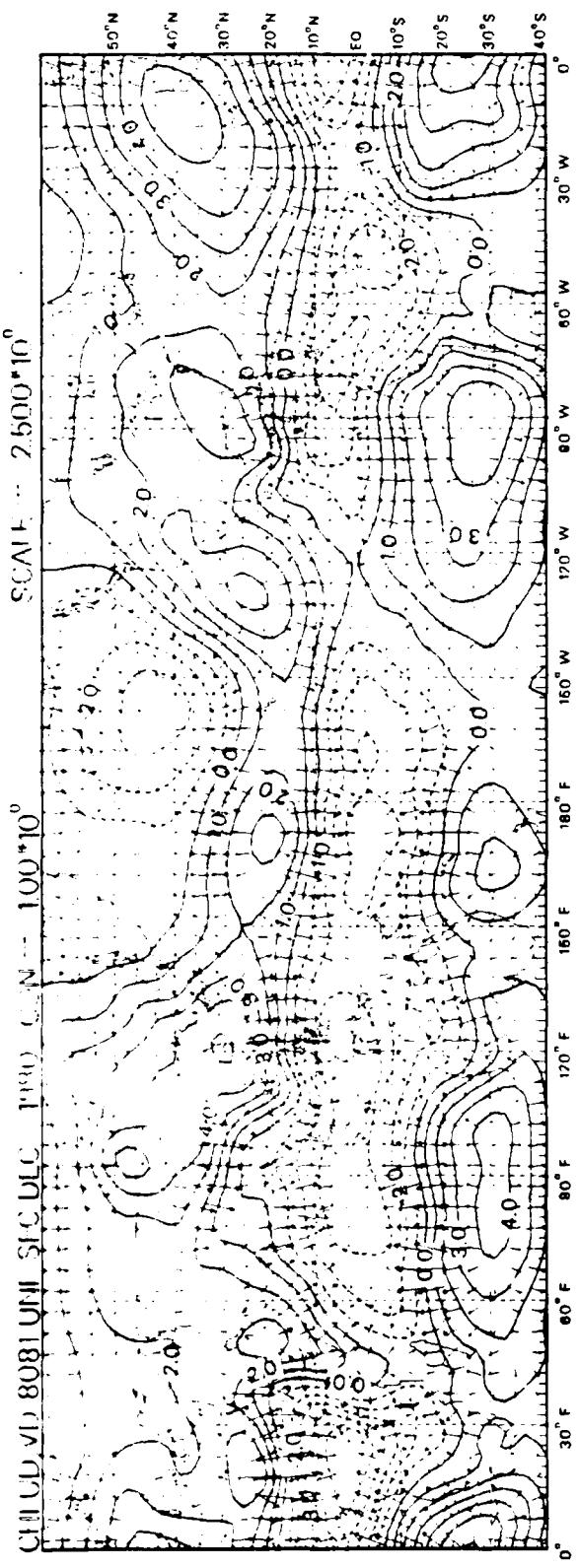


114

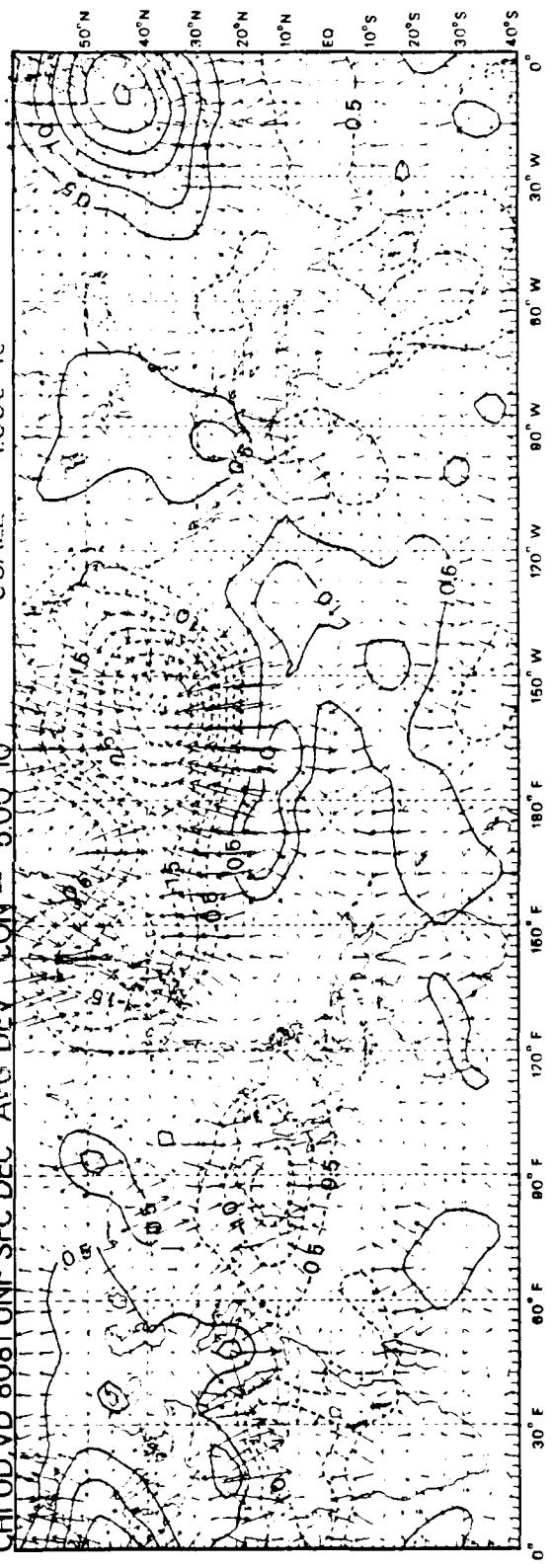
D56



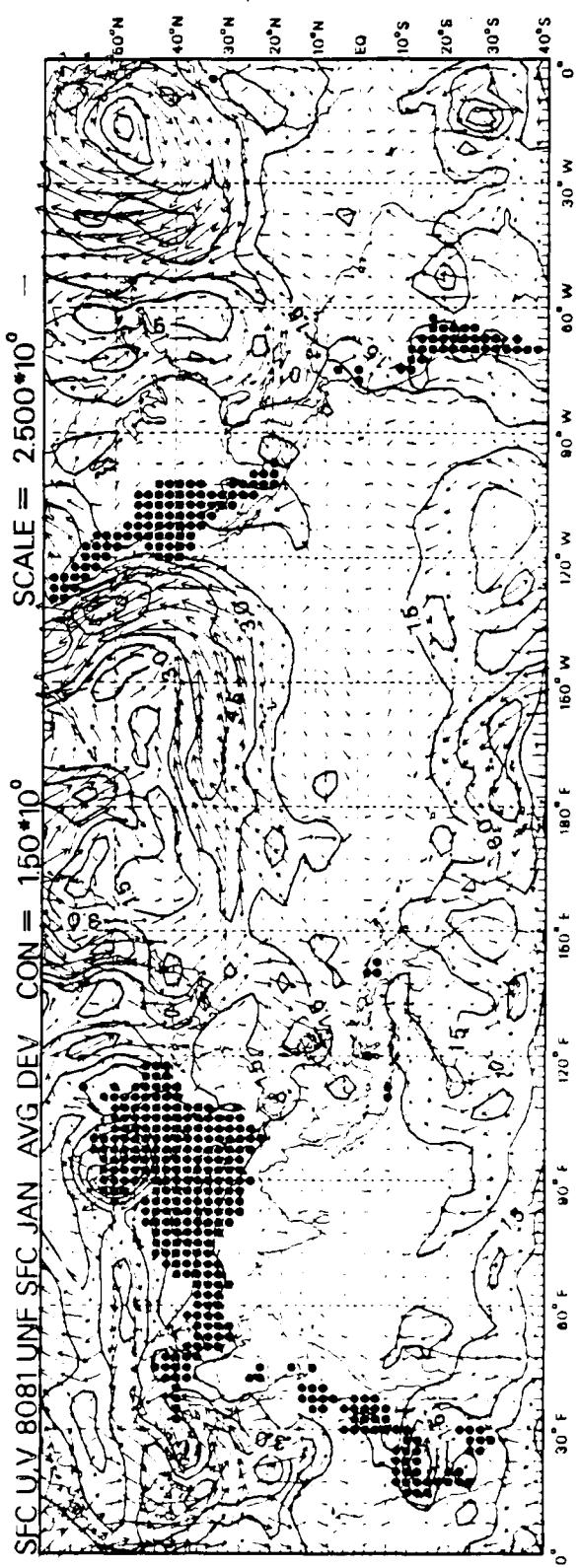
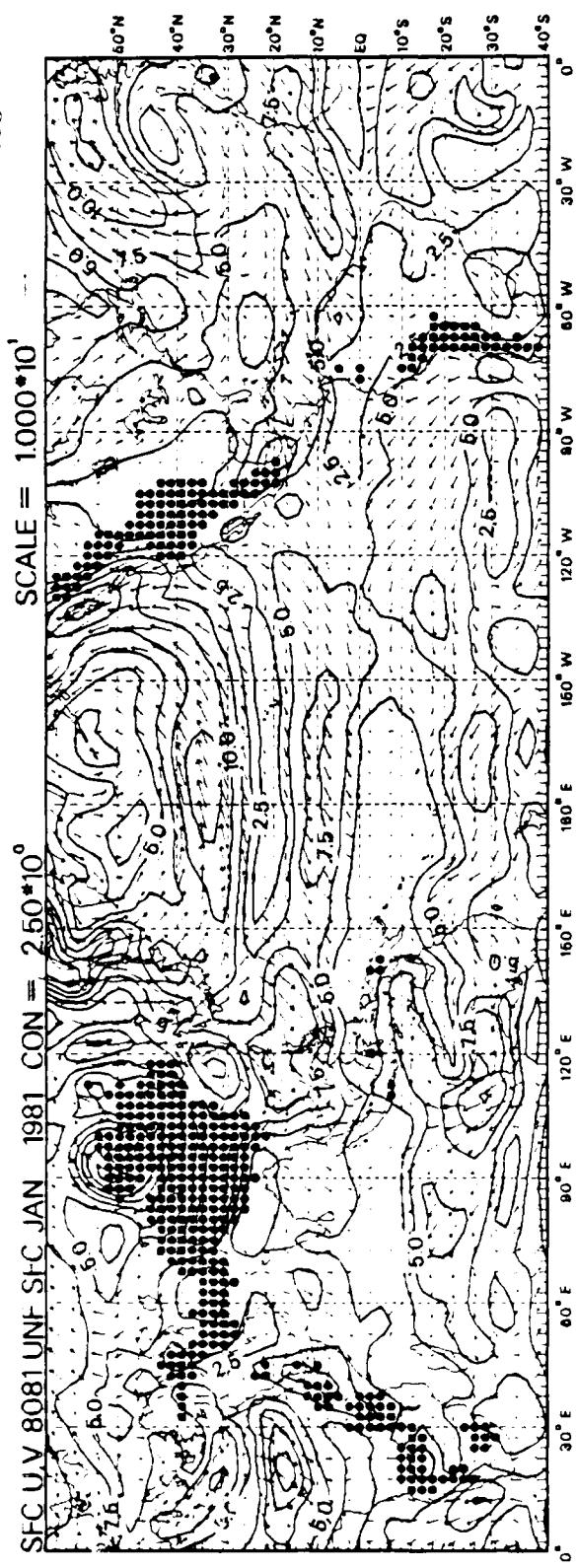
1057



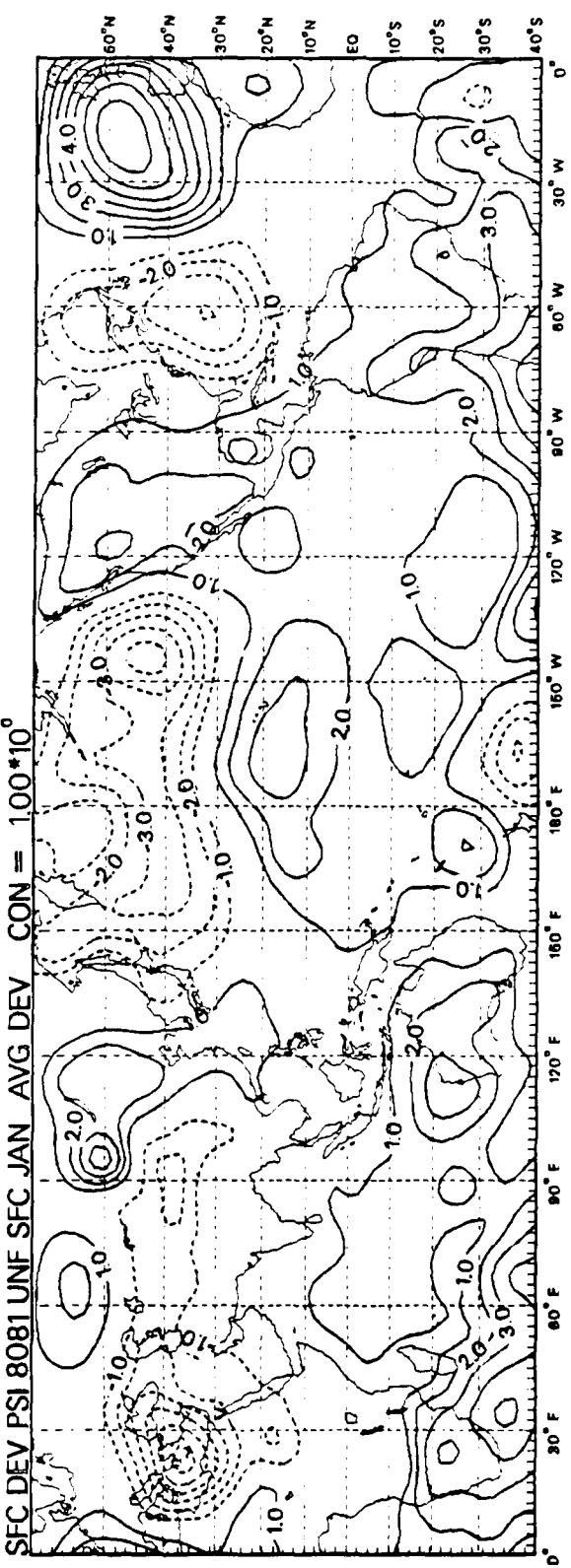
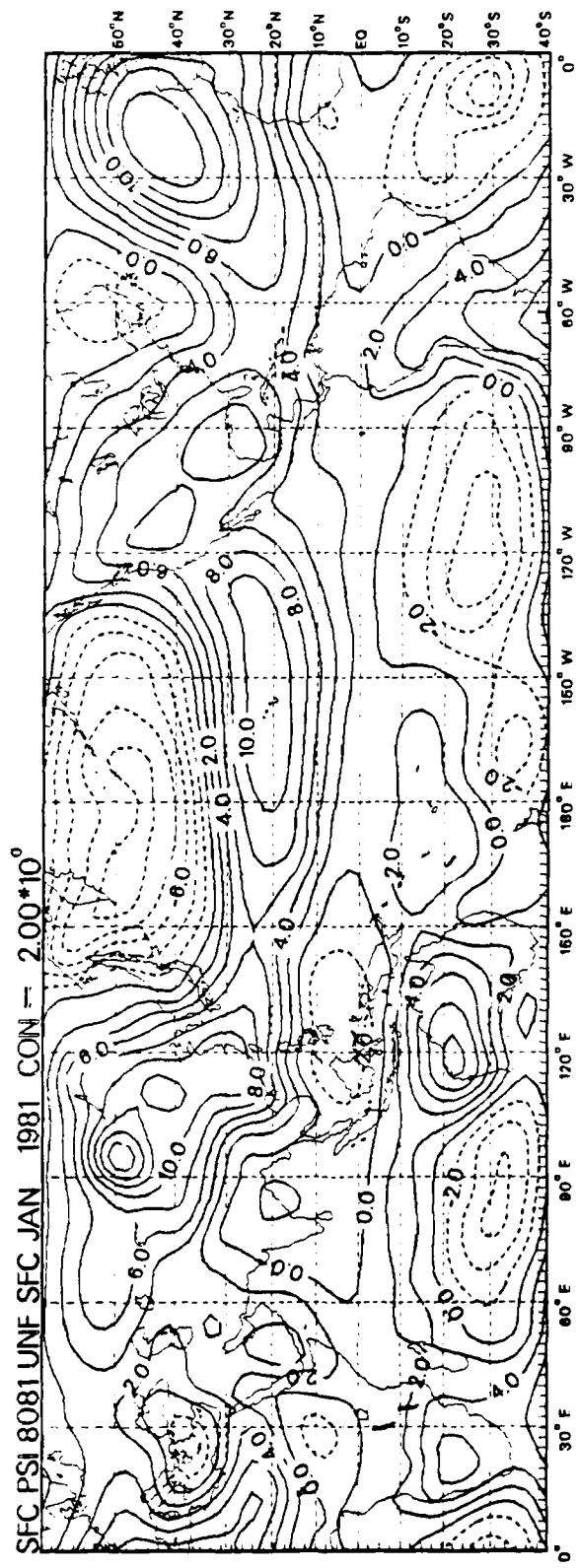
CHI UD VD 8081 UNF SEC DEC CON = 5.00*10⁻¹



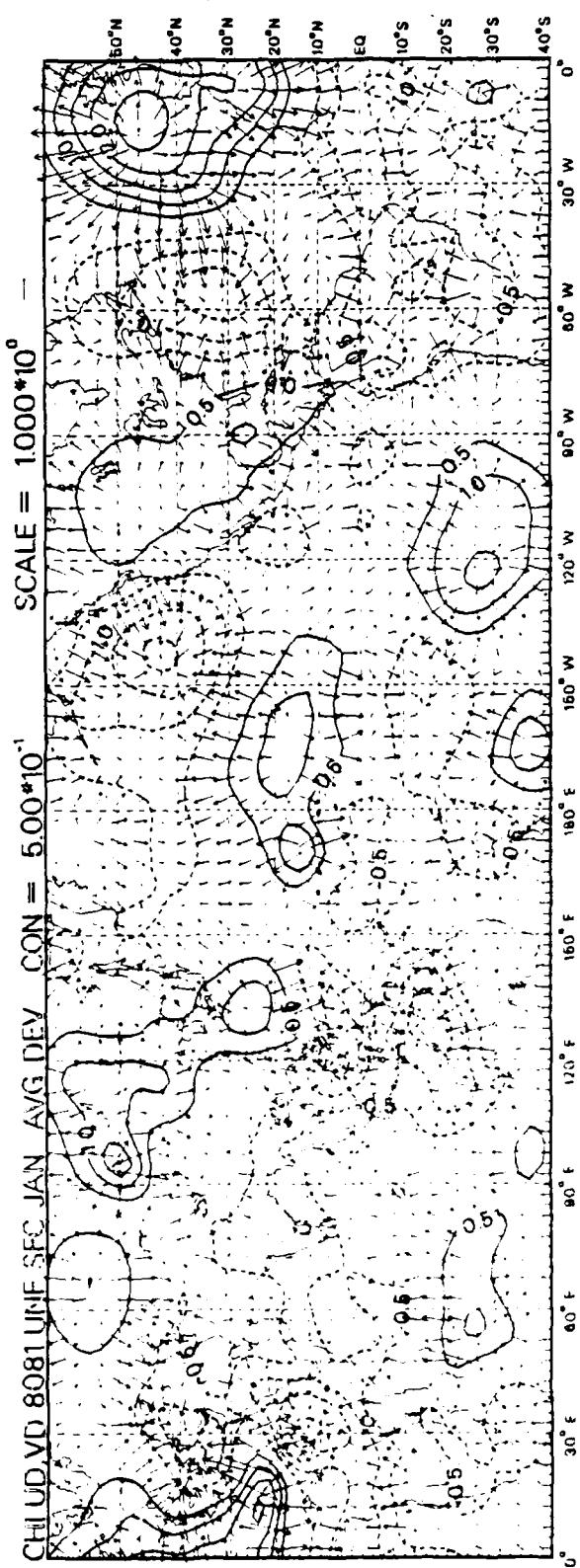
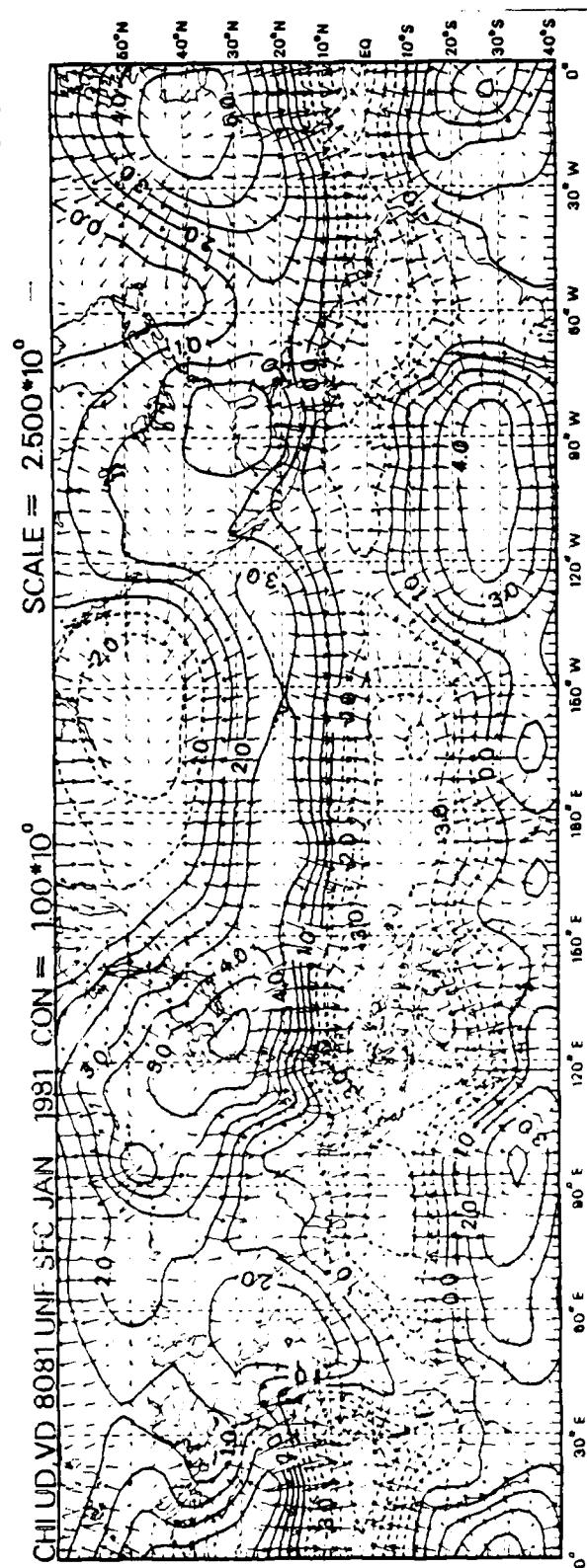
058



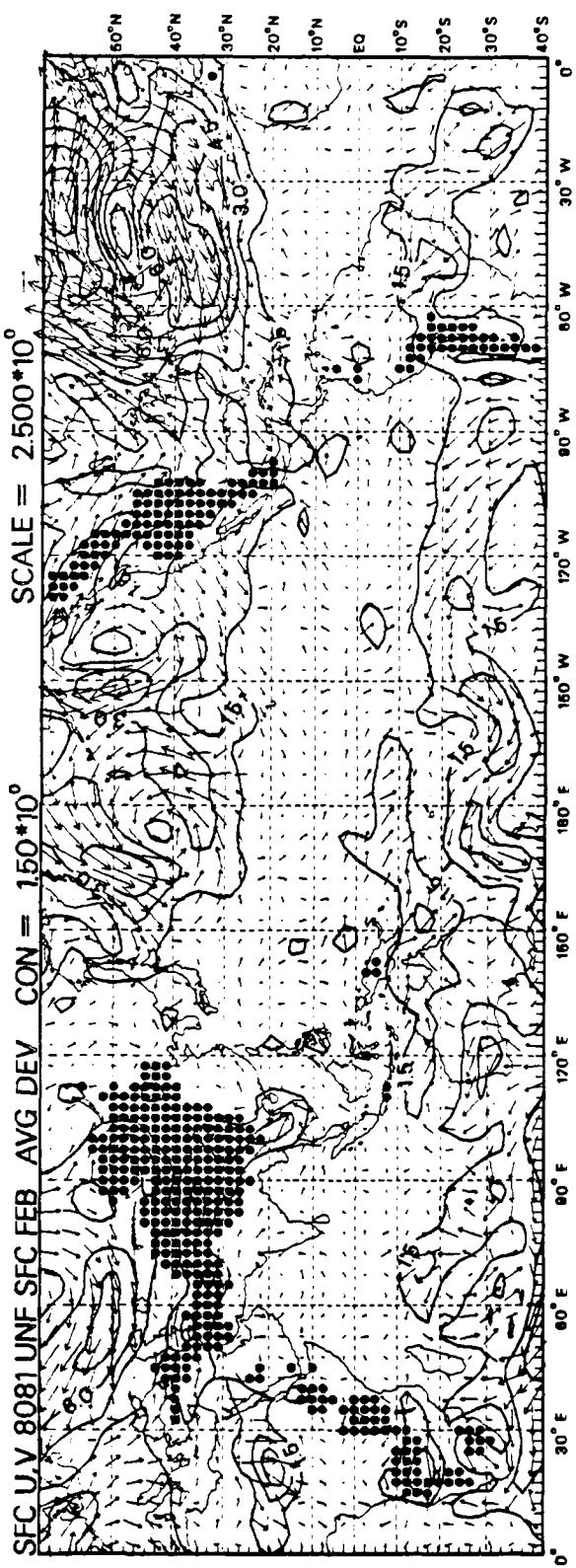
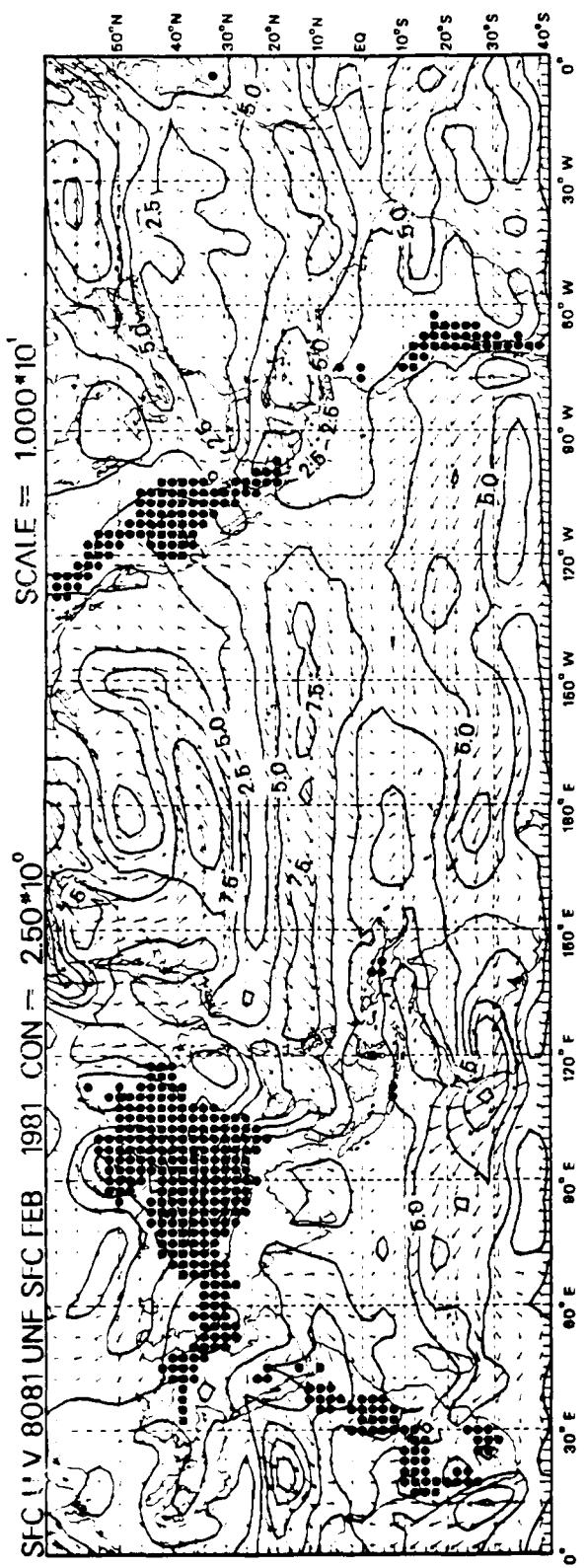
D5.9



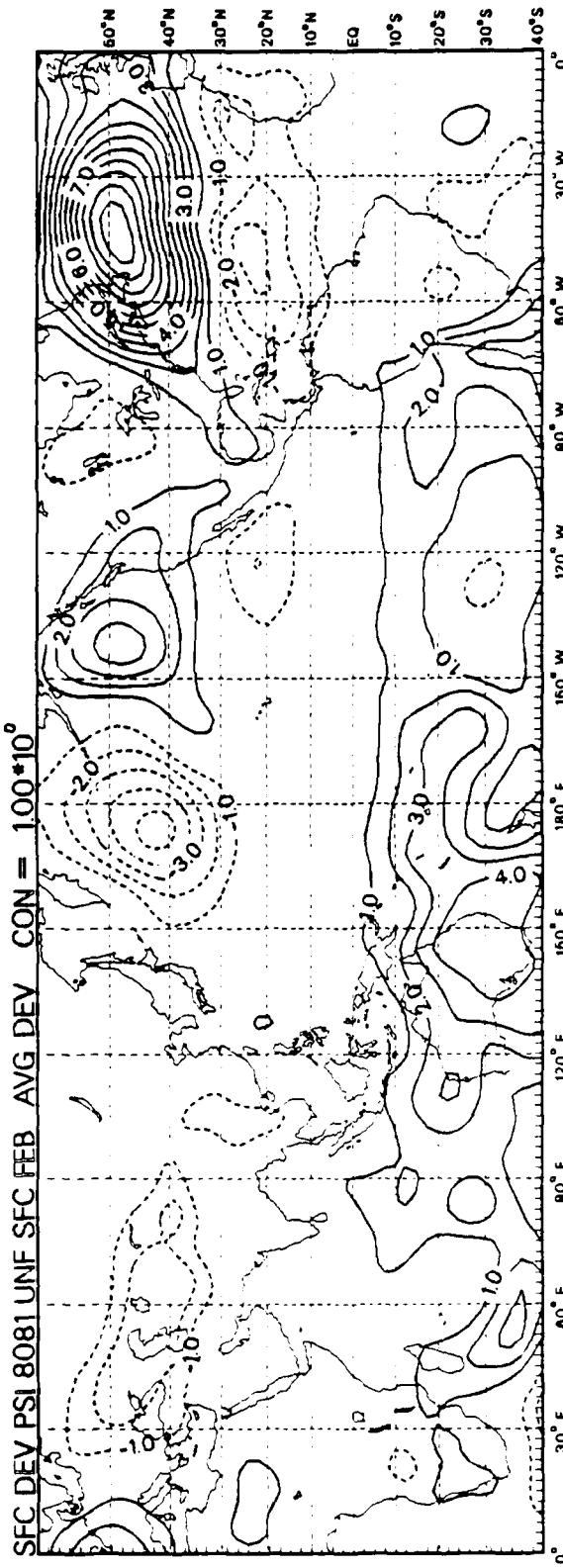
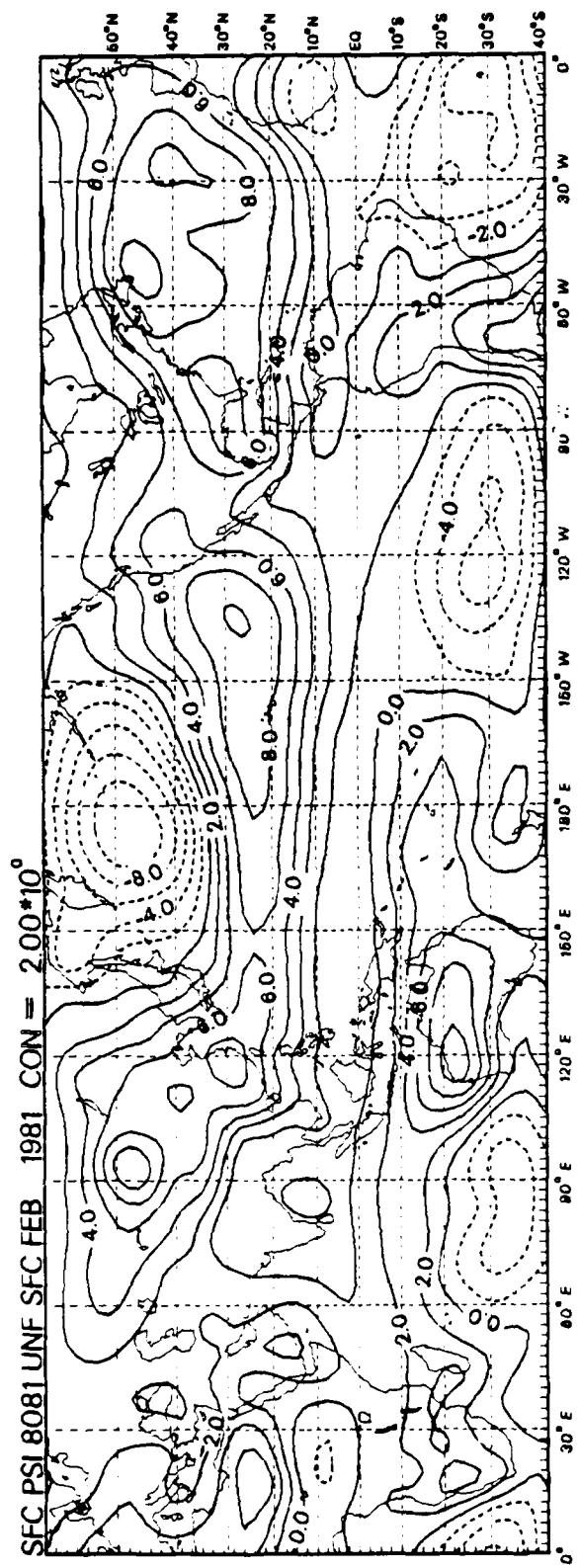
D60



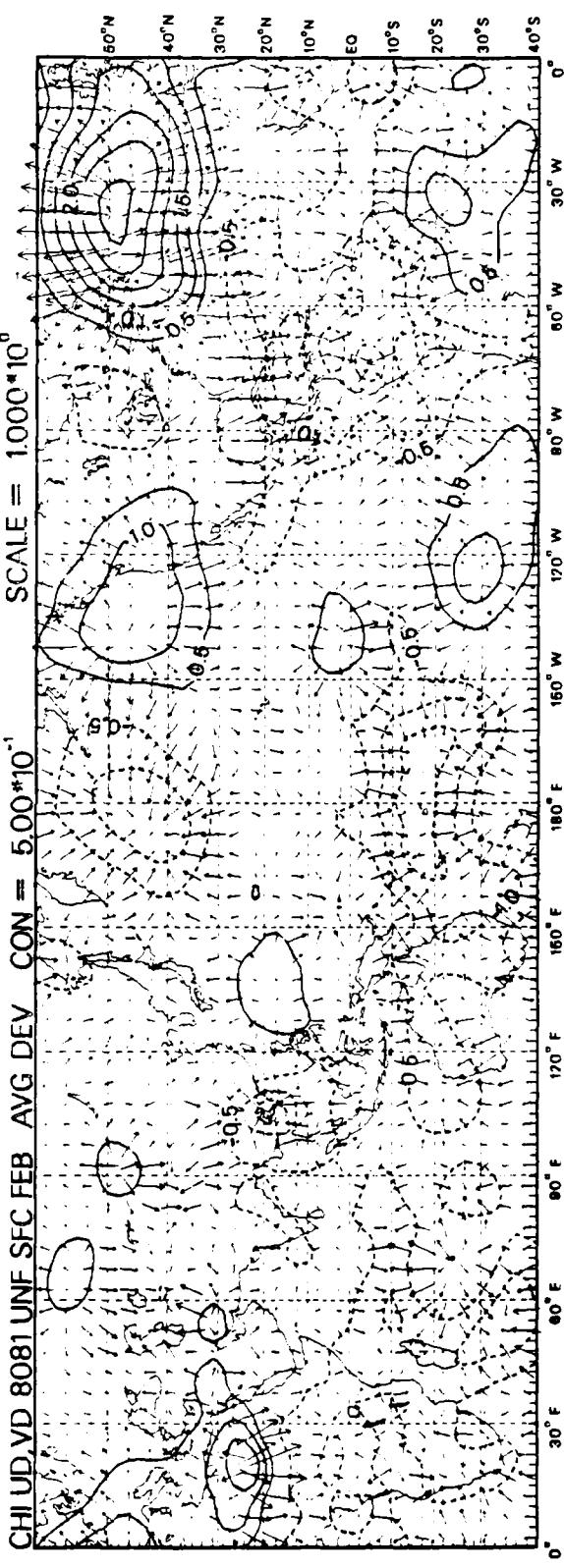
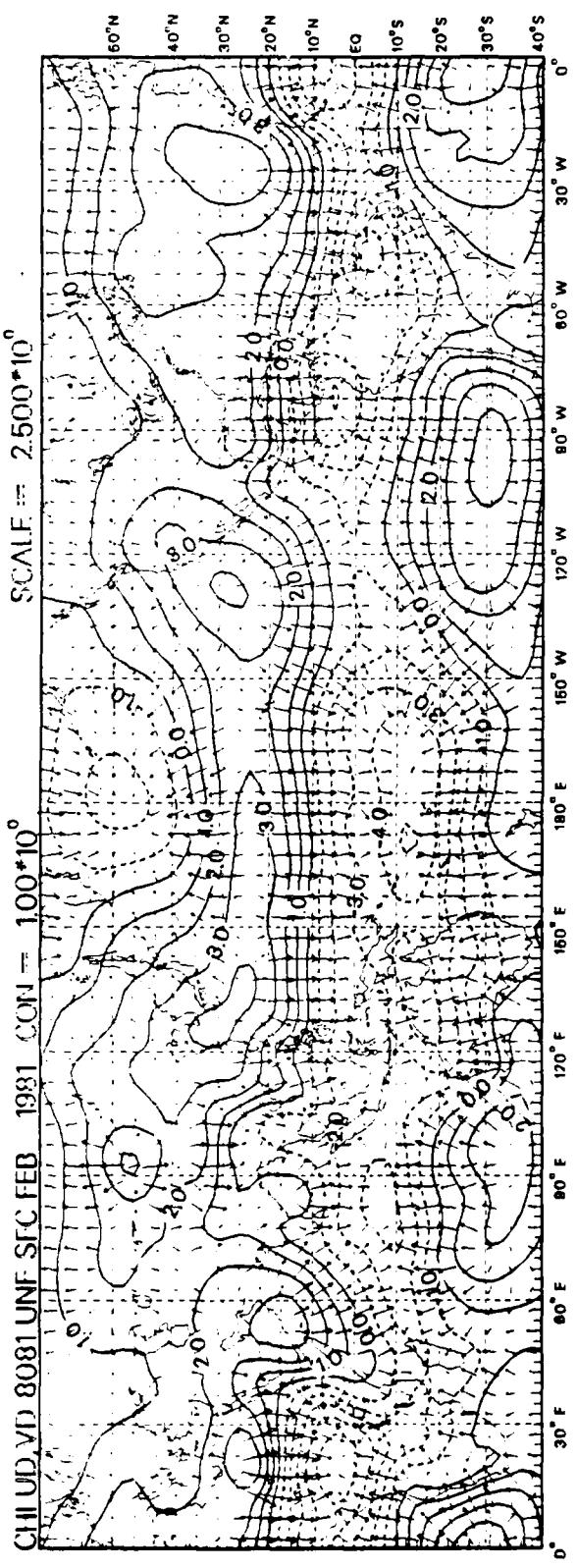
D61



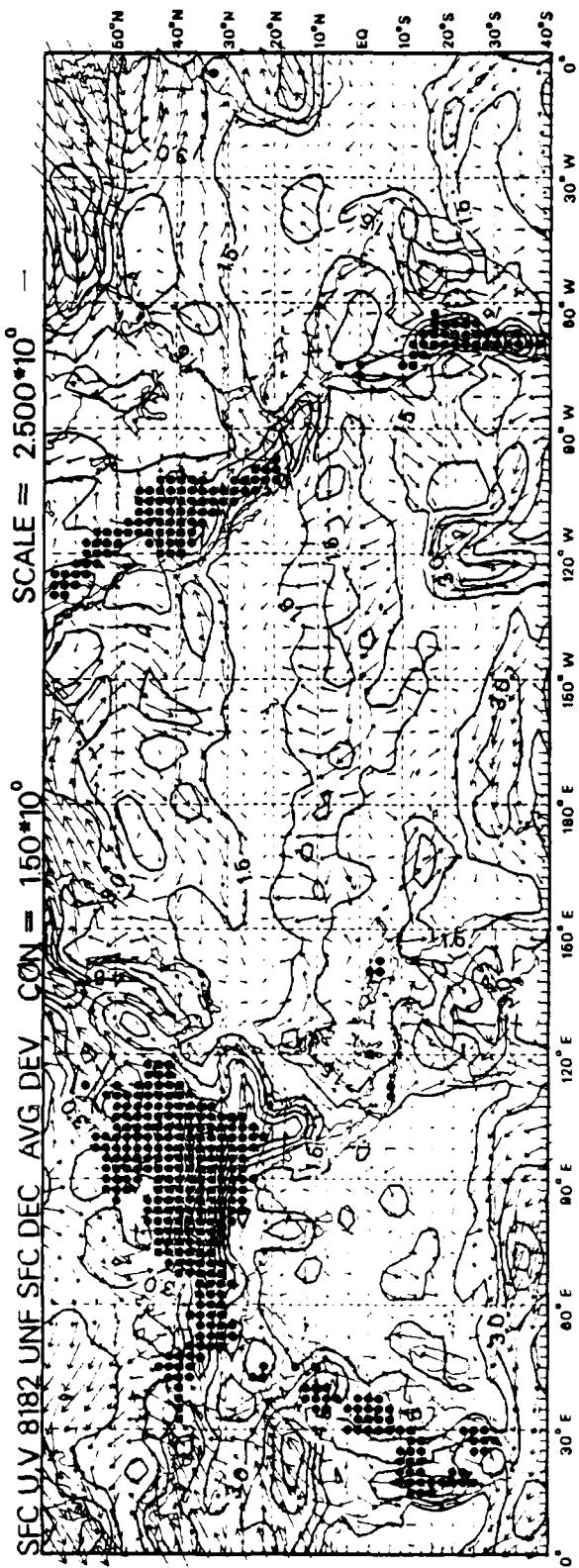
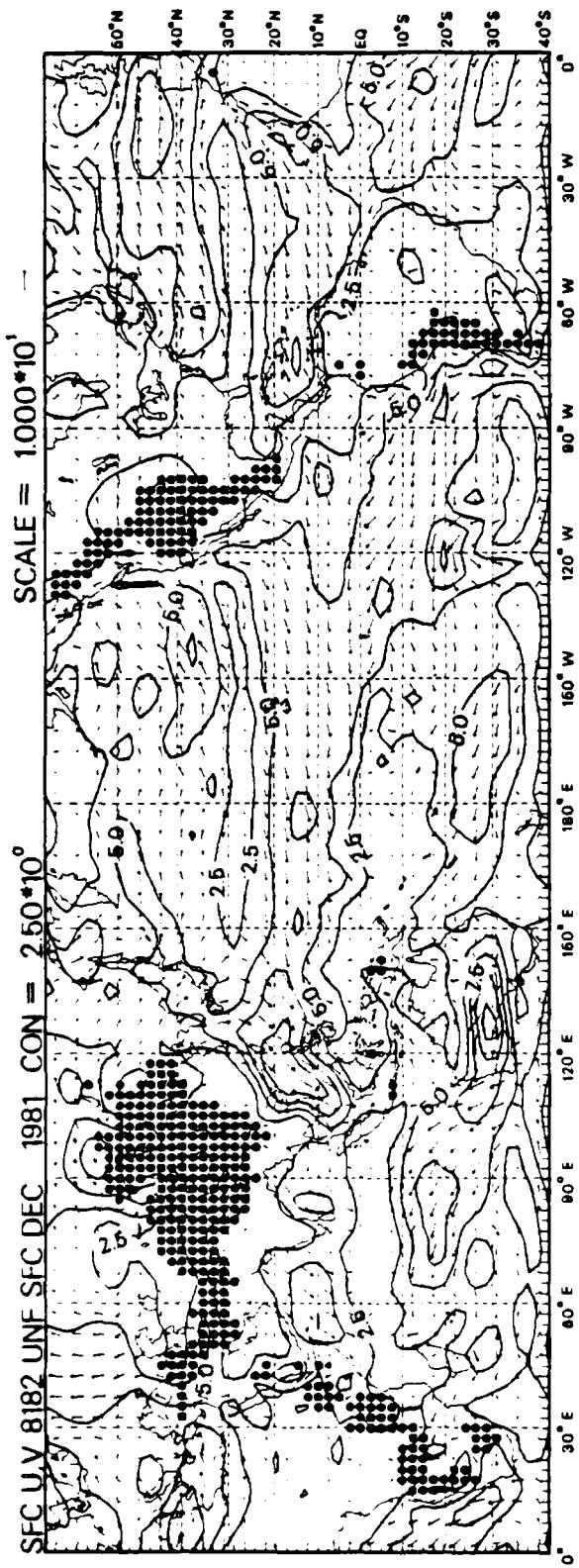
120



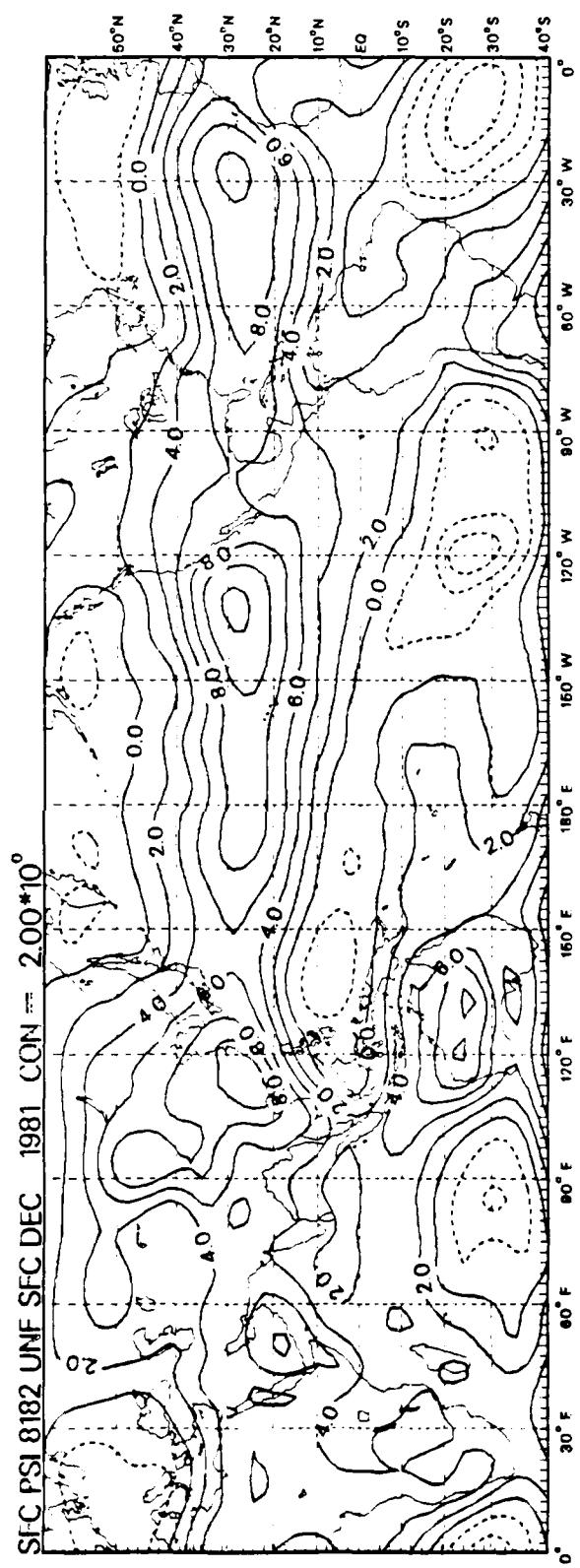
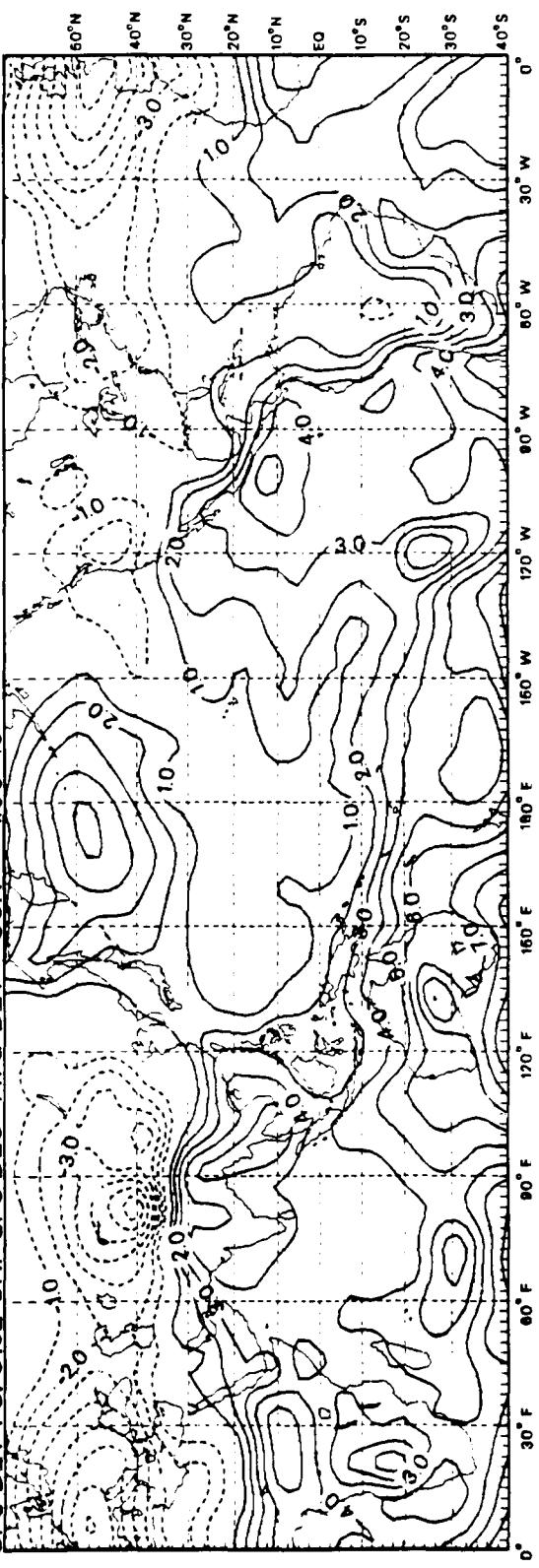
D63



D64

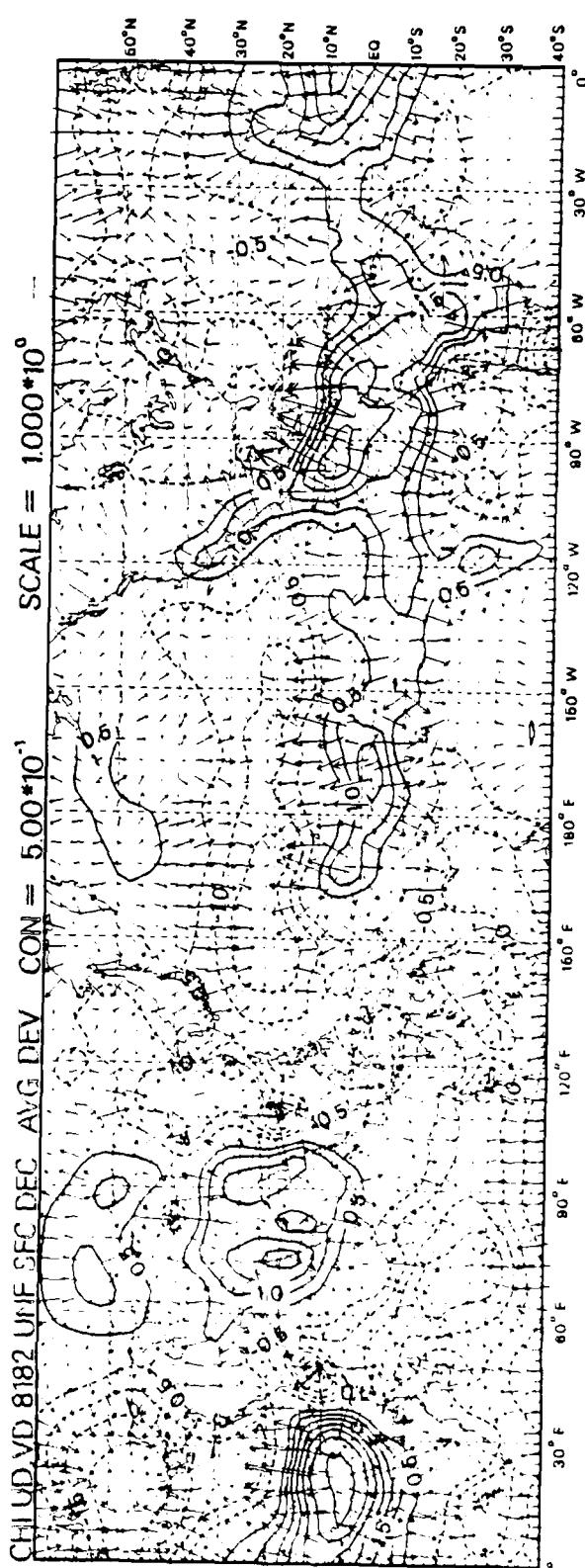
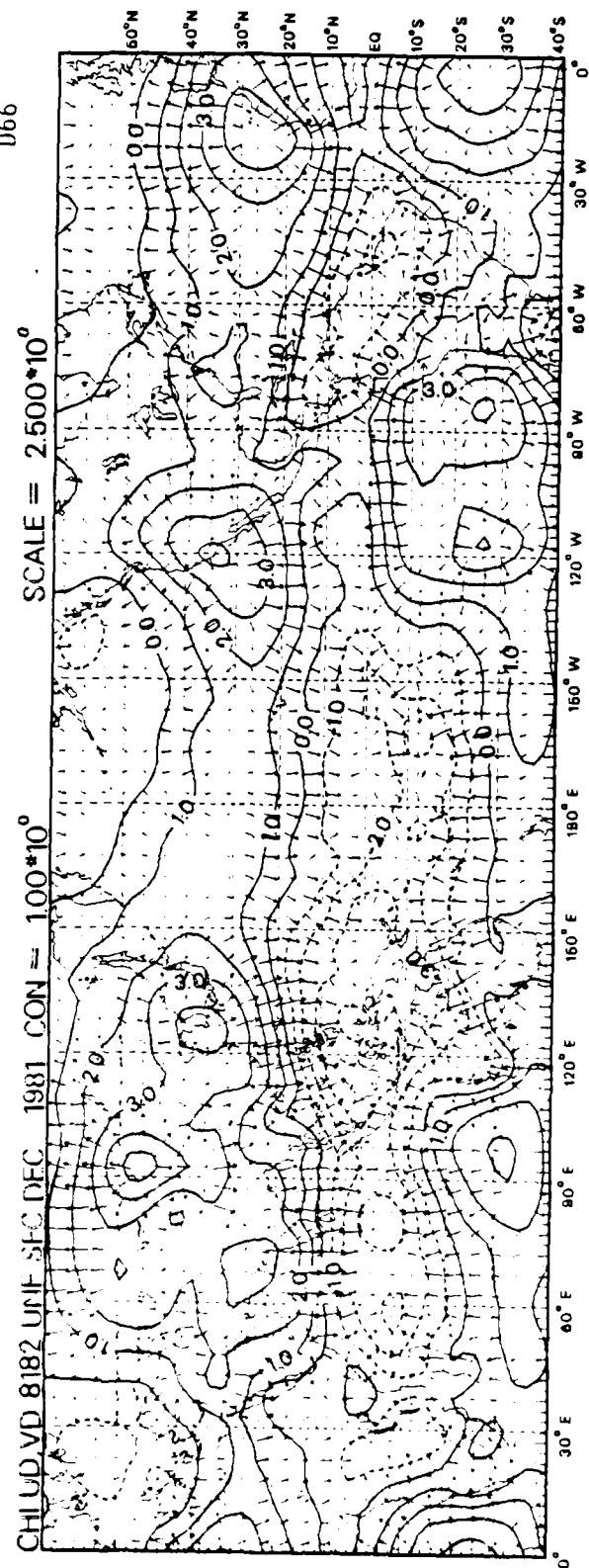


D65

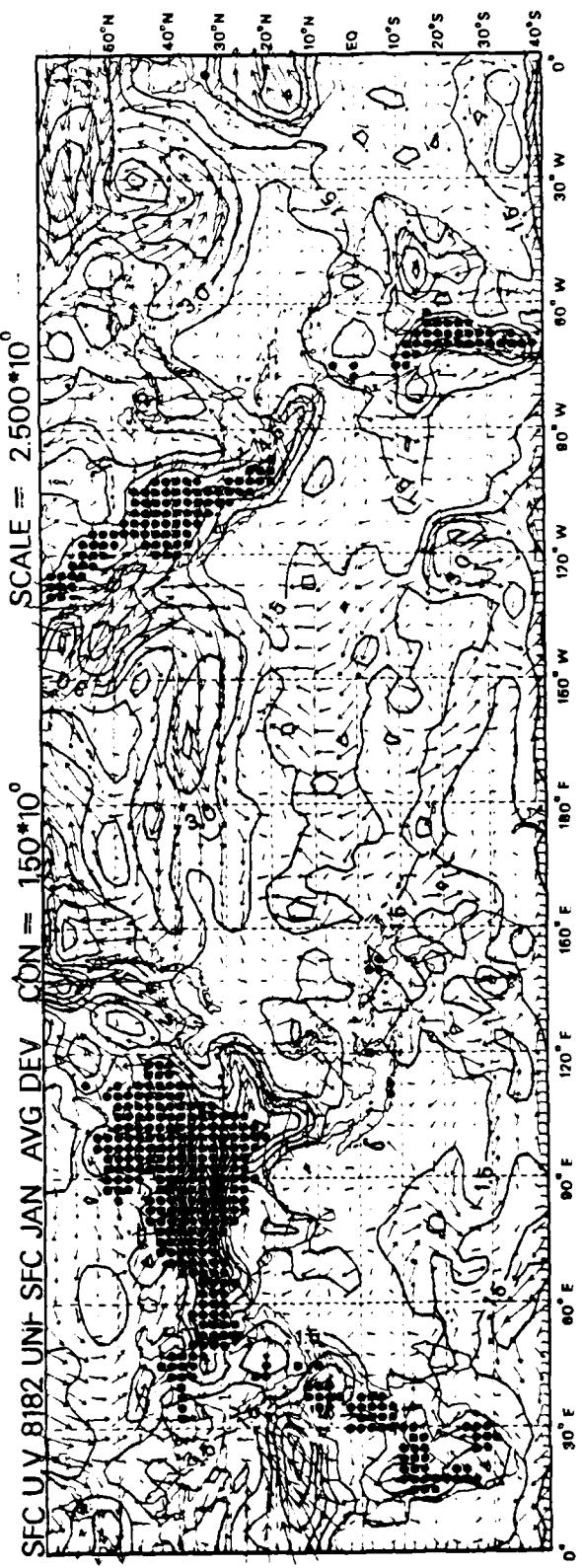
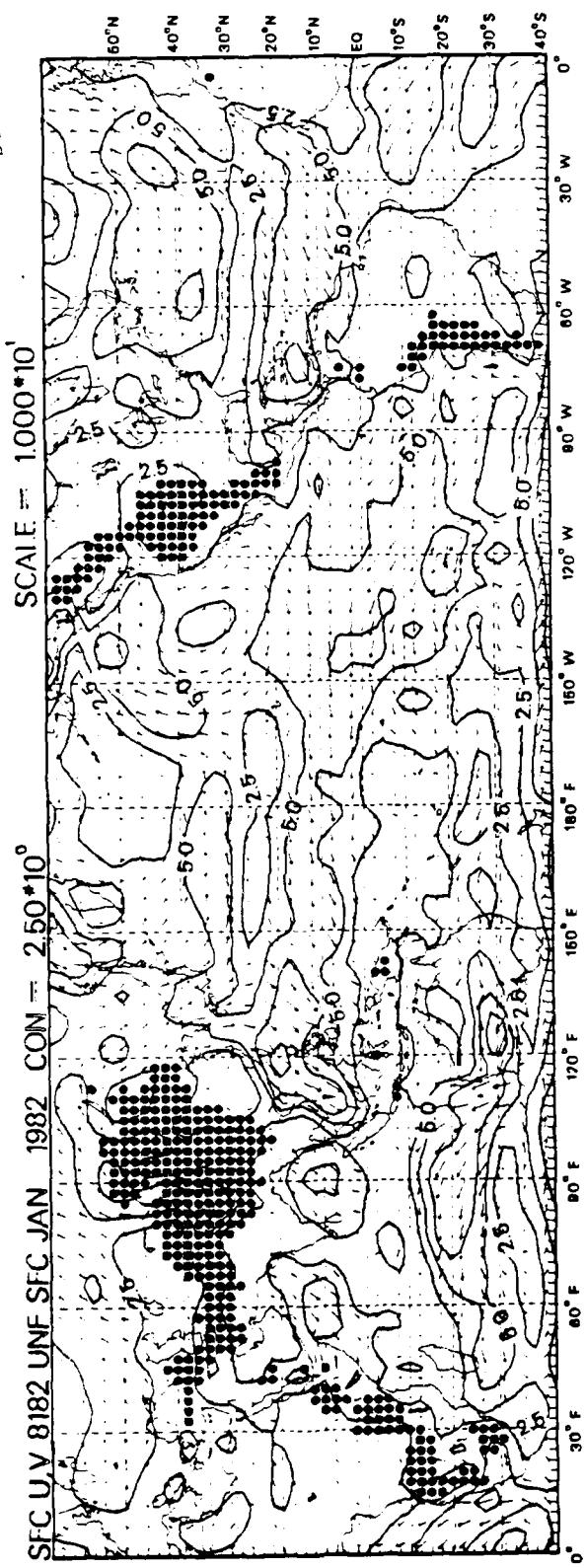
SFC DEV PSI 8182 UNF SFC DEC AVG DEV CON = 1.00×10^0 

124

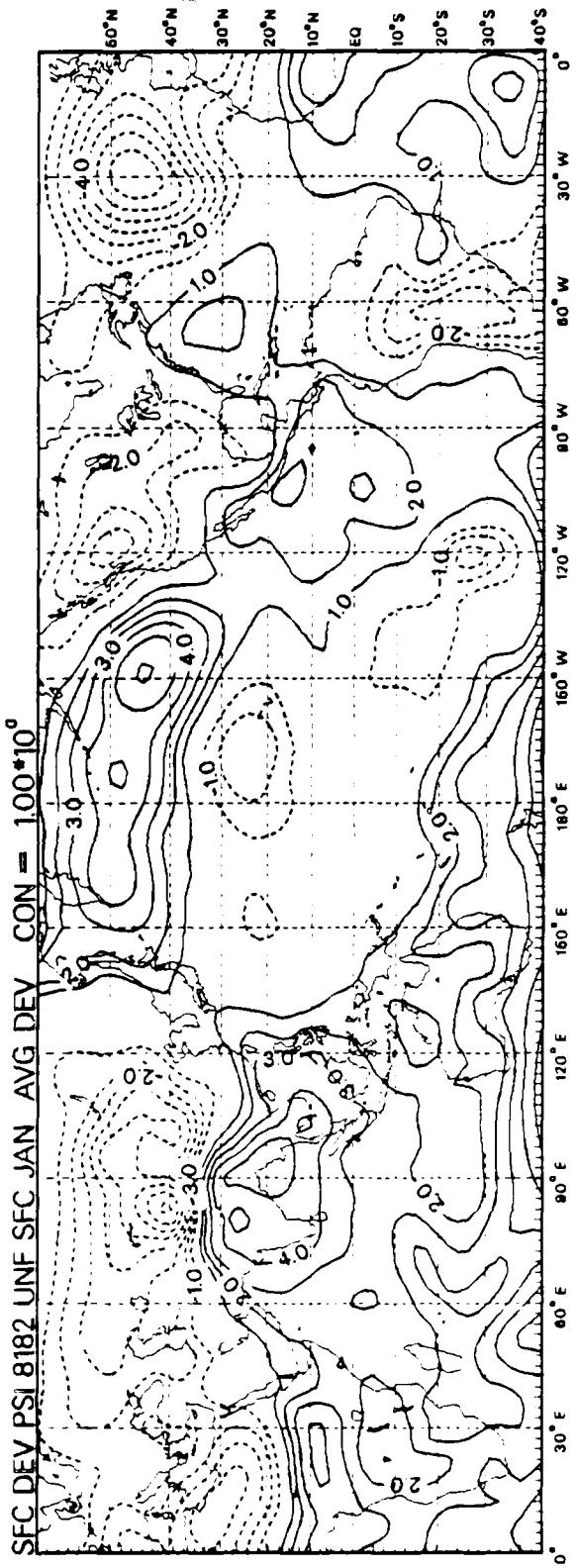
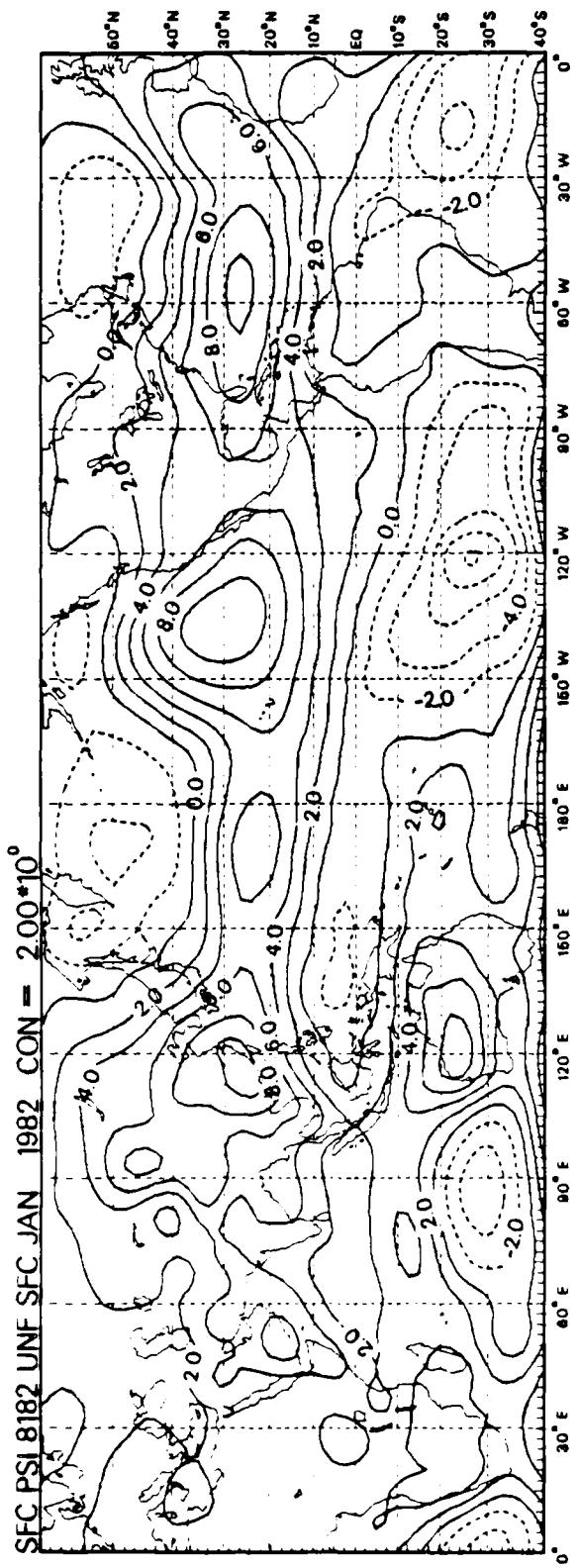
D66



067

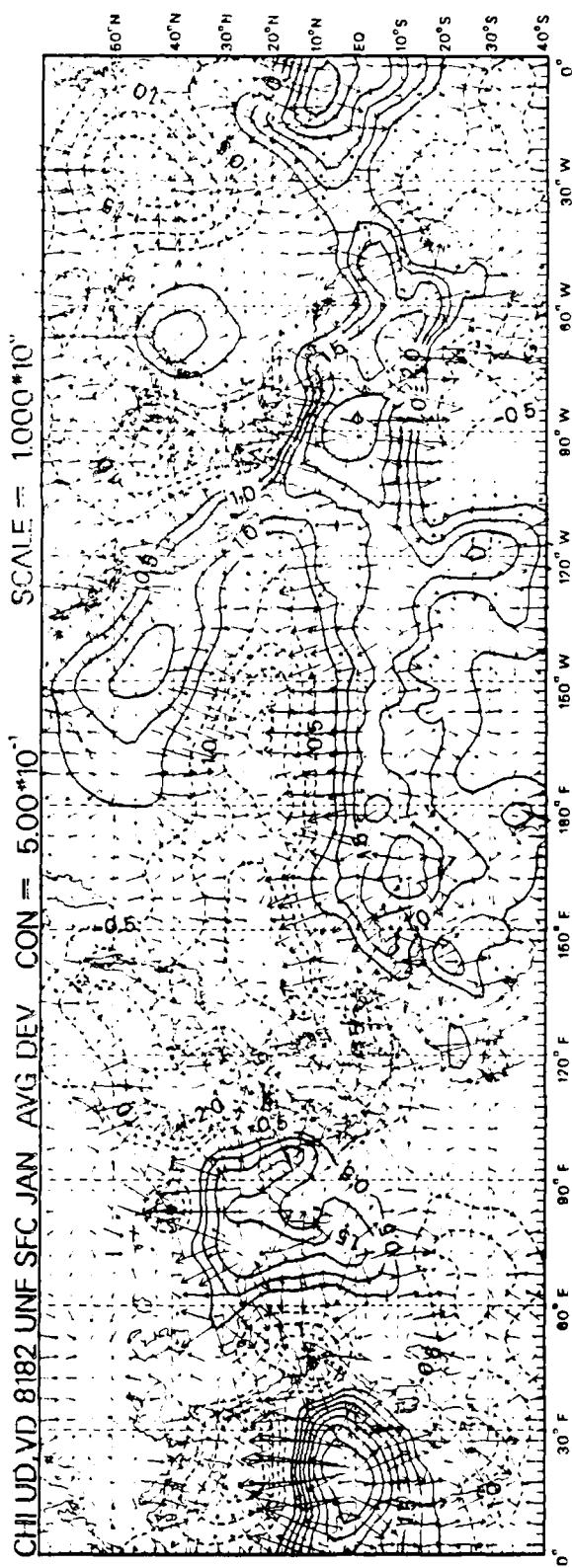
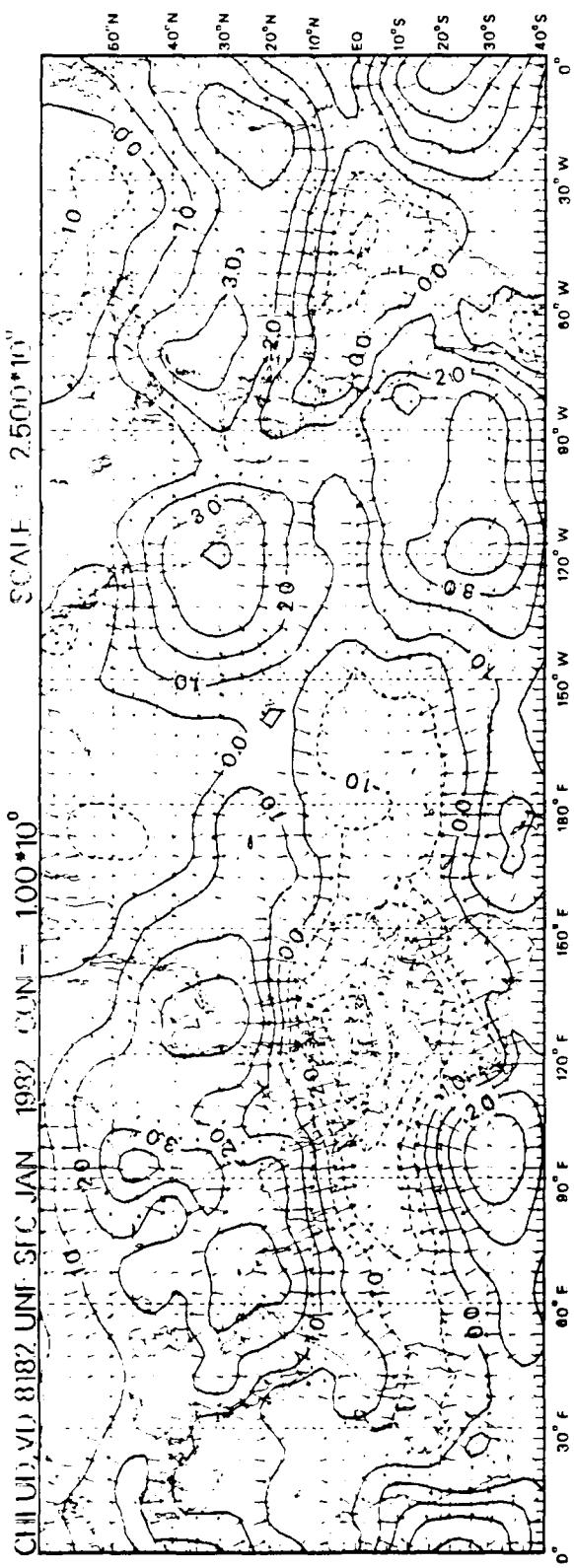


D68

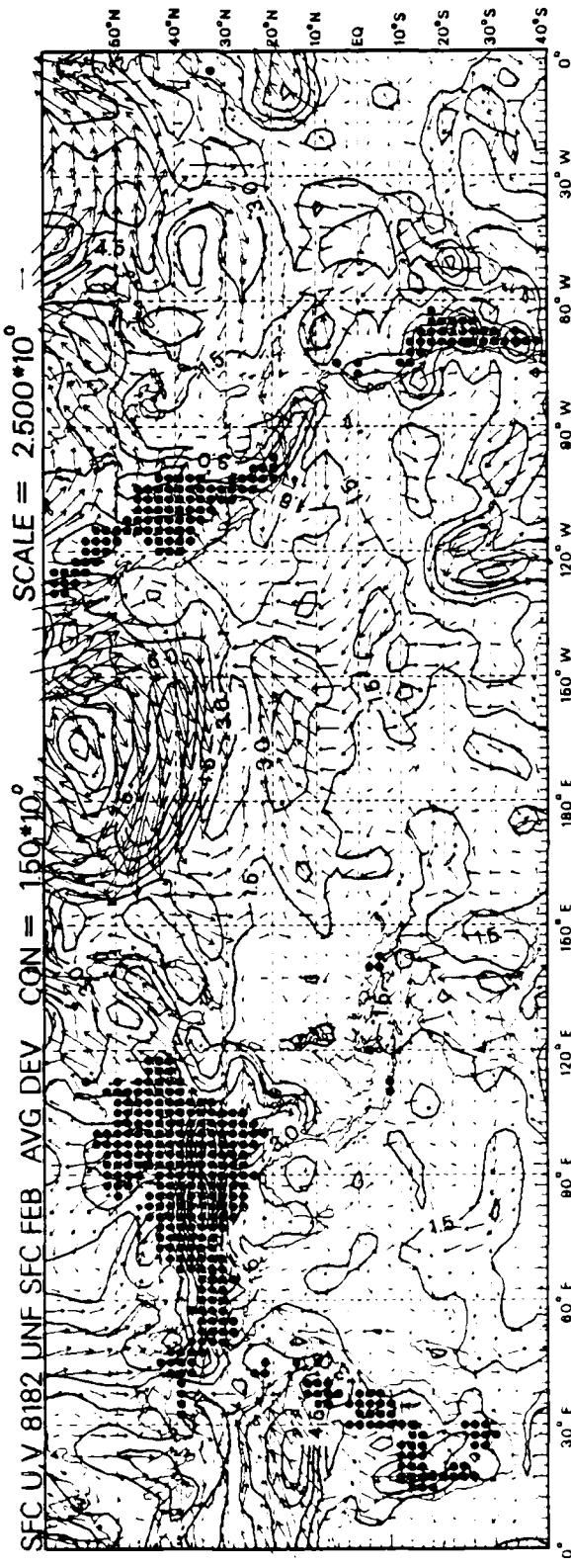
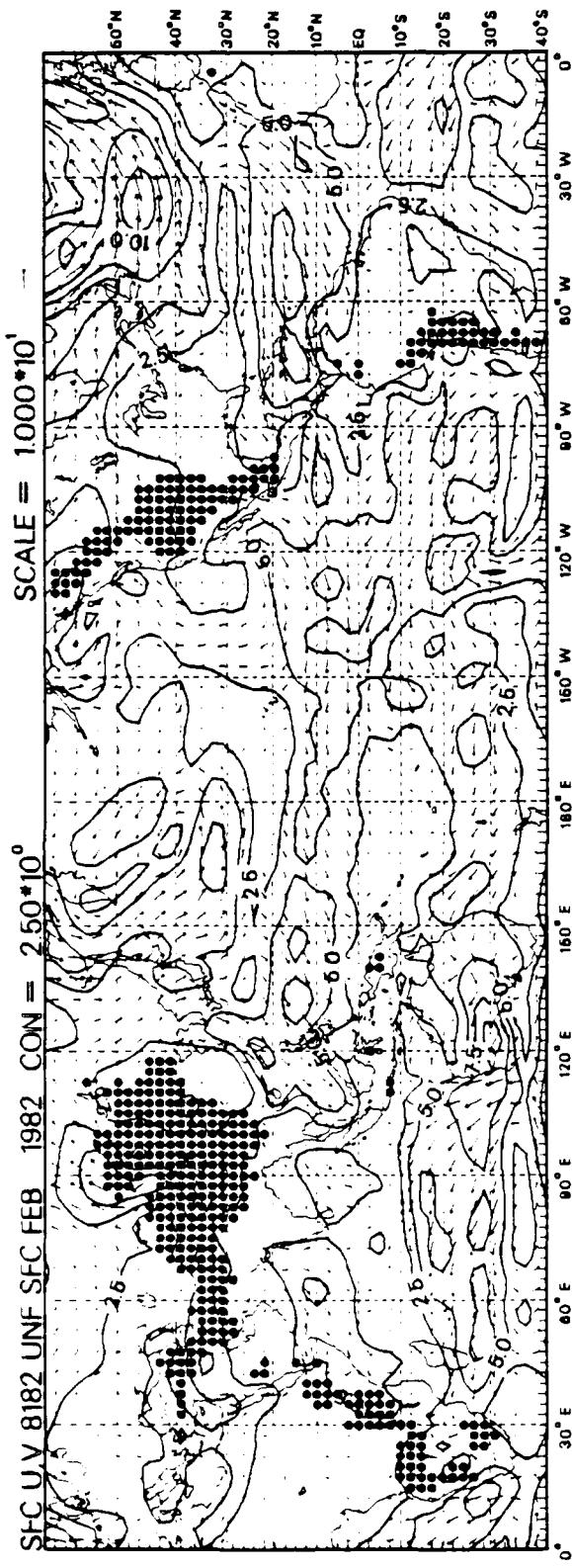


127

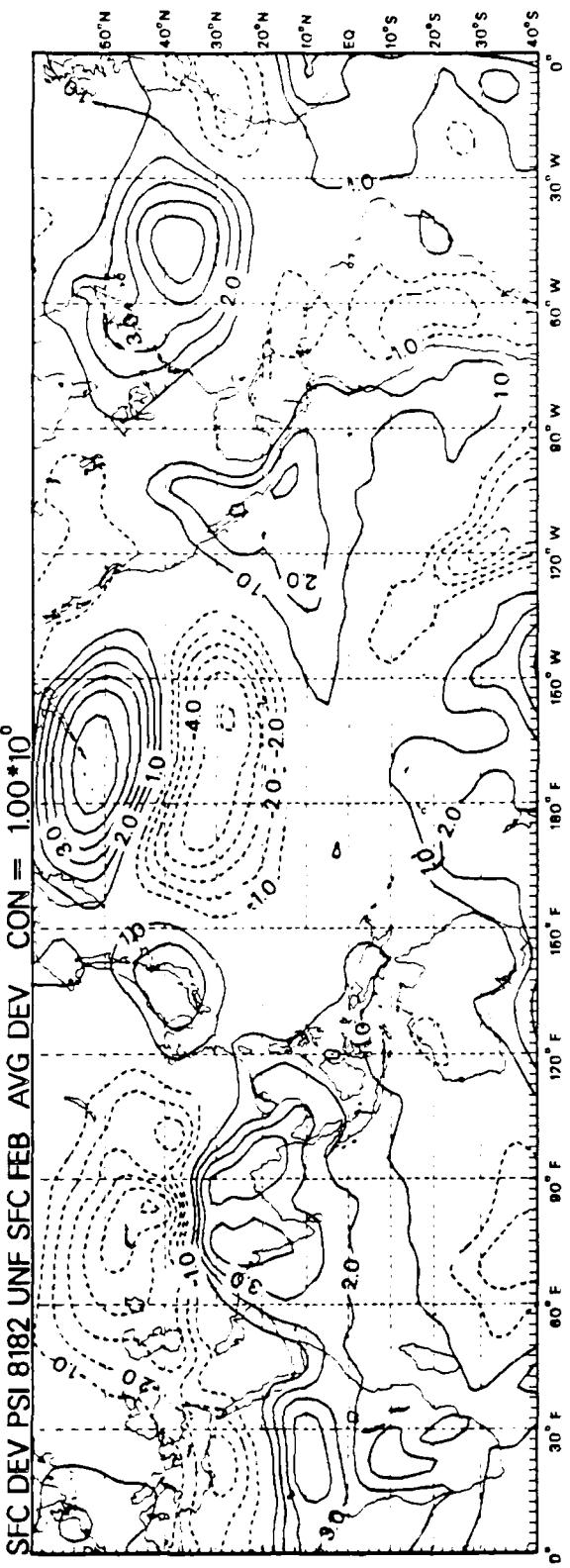
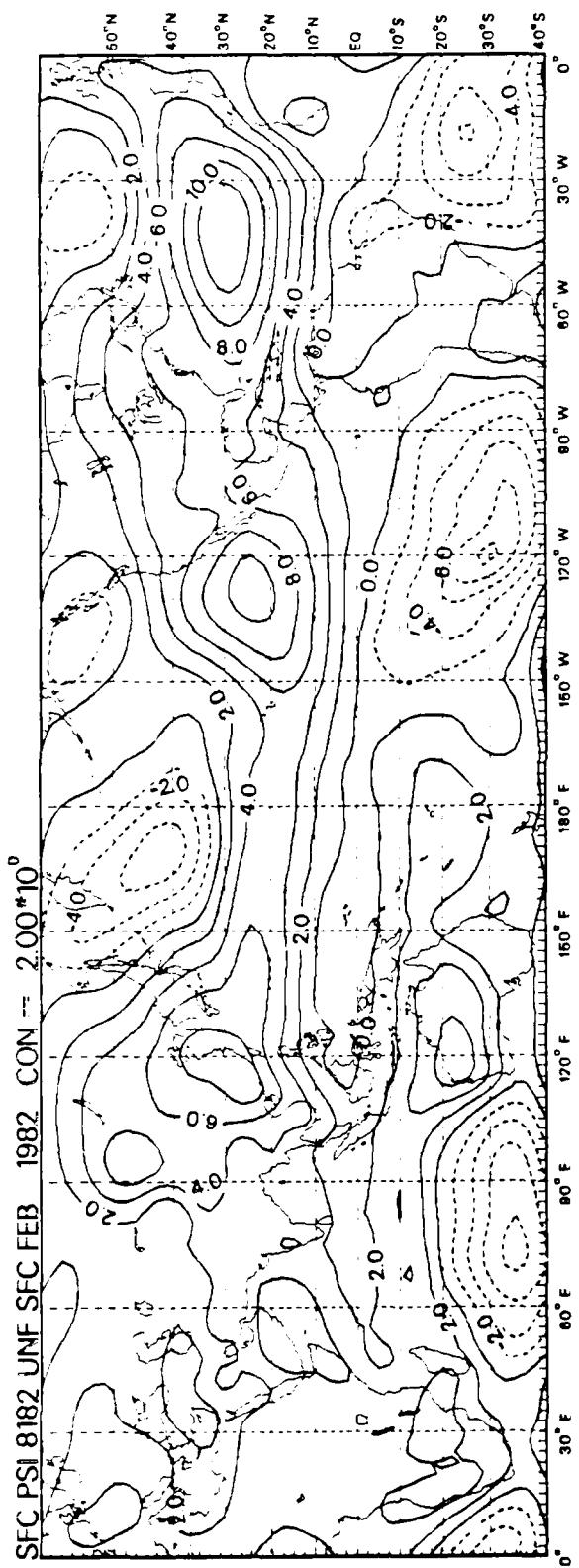
690



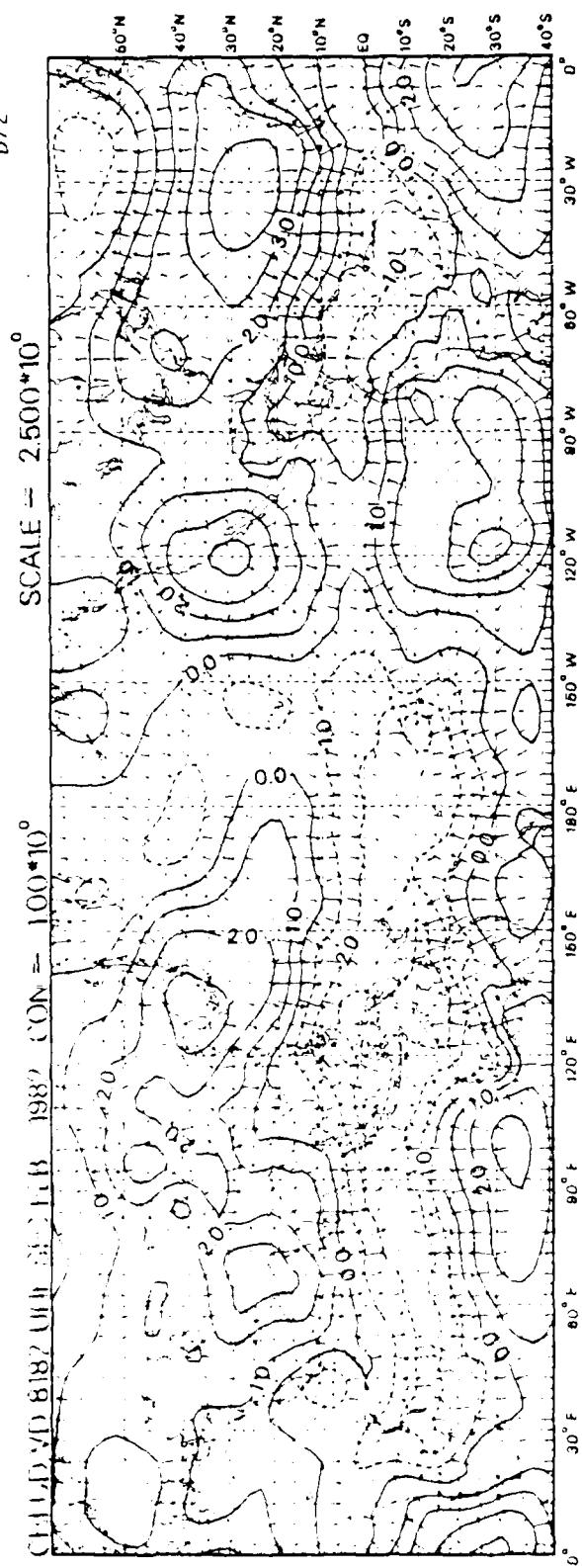
070



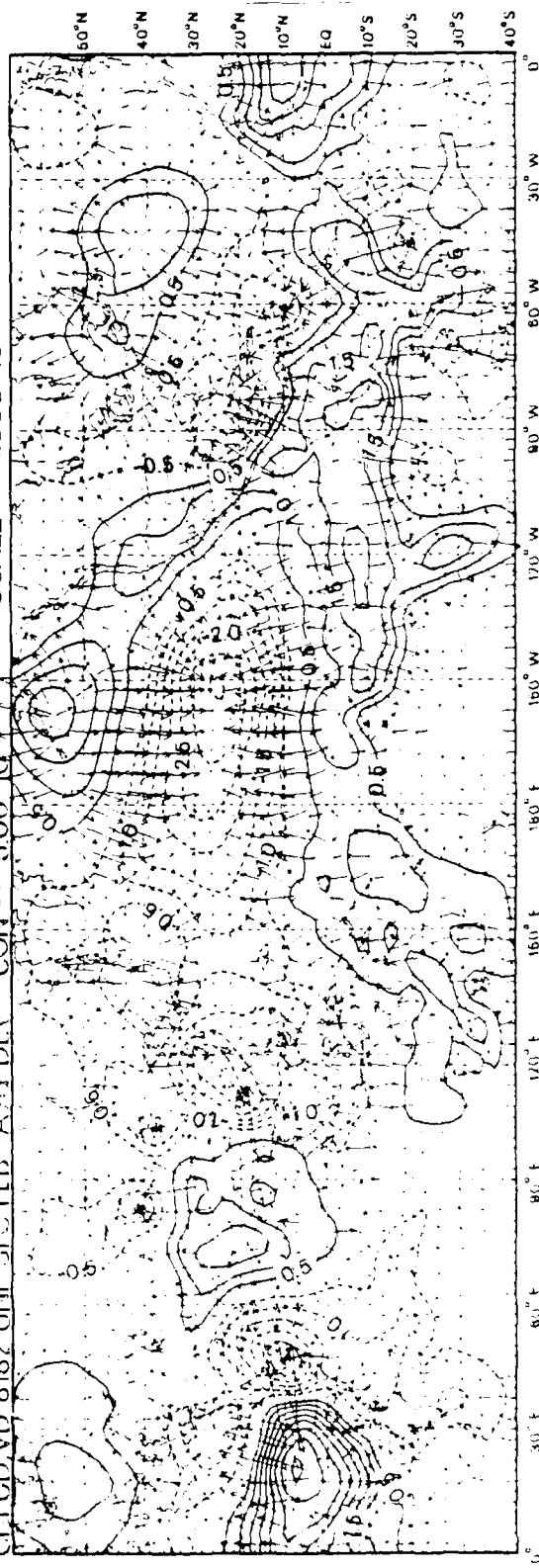
D71



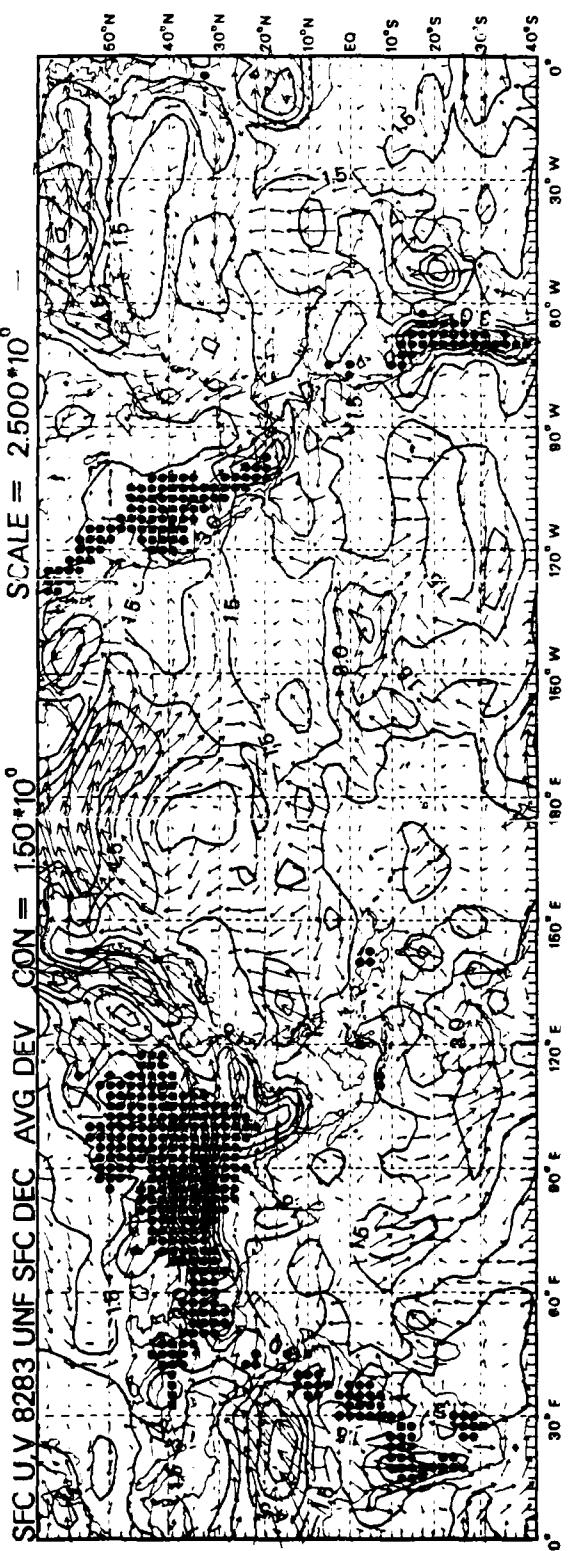
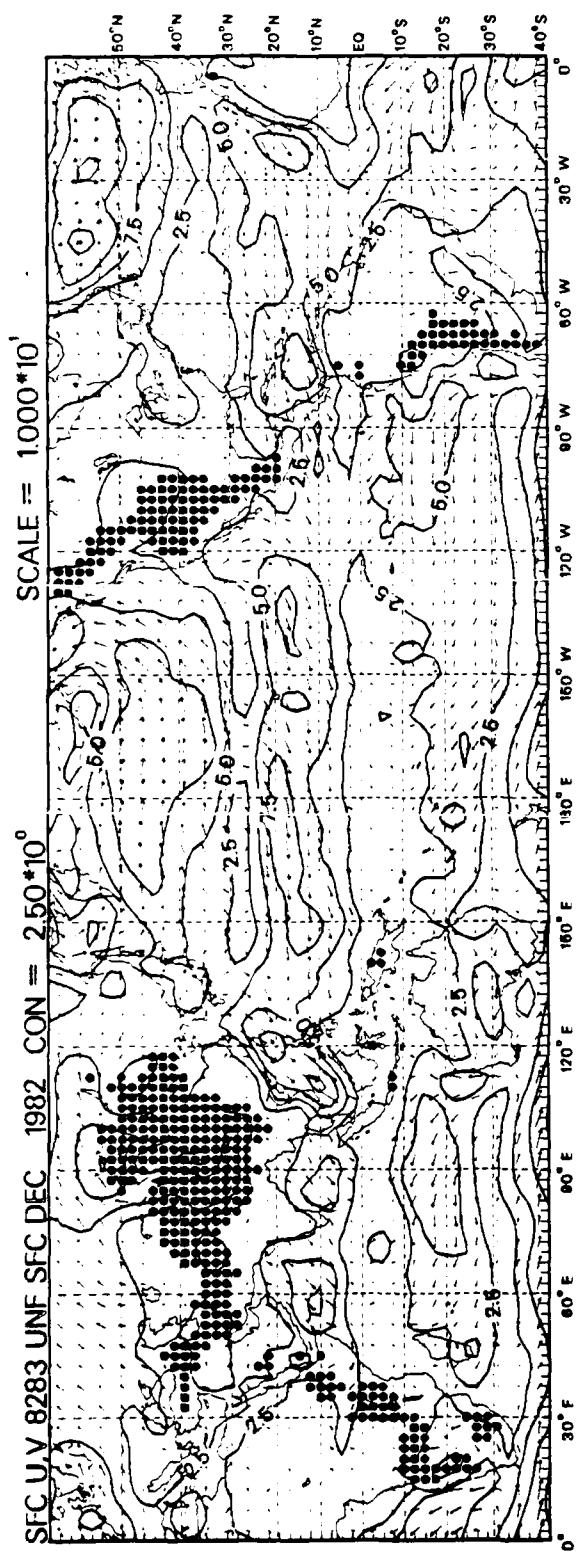
072



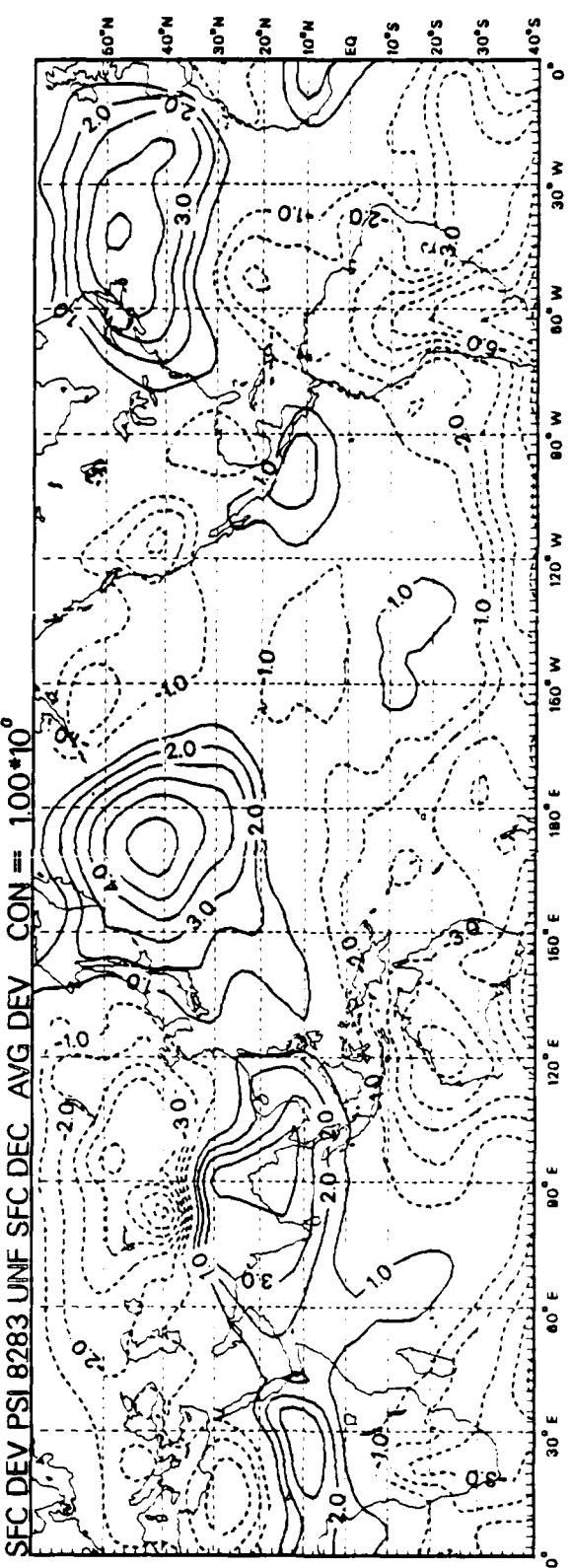
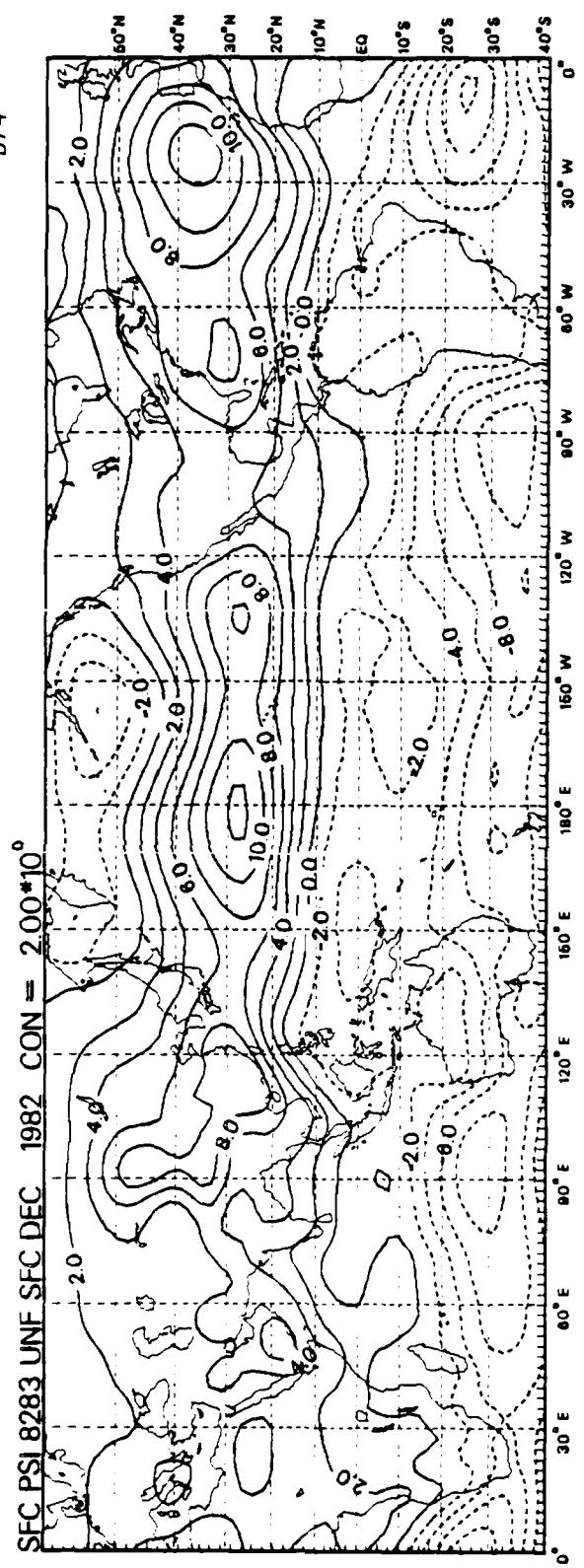
SCALF = 1.000 * 10⁰ CON = 5.00 * 10⁻¹ DEV = 0.05 SEC_EER = 0.05 SEC_DER = 0.05



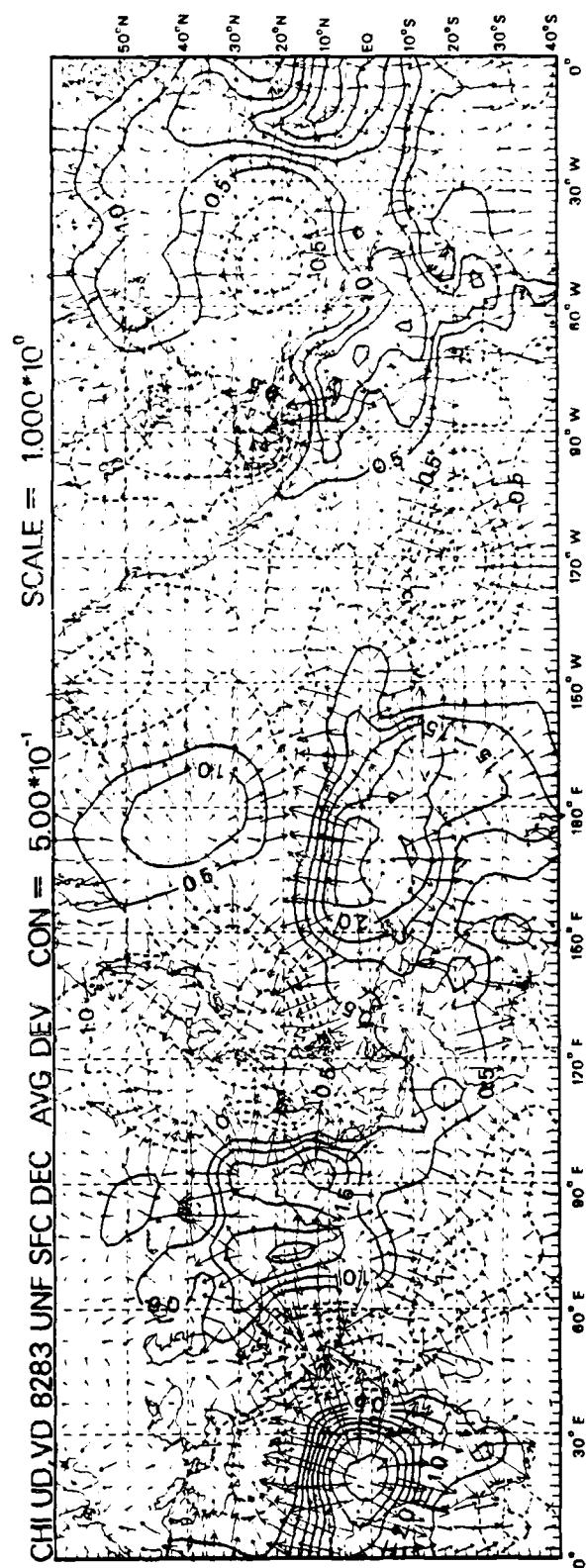
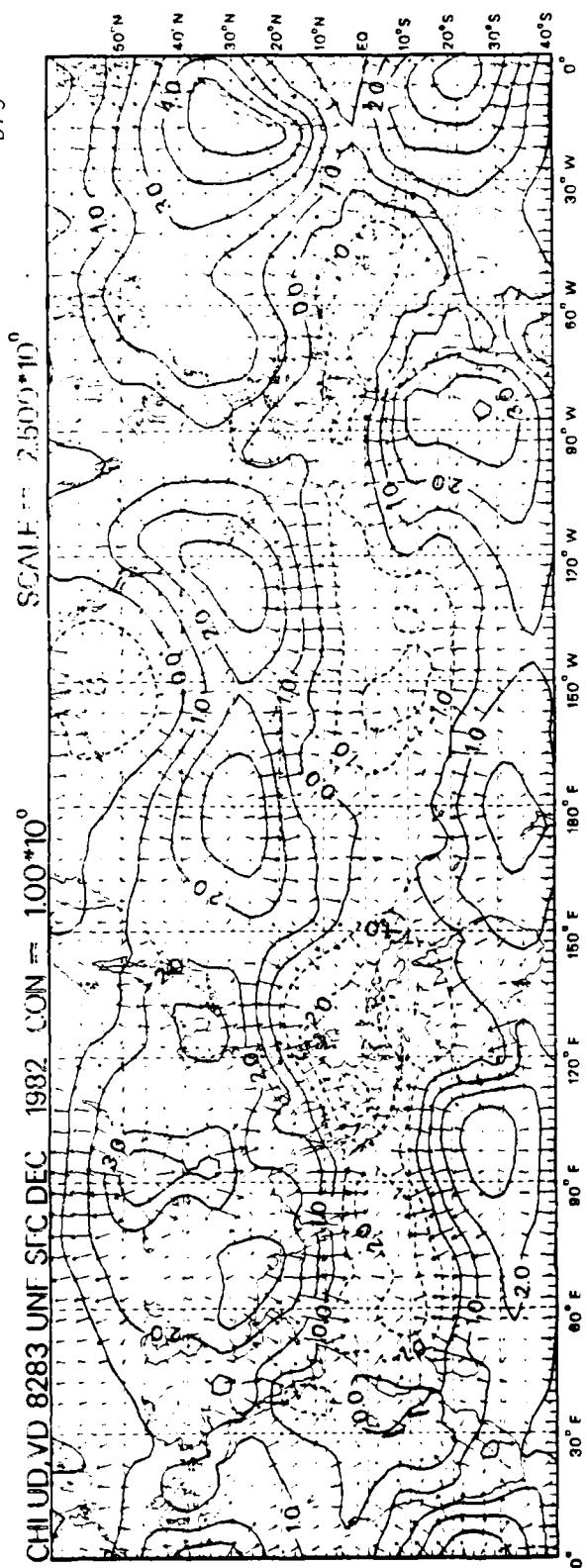
1073



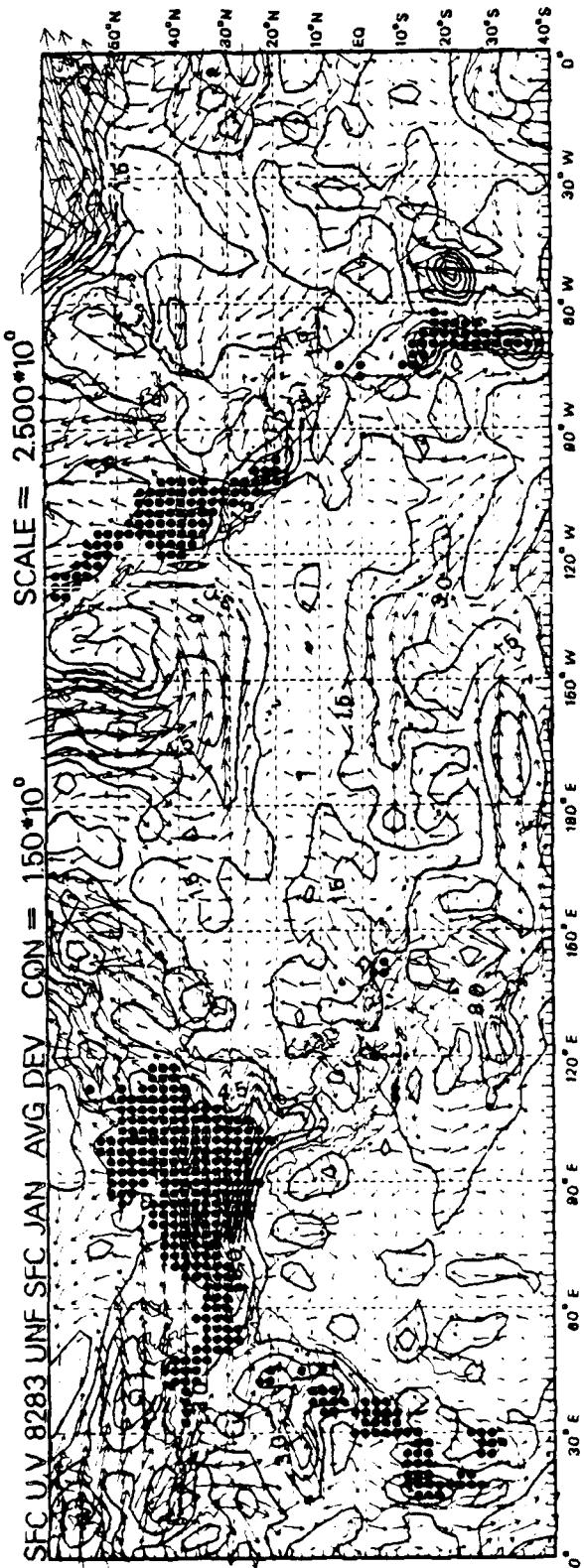
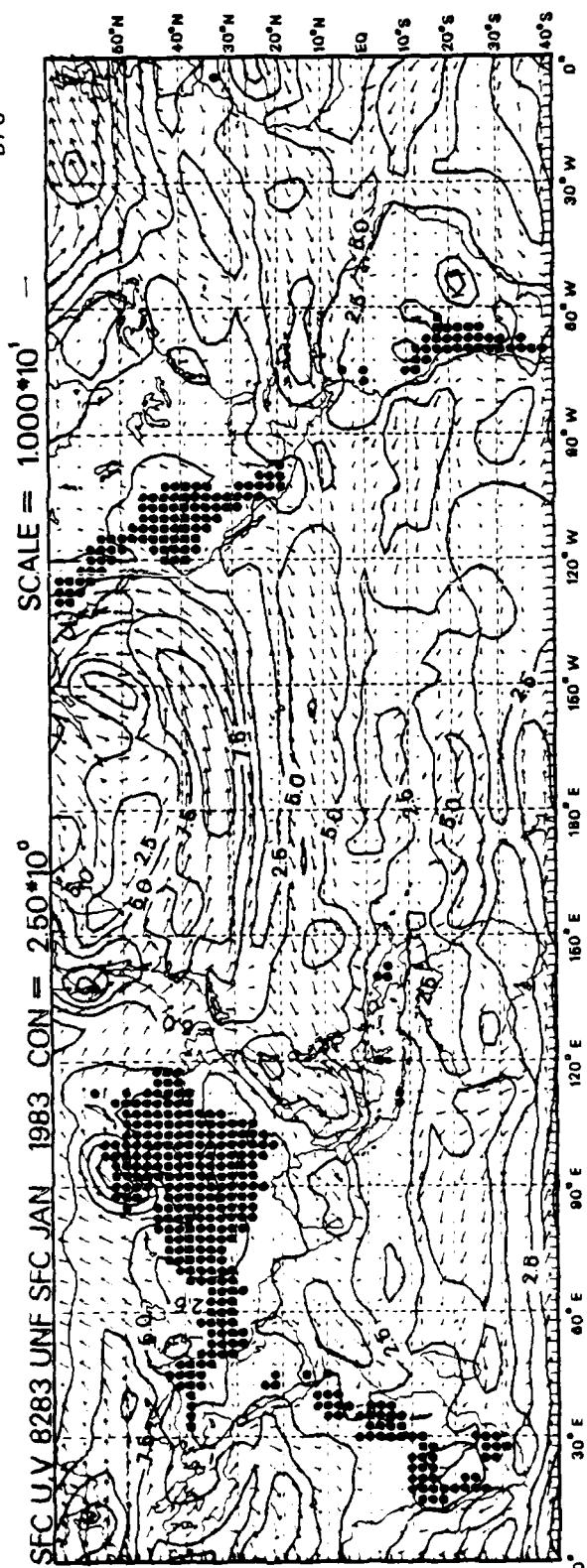
D74

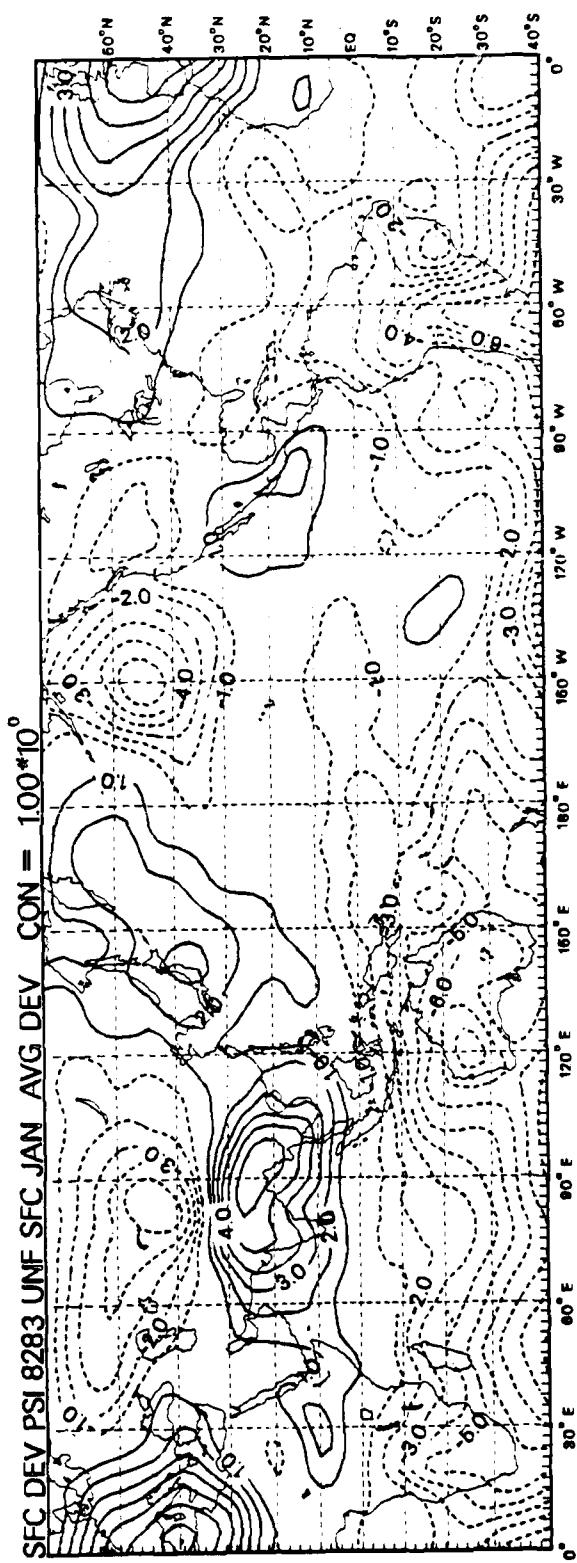
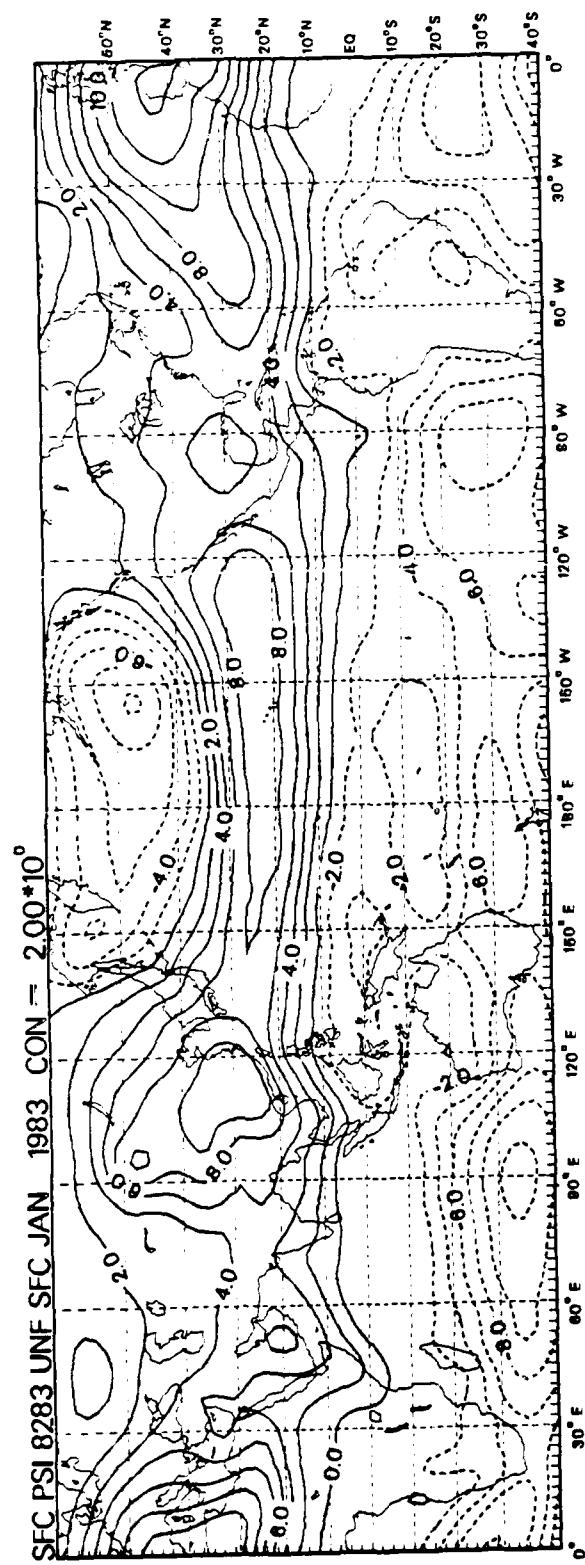


D75



D76



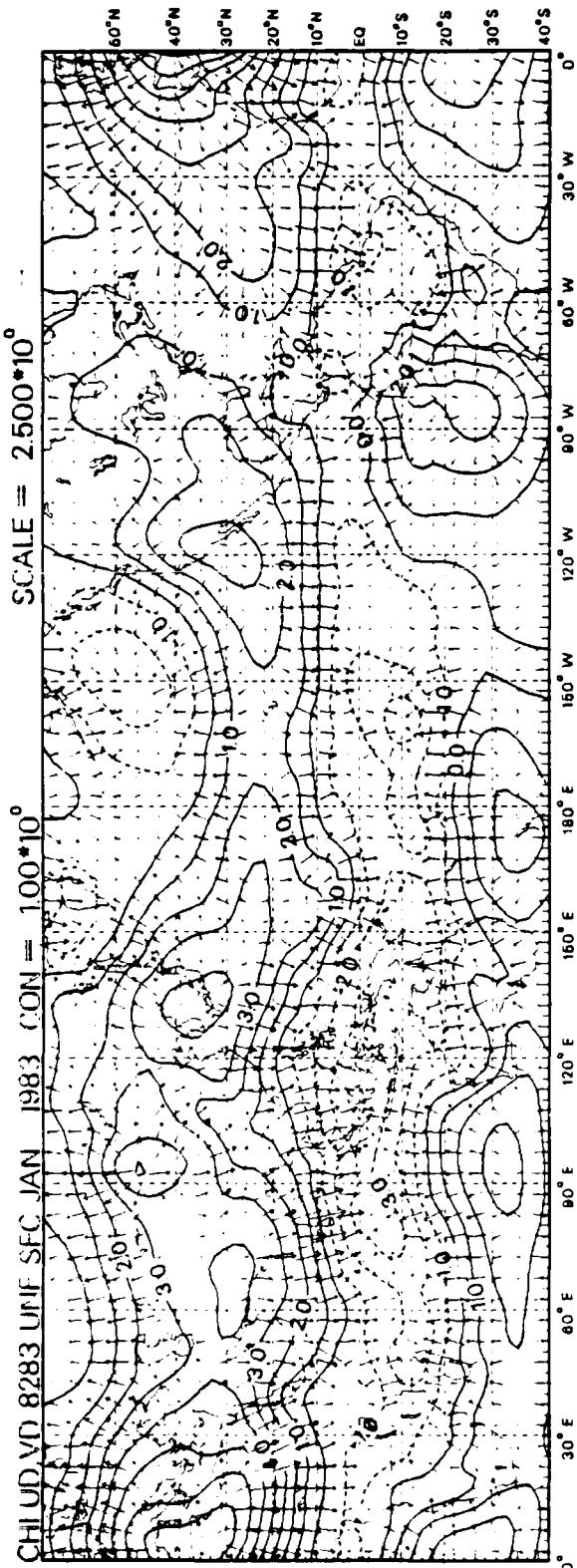


D78

SCALE = $2.500 \cdot 10^6$

$100 \cdot 10^6$

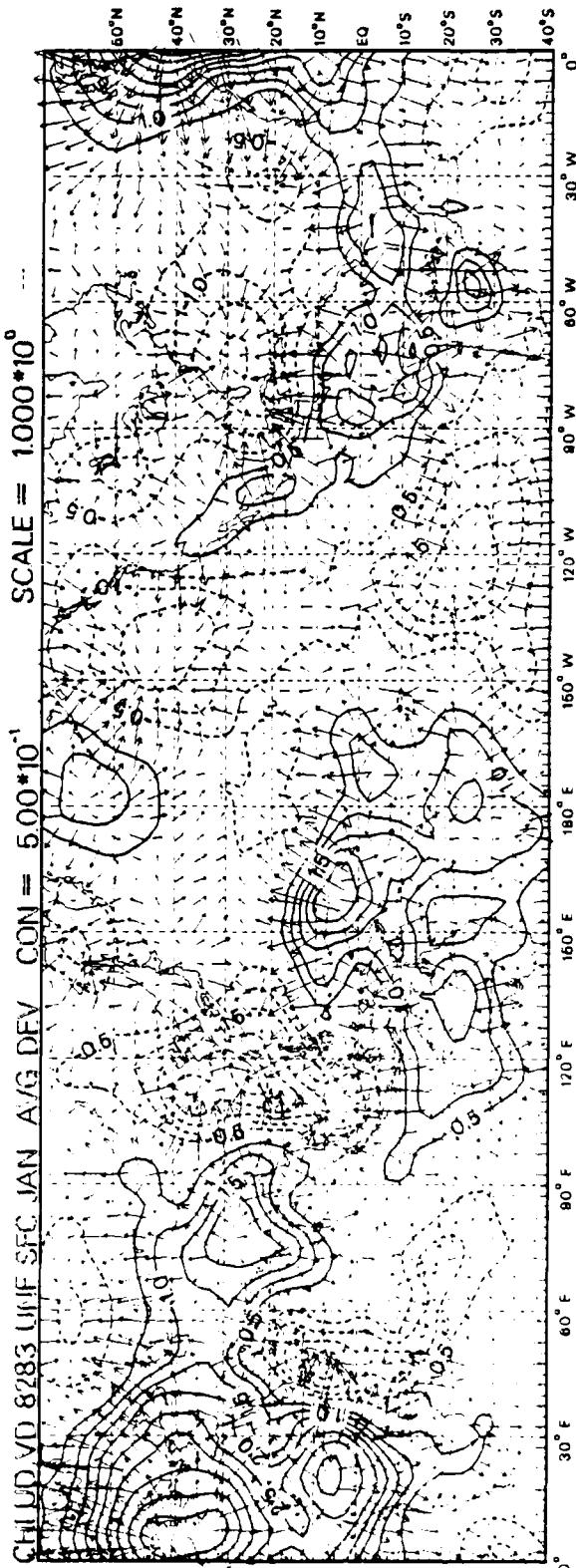
CON =



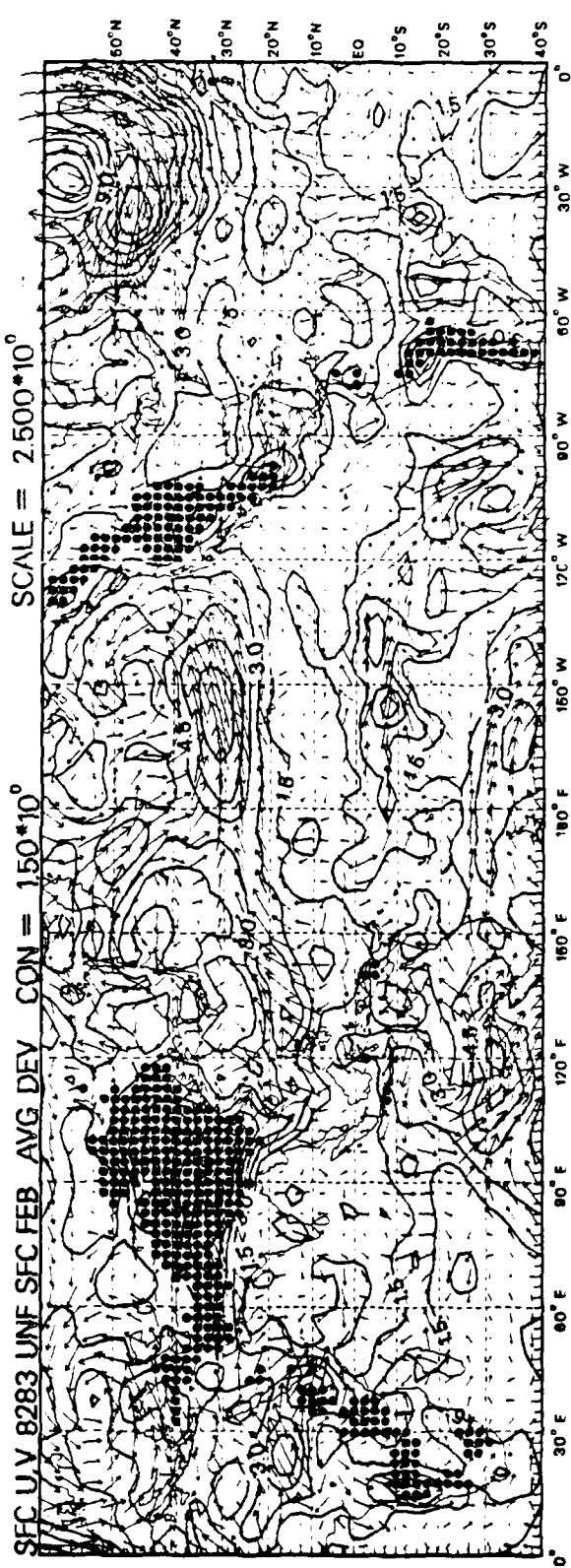
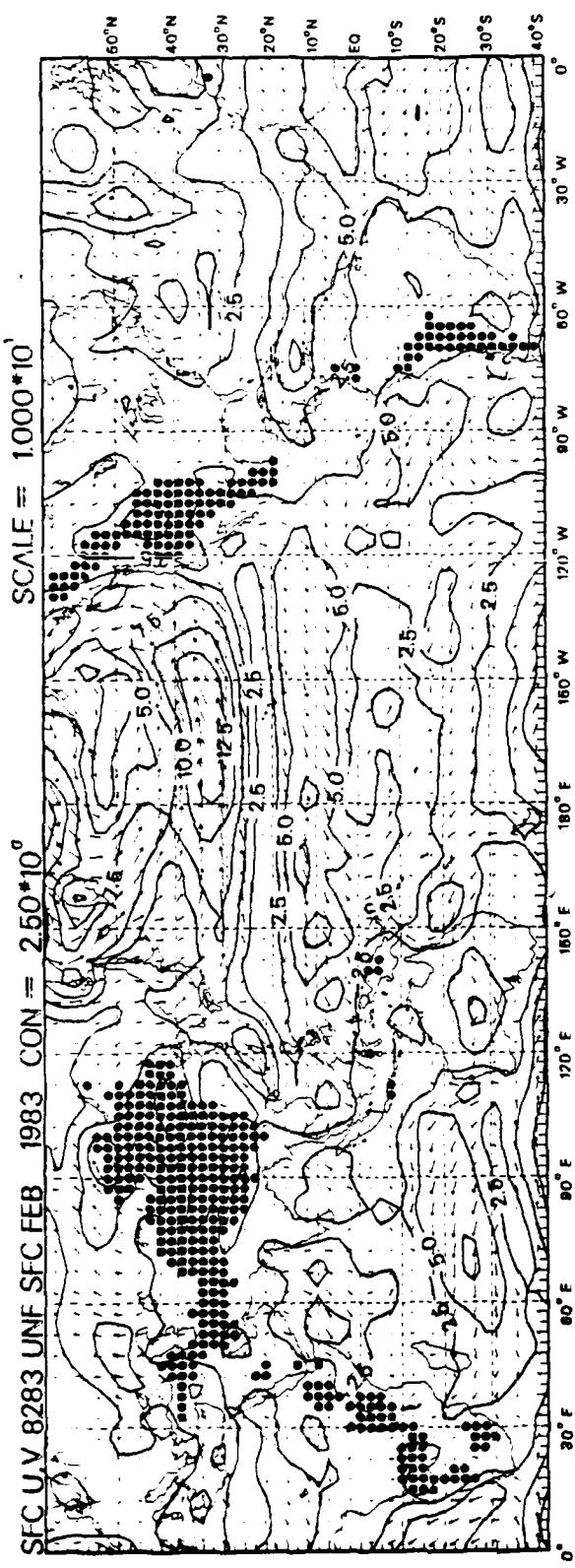
SCALE = $1.000 \cdot 10^6$

$500 \cdot 10^6$

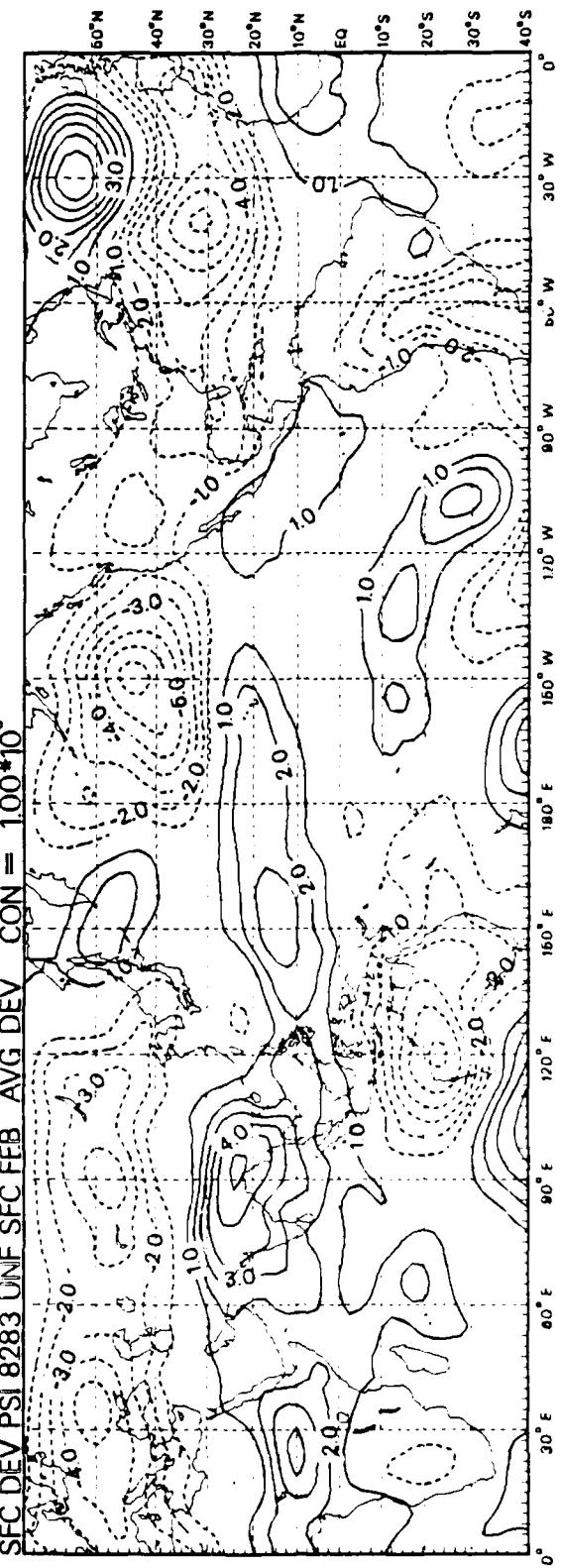
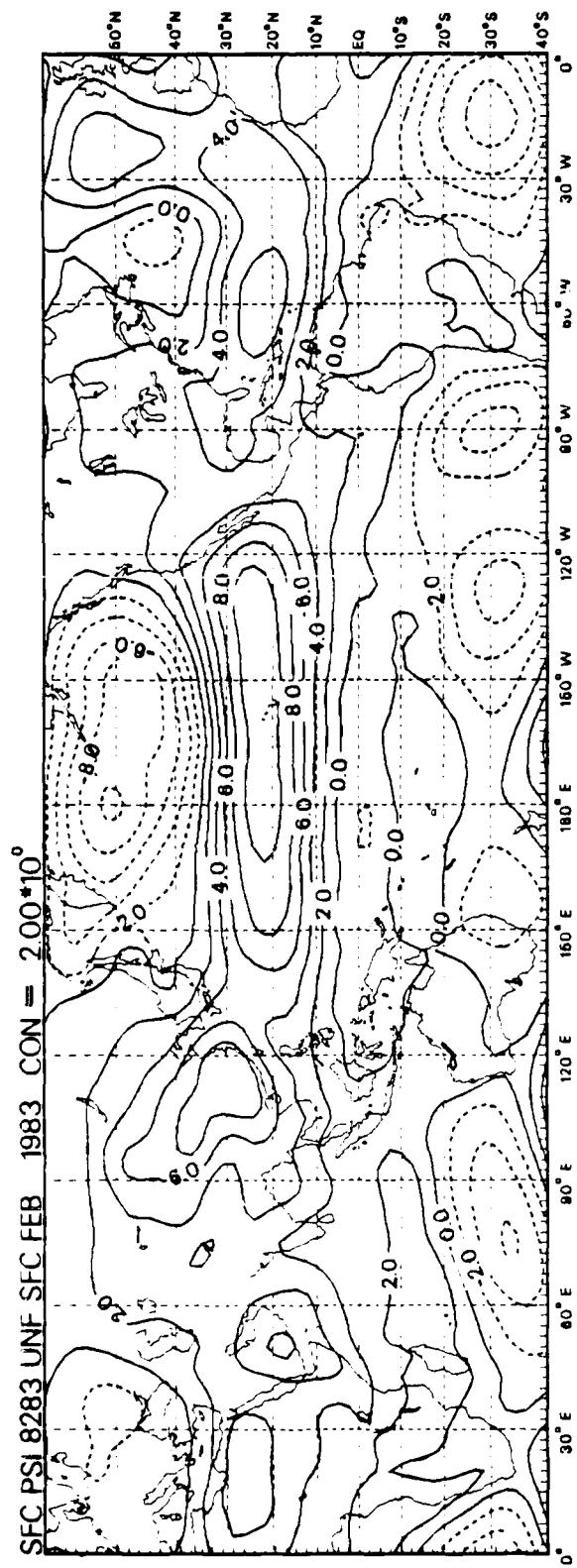
CON =

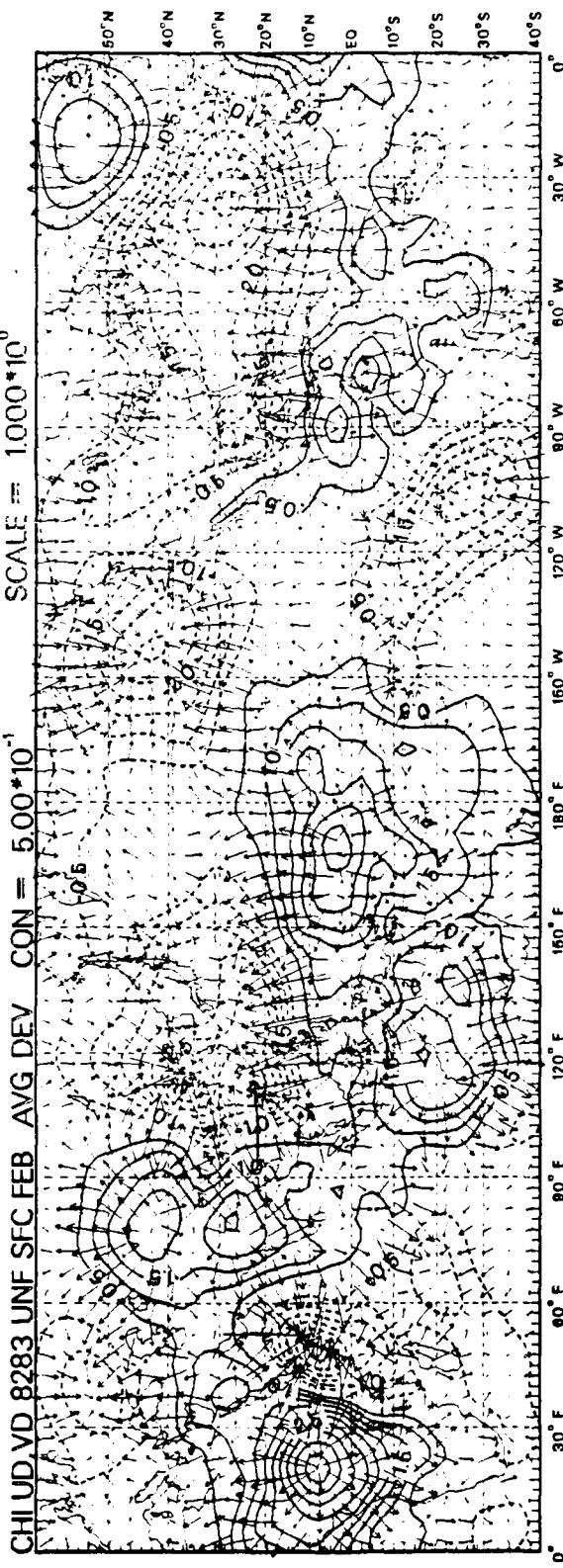
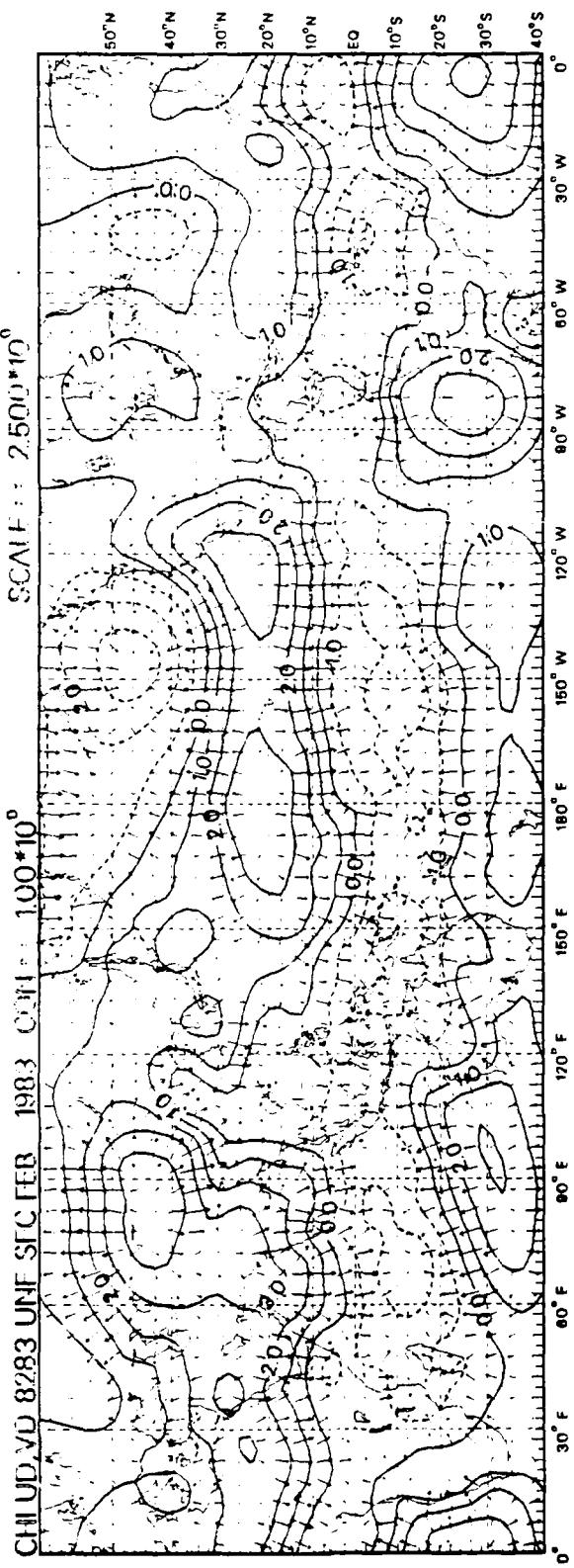


D79



D80



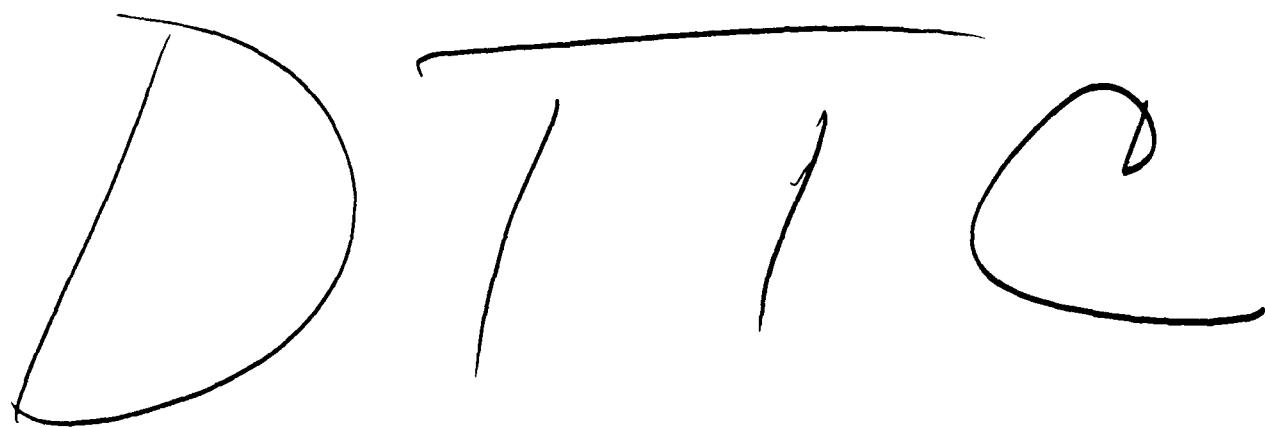


DISTRIBUTION LIST

	No. of copies
1. Defense Technical Information Center Cameron Station Alexandria, Virginia 22304-6145	2
2. Library, Code 0142 Naval Postgraduate School Monterey, California 93943-5100	2
3. Department of Meteorology Library, Code 63 Naval Postgraduate School Monterey, California 93943-5100	1
4. Climate Analysis Center NMC/NOAA Washington, D.C. 20233	3
5. Professor R. J. Renard, Code 63Rd Naval Postgraduate School Monterey, California 93943 5100	1
6. Professor C. P. Chang, Code 63Cp Naval Postgraduate School Monterey, California 93943 5100	50
7. Professor J. S. Hoyle, Code 63By Naval Postgraduate School Monterey, California 93943 5100	2
8. Dr. K. M. Lau Goddard Space Flight Center Climate and Radiation Branch NASA, Code 613 Greenbelt, Maryland 20771	2

9. Research Administration Office
Code 012
Naval Postgraduate School
Monterey, CA 93943-5000

1



7-86